Branched Polymers *via* CCTP with Vinyl end Groups and their Application in Wound Care Materials

By Samuel Robert Lowe

A thesis submitted in partial requirements for the degree of

Doctor of Philosophy in Chemistry

Department of Chemistry

University of Warwick

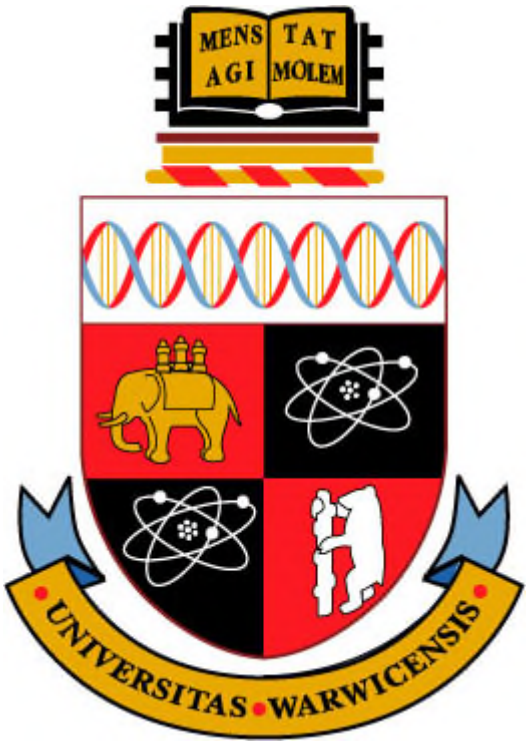

May 2017

CONTENTS

LIST OF FIGURES

LIST OF SCHEMES

LIST OF TABLES

LIST OF EQUATIONS

Abbreviations

[η]	Intrinsic Viscosity
α	Mark-Houwink Parameter
ρ_p	Polymer Network Density
AIBN	2,2'-azobis(isobutyrylnitrile)
AMPS	2-Acrylamido-2-MethylPropane Sulfonic acid
ASTM	Analytical Standard Testing Method
ATRP	Atom-Transfer-Radical-Polymerisation
BI	Bromine Index
CCT	Catalytic Chain Transfer
CCTA	Catalytic Chain Transfer Agent
CCTP	Catalytic Chain Transfer Polymerisation
CoBF	Co(II) dimethylglyoxime-difluoroboryl
Co(III)-H	Co(III) hydride
CRP	Controlled Radical Polymerisation
C_s	Chain Transfer Constant
CS	Compressive Strength
CTA	Chain Transfer Agent
Đ	Dispersity
d_f	Fractal Dimension
Da	Dalton
DMTA	Dynamic Mechanical Thermal Analysis
DP	Degree of Polymerisation
DRI	Differential Refractive Index
DSC	Differential Scanning Calorimetry
EGDA	EthyleneGlycol DiAcrylate
EGDMA	EthyleneGlycol DiMethAcrylate
FRP	Free Radical Polymerisation
G'	Elasticity modulus

G''	Viscous modulus
G*	Complex modulus
GC-FID	Gas Chromatography – Flame Ionisation Detection
GPC	Gel Permeation Chromatography
HEA	2-HydroxyEthyl Acrylate
HEMA	2-HydroxyEthyl MethAcrylate
IPN	Inter-Penetrating Network
IV	Intrinsic Viscosity
LCST	Lower Critical Solution Temperature
LogM	Log Molecular Weight
LVER	Linear ViscoElastic Region
MAA	Methacrylic Acid
MALS	Multi-Angle Light Scattering
MMA	Methyl Methacrylate
M_c	Molecular Weight between Cross-Linking Points
M_n	Number average molecular weight
M_P	Peak average molecular weight
M_w	Weight average molecular weight
MW	Molecular Weight
MWD	Molecular Weight Distribution
NMR	Nuclear Magnetic Resonance
pAMPS	poly(2-Acrylamido-2-MethylPropane Sulfonic acid)
PEG	PolyEthyleneGlycol
PEGDA	Poly(Ethylene Glycol) DiAcrylate
PEGDMA	Poly(Ethylene Glycol) DiMethAcrylate
PEGMEMA	Poly(Ethylene Glycol) MethylEther Methacrylate
PEO	PolyEthylene Oxide
ppm	Parts per million
PS	PolyStyrene
RAFT	Reversible Addition-Fragmentation chain Transfer polymerisation

R	Gas Constant
R_{diff}	Rate of Diffusion
R_{relax}	Rate of Relaxation
RI	Refractive Index
SBF	Simulated Body Fluid
SCVP	Self-Condensing Vinyl Polymerisation
SEM	Scanning Electron Microscopy
SEC	Size Exclusion Chromatography
TMS	TetraMethyl Silane
T_g	Glass Transition Temperature
T_m	Melt Transition Temperature
THF	TetraHydoFuran
TPU	Tecophilic PolyUrethane
UC	Universal Calibration
UV	Ultra Violet
VA-044	2,2'-Azobis[2-(2-imidazolin-2-yl)propane] Dihydrochloride
V_h	Hydrodynamic Volume
v_e	Cross-linking Density
VISC	Viscometry detector
V_R	Retention Volume

This thesis is dedicated to Stephen Mark Lowe

1963-2013

‘Spero Meliora’

Acknowledgments

My first thanks must go to Dave, for taking me on into his research group and for sourcing the funding of this PhD. As all PhDs should be, this has been a challenging experience and Dave has pushed me to improve, not only in the lab, but in the wider skills every effective researcher should possess. Dave's patience, guidance and tutelage are the reason I have been able to complete this PhD.

I am incredibly grateful for extraordinary contribution of Tara Schiller, who has gone beyond the call of duty in training me in my materials testing techniques, providing me access to the Warwick Manufacturing Group and for reading and commenting upon this thesis. Thanks also go to Nancy for giving a valuable insight into industrial research, and for her guidance and perspective on my work.

Thanks to the post-docs for their guidance at various points through my work; Paul, Olivier, Gabit and Kristian. Thanks go to the denizens of C210, past and present; Kay, Jamie, Raj, Dan, Sam, Jenny, Nut, Patrick and Danielle, you've certainly spiced up the past four years: Kay, Raj and Jamie for being there at the beginning and showing me the ropes; Dan for help with all things GPC and for taking up the challenge of reading and editing this thesis; Sam for the rolling ball of crises and leudity in the corner; Jenny for your acute sense of perspective; Nut for your bubbly, joyful optimism and helpfulness; Patrick and Danielle for your (ultimately successful) encouragement for me to purchase a boat.

Finally, thanks must go to my amazing wife; Florence and my family. Thank you to Florence for putting up with the 5.00 am starts, the 22.00 pm finishes and for patiently supporting me all the way through this process with hot meals and sage

advice. Thank you to my mother for raising me, supporting me and being the person to call and moan at during the long night time drives. Dubious thanks must also be extended to Tim, Douglas, Brian, Roger and Doreen for inspiring me to do a PhD in Chemistry.

Declaration

Experimental work contained in this thesis is original research carried out by the author, in the Department of Chemistry at the University of Warwick between October 2013 and November 2016, and at the Warwick Manufacturing Group at the University of Warwick between October 2013 and November and 2016.

Results from other authors are referenced throughout in the usual manner.

Date: 25/05/2017

Samuel Lowe

Abstract

Chronic wounds represent a significant problem to healthcare systems globally, wound generated from burns and diabetic ulcers have a 20 % chance of becoming chronic. In this thesis work was conducted to try and develop novel networks to act as chronic wound treatment systems.

Initially Catalytic Chain Transfer Polymerization (CCTP) was utilized to develop low molecular weight branched polymers with ω-vinyl end groups for use as novel gelators. Poly(methacrylic acid) (pMAA) was chosen as a building block due to its anionic nature and possibilities in the region of drug delivery and wound care. Branched acidic polymers of different molecular weights and degrees of branching were synthesized with good control. In addition to this branched and linear species of poly[(polyethylene glycol) methyl ether methacrylate] pPEGMEMA were synthesized by the same technique. All polymers were investigated kinetically and with multi-detector SEC to determine branching.

A poly(2-hydroxyethyl acrylate) hydrogel system was optimized by both thermal and photo initiation prior to the addition of branched acid polymers. Branched acid polymers exhibited a hardening effect upon thermally cured gels by rheology with a corresponding decrease in swelling suggesting reduction in the mesh size due to acting as gelators. However, in a photo-cure system the reverse effect was observed with softening and increase in swelling signifying an increase in mesh size.

A poly(2-acrylamido-2-methylpropane sulfonic acid) (pAMPS) hydrogel system was then utilized to study this effect with different degrees of branching and molecular weights of polymers. Studies by rheology, swelling and compression indicate that the

branched acid polymers were exhibiting a chain transfer effect from the ω-vinyl end group, inhibiting gel formation and therefore rendering them unsuitable for use as gelators.

An inter-penetrating network (IPN) of pAMPS and a thermoplastic elastomer (TPU) was formed by photo-curing a TPU film swollen in a solution of AMPS monomer and initiator. This process yielded a versatile, highly absorbent and transparent network which was able to rapidly absorb large quantities of fluids. Calcium testing and adhesion testing show that this material has significant potential in the field of wound dressings.

1. Introduction; the synthesis of branched polymers *via* radical polymerisation and the use of branched polymers in wound care hydrogels

The work in this thesis describes the synthesis of branched acidic and neutral polymers, by catalytic chain transfer polymerisation (CCTP), and their inclusion into hydrophilic polymer networks for use in wound-healing bandages. Areas relating to these materials will be discussed in this thesis.

A review of radical polymerisation will be conducted, beginning with free radical polymerisation and moving on to consider controlled radical polymerisation (CRP) before addressing the technique of choice – CCTP. Here we shall look at how it has been developed and applied to date with a special emphasis upon the growth of branched polymerisation using this technique. The motivation for the use of CCTP will also be explained.

This discussion will then cover hydrogels, their initial discovery, their development through time in addition to where the forefront in this technology now resides. The application of hydrogel networks into wound care materials will be explored as well as the wound healing process itself.

1.1 Free Radical Polymerisation

Chain growth polymerisation (as opposed to step growth polymerisation) is a form of polymerisation encompassing; free radical polymerisation (FRP), coordination polymerisation, anionic and cationic polymerisation.[1,2] It is characterised by the addition of unsaturated monomeric species to an active chain end one at a time. IUPAC define the chain growth polymerisation technique of (FRP) as;

"A chain polymerisation in which the kinetic chain carriers are radicals. Note: Usually, the growing chain end bears an unpaired electron"[3]

1.1.1 History

Polymerisation can find its first roots in 1832, when Jöns Jacub Berzelius first coined the word polymeric (derived from the Greek πολυμερη΄σ) to describe compounds with the same proportionate composition (empirical) but different numbers of constituent atoms.[4] In 1863 Berthelot described the conversion of monomers to their respective "polymerides" as polymeric transformation, and through his work is described as the first polymer chemist.[5] Despite this, it was not until 1920 with Staudinger's formation of long chain molecules by a chain growth method, theorised at the time to be due to free radical chemistry, that the study of polymer chemistry began in earnest.[6] This was followed by work in 1929 describing chain termination *via* ring formation and work in 1931 describing the activation of monomeric species prior to the very rapid addition of further monomeric species, one by one, to the chain end.[7,8] In 1937 Flory published his "the mechanism of vinyl polymerisations", a paper widely seen as being the cornerstone of modern FRP kinetic theory.[2]

Today, FRP accounts for just under half of the commercial polymers synthesised and encountered on a day to day basis.[5] This pervasiveness is a result of the high tolerances the technique exhibits towards impurities and the ease of synthesis when compared to the controlled radical polymerisation (CRP) techniques of reversible addition-fragmentation chain transfer polymerisation (RAFT), atom transfer radical polymerisation (ATRP), single electron transfer living radical polymerisation (SET-LRP) and ionic polymerisations. Unfortunately the technique's facile use comes with poor control over the rates of reaction and the deactivation of the reactive, non-selective, radical species, which subsequently leads to poor control of polymer molecular weight and architecture.[1]

1.1.2 Mechanism

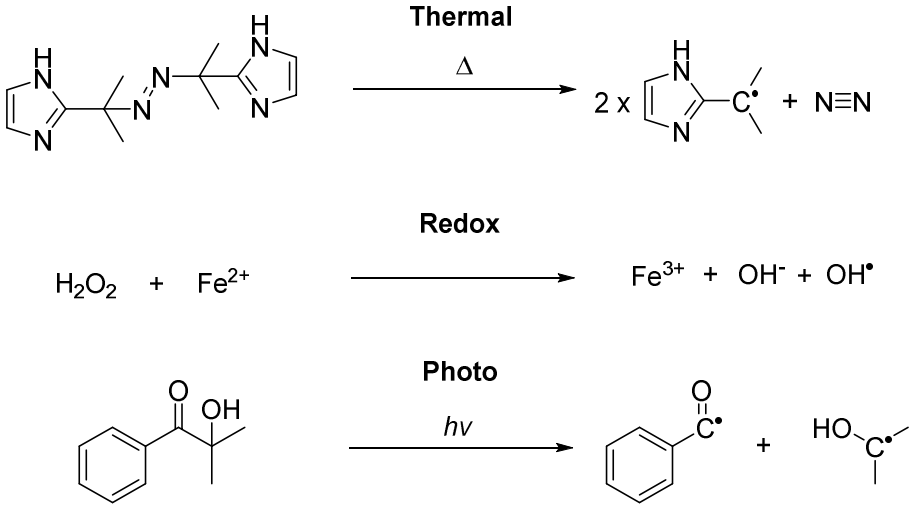

Scheme 1.1; Types of radical initiators including; the thermal initiator *VA-044™*, Iron/peroxide redox initiation coupling and *Irgacure 1173™* photo initiator.

Initiation of polymerisation in FRP usually involves the decomposition of a small-molecule to form radical species. Different forms of external stimuli can be used to

initiate this process including heat, redox reactions or irradiation with light at a certain wavelength (**Scheme 1.1**).

Whatever the stimuli used for the generation of the initiating free radical, these species go on to add to a first monomer unit causing the first step in the polymerisation cycle – initiation, thus begetting a radical capable of propagation (**Scheme 1.2**). Radicals formed from this initiation step go on to propagate sequentially from the chain end radical with additional monomer units until either the monomer is depleted or termination occurs through one of the mechanisms described below. The rate of propagation is dependent upon the concentration of monomer, radical and the propagation rate constant, which is in turn dependent upon the type of monomer and the conditions of the reaction (**Scheme 1.2**). Propagation is unable to alter the concentration of radicals – this occurs through termination as discussed below.

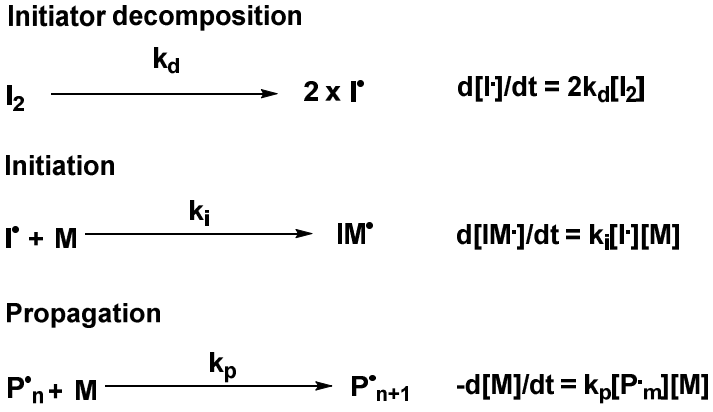

Scheme 1.2; Reaction schemes and rate equations for initiator decomposition, Initiation and propagation of monomer in FRP, where I_2 is the initiator, I is the initiator fragment, M is the monomer, P is the polymer and, k_d, k_i and k_p are the rate of initiator decomposition, initiation and propagation, respectively.

Termination in free radical polymerisation is uncontrolled, leading to the synthesis of polymers with very high polydispersities (Đ), when termination does occur it results in the formation of "dead" deactivated chain ends and a decrease in the concentration of radicals (unless more are subsequently generated by initiator decomposition). Chain death can occur through three modes; combination, disproportionation and chain transfer, the relative proportions of which are determined by the monomer and solvent system in use as well as environmental conditions, such as temperature (**Scheme 1.3**).

Termination mechanisms

Combination

Disproportionation

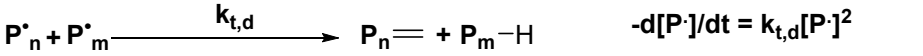

Chain Transfer

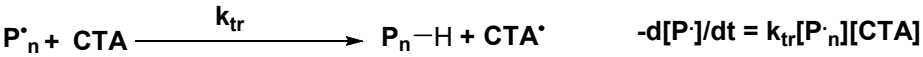

Scheme 1.3; Reaction schemes and rate equations for termination and chain transfer FRP where P_n and P_m are polymer chains consisting of n and m monomer units respectively, P_{n+m} is a terminated polymer chain of n + m monomer units, P_{n-H} is a polymer chain of n units terminated by H, $P_{m=}$ is a polymer chain of m units terminated by a double bond, CTA is a chain transfer agent (whether monomer, solvent, polymer or an added species), and $k_{t,c}$, $k_{t,d}$ and k_{tr} are the rate constants of termination by combination, disproportionation and chain transfer respectively.

Termination through combination of two growing chain ends leads to the formation of species with the sum of the two molecular weights (MW) of the respective species; as a result this produces species with higher than average MW. Termination through disproportionation occurs through the transfer of hydrogen from one growing radical chain end to another, this results in the formation of an unsaturated polymeric chain end and a saturated polymeric chain end. The rate constants of termination are significantly higher than those of propagation but is generally prevented from dominating due to the low concentrations of radicals, however, at higher conversions when the monomer is depleted termination becomes dominant.

1.1.3 Chain Transfer

Chain transfer takes place in FRP when an atom (normally hydrogen) is transferred from the propagating chain end to a chain transfer agent (CTA), which can be; monomer, polymer, solvent, initiator or other species deliberately added to affect chain transfer.[2] Chain transfer has a direct impact upon the degree of polymerisation (DP_n), lowering the DP_n through prematurely terminating the polymer chain before it reaches the kinetic chain length. Normally chain transfer in FRP has no effect upon the rate of polymerisation, only reducing the DP_n, although some cases do exist to the contrary where the relative rates of propagation, chain transfer and reinitiation lead to a decreased rate of polymerisation (**Table 1.1**).[1]

k_p:k_{tr}	k_a:k_p	Resulting Chain Transfer	Effect on R_p	Effect on DP_n
$k_p >> k_{tr}$	$k_a \approx k_p$	Normal Chain transfer	None	Decrease
$k_p << k_{tr}$	$k_a \approx k_p$	Telomerisation	None	Large decrease
$k_p >> k_{tr}$	$k_a < k_p$	Retardation	Decrease	Decrease
$k_p >> k_{tr}$	$k_a < k_p$	Degradative chain transfer	Large decrease	Large decrease

Table 1.1: Effect of chain transfer on rate of polymerisation, R_p and DP_n of resulting polymers based on the relative rates of propagation, k_p, transfer, k_{tr} and reinitiation, k_a. Adapted from reference.[9]

Chain transfer, although often an undesirable side reaction, can be harnessed through the addition of specific chain transfer agents to control the DP_n of a polymer without having to add large quantities of initiator. Thiols are the most commonly used chain transfer agent in FRP (with a C_s of 1-10, the highest value among conventional CTAs), as they readily transfer hydrogen to propagating species, yielding a saturated chain end and a thiyl radical. The thiyl radical is then capable of initiating further polymerisation. The consequences of this form of chain transfer are; the inclusion of additional functionality (not always desirable) and the

steady consumption of the CTA. In the *'Strathclyde methodology'* thiol CTAs are pushed to their limit to mitigate the effects of the Norrish-Trommsdorff, or gel effect (localised increases in the viscosity of a polymers solution leading to overall increase in rate of polymerisation potentially causing gelation) in FRP in the presence of vinyl and divinyl monomers.[10-13]

1.2 Catalytic Chain Transfer Polymerisation (CCTP)

Catalytic chain transfer polymerisation (CCTP) is a method of harnessing the simplicity of FRP and controlling the molecular weight of the polymers produced by enhancing the rate of chain transfer. This is achieved through the addition of the highly effective cobalt (II) macrocycles as CTA, the most effective of which is CoBF (or one of its derivatives). The benefits of this method include; its simplicity (as demonstrated by its industrial uptake), the formation of vinyl end groups with near to 100 % fidelity, allowing for exploitation of this functionality, and, due to the high chain transfer constant of the CTA, only very small amounts of the benign CTA are required (ppm levels).

1.2.1 Initial development

Catalytic chain transfer was first discovered by Boris Smirnov and Alexander Marchenko in 1975 as a result of research into the use of transition metal compounds to catalyse the redox decomposition of peroxy initiators in free radical polymerisations.[14-19] Co (II) porphyrins (**Figure 1.1** - **1**) promoted by Ponomarev based upon the structure of Vitamin B12 **(2)** were discovered to be effective at controlling and limiting the molecular weight of polystyrene and PMMA formed from free radical polymerisation *via* chain transfer.[20] The added benefit of this

method was the very low quantities of catalyst required to achieve this relative to the conventional chain transfer agents. [14,15,17] The chain transfer constant (C_s) for (**1**) in the free radical polymerisation of methyl methacrylate is $2.4x10^3$ compared to ~40 in the case of a thiol chain transfer agent.[21]

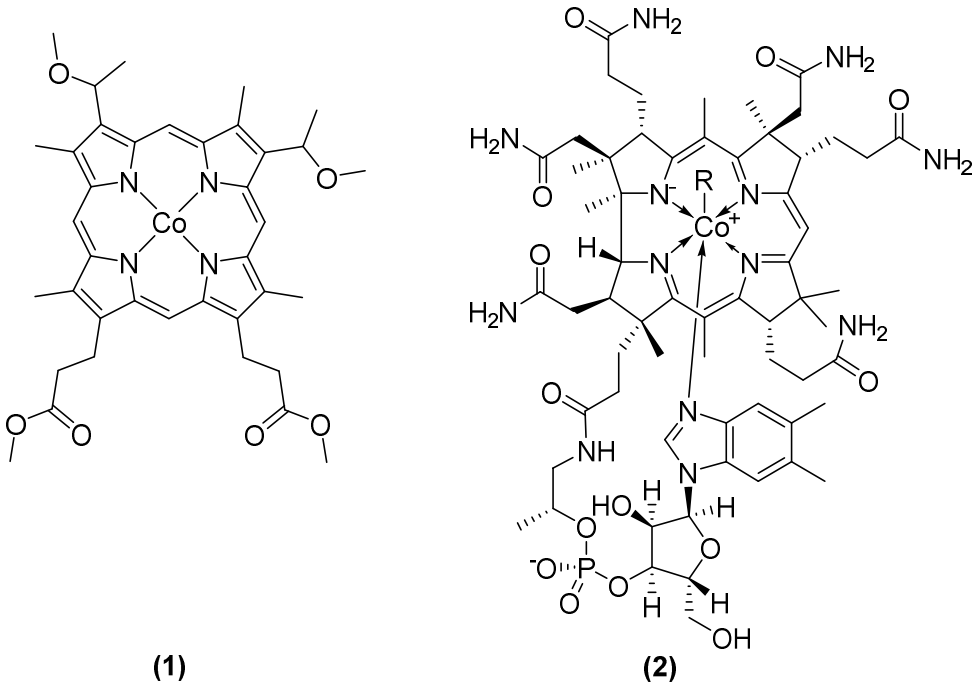

(1) **(2)**

Figure 1.1: (1) Cobalt tetramethoxy hematoporphyrin-IX (shown without neutral axial ligands) and (2) Vitamin B12 with corryn ring as opposed to porphyrin ring.[15]

Further work assisted by the Enikolopyan group led to an understanding of the fundamental mechanism of reaction in 1977, this is discussed below.

Initial research in the USSR dealt with; catalytic inhibition by aprotic solvents,[22] mechanistic investigations,[22] the development of cobaloxime compounds (**3**) as potent second generation chain transfer catalysts,[23,24] investigation into the structural basis of activity,[25,26] and kinetic studies into the formation of low molecular weight polymers and oligomers.[27,28] Further commercial development

was stymied by the issuing of a USSR patent detailing '*for office use only*' in 1980, restricting research to the institution of the researcher.[23,29]

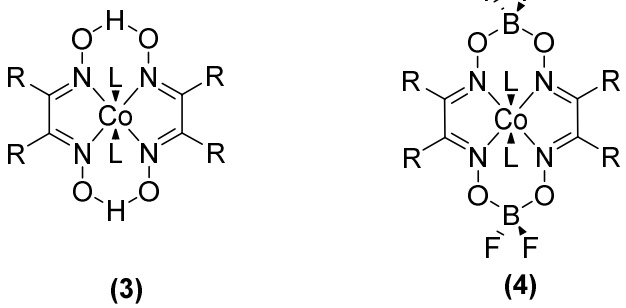

(3) **(4)**

Figure 1.2; Cobaloxime general structure (unspecified neutral axial ligands denoted by L) (3), CoBF general structure (4).

Take up of the technique by DuPont under Steven Ittel led to the development of patents for air stable CCTP catalysts based upon cobaloximes with BF_2 bridging ligands (CoBF) (**4**), allowing for the ready commercialisation of CCTP for methacrylates and styrene.[30-33]

The initial stage of publications generated in the Russian literature went largely unnoticed outside of Russia and further patents from this period also led to this technique being ignored in the west for a number of years.[15,16,18,19,34] The next stage of the development of CCT was to occur through industrial development. Issues at this point were encountered with the perceived unreactivity of CCTP macromonomers and the narrow range of monomers accessible to the technique (being limited to α-methyl substituted monomers and styrene).

In the early 1990s interest in CCTP was revived through the use of CCTP oligomers as addition-fragmentation chain-transfer (AFCT) agents for the formation of telechelic and diblock polymers through free radical polymerisation (**Scheme 1.4**).[35-37]

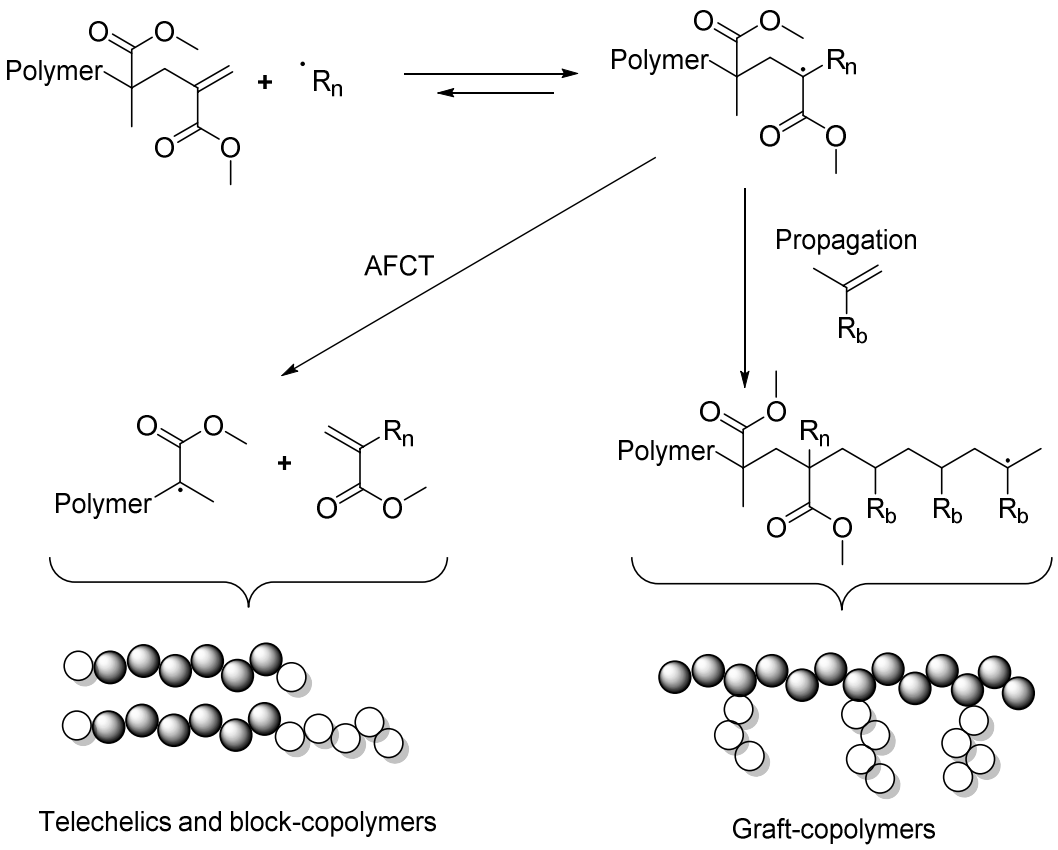

Scheme 1.4; Alternative proposed pathways for reaction with CCTP ω-vinyl terminated polymers, showing addition fragmentation chain transfer and propagation. Figure adapted from reference.[14]

The late 1990s through to the 2000s saw industrial interest increase and with this a corresponding increase in academic publication. This can be seen through a range of patents issued from companies such as the Glidden Paint company (which became part of ICI/Dulux and now Akzo), DuPont and ICI/Zeneca Specialities (later to become a part of DSM). Glidden's patents demonstrate the use of cobaloximes (**4**) as catalysts, however, the patent was quite narrow in that it made very limited claims only to the parent cobaloxime (**3**).[38] The narrowness of the claim was exploited by DuPont who expanded upon the range of cobaloxime functionalities available. In turn DuPont also made a similar mistake in not filing broad enough claims and an "error" in the wording of their patents, where they claimed "R" in

structure **4** as phenyl but not aryl, led to its exploitation by ICI/Zeneca who further developed a range of compounds where R is a substituted phenyl (aryl).

The development of cobaloximes first explored analogues of **3** which proved to be cheaper to produce and with a higher chain transfer constant (C_s $2x10^4$).[14] These were soon replaced by cobaloximes with a BF_2 bridge as opposed to a H bridge (**4**), this once again increased the chain transfer constant (C_s $4x10^4$) whilst at the same time increasing the stability of the complexes to acidic hydrolysis and oxidation to Co(III).[27,31]

The use of (**4**) increased the utility of the catalysts and CCTP has now been used in a wide range of applications both in fine chemicals (rheology modifiers,[39] macromonomers as hair care additives[40], paint and coatings, automotive refinish, ink-jet inks, contact lenses) and in industrial applications (thermoformed sheets of MMA for sinks, baths and shower trays).[41]

1.2.2 Mechanism

There are three proposed mechanisms for catalytic chain transfer polymerisation, a technique that has been found to be truly catalytic through the recovery of the regenerated cobalt complex.[15,16,18,19] Two of the three techniques are characterised by activation of a substrate by the cobalt complex prior to attack by the monomer; the third involves a sequential reaction of two species with the metal centre (**Scheme 1.5**). The matter of contention between the three mechanisms is the action of hydrogen transfer in the initiation of a new propagating radical chain.

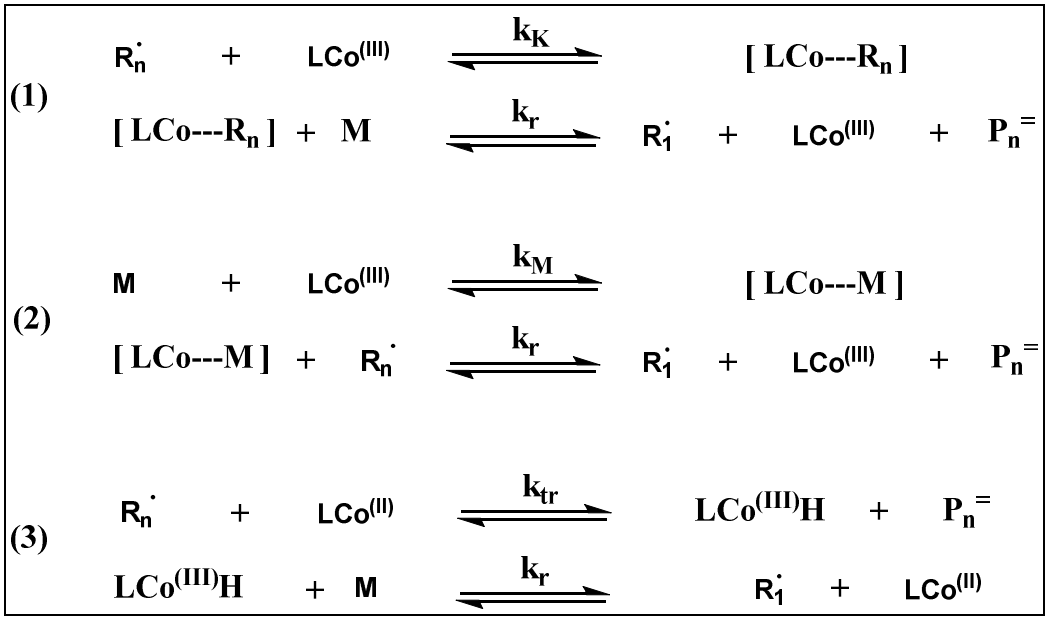

Scheme 1.5; Proposed mechanisms for CCTP. Where R_n and R_1 are the polymeric and monomeric radicals respectively, M is the monomer, LCo(II) is the cobalt chelate CTA and $P_{n=}$ is a polymer with unsaturated chain end. Adapted from reference.[15]

The first proposed mechanism (**1**) requires the formation of an intermediate Co complex through reaction with the propagating radical followed by hydrogen abstraction from the monomer by the complex to give a new propagating radical chain.[28,29] This mechanism was tested, and although the initial step has been observed, the mechanism is improbable as the monomer is not directly involved in the hydrogen abstraction step.[42] The second mechanism (**2**) involves using a Michaelis-Menton-type mechanism akin to enzymatic action.[16] This mechanism shows a dependence of the rate of chain transfer upon the concentration of monomer, which was quickly disproved.[34,43] The third proposed mechanism (**3**) involves the disproportionation of the Co catalyst with a polymeric radical, yielding a Co(III) hydride followed by the reinitiation of a monomer to form a new

propagating chain. Although the LCo(III)H has never been observed in context, kinetic studies by Smirnov and co-workers,[18,19] and, later work carried out by O'Driscoll and Gridnev in combination with well documented work on cobalt hydrides,[27,44-46] have led to general agreement on this mechanism.[15,42,47-50]

As with conventional chain transfer, the effect of CCTP is to reduce the molecular weight without reducing the rate of polymerisation in the reaction. It differs from conventional chain transfer in that the CTA is recovered in the process and is capable of reinitiating polymerisation, as a result the mechanism can be displayed as a catalytic cycle (**Figure 1.3**).

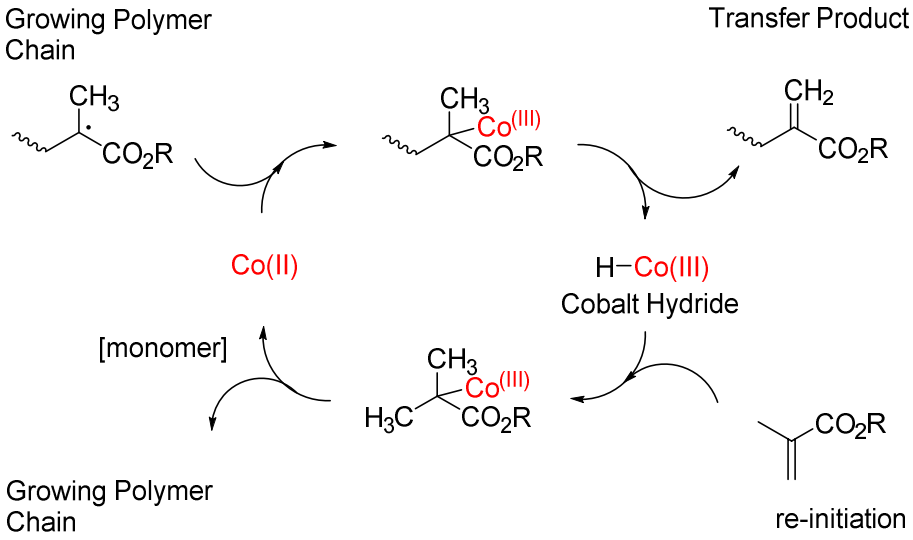

Figure 1.3; Mechanism for catalytic chain transfer of methacrylates cobalt complex COBF.

There still remain a few unexplained anomalies in the proposed mechanism, caused by the difficulty of analysing the active species due to the paramagnetism of the catalyst, rendering NMR difficult. One such anomaly is that it is considered unlikely that hydrogen abstraction occurs *via* β-hydride elimination, rather that abstraction

occurs *via* a radical pathway, and, is supported by kinetic isotope experiments by Gridnev.[51]

1.2.3 Monomer and Catalysts

Monomer

When considering CCTP, monomers can be split into two categories; active and inactive species. Active species will invariably have an α-methyl group (the exception being styrene), holding a H-atom that can easily be abstracted by the catalyst complex. The steric bulk afforded by the α-methyl group, allows for the Co(III)-C bond formed to be labile, resulting in hydrogen abstraction and the formation of Co(III)-H and an ω-vinyl terminated polymer chain.[52] Conversely, compounds without an α-methyl group, have secondary propagating radicals and lack the easily abstractable H-atom. This lends itself to the formation of a relatively stable Co(III)-C bond – even observable by MALDI-TOF,[49] removing active catalyst from the catalytic cycle and reducing the C_s of the catalyst in the system.[16,24,53] When an H-atom is abstracted in these systems, it is abstracted from the backbone, rather than an α-methyl substituent, leading to the formation of an internal, or backbone, vinyl bond, which is less active for further modification.

Catalysts

Functioning CCTP species are always low-spin cobalt(II) complexes with octahedral geometry (O_h), made up of a macrocyclic tetra chelate ligand with square planar geometry, leaving two axial coordination sites available for action of catalysis.[15,21,54] Cobalt (II) complexes can exist in either the high- or low-spin (**Figure 1.4**), depending upon the ligand – although no empirical reasoning has been found for

why certain macrocycles with oxygen or nitrogen atoms bonding give high- or low-spin complexes with respect to their effect upon the band gap of the complex.

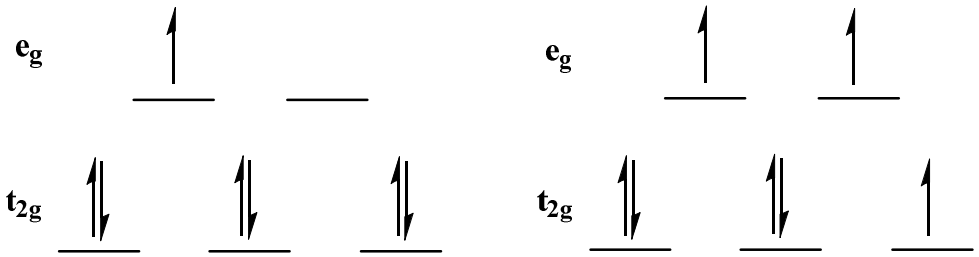

Figure 1.4; d-electron configuration of d^7 Co(II) complexes in low (left) and high spin (right) states.

Catalyst development from vitamin B12 and the introduction of porphyrin ligands (**Figure 1.1**) were quickly optimised, first with the development of cobaloximes (C_s = 2 x 10^4),[21] and then the introduction of hydrolytic stability with a BF_2 bridging ligand (**4**, **Figure 1.2**).[15,32,33] The new cobaloximes, with significantly enhanced hydrolytic stability in oxygenated and aqueous solutions, allowed the facile utilisation of CCTP industrially as the catalyst could be handled in its solid form in air, with the added advantage of even higher activity (C_s = 4 x 10^4).[14,27] Solubility and stability of the complexes to different industrial applications can be tuned through the axial and equatorial R groups of the ligands, further increasing the range of their applications.[15,27,55]

Measurement of catalyst efficiency

The activity of a CTA for any given system (monomer, solvent, temperature, CTA) is given by the chain transfer constant (C_s) – defined as the ratio of the rate of chain transfer to the rate of propagation (k_{tr}/k_p).[37,56,57] Conventional CTAs such as thiols have a C_s value of 1-10 for methacrylates, whereas CCTP catalysts like CoBF will typically have C_s values in the region 10^4 for methyl methacrylate, thus requiring

significantly lower concentrations of CTA in order to afford the same effect upon MW. In CCTP Mayo plots are often used as a measure of the purity of the catalyst – due to the paucity of available methods of characterisation – relative to known systems (homopolymerisation of MMA with CoBF, giving a C_s of 4 x 10^4).[58]

$$\frac{1}{DP_n} = \frac{1}{DP_n^0} + C_s\frac{[S]}{[M]}$$

Equation 1.1: Mayo equation, where DP_n is the number average degree of polymerisation in the presence of CTA, DP_n^0 is the number average degree of polymerisation without CTA, C_s is the chain transfer constant, [S] and [M] are the concentration of CTA and monomer respectively.[15]

The Mayo equation (**Equation 1.1**) used for the calculation of C_s is carried out through a series of polymerisations conducted across a range of ratios of CTA to monomer, including one with no CTA present, and stopped at low conversion (generally < 10 %), to avoid the effects of reduced monomer concentration and termination. From this can be extracted a linear plot of $1/DP_n$ *vs.* [S]/[M] yielding a slope with a value of C_s and an intercept of DP_n^0 for that system. This system holds for all but very low DP_n (< 20) when a modified Mayo equation (Equation 1.2) must be used due to the significant effects of the formation of monomeric product.[43]

$$\frac{1}{DP_n - 2} = \frac{1}{DP_n^0} + C_s\frac{[S]}{[M]}$$

Equation 1.2; Modified Mayo equation for low DP, where DP_n is the number average degree of polymerisation in the presence of CTA, DP_n^0 is the number average degree of polymerisation without CTA, C_s is the chain transfer constant, [S] and [M] are the concentration of CTA and monomer respectively.[15]

Number average DP can be calculated either from M_n^{SEC}, or by division of M_w^{SEC} by two times the monomer mass. M_w should only be used for systems where the Đ is

approximately 2 due to a high rate of chain transfer – as is the case with CCTP. M_w is conventionally used in this case due to the high susceptibility of M_n to baseline deviation, so rendering lower accuracy.[59-61]

1.2.4 Applications of CCTP polymers

The development of CCTP has been intrinsically linked with its industrial applicability due to the early realisation that it could be used to control molecular weight in free radical polymerisations. However, there has been development from an academic perspective which this section will briefly address, as the industrial aspect has already been discussed in the historic overview.

CCTP-generated macro-monomers have found a variety of uses in the academic field. CCTP macromonomers have been copolymerised with acrylics and secondary radical-generating monomers to form grafts and combs.[36] Methacrylate CCTP macromonomers have been shown to act as CTAs through a β-scission addition-fragmentation mechanism,[37,62,63] which has been used in the case of CCTP α-methyl styrene dimers to control the MW of free radical styrene polymerisation.[64] This feature has also been used to control the polymerisation temperature in the UV curing of dental resins.[65] More recently the generation of CCTP macromonomers as CTAs has been used to generate narrow Đ block copolymers in a technique dubbed sulphur free RAFT.[66]

Telechelic polymers have also utilised the β-scission addition fragmentation mechanism in its action upon a CCTP derived poly(2-hydroxyethyl methacrylate) dimer as a CTA in the synthesis of α,ω-dihydroxy telechelic poly(methyl

methacrylate).[67] This subject area has been comprehensively investigated in the literature.[21,37,67,68]

Macromonomers have also been utilised in combination with RAFT to form grafted architectures. Well defined polymer chains were formed by RAFT prior to termination by CCTP, yielding ω-vinyl terminated macromonomers with low Đ. These polymers were then copolymerised with acrylic monomer to give comb-like and star-like structures. Copolymerisation of a macromonomer with a difunctional acrylic has been used to form core-cross-linked star structures for use as rheological modifiers, where the hydrophilicity of the chain tunes the solubility of the structure in different solvents.[39]

1.3 Branched Polymers

Polymer topology has an important impact upon a number of properties of polymers.[69] Branched polymers have garnered substantial interest over the past 25 years due to their potential as viscosity and rheological modifiers, as well as their high level of functionality and their potential to impart increased solubility.[1,70,71] These properties have seen them taken up for applications such as; coatings, resins,[72,73] viscosity modifiers, [74,75] biomedical applications and even drug delivery devices.[76,77]

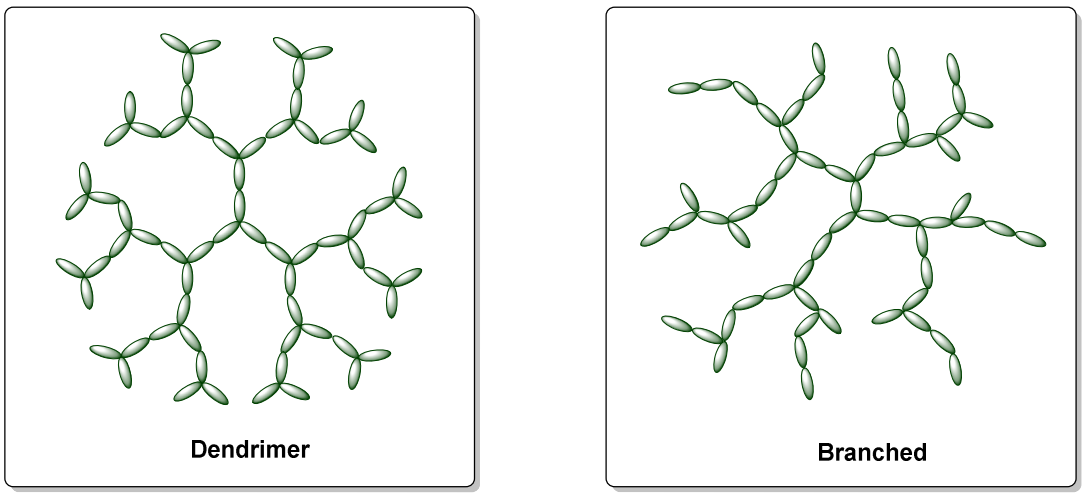

Figure 1.5; General structure of macromolecules of dendritic (left) and branched (right) architecture.

Branched species can be divided into two broad classifications; dendrimers and branched/hyperbranched polymers (**Figure 1.5**). Dendrimers, which are characterised as being perfectly symmetric, ideally monodisperse, macromolecules are very appealing to biomedical applications due to their high peripheral functionality,[78,79] however, their highly demanding synthetic protocols often lead to high costs which limit their applicability. Branched and hyperbranched polymers offer a more facile route towards highly functional polymers that can be synthesised by one-pot processes with relatively simple purification requirements, although, at the cost of being less well defined. This thesis focusses upon the synthesis and use of highly branched polymers, therefore the following sections will focus upon synthetic routes towards these species.

1.3.1 Synthesis of branched polymers

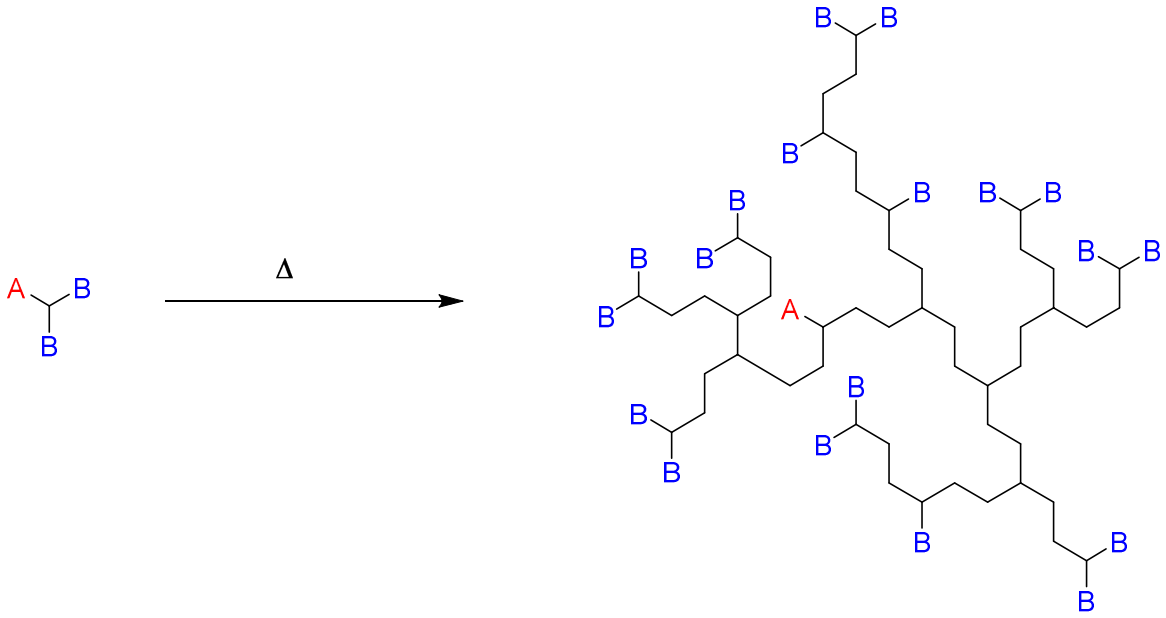

Scheme 1.6; General reaction scheme depicting single monomer methodology self-condensation reaction of AB_2 monomers.

Classical synthesis of branched polymers involves the use of AB_x monomers under Flory's single monomer methodology, whereby A groups only react with B groups, and the relative reactivities of groups A and B are equal (**Scheme 1.6**).[80] This technique theoretically has the advantage that if an ideal selectivity between A and B monomers is maintained, then cross-linking should be impossible, however, the reality is that cross-linking cyclisation and side reactions between B groups do occur.[81] Unfortunately, there are very few step growth monomers commercially available that fulfil this brief. A double monomer methodology was also developed whereby both homopolymerisation and copolymerisation of AB_x+B_y monomers is permitted, this allows for the introduction of additional functionality as well as the tuning of the length of branching in the polymer and, therefore, the topology.

In this work only radical polymerisation techniques are used in the synthesis of branched polymers, as a result, non-radical approaches will not be considered further. Step growth (as opposed to chain growth) methods are widely used and have had extensive uptake industrially and academically. As a result there are a number of comprehensive, contemporary reviews on the subject.[70,82-87]

1.3.2 Network formation

Due to the inclusion of multifunctional monomers, necessary for the formation of branched polymers, the synthesis of cross-linked networks should be briefly considered. An infinite polymer network (in which the MW tends towards infinity) can occur through two main techniques when considering branched polymers. The first is cross-linking during polymerisation, the second is through post-polymerisation modification. These networks have found many varied applications, and will be considered later in this chapter.

Flory[80,88-92] and Stockmayer[93] laid the foundations for the mathematical consideration of cross-linked gel networks, treating the free radical formation of networks as being analogous to the step polymerisation of multi-functional reactants.[1] Unfortunately, this theory failed to anticipate the role of cyclisation in gel formation and so tended to over predict the gel point.

Definition of the point of gelation in conventional free radical polymerisation (in the absence of a CTA) has been investigated in a range of radical polymerisations where the concentration of the diene is typically kept below 1 mol %. Systems where the reactivity of the mono and di-vinyl monomer are relatively similar include MMA-EGDMA[94,95] and styrene-divinyl benzene.[96] In these systems, the reactivity of the

two is assumed to be equal so that for an A + BB polymerisation, the extent of the reaction ρ of A double bonds is equal to the ρ for B double bonds. The extent of the reaction can therefore be written as ρ[A] and ρ[BB], where the total concentration of reacted BB units is ρ^2[BB]. The cross-link number is simply the number of fully reacted BB units and the critical gel-point occurs when the number of cross-links per chain is equal to 1/2 (**Equation 1.3**).[1]

$$\rho_c = \frac{[A] + [B]}{[B]\bar{X}_w}$$

Equation 1.3; Gel-point, ρ_c, for radical polymerisation of monofunctional monomer A, and difunctional monomer BB, where [A] is the concentration of A vinyl bonds, [B] is the concentration of B vinyl bonds and $\overline{X}_m$ is the weight average degree of polymerisation.

At very low concentrations of BB (< 0.1 mol %), this equation proves accurate, as $\overline{X}_m$ is defined as the weight average degree of polymerisation for the homopolymerisation of A. This equation shows extensive cross-linking in a MMA-EGDMA co-polymerisation, with EGDMA (< 0.5 wt. %) occurring at 12.5 % conversion.[97,98] However, it is shown that calculated values underestimate ρ_c at higher concentrations of divinyl monomer BB, this is because, as with the Flory-Stockmayer theory, the equation does not take into account the effects of cyclisation and the reduced reactivity of pendent functionality relative to free monomer species.[94,99,100] These studies all show that with even very low concentrations of divinyl monomer, a cross-linked gel network should be formed. Multiple strategies have been investigated to overcome these limitations, to allow for the formation of soluble branched species, the chain growth varieties of which will be discussed herein.

1.3.3 Branched polymers by chain growth

Self-condensing vinyl polymerisation (SCVP) was first reported by Fréchet *et al* in 1995, immediately opening the door to the application of chain growth strategies for the synthesis of branched, soluble polymers.[101] These techniques included self-condensing ring opening polymerisation (SCROP), chain transfer and, RAFT and ATRP driven SCVP.[71]

1.3.3.1 Self-Condensing Vinyl Polymerisation (SCVP)

SCVP is a process in which a monomer of AB_2 character, where the B_2 character is the vinyl group through which chain growth can occur and A is an activatable group from which vinyl polymerisation can be initiated.[71,87] Fréchet's initial method involved the polymerisation 3-(1-chloroethyl)ethenyl benzene in the presence of $SnCl_4$ to act as a lewis acid for the initiation of cationic polymerisation. This method yields branched polymers, but also gives high Đ and gelation at long reaction times due to the non-living nature of the reactions, despite the use of AB_x functionality, for which no gelation should occur.[102] This method was improved through copolymerisation with traditional vinyl monomers, which allows for the tuning of the degree of branching.[103,104] SCVP has since been developed to accommodate group transfer polymerisation (GTP),[105,106] atom transfer radical polymerisation (ATRP),[107-109] nitroxide mediated radical polymerisation (NMP)[107] and reversible fragmentation polymerisation (RAFT)[110,111] with additional control being imparted through the use of these 'living' techniques.

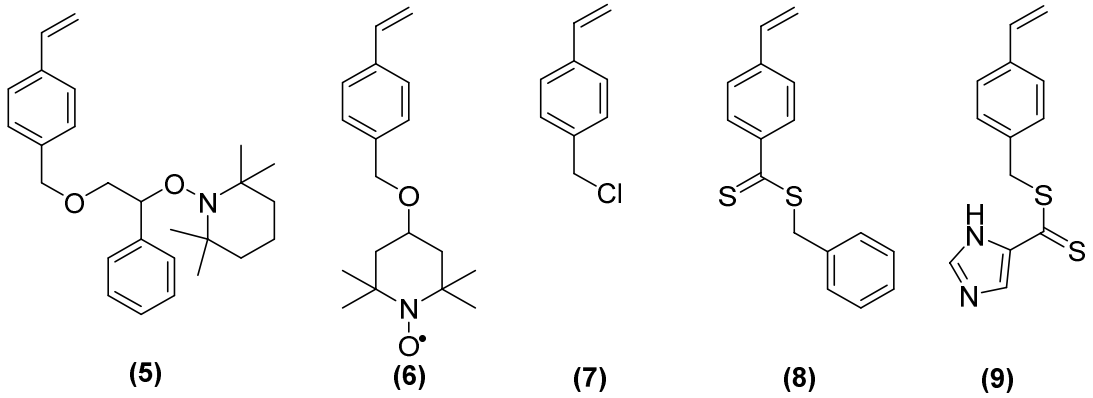

(5) (6) (7) (8) (9)

Figure 1.6; Influential monomers in the development of SCVP with living polymerisation techniques.

SCVP-NMP was used to create hyperbranched and star polymers using monomer with a polymerisable styryl group and an initiating/propagating moiety comprised of a nitroxide linked to a benzylic carbon atom (**5** in **Figure 1.6**). This led to a readily cleavable N-O bond for the formation of a propagating radical. Development of monomer structure led to nitroxides integrated into the branch points of the material, creating weak points that can be cleaved to form macroinitiators for the further polymerisation close to branching points (**6** in **Figure 1.6**).[112,113]

SCVP-ATRP initially made use of **7** in the presence of Cu(I)Br, however, this was found to produce predominantly linear polymers (**Figure 1.6**).[108,114] It was discovered that a constant concentration of Cu(I) was required for the formation of branched structures, subsequently high concentrations of initiator and the use of Cu(0) was used, allowing for the constant oxidation of deactivated Cu(II) species.[115] This method has the benefit of not having a 'weak' point in its structure (unlike SCVP-NMP and –RAFT). The use of halide initiating species in ATRP has also allowed for the copolymerisation of fluorinated monomers for the formation of fluorinated hyperbranched polymers.[116]

SCVP-RAFT was first used for the polymerisation of monomer incorporating a polymerisable dithioester (**8** in **Figure 1.6**) to produce branched styrene polymers with a weak dithioester bond.[111] This weakness was disposed of when 9 was applied, in which the dithioester group was on the chain end in the polymerisation of NIPAM (**Figure 1.6**).[117,118] Modification of this technique allowed for the synthesis of block, hyperbranched polymers with stimuli responsive properties.[110]

1.3.3.2 Conventional Chain Transfer

To monomer or polymer

Conventional chain transfer can take the form of; transfer to monomer, polymer or a chain transfer agent (CTA). The simplest method is to harness chain transfer to monomer *i.e.* polymerisation through monomers with non-stabilised radicals, such as ethylene or vinyl acetate.[71] Many monomers, including acrylates, undergo chain transfer, although at a reduced rate in CRP, leading to an insignificant amount of branching.[119,120] In order to promote chain transfer, thiol functionality – ubiquitous to chain transfer - was introduced onto co-monomers for the copolymerisation of styrene with vinyl benzyl thiol to give highly branched polymers.[121] Unfortunately such monomers are inherently unstable due to their liability to undergo Michael addition from the thiol group to the electron poor vinyl group. An alternative route, investigated by Rimmer and co-workers, involves the introduction of chain transfer to a co-monomer, used in the polymerisation of N-vinyl pryrrolidinone and vinyl acetate (**10** in **Scheme 1.7**).[122]

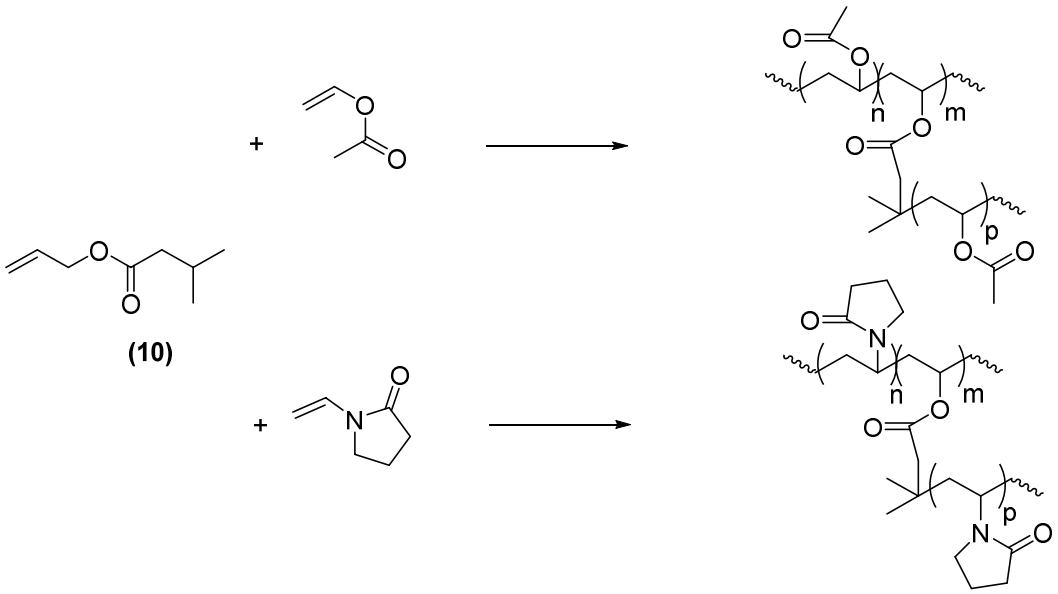

Scheme 1.7; Copolymerisation with a branching comonomer, (10), which transfers via abstraction of the 2-propyl hydrogen during the polymerisation of monomers that propagate via non-stabilised radicals. Adapted from reference.[71]

Although this route represents an economical and effective route to the production of highly branched polymers, the lack of control over polymerisation and end groups limits its applicability.

Control of multifunctional monomer polymerisations using a conventional CTA

Normally, free radical polymerisation in the presence of even very low concentrations of di-functional monomers (*e.g.* ethyleneglycol dimethacrylate or divinyl benzene) would yield an insoluble, cross-linked network, with the cross-linking concentration per chain exceeding unity.[98] However, the application of thiols as a CTA enables the copolymerisation of mono-vinyl monomer with low concentrations of multi-vinyl monomers in a route now commonly known as the "Strathclyde methodology" after the institution in which it was conceived by Sherrington *et al.* (**Scheme 1.8**).[13,123-128] The Strathclyde route occurs through a reduction of molecules produced per kinetic chain length, thereby delaying the

onset of gelation in free radical polymerisation in the presence of a multi-vinyl monomer. This route provides a facile, cost-effective route to branched polymers, yielding (some) polymers with thiol functionality. This method can also be used to synthesise branched polymers in emulsion,[129] however, there are multiple adverse challenges described herein. The malodorous and toxic thiol CTA is non-catalytic and so has to be used at equivalent concentrations, the degree of branching is limited to low concentrations of multi-functional polymer meaning that truly-hyperbranched polymers are not accessible. In addition to this the process is limited to resonance stabilised, electron-deficient monomers as the thiol would quench non-stabilised radicals.[128] Finally, despite imparting thiol functionality, this is not universal as this is only imparted to an optimum of 50 % of the chains, as each chain transfer event will also terminate a chain with a hydrogen atom.

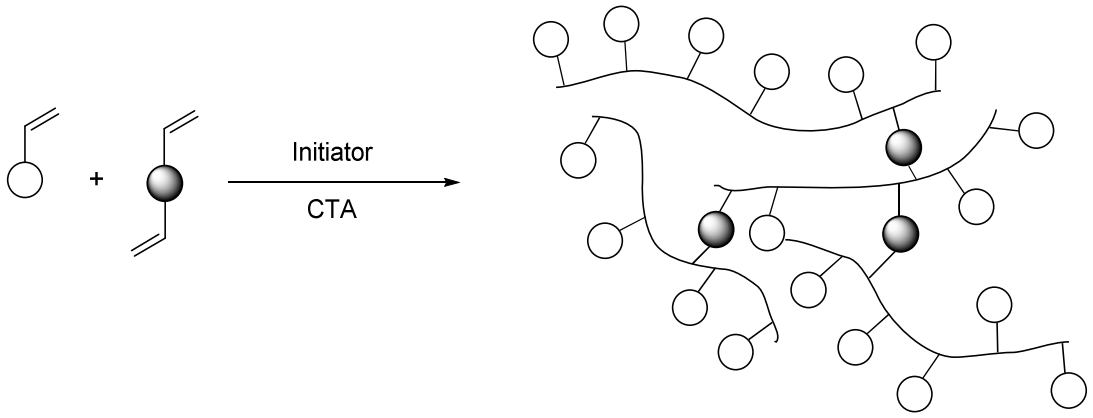

Scheme 1.8 ; Synthesis of branched vinyl polymer through copolymerisation of a mono- and a di-vinyl monomer and chain transfer agent through the Strathclyde route. Adapted from reference.[71]

Polymers produced by the "Strathclyde methodology" give poorly defined Đ and poor control over terminal functionality. In the work described in this thesis, a similar FRP process is used with the application of a catalytic chain transfer agent

(CCTA) to synthesise branched species with high vinyl functionality for application as cross-linking agents in wound care materials.

1.3.4 Branched polymers by CCTP

Investigations into the synthesis of branched polymer by CCTP began in the 1980s with the attempted homopolymerisation of triethylene glycol dimethacrylate (TEGDMA) using a cobalt(II) hematoporphyrin tetramethyl ester complex as the CCTA. Although soluble oligomers were observed, the resulting polymers were inconsistent and were not fully characterised.[130] This first attempt was followed by the filing of a patent in 1986 by Abbey using TEGDMA and a Co(II) catalyst *in situ,* unfortunately too much catalyst was used, resulting in mostly linear polymers.[38,131]

Over a decade later Guan published his first patent in this area for E.I. DuPont Nemours and company in 1998, detailing homopolymerisation of a multitude of different di- and tri-vinyl monomers as well as their copolymerisation with a range of different mono-vinyl monomers.[132] This was followed a number of years later by its publication in the academic literature, where the polymers produced were noted for their low solution viscosity, high vinyl group concentration and the monitoring of the molecular weight through multi-detector SEC, in particular viscometry.[133] A mechanism of trimerization followed by cascade branching was also proposed at the same time (**Scheme 1.9**). A subsequent paper showed good control over the process and topology through a directly proportional increase in the M_w of the polymers with increasing branching.[69]

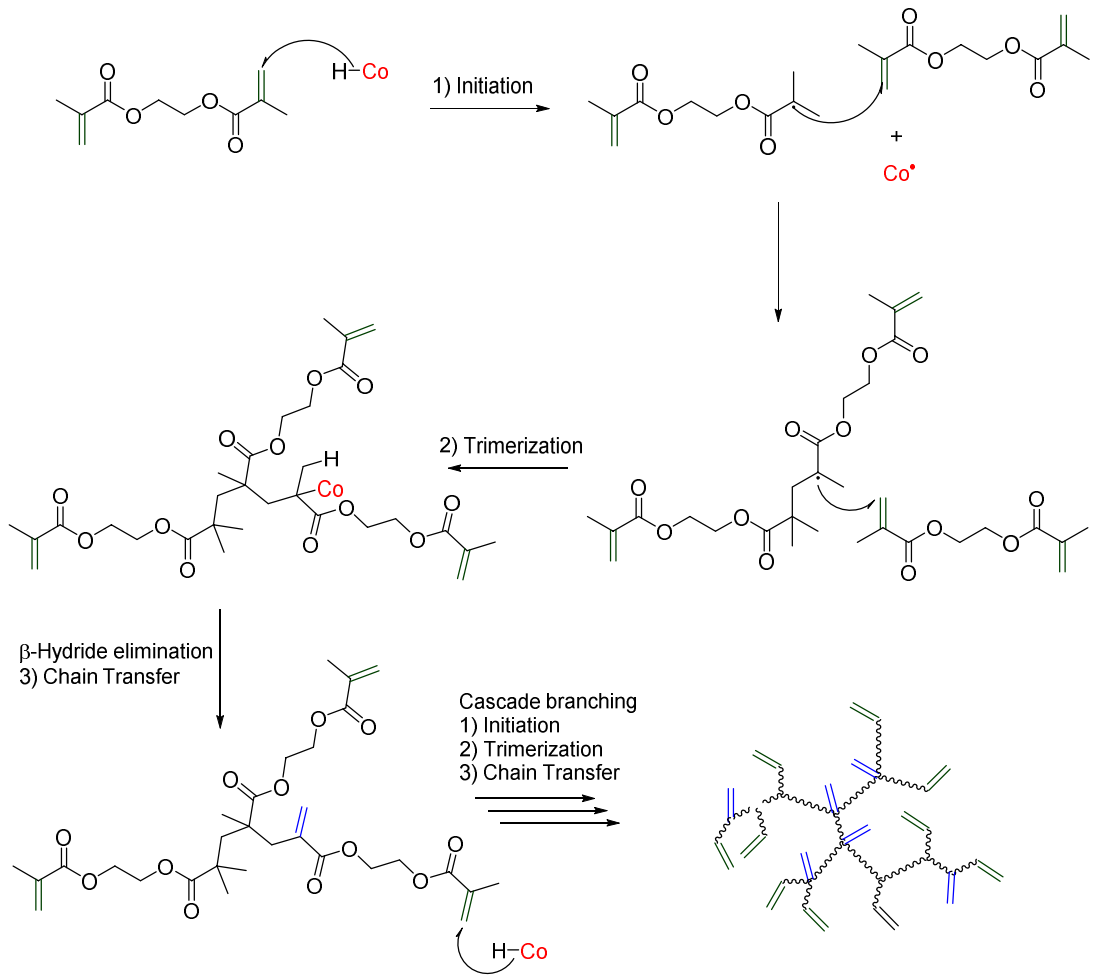

Scheme 1.9; Proposed mechanism for CCTP of EGDMA through cascade branching postulated by Guan,[133] leading to the formation of vinyl terminated polymers.

Work conducted around the same time by Sherrington *et al.* from the University of Strathclyde, Viscotek and Ineos Acrylics compared the 'Strathclyde methodology' to CCTP through the copolymerisation of MMA with tripropylene glycol diacrylate (TPGDA). This work showed that the polymers produced by CCTP increased in M_w with decreasing concentration of CCTA but the M_n did not. This, they reasoned, was evidence of backbiting rather than branching.[13] At a similar time a set of Russian papers were released in which a Co(II) prophyrin complex was used to inhibit the onset of the gel effect in the copolymerisation of styrene with dimethacrylates.[134] This was followed by an attempt to use the alkyl substituent chain length of the

methacrylate monomer to control polymerisations in bulk by hindering the radical chain end, this ultimately only ever produced uncontrolled reactions.[135,136]

Further investigations by Sherrington, comparing CCTP to the 'strathclyde methodology', concluded that the formation of insoluble polymers was due to the occurrence of backbiting cyclisation reactions, postulating that greater control was exhibited in the case of the 'strathclyde methodology'.[127] In this study the radius of gyration, g', was used to show the difference in branching, however, higher concentrations of divinyl monomer were used in the 'Strathclyde methodology' and so showing a higher degree of branching.

In 2006 Kurmaz published the homopolymerisation of EGDMA and other di-vinyl monomers by CCTP.[137] This work was subsequently affirmed by publications issued by Haddleton, McEwan, and Smeets. Haddleton *et al.* published the homopolymerisation of EGDMA followed by its functionalization by thiol Michael addition, confirming the presence of a significant degree of branching within these materials.[138] Smeets then published a similar study functionalising pEGDMA through reductive amination to form core-crosslinked, functionalised micelles.[139] Both of these pieces of work were accompanied by multi-detector SEC, indicating the formation of a high degree of branching, and, NMR and post-polymerisation functionalization indicating high concentrations of vinyl functionality.

1.4 Hydrogels

1.4.1 Definition and Classification

Hydrogels are swollen polymer networks derived from hydrophilic monomers which, can retain very large volumes of water relative to their weight, yet remain insoluble due to the presence of crosslinking; they also are characterised as being soft and rubbery (as opposed to brittle and glass-like), with high flexibility (strain at break) and low stiffness (modulus) in their material properties.[140-142] These cross-linkers can take one of two forms; chemical (or covalent) and physical crosslinking. In simple, single component networks (monoliths) chemical cross-linked systems are characterised as being tough (the ability to absorb relatively large amounts of energy without fracturing) with greater consistency yet no self-healing properties. Physical hydrogels are generally weaker due to being held together by inter-molecular forces such as; ionic, Van-der-Vaals and hydrogen bonding. However, physical gels have the capacity for greater stimuli responsive and self-healing behaviour.[143,144]

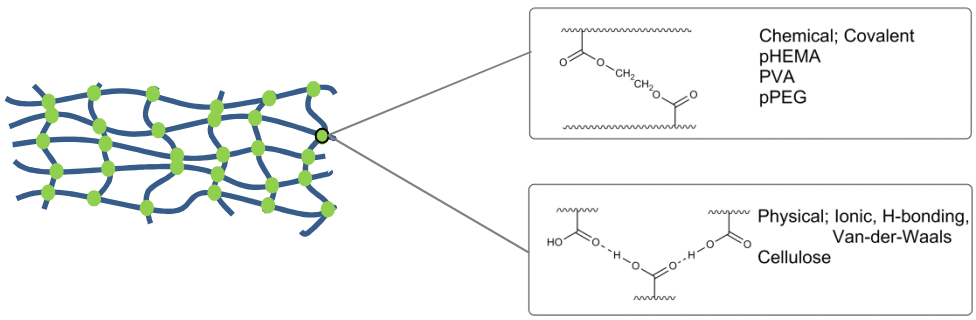

Figure 1.7; Categorisation of a hydrogel network (left) as either a chemically (top right) or a physically (bottom right) cross-linked network.

Hydrogels can be further defined according to the source of the monomeric units into natural or synthetic networks. Since their initial development, hydrogels have

been used in wound care dressings due to their abilities to absorb very large volumes of fluids and contain water soluble active ingredients for delivery.[141] The focus of this project has been the development of a hydrogel for the purposes of chronic wound care treatment.

1.4.2 Complex multi-component networks

Single network hydrogels characteristically have poor mechanical properties and slow response to swelling, one method for enhancing these characteristics is to form 'alloys' of different networks or inter-penetrating networks (IPNs). IPNs are combinations of two (or more) cross-linked polymer networks, where at least one of the networks is cross-linked or polymerised in the presence of the other.[145-147] IPNs can be defined by their method of synthesis into; simultaneous IPNs – synthesis simultaneously by orthogonal routes, or sequential IPNs – where a single network is swollen into a solution, containing the second network's monomer, initiator with or without cross-linker prior to cure.[145-148] When a cross-linker is present for each network, then a fully-IPN results, if one network is without a cross-linker, the network is defined as being a semi-IPN as the linear polymers are considered to be embedded in the second network.[149,150] These linear polymers can in some cases be further selectively cross-linked to form fully-IPN.[151,152] There have been a wide range of IPNs developed utilising natural polymers including: alginate,[153-155] chitosan,[156-158] starch,[159,160] cellulose,[161,162] gelatin,[163,164] and silk fibrin among many others,[165,166] however, these materials demonstrate a high degree of variability on the molecular level leading to them being difficult to

reproduce consistently. These materials lie outside of the field of interest of this thesis, as this investigation is concerned with purely synthetic IPNs.

Synthetic IPNs are made up of two synthetic networks, unlike networks that include natural species, these materials are entirely reproducible, and can be tailor designed and made.[145] Natural hydrogels suffer from variations in properties due to the inherent inconsistency of the monomeric units with respect to their structure. Synthetic IPNs can be divided into two categories according to composition; entirely non-ionic networks,[167-169] and ionic IPNs, where one or both of the networks are cationic,[170,171] anionic[172,173] or ampholytic.[174,175] Synthetic networks have seen applications in a variety of fields.

Both synthetic and natural IPNs have seen application in the field of wound care dressings, IPNs with natural polymers make up the massive majority of these materials, however, these sit outside of the remit of this work. Synthetic IPNs have seen some development over the past two decades both industrially,[176-179] and academically,[180-189] these materials have focused upon having a mildly hydrophobic layer and a hydrophilic layer,[180,187] with many attempting to incorporate environmental stimuli responsive behaviour such as pH, temperature[181,182] or both.[183,184] Most of the networks developed involve the use of a polyurethane layer due to the ability to form mechanically tuneable and biocompatible sheets, allowing for easy, sequential synthesis of an IPN through the use of polyurethane sheets as the first network.[176,177,181-185,190] Work in this thesis has attempted to take this premise in combination with the biocompatible monomer 2-acrylamido-s-

methylpropane sulfonic acid (AMPS) to form mechanically robust, mildly adhesive, rapidly absorbent materials for a wound care application.

1.4.3 Branched polymers in hydrogels

Branched polymers are highly appealing species for inclusion into networks, this can be attributed to their simple one pot synthesis, lack of chain entanglements, and, high concentration of functional groups at the periphery, making them suitable for further reaction and cross-linking.[191] Branched polymers can be incorporated into hydrogels as macromonomers through two mechanisms; physical non-covalent attachment to form a supramolecular network,[192] or through covalent bonding, to act as permanent cross-linkers within an extended network.

Physical 'supramolecular networks' have been widely researched, affording the benefits of being easily self-healing[193-196] and stimuli-responsive[197-199] due to the transient nature of the cross-linking system which can occur through any combination of; hydrophobic,[200] hydrogen bonding,[194] electrostatic interactions,[201] host-guest interactions[202] and metal coordination.[203] These materials have seen widespread research in the biomedical field[204] as well as in drug delivery,[205] 3D printing,[206] oil recovery[207] and tissue engineering.[208]

Development into the covalent inclusion of hyperbranched polymers into polymeric networks has seen extensive application-driven research.[209] Most of the research has centred upon biomedical applications such as tissue engineering,[210-213] drug delivery,[210] dental composites[214] and biodegradable materials.[215-217] Due to the ease of synthesis of hyperbranched polymers (relative to dendrimers) a number of commercial hyperbranched polymers have been developed and much of the recent

research has centred upon the modification and application of these polymers. Some of the favoured products include; Boltorn™ – a polyester,[211,212,214,218] Hybrane™ – a polyesteramide,[211,212,214] polyglycerol – a polyether[210] and Epox™ – a polyamide.[214] Of particular interest to this work are examples making use of either implicit vinyl functionality[219] or branched polymers modified to give vinyl functionality,[210-214] and subsequently applied in free radical polymerisation.

In 2001 the research group of Carl-Eric Wilen investigated the copolymerisation of unsaturated hyperbranched polyesters with styrene, vinyl acetate and methyl methacrylate respectively. In this work it was found that due to solubility issues vinyl acetate forms a biphasic system resulting in a lack of gelation, styrene forms stars and weak gels, and, methyl methacrylate forms entangled and cross-linked networks at higher concentrations of branched polymer than conventional cross-linker. This was attributed to the lower solution viscosity caused by the branched polymers, also allowing for a higher degree of conversion prior to gelation.[219] In 2006 Hennink *et al.* functionalised hyperbranched polyglycerol with methacryoyl groups and compared the effects of photo and thermal curing systems upon these networks, finding excellent conversion and tuneable mechanical properties relative to the degree of functionalization.[210] A similar strategy was employed by Peinado *et al.* in the photopolymerisation of functionalised polyesters and polyesteramides to give methacrylate based networks with tuneable mechanical properties.[211,212] Khademhosseini *et al.* tuned the functionality of polyesters in homo-photopolymerisation to yield tuneable morphology and structural properties for the controlled encapsulation and release of model drug dexamethasone acetate.[213]

Most of these techniques require the post-synthetic modification of branched polymers to give vinyl-terminated species. One of the benefits of CCTP is that highly branched polymers can be produced in a one-pot synthesis with ω-vinyl end group functionality at very high fidelity.[133,138] The work in this thesis aims to harness the techniques described above to incorporate highly branched CCTP produced methacrylate polymers into hydrogels as novel gelators.

1.5 Introduction to Hydrogels in wound healing devices

1.5.1 Wound Healing Cycle

A wound can be defined as a situation when the integrity of any tissue is compromised, whether that be a simple break in the epithelial layer or deeper damage to subcutaneous tissue such as muscle, vessels, organs and bone.[220] Wounds can follow two principle routes – the acute wound healing process through which a wound will repair itself, or the chronic process whereby the wound fails to progress through the regular stages of the healing process.

1.5.2.1 Acute wounds

Acute wounds are often classified as taking 5-10 days, or within 30 days to heal and result in both functional and anatomical restoration. These wounds are conventionally caused by loss of tissue or surgical procedure.[221,222]

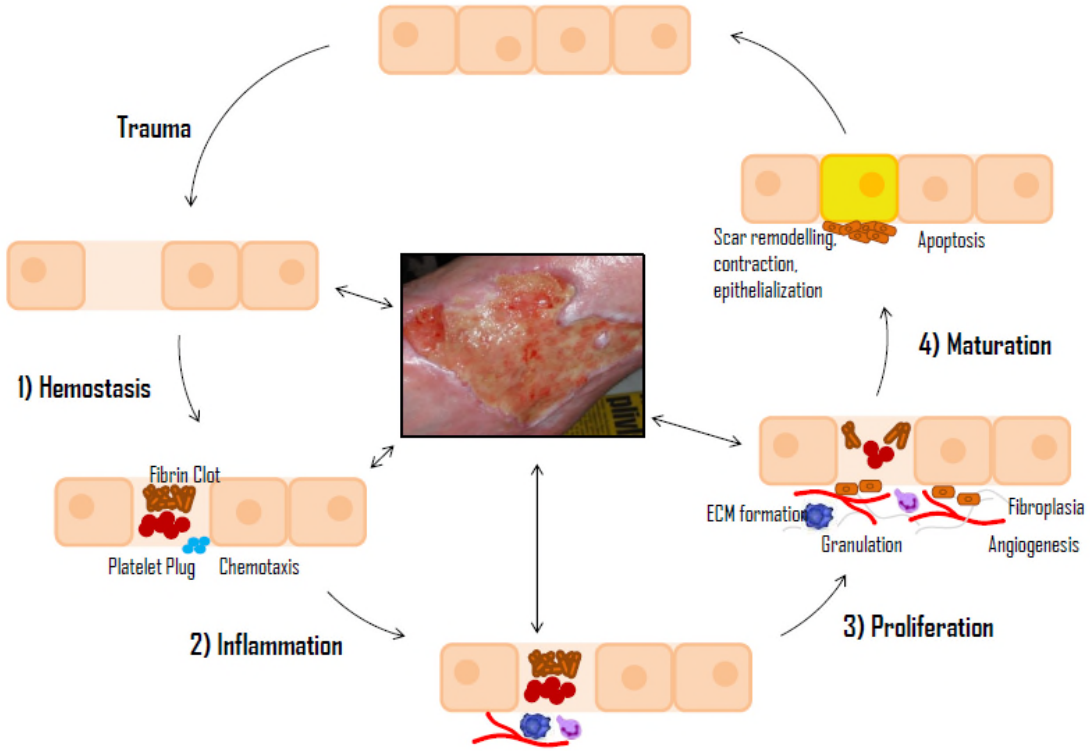

Figure 1.8; Acute wound healing cycle going through the phases of hemostasis, inflammation, proliferation and maturation after trauma with a chronic wound shown.[223-225]

The wound healing process is a continuous process divided up into arbitrary stages to enable identification of the physiological processes occurring in the damaged tissue.[226] The process involves a cascade of precisely regulated steps, with chemical and biological species appearing and disappearing at different stages.[227,228] The processes are combined into four time-dependent phases: (i) coagulation and haemostasis, (ii) inflammation, (iii) proliferation and (iv) the extended process of wound remodelling or maturation (**Figure 1.8**).

Haemostasis and coagulation take place in the wound immediately after the event of injury, with the primary aim of preventing exsanguination through the creation of a clot.[220] Initially an insoluble plug made of fibrin is deposited; this process is regulated by endothelial cells and thrombocytes to facilitate later stages of the

process,[221,229-231] and is aided by temporary vasoconstriction prior to passive relaxation by hypoxia and acid hydrolysis.[232] When platelets come into contact with exposed collagen, clotting factors are released which cause aggregation of fibrin, fibronectin, vitronectin and thrombospondin. This clot later forms the matrix necessary for cell migration.[221,230,231,233]

Inflammation aims to form an immune barrier against the invasion of microorganisms and is divided into an early (24 - 36 hours) and later phase (48 - 72 hours).[220] In the early phase, neutrophil infiltration acts to prevent infection through phagocytosis in order to maintain a bacterial balance in the wound site. Neutrophils are attracted after injury by chemoattractive agents released by platelets and bacteria, whereupon they adhere to endothelial cells, moving with the blood flow and releasing proteolytic enzymes and oxygen derived free-radicals. Once all contamination has been removed, neutrophils are extruded from the wound site as slough and any remaining cellular fragments are broken down by macrophages. In the later phase, macrophages are attracted to the wound site by chemoattractive agents and continue the process of phagocytosis. Macrophages also act as regulating cells, releasing tissue growth factors and other mediators, encouraging the activation of fibroblasts and endothelial cells. Lymphocytes are then attracted and serve an important role in collagenase regulation for collagen development and the construction (and degradation) of the extracellular matrix.

Proliferation is primarily concerned with tissue repair, lasting about two weeks from the third day of repair. During this phase a newly synthesised extracellular matrix is deposited to replace the scab made of fibrin and fibronection, whilst at

the same time undergoing fibroblast migration. This manifests itself as extensive tissue granulation, but there are a number of processes occuring, as briefly discussed herein. Fibroblast migration occurs through the proliferation of fibroblasts to produce matrix proteins. Within a week enough ECM has been generated and fibroblasts change phenotype to myofibroblasts and extend pseudopodia to attach to fibronectin and collagen, causing wound contraction followed by their apoptosis. Collagens, synthesised by the fibroblasts at this stage, impart structure and rigidity within the ECM and are crucial to the final stage of remodelling. Angiogenesis and remodelling is the process of growth and development of blood vessels and tissue within the ECM. This occurs through the creation of chemical concentration gradients so that the cells can move down concentration gradients through chemotaxis. Cell mobility in this fashion requires three actions: protrusion at the cell front, adhesion to attach the actin cytoskeleton to substratum and finally traction allowing the cell to be propelled forward. The final component of proliferation is epithelialisation – the growth of the external skin layer through the migration of cells across the surface, followed by rapid mitosis to create a new skin barrier on top of the wound site.

The final stage of recovery is the remodelling or maturation stage, this phase can last up to 2 years (sometimes longer) and is responsible for the development of the new epithelium and scar tissue. This process leads to an increase in the diameter of collagen bundles, degradation of hyalauronic acid and fibronectin, causing an increase in the tensile strength of the ECM. The matrix and collagen are gradually remodelled from a highly disorganised, mechanically weak network through cyclic degradation and synthesis to create an organised structure with higher density.

Capillary growth continues and the density of fibroblasts and macrophages decreases by apoptosis until a conclusion of steady state is reached at which blood flow is reduced, cell count is diminished and a functional scar tissue covers the wound site at roughly 80 % functionality relative to the original tissue.

1.5.2.2 Chronic wounds

Chronic wounds develop as a result of the normal (acute) wound care processes breaking down, with a simple definition as being a break in the skin of long duration (> 6 weeks) or frequent recurrence.[234-236] With chronic wounds this process is prolonged at one of these stages – usually inflammation - and the wound ceases to heal. This is often due to infection, tissue hypoxia, release of excessive amounts of inflammatory cytokines or, large levels of exudates, and is often accompanied by further underlying medical issues.[220,237] These conditions cause the wound to regress and the inflammatory stage to be exaggerated, causing the perpetuation of a non-healing state. These wounds proceed in an uncontrolled manner and frequently lead to poor functional and anatomical recovery with relapse being commonplace.[220,238]

1.5.3 Hydrogels as chronic wound care dressings

1.5.3.1 Chronic wound care

In 1960, after millennia of ignorance,[239] the western world accepted that a moist environment was critical for wound recovery.[240] Moisture-retentive occlusive wound-dressing environments were found to have twice the healing rate as wounds left exposed to air.[240] In contrast it was found that dry wound healing environments caused further significant tissue death.[241] Since the seminal

publication by Winter, further, overwhelming evidence has accumulated and a number of polymer based wound dressings have been designed and commercialised to manage the wound environment (**Table 1.2**).[239,242] These dressings are shown to increase the rate and degree of re-epithelialisation,[243] stimulate collagen synthesis,[244] promote angiogenesis[245] and relieve pain.[246,247] Occlusive dressings create an effective barrier against external contaminations and the ingress of foreign bodies. This significantly reduces infection rates relative to non-occlusive dressings,[248] with some materials having the added benefit of reducing the pH of wound bed, therefore, making it inhospitable to microbial growth.[243]

The ideal chronic wound dressing would be able to: remove excess exudate, maintain a moist environment, protect against contaminant, cause no trauma upon removal, leave no debris in the wound bed, relieve pain, provide thermal insulation and induce no allergic reactions.[249,250] Due to the complexity and range of types of chronic wound, there is no single 'ideal wound dressing' material, however, a range of different materials have been developed, each with a distinct profile for the ideal environment of application, duration and weaknesses (**Table 1.2**).

Product	Advantages	Disadvantages	Indications	Comment
Gauzes	Inexpensive, Accessible	Drying, Poor barrier	Packing deep wounds	Change every 12-24 hours
Films	Moisture-retentive Transparent Semiocclusive Protects wound from contamination	No Absorption Fluid trapping Skin stripping	Wounds with minimal exudate Secondary dressing	Can leave in place up to 7 days or until fluid leaks
Hydrogels	Moisture-retentive Nontraumatic removal Pain relief	May overhydrate	Dry wounds Painful wounds	Change every 1-3 days
Hydrocolloids	Long wear-time Absorbent Occlusive Protects wound from contamination	Opaque Fluid trapping Skin stripping Malodorous discharge	Wounds with light to moderate exudate	Can leave in place up to 7 days or until fluid leaks
Alginates and hydrofibers	Highly absorbent Hemostatic	Fibrous debris Lateral wicking (alginates only)	Wounds with moderate to heavy exudate Mild hemostasis	Can leave in place until soaked with exudate
Foams	Absorbent Thermal insulation Occlusive	Opaque Malodorous discharge	Wounds with light to moderate discharge	Change every 3 days

Table 1.2; Summary of basic wound dressings. Adapted from reference.[236]

1.5.3.2 Hydrogels in chronic wound care

Hydrogels are defined as polymer networks swollen into an aqueous solvent, as a direct result of this composition they are intrinsically capable of maintaining a moist wound-healing environment.[236,251] These materials are reported to be suitable for wounds with low levels or no exudate such as: necrotic wounds, pressure ulcers, burn wounds and dry chronic wounds.[252,253] Use in wounds with high levels of exudate can cause maceration of the damaged tissue (peri-wound tissue).[254]

Hydrogels promote autolytic-debridement (a non-invasive removal of damaged tissue) of slough and necrotic tissue through the rehydration and subsequent separation of the damaged material from healthy material, this means debridement can occur in patients where a 'sharp' debridement is not feasible.[255] The low adhesion associated with hydrogels allows for easy, painless removal with minimal trauma to the wound bed. Hydrogels also benefit from having a cooling effect, which is reported to give significant pain relief.[256,257] Some examples of commercially available hydrogels include; Intrasite™, Nu-gel™, Aquaform™ polymers, sheet dressings, hydrogel impregnated gauze and water based gels.

In this thesis a number of monolithic networks are studied and the effects of the addition of branched polymers synthesised by CCTP are monitored with respect to the material properties of the resulting networks. Beyond this a synthetic IPN is studied in terms of its material properties with a wound care application in mind.

1.6 *References*

(1) Odian, G. In *Principles of Polymerization*; 4th ed.; John Wiley & Sons: **2004**.

(2) Flory, P. J. *J. Am. Chem. Soc.* **1937**, *59*, 241.

(3) Jenkins, A. D.; Kratochvíl, P.; Stepto, R. F. T.; Suter, U. W. *Pure Appl. Chem.* **1996**, *68*, 2287.

(4) Berzelius, J.; Jahres-Bericht: **1832**, p 44.

(5) Braun, D. *Int. J. Polym. Sci.* **2009**, *2009*.

(6) Staudinger, H. *Ber. Dtsch. Chem. Ges.* **1920**, *53*, 1073.

(7) Staudinger, H.; Brunner, M.; Frey, K.; Garbsch, P.; Signer, R.; Wehrli, S. *Ber. Dtsch. Chem. Ges.* **1929**, *62*, 241.

(8) Staudinger, H.; Kohlschütter, H. *Ber. Dtsch. Chem. Ges.* **1931**, *64*, 2091.

(9) McEwan, K., PhD Thesis, **2012**.

(10) Chisholm, M.; Hudson, N.; Kirtley, N.; Vilela, F.; Sherrington, D. C. *Macromolecules.* **2009**, *42*, 7745.

(11) Norrish, R.; Brookman, E. *Proc. R. Soc. London, Ser. A* **1939**, 147.

(12) Trommsdorff, V. E.; Köhle, H.; Lagally, P. *Makromol. Chem.* **1948**, *1*, 169.

(13) Costello, P. A.; Martin, I. K.; Slark, A. T.; Sherrington, D. C.; Titterton, A. *Polymer* **2002**, *43*, 245.

(14) Gridnev, A. *J. Polym. Sci., Part A: Polym. Chem.* **2000**, *38*, 1753.

(15) Gridnev, A. A.; Ittel, S. D. *Chem. Rev.* **2001**, *101*, 3611.

(16) Smirnov, B. R.; Belgovskii, I. M.; Ponomarev, G. V.; Marchenko, A. P.; Enikolopyan, N. S. *Doklady Akademii Nauk SSR*

1980, *254*, 127.

(17) Enikolopyan, N. S.; Smirnov, B. R.; Ponomarev, G. V.; Belgovskii, I. M. *J Polym Chem Polym Chem Ed* **1981**, *19*, 879.

(18) Smirnov, B. R.; Morozova, I. S.; Pushchaeva, l. M.; Marchenko, A. P.; Enikolopyan, N. S. *Dokl. Akad. Nauk. SSSR.* **1980**, *253*, 609.

(19) Smirnov, B. R.; Morozova, I. S.; Marchenko, A. P.; Markevich, M. A.; Pushchaeva, l. M.; Enikolopyan, N. S. *Dokl. Akad. Nauk. SSSR.* **1980**, *253*, 891.

(20) Davis, T. P.; Haddleton, D. M.; Richards, S. N. *J. Macromol. Sci. C* **1994**, *34*, 243.

(21) Haddleton, D. M.; Maloney, D. R.; Suddaby, K. G.; Muir, A. V. G.; Richards, S. N. *Macromol. Symp.* **1996**, *111*, 37.

(22) Karmilova, L. V.; Ponomarev, G. V.; Smirnov, B. R.; Belgovskii, I. M. *Usp. Khim.* **1984**, *53*, 223.

(23) Belgovskii, I. M.; Gridnev, A. A.; Marchenko, A. P.; Smirnov, B. R.; Enikolopov, N. S. Russ. Patent 940,487, **1980**.

(24) Gridnev, A. *Polym. Sci. USSR* **1989**, *31*, 2369.

(25) Gridnev, A.; Lampeka, Y. D.; Smirnov, B.; Yatsimirskii, K. *Theor. Exp. Chem.* **1987**, *23*, 293.

(26) Goncharov, A.; Gridnev, A.; Lampeka, Y. D.; Gavrish, S. *Theor. Exp. Chem.* **1989**, *25*, 642.

(27) Sanayei, R. A.; O'Driscoll, K. F. *J. Polym. Sci. A Polym. Chem.* **1989**, *26*, 1137.

(28) Smirnov, B. R.; Marchenko, A. P.; Korolev, G. V.; Bel'govskii, I. M.; Yenikolopyan, N. S. *Polym. Sci. USSR* **1981**, *23*, 1158.

(29) Enikolopov, N. S.; Korolev, G. V.; Marchenko, A. P.; Ponomarev, G. V.; Smirnov, B. R.; Titov, V. I. Russ. Patent 664,434, **1980**.

(30) Janowicz, A. H.; Melby, L. R. US4680352 A, **1987**.

(31) Janowicz, A. H.; Google Patents: US4886861 A, **1987**.

(32) Melby, L. R.; Janowicz, A. H.; Ittel, S. D. DE3665868, **1986**.

(33) Melby, L. R.; Janowicz, A. H.; Ittel, S. D. DE3667062, **1986**.

(34) Smirnov, B. R.; plotnikov, V. D.; Ozerkovskii, B. V.; Roshchupkin, V. P.; Enikolopyan, N. S. *Vysokomol Soedin A+* **1981**, *23*, 2588.

(35) Darmon, M. J.; Berge, C. T.; Antonelli, J. A. US5264530 A, **1993**.

(36) Cacioli, P.; Hawthorne, D.; Laslett, R.; Rizzardo, E.; Solomon, D. *J. Macromol. Sci. Chem.* **1986**, *23*, 839.

(37) Moad, C. L.; Moad, G.; Rizzardo, E.; Thang, S. H. *Macromolecules.* **1996**, *29*, 7717.

(38) Lin, J. C.; Abbey, K. J. US4680354, **1987**.

(39) Antonelli, J. A.; Scopazzi, C. US5310807, **1981**.

(40) Slavin, S.; Haddleton, D. M.; Appl., P. I., Ed. 2011.

(41) Lynch, C. P.; Irvine, D. J.; Beverly, G. M. WO9804603, **1998**.

(42) Heuts, J. P. A.; Forster, D. J.; Davis, T. P. *Macromol. Rapid Comm.* **1999**, *20*, 299.

(43) Gridnev, A.; Belgovskii, I.; Yenikolopyan, N. *Vysokomol Soedin B+* **1986**, *28*, 85.

(44) Burczyk, A. F.; O'Driscoll, K. F.; Rempel, G. L. *J Polym Chem Polym Chem Ed* **1984**, *22*, 3255.

(45) Schrauzer, G. N. *Acc. Chem. Res.* **1968**, *1*, 97.

(46) Chao, T.-H.; Espenson, J. H. *J. Am. Chem. Soc.* **1978**, *100*, 129.

(47) Heuts, J. P. A.; Roberts, G. E.; Biasutti, J. D. *Aust. J. Chem.* **2002**, *55*, 381.

(48) Gridnev, A. A. *Polym J* **1992**, *24*, 613.

(49) Roberts, G. E.; Heuts, J. P.; Davis, T. P. *Macromolecules.* **2000**, *33*, 7765.

(50) Roberts, G. E.; Davis, T. P.; Heuts, J. P.; Ball, G. E. *Macromolecules.* **2002**, *35*, 9954.

(51) Gridnev, A. A.; Ittel, S. D.; Wayland, B. B.; Fryd, M. *Organometallics* **1996**, *15*, 5116.

(52) Morrison, D. A.; Davis, T. P.; Heuts, J.; Messerle, B.; Gridnev, A. A. *J. Polym. Sci., Part A: Polym. Chem.* **2006**, *44*, 6171.

(53) Woska, D. C.; Xie, Z. D.; Gridnev, A. A.; Ittel, S. D.; Fryd, M.; Wayland, B. B. *J. Am. Chem. Soc.* **1996**, *118*, 9102.

(54) Gridnev, A. A.; Ittel, S. D.; Fryd, M.; Wayland, B. B. *Organometallics* **1993**, *12*, 4871.

(55) Suddaby, K. G.; Haddleton, D. M.; Hastings, J. J.; Richards, S. N.; O'Donnell, J. P. *Macromolecules.* **1996**, *29*, 8083.

(56) Mayo, F. R. *J. Am. Chem. Soc.* **1943**, *65*, 2324.

(57) P. Davis, T.; D. Zammit, M.; P.A. Heuts, J.; Moody, K. *Chem. Commun.* **1998**, 2383.

(58) Smirnov, B.; Pushchayeva, L.; Plotnikov, V. *Polym. Sci. USSR* **1989**, *31*, 2607.

(59) Suddaby, K. G.; Maloney, D. R.; Haddleton, D. M. *Macromolecules.* **1997**, *30*, 702.

(60) Heuts, J. P. A.; Davis, T. P.; Russell, G. T. *Macromolecules.* **1999**, *32*, 6019.

(61) Heuts, J. P. A.; Forster, D. J.; Davis, T. P.; Yamada, B.; Yamazoe, H.; Azukizawa, M. *Macromolecules.* **1999**, *32*, 2511.

(62) Smeets, N. M. B.; Jansen, T. G. T.; Sciarone, T. J. J.; Heuts, J. P. A.; Meuldijk, J.; Van Herk, A. M. *J. Polym. Sci., Part A: Polym. Chem.* **2010**, *48*, 1038.

(63) Haddleton, D. M.; Maloney, D. R.; Clarke, K. G. S. A.; Richards, S. N. *Polymer* **1997**, *38*, 6207.

(64) Ishigaki, H.; Okada, H.; Suyama, S. JP03212402A, **1991**.

(65) Nagashima, M.; Kazama, H. JP11071220A, **1999**.

(66) Engelis, N. G.; Anastasaki, A.; Nurumbetov, G.; Truong, N. P.; Nikolaou, V.; Shegiwal, A.; Whittaker, M. R.; Davis, T. P.; Haddleton, D. M. *Nat Chem* **2016**, *advance online publication*.

(67) Haddleton, D. M.; Topping, C.; Hastings, J. J.; Suddaby, K. G. *Macromol. Chem. Phys.* **1996**, *197*, 3027.

(68) Haddleton, D. M.; Topping, C.; Kukulj, D.; Irvine, D. *Polymer* **1998**, *39*, 3119.

(69) Guan, Z. *J. Polym. Sci., Part A: Polym. Chem.* **2003**, *41*, 3680.

(70) Voit, B. I.; Lederer, A. *Chem. Rev.* **2009**, *109*, 5924.

(71) England, R. M.; Rimmer, S. *Polym. Chem.* **2010**, *1*, 1533.

(72) Bruchmann, B.; Königer, R.; Renz, H. *Macromol. Symp.* **2002**, *187*, 271.

(73) Bruchmann, B. *Macromol. Mater. Eng.* **2007**, *292*, 981.

(74) Mulkern, T.; Tan, N. B. *Polymer* **2000**, *41*, 3193.

(75) Hong, Y.; Coombs, S.; Cooper-White, J.; Mackay, M.; Hawker, C.; Malmström, E.; Rehnberg, N. *Polymer* **2000**, *41*, 7705.

(76) Chen, S.; Zhang, X.-Z.; Cheng, S.-X.; Zhuo, R.-X.; Gu, Z.-W. *Biomacromolecules* **2008**, *9*, 2578.

(77) Wang, Y.; Grayson, S. M. *Adv. Drug. Deliver. Rev.* **2012**, *64*, 852.

(78) Boas, U.; Heegaard, P. M. *Chem. Soc. Rev.* **2004**, *33*, 43.

(79) Svenson, S.; Tomalia, D. A. *Adv. Drug. Deliver. Rev.* **2012**, *64*, 102.

(80) Flory, P. J. *J. Am. Chem. Soc.* **1952**, *74*, 2718.

(81) Komber, H.; Ziemer, A.; Voit, B. *Macromolecules.* **2002**, *35*, 3514.

(82) Segawa, Y.; Higashihara, T.; Ueda, M. *Polym. Chem.* **2013**, *4*, 1746.

(83) Carlmark, A.; Malmström, E.; Malkoch, M. *Chem. Soc. Rev.* **2013**, *42*, 5858.

(84) Konkolewicz, D.; Monteiro, M. J.; Perrier, S. b. *Macromolecules.* **2011**, *44*, 7067.

(85) Hoogenboom, R. *Angew. Chem. Int. Ed.* **2010**, *49*, 3415.

(86) Peleshanko, S.; Tsukruk, V. V. *Prog. Polym. Sci.* **2008**, *33*, 523.

(87) Huang, Y.; Wang, D.; Zhu, X.; Yan, D.; Chen, R. *Polym. Chem.* **2015**, *6*, 2794.
(88) Flory, P. J. *J. Am. Chem. Soc.* **1939**, *61*, 3334.
(89) Flory, P. J. *J. Am. Chem. Soc.* **1940**, *62*, 2261.
(90) Flory, P. J. *J. Am. Chem. Soc.* **1941**, *63*, 3083.
(91) Flory, P. J.; Rehner, J. *J. Chem. Phys.* **1943**, *11*, 521.
(92) Flory, P. J. *J. Am. Chem. Soc.* **1956**, *78*, 5222.
(93) Jacobson, H.; Beckmann, C. O.; Stockmayer, W. H. *J. Chem. Phys.* **1950**, *18*, 1607.
(94) Landin, D.; Macosko, C. *Macromolecules.* **1988**, *21*, 846.
(95) Li, W.-H.; Hamielec, A.; Crowe, C. *Polymer* **1989**, *30*, 1513.
(96) Storey, B. T. *J. Polym. Sci., Part A.* **1965**, *3*, 265.
(97) Walling, C. *J. Am. Chem. Soc.* **1949**, *71*, 1930.
(98) Yoshimura, M.; Mikawa, H.; Shirota, Y. *Macromolecules.* **1978**, *11*, 1085.
(99) Hild, G.; Okasha, R. *Makromol. Chem.* **1985**, *186*, 93.
(100) Hild, G.; Okasha, R. *Makromol. Chem.* **1985**, *186*, 389.
(101) Frechet, J. M.; Henmi, M.; Gitsov, I.; Aoshima, S. *Science* **1995**, *269*, 1080.
(102) Müller, A. H.; Yan, D.; Wulkow, M. *Macromolecules.* **1997**, *30*, 7015.
(103) Puskas, J. E.; Grasmüller, M. In *Macromol. Symp.*; Wiley Online Library: 1998; Vol. 132, p 117.
(104) Simon, P. F.; Müller, A. H. *Macromolecules.* **2001**, *34*, 6206.
(105) Simon, P. F.; Radke, W.; Müller, A. H. *Macromol. Rapid Comm.* **1997**, *18*, 865.
(106) Sakamoto, K.; AIMIYA, K.; Kira, M. *Chem. Lett.* **1997**, *1997*, 1245.
(107) Hawker, C. J.; Frechet, J. M.; Grubbs, R. B.; Dao, J. *J. Am. Chem. Soc.* **1995**, *117*, 10763.
(108) Weimer, M. W.; Fréchet, J. M.; Gitsov, I. *J. Polym. Sci., Part A: Polym. Chem.* **1998**, *36*, 955.
(109) Matyjaszewski, K.; Nakagawa, Y.; Gaynor, S. G. *Macromol. Rapid Comm.* **1997**, *18*, 1057.
(110) Carter, S.; Rimmer, S.; Sturdy, A.; Webb, M. *Macromol. Biosci.* **2005**, *5*, 373.
(111) Wang, Z.; He, J.; Tao, Y.; Yang, L.; Jiang, H.; Yang, Y. *Macromolecules.* **2003**, *36*, 7446.
(112) Tao, Y.; He, J.; Wang, Z.; Pan, J.; Jiang, H.; Chen, S.; Yang, Y. *Macromolecules.* **2001**, *34*, 4742.
(113) Niu, A.; Li, C.; Zhao, Y.; He, J.; Yang, Y.; Wu, C. *Macromolecules.* **2001**, *34*, 460.
(114) Gaynor, S. G.; Edelman, S.; Matyjaszewski, K. *Macromolecules.* **1996**, *29*, 1079.
(115) Matyjaszewski, K.; Pyun, J.; Gaynor, S. G. *Macromol. Rapid Comm.* **1998**, *19*, 665.
(116) Cheng, C.; Wooley, K. L.; Khoshdel, E. *J. Polym. Sci., Part A: Polym. Chem.* **2005**, *43*, 4754.
(117) Carter, S.; Hunt, B.; Rimmer, S. *Macromolecules.* **2005**, *38*, 4595.

(118) Rimmer, S.; Carter, S.; Rutkaite, R.; Haycock, J. W.; Swanson, L. *Soft Matter* **2007**, *3*, 971.

(119) Lovell, P.; Shah, T.; Heatley, F. *Polym. Commun.* **1991**, *32*, 98.

(120) Ahmad, N. M.; Charleux, B.; Farcet, C.; Ferguson, C. J.; Gaynor, S. G.; Hawkett, B. S.; Heatley, F.; Klumperman, B.; Konkolewicz, D.; Lovell, P. A. *Macromol. Rapid Comm.* **2009**, *30*, 2002.

(121) Liu, J.; Wang, Y.; Fu, Q.; Zhu, X.; Shi, W. *J. Polym. Sci., Part A: Polym. Chem.* **2008**, *46*, 1449.

(122) Sarker, P.; Ebdon, J. R.; Rimmer, S. *Macromol. Rapid Comm.* **2006**, *27*, 2007.

(123) Isaure, F.; Cormack, P. A.; Sherrington, D. C. *J. Mater. Chem.* **2003**, *13*, 2701.

(124) Slark, A. T.; Sherrington, D. C.; Titterton, A.; Martin, I. K. *J. Mater. Chem.* **2003**, *13*, 2711.

(125) Isaure, F.; Cormack, P. A.; Sherrington, D. C. *Macromolecules.* **2004**, *37*, 2096.

(126) O'brien, N.; McKee, A.; Sherrington, D.; Slark, A.; Titterton, A. *Polymer* **2000**, *41*, 6027.

(127) Camerlynck, S.; Cormack, P. A. G.; Sherrington, D. C.; Saunders, G. *J. Macromol. Sci. B.* **2005**, *44*, 881.

(128) Baudry, R.; Sherrington, D. *Macromolecules.* **2006**, *39*, 1455.

(129) Liu, Y.; Haley, J. C.; Deng, K.; Lau, W.; Winnik, M. A. *Macromolecules.* **2008**, *41*, 4220.

(130) Golikov, I.; Semyannikov, V.; Mogilevich, M. *Vysokomol Soedin B+* **1985**, *27*, 304.

(131) Abbey, K. J. US4608423, **1986**.

(132) Guan, Z. US5767211, **1998**.

(133) Guan, Z. *J. Am. Chem. Soc.* **2002**, *124*, 5616.

(134) Kurmaz, S. V.; Perepelitsina, E. O.; Bubnova, M. L.; Estrina, G. A.; Roshchupkin, V. P. *Mendeleev Commun.* **2002**, *12*, 21.

(135) Kurmaz, S. V.; Perepelitsina, E. O.; Bubnova, M. L.; Estrina, G. A. *Mendeleev Commun.* **2004**, *14*, 125.

(136) Kurmaz, S.; Bubnova, M.; Perepelitsina, E.; Estrina, G. *Polym. Sci. Ser. A.* **2006**, *48*, 696.

(137) Kurmaz, S.; Perepelitsina, E. *Russ. Chem. Bull.* **2006**, *55*, 835.

(138) McEwan, K. A.; Haddleton, D. M. *Polym. Chem.* **2011**, *2*, 1992.

(139) Krasznai, D. J.; McKenna, T. F. L.; Cunningham, M. F.; Champagne, P.; Smeets, N. M. B. *Polym. Chem.* **2012**, *3*, 992.

(140) Hennink, W. E.; van Nostrum, C. F. *Adv. Drug. Deliver. Rev.* **2002**, *54*, 13.

(141) Hoffman, A. S. *Adv. Drug. Deliver. Rev.* **2002**, *54*, 3.

(142) Peppas, N. A.; Bures, P.; Leobandung, W.; Ichikawa, H. *Eur. J. Pharm. Biopharm.* **2000**, *50*, 27.

(143) Halacheva, S. S.; Freemont, T. J.; Saunders, B. R. *J. Mater. Chem. B.* **2013**, *1*, 4065.

(144) Wichterle, O.; Lim, D. *Nature* **1960**, *185*, 117.

(145) Dragan, E. S. *Chem. Eng. J.* **2014**, *243*, 572.

(146) Myung, D.; Waters, D.; Wiseman, M.; Duhamel, P. E.; Noolandi, J.; Ta, C. N.; Frank, C. W. *Polym. Advan. Technol.* **2008**, *19*, 647.

(147) Sperling, L. H. *Interpenetrating polymer networks*; John Wiley & Sons, Inc. , **2004**.

(148) Wang, J. J.; Liu, F. *Polym. Bull.* **2013**, *70*, 1415.

(149) Chivukula, P.; Dušek, K.; Wang, D.; Dušková-Smrčková, M.; Kopečková, P.; Kopeček, J. *Biomaterials* **2006**, *27*, 1140.

(150) Hoare, T. R.; Kohane, D. S. *Polymer* **2008**, *49*, 1993.

(151) Dragan, E. S.; Lazar, M. M.; Dinu, M. V.; Doroftei, F. *Chem. Eng. J.* **2012**, *204*, 198.

(152) Yin, L.; Fei, L.; Tang, C.; Yin, C. *Polym. Int.* **2007**, *56*, 1563.

(153) Samanta, H. S.; Ray, S. K. *Carbohydr. Polym.* **2014**, *99*, 666.

(154) Wang, Q.; Zhang, J.; Wang, A. *Carbohydr. Polym.* **2009**, *78*, 731.

(155) Kim, S. J.; Yoon, S. G.; Kim, S. I. *J. Appl. Polym. Sci.* **2004**, *91*, 3705.

(156) Crini, G.; Badot, P.-M. *Prog. Polym. Sci.* **2008**, *33*, 399.

(157) Ngah, W. W.; Teong, L.; Hanafiah, M. *Carbohydr. Polym.* **2011**, *83*, 1446.

(158) Kim, S. J.; Shin, S. R.; Spinks, G. M.; Kim, I. Y.; Kim, S. I. *J. Appl. Polym. Sci.* **2005**, *96*, 867.

(159) Murthy, P. K.; Mohan, Y. M.; Sreeramulu, J.; Raju, K. M. *React. Funct. Polym.* **2006**, *66*, 1482.

(160) Dragan, E. S.; Apopei, D. F. *Chem. Eng. J.* **2011**, *178*, 252.

(161) Wang, J.; Zhou, X.; Xiao, H. *Carbohydr. Polym.* **2013**, *94*, 749.

(162) Cai, Z.; Kim, J. *J. Appl. Polym. Sci.* **2009**, *114*, 288.

(163) Singh, D.; Choudhary, V.; Koul, V. *J. Appl. Polym. Sci.* **2007**, *104*, 1456.

(164) Aduba, D. C.; Hammer, J. A.; Yuan, Q.; Yeudall, W. A.; Bowlin, G. L.; Yang, H. *Acta. Biomater.* **2013**, *9*, 6576.

(165) Gil, E. S.; Hudson, S. M. *Biomacromolecules* **2007**, *8*, 258.

(166) Kundu, J.; Poole-Warren, L. A.; Martens, P.; Kundu, S. C. *Acta. Biomater.* **2012**, *8*, 1720.

(167) Chirila, T. V.; George, K. A.; Abdul Ghafor, W. A.; Pas, S. J.; Hill, A. J. *J. Appl. Polym. Sci.* **2012**, *126*.

(168) Lee, Y.; Kim, D. N.; Choi, D.; Lee, W.; Park, J.; Koh, W. G. *Polym. Advan. Technol.* **2008**, *19*, 852.

(169) Liu, Y. Y.; Lü, J.; Shao, Y. H. *Macromol. Biosci.* **2006**, *6*, 452.

(170) Silan, C.; Akcali, A.; Otkun, M. T.; Ozbey, N.; Butun, S.; Ozay, O.; Sahiner, N. *Colloids. Surf., B.* **2012**, *89*, 248.

(171) Huang, Y.; Liu, M.; Wang, L.; Gao, C.; Xi, S. *React. Funct. Polym.* **2011**, *71*, 666.

(172) Ali, S. W.; Zaidi, S. A. R. *J. Appl. Polym. Sci.* **2005**, *98*, 1927.

(173) Baskan, T.; Tuncaboylu, D. C.; Okay, O. *Polymer* **2013**, *54*, 2979.

(174) Xu, K.; Tan, Y.; Chen, Q.; An, H.; Li, W.; Dong, L.; Wang, P. *J. Colloid. Interf. Sci.* **2010**, *345*, 360.

(175) Masaki, M.; Kokufuta, E. *Colloid. Polym. Sci.* **2013**, *291*, 669.

(176) Turner, J.; Martineau, L.; Shek, P. US20040105880 A1, **2003**.

(177) Peng, H.; Mok, M.; Martineau, L.; Shek, P. US20050218541 A1, **2004**.

(178) Dillon, M. US7087135 B2, **2005**.

(179) Branco, D. A. C. C.; Chaudhuri, O.; Mooney, D. J. WO2015192017 A1, **2015**.

(180) Weiss, R. A.; Goldman, M. P. *Dermatol. Surg.* **2001**, *27*, 449.

(181) Reddy, T. T.; Kano, A.; Maruyama, A.; Hadano, M.; Takahara, A. *Biomacromolecules* **2008**, *9*, 1313.

(182) Thimma Reddy, T.; Kano, A.; Maruyama, A.; Hadano, M.; Takahara, A. *J. Biomed. Mater. Res. B.* **2009**, *88*, 32.

(183) Reddy, T. T.; Takahara, A. *Polymer* **2009**, *50*, 3537.

(184) Thatiparti, T. R.; Kano, A.; Maruyama, A.; Takahara, A. *J. Polym. Sci., Part A: Polym. Chem.* **2009**, *47*, 4950.

(185) Hayashi, M.; Matsushima, S.; Noro, A.; Matsushita, Y. *Macromolecules.* **2015**.

(186) Tang, Q.; Yu, J.-R.; Chen, L.; Zhu, J.; Hu, Z.-M. *Curr. Appl. Phys.* **2010**, *10*, 766.

(187) Gupta, A.; Upadhyay, N. K.; Parthasarathy, S.; Rajagopal, C.; Roy, P. K. *J. Appl. Polym. Sci.* **2013**, *128*, 4031.

(188) Chang, C.-H.; Liu, H.-W.; Huang, C.-C. *Bio-Med. Mater. Eng.* **2014**, *24*, 2081.

(189) Liu, H.-W.; Chaw, J.-R.; Shih, Y.-C.; Huang, C.-C. *Bio-Med. Mater. Eng.* **2014**, *24*, 2065.

(190) Chang, C. H.; Liu, H. W.; Huang, C. C. *Biomed Mater Eng* **2014**, *24*, 2081.

(191) Gao, C.; Yan, D. *Prog. Polym. Sci.* **2004**, *29*, 183.

(192) Voorhaar, L.; Hoogenboom, R. *Chem. Soc. Rev.* **2016**.

(193) Chen, H.; Ma, X.; Wu, S.; Tian, H. *Angew. Chem. Int. Ed.* **2014**, *53*, 14149.

(194) Cui, J.; del Campo, A. *Chem. Commun.* **2012**, *48*, 9302.

(195) Akay, G.; Hassan-Raeisi, A.; Tuncaboylu, D. C.; Orakdogen, N.; Abdurrahmanoglu, S.; Oppermann, W.; Okay, O. *Soft Matter* **2013**, *9*, 2254.

(196) Ge, Z.; Zhou, Y.; Tong, Z.; Liu, S. *Langmuir* **2011**, *27*, 1143.

(197) Miasnikova, A.; Laschewsky, A.; De Paoli, G.; Papadakis, C. M.; Müller-Buschbaum, P.; Funari, S. S. *Langmuir* **2012**, *28*, 4479.

(198) Charbonneau, C.; Chassenieux, C.; Colombani, O.; Nicolai, T. *Macromolecules.* **2011**, *44*, 4487.

(199) Nakahata, M.; Takashima, Y.; Yamaguchi, H.; Harada, A. *Nat. Commun.* **2011**, *2*, 511.

(200) Tirtaatmadja, V.; Tam, K.; Jenkins, R. *Macromolecules.* **1997**, *30*, 3271.

(201) Van Tomme, S. R.; van Steenbergen, M. J.; De Smedt, S. C.; van Nostrum, C. F.; Hennink, W. E. *Biomaterials* **2005**, *26*, 2129.

(202) Li, J.; Harada, A.; Kamachi, M. *Polym. J.* **1994**, *26*, 1019.

(203) Chujo, Y.; Sada, K.; Saegusa, T. *Macromolecules.* **1993**, *26*, 6320.

(204) Wang, H.; Heilshorn, S. C. *Adv. Mater.* **2015**, *27*, 3717.

(205) Yu, L.; Ding, J. *Chem. Soc. Rev.* **2008**, *37*, 1473.

(206) Tsai, Y.-C.; Li, S.; Hu, S.-G.; Chang, W.-C.; Jeng, U.-S.; Hsu, S.-h. *ACS Appl. Mater. Interfaces.* **2015**, *7*, 27613.

(207) Liu, H.; Xiong, C.; Tao, Z.; Fan, Y.; Tang, X.; Yang, H. *RSC Adv.* **2015**, *5*, 33083.

(208) Boekhoven, J.; Stupp, S. I. *Adv. Mater.* **2014**, *26*, 1642.

(209) Olofsson, K.; Andrén, O. C.; Malkoch, M. *J. Appl. Polym. Sci.* **2014**, *131*.

(210) Oudshoorn, M. H. M.; Rissmann, R.; Bouwstra, J. A.; Hennink, W. E. *Biomaterials* **2006**, *27*, 5471.

(211) Pedrón, S.; Bosch, P.; Peinado, C. *J. Photochem. Photobiol., A.* **2008**, *200*, 126.

(212) Pedrón, S.; Anseth, K.; Benton, J. A.; Bosch, P.; Peinado, C. *Macromol. Symp.* **2010**, *291*, 307.

(213) Zhang, H.; Patel, A.; Gaharwar, A. K.; Mihaila, S. M.; Iviglia, G.; Mukundan, S.; Bae, H.; Yang, H.; Khademhosseini, A. *Biomacromolecules* **2013**, *14*, 1299.

(214) Dodiuk-Kenig, H.; Lizenboim, K.; Eppelbaum, I.; Zalsman, B.; Kenig, S. *J. Adhes. Sci. Technol.* **2004**, *18*, 1723.

(215) Pitarresi, G.; Palumbo, F. S.; Giammona, G.; Casadei, M. A.; Micheletti Moracci, F. *Biomaterials* **2003**, *24*, 4301.

(216) Tao, W.; Yan, L. *J. Appl. Polym. Sci.* **2010**, *118*, 3391.

(217) Zant, E.; Grijpma, D. W. *Biomacromolecules* **2016**, *17*, 1582.

(218) Henriksson, M.; Fogelström, L.; Berglund, L. A.; Johansson, M.; Hult, A. *Compos. Sci. Technol.* **2011**, *71*, 13.

(219) Liu, H.; Wilén, C.-E. *J. Polym. Sci., Part A: Polym. Chem.* **2001**, *39*, 964.

(220) Velnar, T.; Bailey, T.; Smrkolj, V. *J. Int. Med. Res.* **2009**, *37*, 1528.

(221) Robson, M. C.; Steed, D. L.; Franz, M. G. *Curr. Prob. Surg.* **2001**, *38*, 72.

(222) Lazarus, G. S.; Cooper, D. M.; Knighton, D. R.; Margolis, D. J.; Percoraro, R. E.; Rodeheaver, G.; Robson, M. C. *Wound. Repair. Regen.* **1994**, *2*, 165.

(223) Schreml, S.; Szeimies, R.-M.; Prantl, L.; Landthaler, M.; Babilas, P. *J. Am. Acad. Dermatol.* **2010**, *63*, 866.

(224) Falanga, V. *Lancet* **2005**, *366*, 1736.

(225) McLister, A.; McHugh, J.; Cundell, J.; Davis, J. *Adv. Mater.* **2016**, n/a.

(226) Richardson, M. *Nurs. Times.* **2003**, *100*, 50.

(227) George Broughton, I.; Janis, J. E.; Attinger, C. E. *Plast. Reconstr. Surg.* **2006**, *117*, 1e.

(228) Hunt, T. K.; Hopf, H.; Hussain, Z. *Adv. Skin. Wound. Care.* **2000**, *13*, 6.

(229) Jespersen, J. *Dan. Med. Bull.* **1988**, *35*, 1.

(230) Pool, J. *Am. J. Med. Technol.* **1977**, *43*, 776.

(231) Lawrence, W. T. *Clin. Plast. Surg.* **1998**, *25*, 321.

(232) Strecker-McGraw, M. K.; Jones, T. R.; Baer, D. G. *Emerg. Med. Clin. North Am.* **2007**, *25*, 1.

(233) Skover, G. *Clin. Podiatr. Med. Surg.* **1991**, *8*, 723.

(234) Boateng, J. S.; Matthews, K. H.; Stevens, H. N. E.; Eccleston, G. M. *J. Pharm. Sci.* **2008**, *97*, 2892.

(235) Zahedi, P.; Rezaeian, I.; Ranaei-Siadat, S.-O.; Jafari, S.-H.; Supaphol, P. *Polym. Advan. Technol.* **2010**, *21*, 77.

(236) Fonder, M. A.; Lazarus, G. S.; Cowan, D. A.; Aronson-Cook, B.; Kohli, A. R.; Mamelak, A. J. *J. Am. Acad. Dermatol.* **2008**, *58*, 185.
(237) Vanwijck, R. *Bull. Mem. Acad. R. Med. Belg.* **2000**, *156*, 175.
(238) Degreef, H. J. *Dermatol. Clin.* **1998**, *16*, 365.
(239) Ovington, L. G. *Home Healthcare Now* **2002**, *20*, 652.
(240) Winter, G. D. *Nature* **1962**, *193*, 293.
(241) Winter, G. *Epidermal wound healing* **1972**, 71.
(242) Rovee, D. T. *Clin. Mater.* **1991**, *8*, 183.
(243) Varghese, M. C.; Balin, A. K.; Carter, D. M.; Caldwell, D. *Arch. Dermatol.* **1986**, *122*, 52.
(244) Alvarez, O. M.; Mertz, P. M.; Eaglstein, W. H. *J. Surg. Res.* **1983**, *35*, 142.
(245) Knighton, D.; Silver, I.; Hunt, T. *Surgery* **1981**, *90*, 262.
(246) Barnett, A.; Berkowitz, R. L.; Mills, R.; Vistnes, L. M. *Am. J. Surg.* **1983**, *145*, 379.
(247) Nemeth, A. J.; Eaglstein, W. H.; Taylor, J. R.; Peerson, L. J.; Falanga, V. *Arch. Dermatol.* **1991**, *127*, 1679.
(248) Hutchinson, J.; Lawrence, J. *J. Hosp. Infect.* **1991**, *17*, 83.
(249) Seaman, S. *J. Am. Podiat. Med. Assn.* **2002**, *92*, 24.
(250) May, S. R. *Chronic Wound Care. A Clinical Sourcebook for Healthcare Professionals. Health Management Publications* **1990**, 301.
(251) Jiang, Q.; Wang, J.; Tang, R.; Zhang, D.; Wang, X. *Int. J. Biol. Macromol.* **2016**.
(252) Borda, L. J.; Macquhae, F. E.; Kirsner, R. S. *Curr. Dermatol. Rep.* **2016**, 1.
(253) Dhivya, S.; Padma, V. V.; Santhini, E. *BioMedicine* **2015**, *5*.
(254) Baker, P. *Adv. Nurse. Pract.* **2005**, *13*, 37.
(255) Lay-Flurrie, K. *Prof Nurse* **2004**, *19*, 269.
(256) Hollinworth, H. *Nurs. Times.* **2001**, *97*, 63.
(257) Eisenbud, D.; Hunter, H.; Kessler, L.; Zulkowski, K. *Ostomy. Wound. Manag.* **2003**, *49*, 52.

2. Synthesis of Water Soluble Branched Polymers *via* CCTP

This chapter investigates the synthesis of linear and branched hydrophilic polymers prepared from MAA, PEGMEMA and relatively high concentrations of the cross-linker EGDMA by Catalytic Chain Transfer Polymerisation (CCTP).[1-3] Initially the theory of branched polymers and the analysis of non-linear species by multi-detector SEC are reviewed through the application of Universal Calibration generated by the coupling of refractive index and viscometry detectors.[4,5] This is followed by a presentation of alternative methods for the analysis of branched polymers by techniques including NMR and GC-FID.

Solution polymerisation was used to synthesise low MW linear polymers of MAA to act as a standard for the synthesis and characterisation of low MW copolymers of MAA and EGDMA.[2,6] As investigations progressed to the synthesis of PEGMEMA branched species, linear analogues are presented to form a standard for analysis of the branched materials produced.

2.1 Characterisation of branched polymers

2.1.1 Application of SEC to branched polymers

Branched and hyperbranched polymers where the branching is irregular represent a significant analytical challenge. The irregular spacing of the branching points renders the use of ^{1}H NMR to determine conversion and degree of polymerisation through the integration of backbone hydrogen environments challenging. Therefore a number of different techniques are used to characterise these materials.

Conventional size exclusion chromatography (SEC) depends upon developing a calibration from the peak molecular weights (M_p) of calibration standards with low dispersity (Đ) of a range of molecular weights, these are then used to produce a plot of log molecular weight (log M) vs. retention volume (V_R).[7] A polynomial fit of the calibrants across the molecular weight region allows for the calculation of the MW of samples according to their V_R.

Conventional SEC is ideal for the analysis of materials with a linear architecture that have minimal interaction with the stationary phase. Unfortunately, it has substantial flaws when it comes to the analysis of non-linear materials where the relationship between MW and V_R is less uniform.[8,9] As the separation in SEC is not dependant on MW but rather the hydrodynamic volume (V_h) of the polymer molecule, the calibration standards would ideally be of the same architecture and composition as the sample, as both of these variables have a significant impact upon V_h.[7,8] As it is not always possible to procure linear standards of a given polymer, or practical to expend large amounts of time and resources synthesising them, most molecular weight values reported in the

literature are apparent values relative to PS, PMMA or PEO calibrations, yielding mere approximations of the real MW.

As, in this work, structures with varying degrees of branching and functionality but similar MW are compared and, since these would have significantly different and incomparable V_R, other detectors are required in order to gain accurate results.[8,9] Two techniques widely used for this are; universal calibration and triple detection – both make use of two or more detectors.[5,10] Universal calibration makes use of a concentration sensitive differential refractive index detector and viscometer, whereas triple detection also makes use of light scattering in addition to those previously mentioned. Unfortunately light scattering is inherently insensitive at low molecular weights, due to low minimal scattering from smaller chains, triple detection is not suitable in this instance and will not be discussed further.[5]

2.1.2 Universal calibration and triple detection SEC

Universal calibration as a method was first developed by Grubisic *et al*. in 1967 and was established as a suitable method for the comparison of polymers of differing functionality, topography and architecture.[5] As mentioned above, universal calibration makes use of two detectors – a concentration-sensitive detector (usually a differential refractive index, DRI) and a viscometer (VISC). The assumption is that separation by SEC is solely reliant on V_h, which is related to intrinsic viscosity (IV) and molecular weight by the Einstein viscosity law (**Equation 2.1**).

$$[\eta] = K\frac{V_h}{M}$$

Equation 2.1; Einstein viscosity law where [η] is intrinsic viscosity, V_h is hydrodynamic volume, M is molecular weight and K is a constant independent of polymer structure in value.

Equation 2.1 shows that V_h can be described as the product of intrinsic viscosity [η] and molecular weight M, meaning that using log[η]M (as opposed to logM in conventional SEC) vs V_h would yield a universal calibration curve, shown convincingly to be valid for non-linear polymer topologies as well as alternative functionalities (**Figure 2.1**).

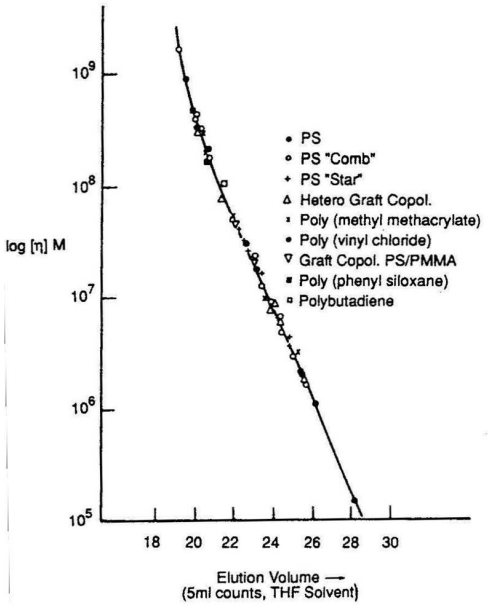

Figure 2.1; Universal calibration plot of log[η]M vs elution volume and its application to a number of architectures and functionalities. Adapted from reference.[5]

The viscometry detection used in the universal calibration can also be used to generate Mark-Houwink plots which allow for a plot of log [η] vs. log MW **Equation 2.2,** the gradient of which is α, this can provide a qualitative insight into the polymer architecture. Furthermore, this is useful for qualitatively comparing branching as

branched materials have a lower V_R and, therefore, should have a lower [η] across any comparable MW range.

$$\boldsymbol{M = K[\eta]^{\alpha}}$$

$$\boldsymbol{\log M = \log K + \alpha \log[\eta]}$$

Equation 2.2; Mark-Houwink equation where M is molecular weight, [η] is the intrinsic viscosity and, K and α are the Mark-Houwink constants (top), log form of Mark-Houwink equation used in Mark-Houwink Plots (bottom).[4]

Equation 2.2 gives a simple, qualitative method for analysing the degree of branching in a polymer relative to a linear standard; consistently branched polymers would expect to see a lower IV across the whole of their molecular weight compared to a linear equivalent due to consistently having a lower value of V_R.[4]

The Mark-Houwink exponent α is derived from the slope of a Mark-Houwink plot (**Equation 2.2**), and gives an indication of the solvated conformation of the polymer in a θ solvent – that being the solvent in which a polymer acts as an ideal chain (when the chemical potential of mixing between the solvent and the polymer chain is zero). The α value is related to the fractal dimensions (d_f) of the polymer or its level of complexity relative to its dimensions. High α values approaching 1, are associated with low d_f values, and symbolise a rigid rod conformation. Low α values approaching 0, are associated with high d_f values represent a hard sphere conformation (**Table 2.1**).[4]

Architecture	Fractal dimension d_f	Mark-Houwink exponent α
Rigid rod	1	-
Linear random coil (good solvent)	$1.67 < d_f < 2$	$0.5 < \alpha < 0.8$
Linear random coil (Θ conditions)	2	0.5
Random branching (good solvent)	$2 < d_f < 2.27$	$0.33 < \alpha < 0.5$
Random branching (Θ solvent)	2.27	0.33
Hard sphere	3	0

Table 2.1; Relationship between fractal dimension, Mark-Houwink exponent α and polymer architecture.[4]

Linear polymers usually assume a random coil conformation, with value of α greater than 0.5, giving a constant increase in IV with increasing molecular weight. Increasing the degree of branching within the same molecular weight region as the linear sample would be expected to cause a decrease in the value of α (trending towards zero), as increasing the molecular weight would have less of an impact upon the value of V_R and the IV. If the value of α in a sample trends towards zero then this is indicative of a material acting more like a hard sphere and, therefore, more likely to have a significant degree of branching.

2.1.3 Semi-quantitative descriptions of branching by SEC with viscometry detection.

The mean-squared radius of gyration (R_g^2) is a representation of the chain size of a polymer in solvent. Zimm and Stockmayer theorised that the R_g^2 would decrease with increasing degrees of branching in polymers of the same molecular weight and,

associated this reduction with the contraction factor, g.[11,12] This is defined as the ratio of radius of gyration of branched to linear polymers at the same molecular weight (**Equation 2.3**).

$$g = \left[\frac{\left(R_g^2\right)_B}{\left(R_g^2\right)_L}\right]_M$$

Equation 2.3; Contraction factor g, where B and L denote the mean-square radius for branched and linear samples, respectively. Subscript M means the branched and linear species are of the same molecular weight.

Radius of gyration can only be measured by multi-angle light scattering (MALS), which doesn't give accurate results at low MW. Zimm and Klib discovered a contraction factor (g') could also be measured by viscometry detection and is defined as the ratio of intrinsic viscosity of branched and linear species of the same molecular weight (**Equation 2.4**).[13] This does not give the same result as the contraction factor derived from the radius of gyration, nor does it equate to intrinsic viscosities derived from branched and linear species of the same retention volume. As a result, this technique must be used in combination with universal calibration.

$$g' = \left[\frac{[\eta]_B}{[\eta]_L}\right]_M$$

Equation 2.4; Contraction factor g' given as a ratio of the intrinsive viscosities ([η]) of branched (B) and linear (L) species at the same molecular weight (M).

This method cannot be used to generate absolute branched numbers, but it is able to give an indication of the relative degree of branching in a series of branched polymers relative to a linear species of the same functionality.[14,15] Linear polymers will have a g'

value of 1, therefore deviation from linearity caused by branching, generates a lower value in g'.

2.2 Synthesis and optimisation of branched acid polymers

2.2.1 Linear MAA homo-polymerisation and pseudo-mayo plots

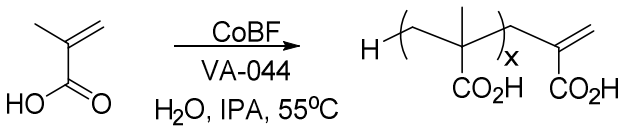

Scheme 2.1; Catalytic chain transfer polymerisation of MAA in the presence of CoBF

Before synthesising branched polyacids, homo-polymerisation of MAA (**Scheme 2.1**), was conducted in order to ascertain the chain transfer constant (C_s) of the monomer/catalyst system according to the Mayo system (**Equation 2.5**). This is a measure of the effectiveness of the chain transfer agent within the system. In order to obtain this information, a mayo plot is constructed by conducting a series of homopolymerisations at different catalyst to monomer ratios and stopping the reaction at very low conversion (< 10 %) in order to gain a sample before termination begins to affect the molecular weight.[16-18] The slope of the resulting curve of 1/DP vs [CoBF] / [MAA] yields the C_s for this particular system (**Figure 2.2**).

$$\frac{1}{DP_n} = \frac{1}{DP_n^0} + C_s\frac{[S]}{[M]}$$

Equation 2.5; The Mayo equation – DP_n is the degree of polymerisation, DP_n^0 is the degree of polymerisation with no CTA, C_s is the chain transfer constant for transfer to CTA, [S] is the concentration of CTA and [M] is the concentration of monomer[19]

Reaction	[CoBF] (mol)	[CoBF] / [MAA]	Conversion (%)[a]	M_w ($gmol^{-1}$)[b]	1/DP
1	1.28×10^{-4}	6.00×10^{-5}	5	2400	0.036
2	7.67×10^{-5}	4.88×10^{-5}	3	3200	0.027
3	5.98×10^{-5}	3.13×10^{-5}	5	3900	0.022
4	2.99×10^{-5}	1.56×10^{-5}	7	6200	0.014

Table 2.2; Data for homopolymerisation of MAA, with varying [CoBF]/[MAA] ratios used to construct a Mayo plot (Figure 2.2).[a] Measured by GC-FID. [b] Measured by conventional SEC-DRI, with 2 x PLgel mixed D columns, calibrated with pMMA standards, with DMF (5 mmol NH_4BF_4) as eluent.

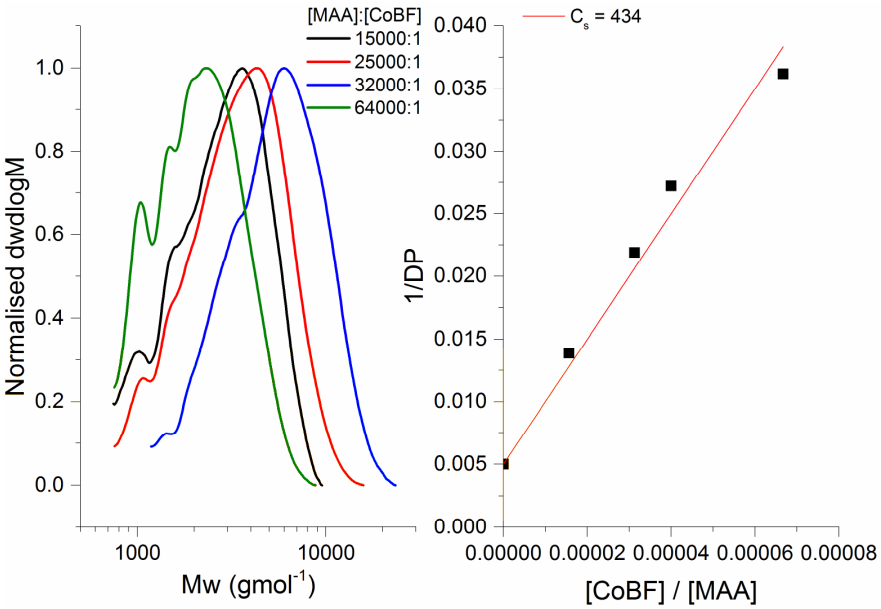

Figure 2.2; SEC traces of pMAA homopolymers at different [MAA]:[CoBF] stopped at low conversion (left). Pseudo-Mayo plot of 1/DP against [CoBF]/[MAA] ratios for pMAA homopolymers (right).

A linear relationship between the reciprocal of degree of polymerisation and the CoBF to monomer molar ratio can be observed from the pseudo-Mayo plot (**Figure 2.2**). The resulting low value of the C_s can be attributed to the high rate of catalyst hydrolysis caused by the presence of high concentrations of acid; this removes much of the catalyst and so reduces its effectiveness in the reaction solution.[2,20-22] This value is

much better than a comparable system using a Co^{II} chain transfer agent without the BF_2 bridging groups as these catalysts are far more susceptible to hydrolysis, even in the solid form.[2,19,21,23] The value obtained is comparable to that obtained previously by Haddleton *et al.* in 2001 for pMAA, and shows that the catalyst is undergoing chain transfer.[2] The value of $1/DP_{n,0}$ was found to be 0.005 which translates to a DP of 200, when factoring in that the ratio of monomer to initiator is 530:1 and, allowing for the effects of reduced chain length due to chain transfer to monomer and solvent, this is a realistic $1/DP_{n,0}$. Having defined the C_s of the catalyst in the system, this was used as a starting point for the addition of a di-vinyl monomer to prepare branched polymers.

2.2.2 Branched MAA polymerisation by CCTP

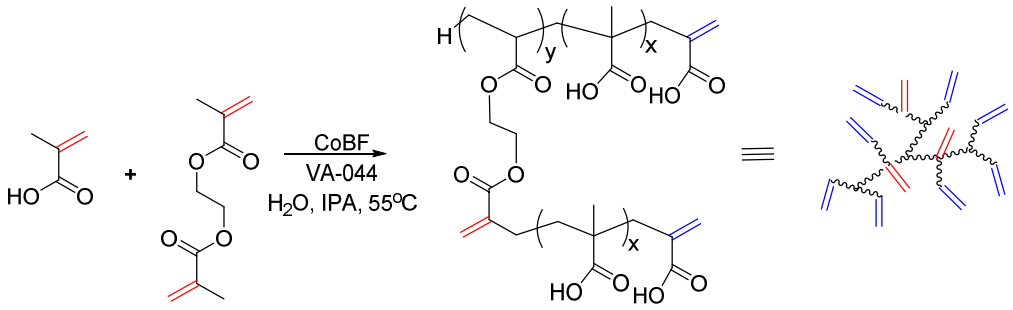

Scheme 2.2; Copolymerisation of MAA and EGDMA via CCTP, initiated by VA-044

In this section, a series of branched acid polymers were synthesised with varying concentrations of both the di-vinyl monomer - ethyleneglycol dimethacrylate (EGDMA) – and chain transfer agent - CoBF - according to published conditions.[2,20]

2.2.2.1 Variation in the concentration of EGDMA

As the application of these branched hydrogels requires that the polymers be water soluble in order to be included in the formulation of hydrogels, the concentration of the sparingly water soluble EGDMA was kept below 15 mol % - above which more

hydrophobic solvent systems are required in order to prevent gelation and, the resulting polymers have very poor water solubility. Both divinyl monomer and the resulting branched polymers show limited water solubility and crash out of solution, leading to uncontrolled free radical polymerisation and cross-linking to form gels. As a result, three polymers with varying concentrations of EGDMA from 0 to 15 wt. % were synthesised with a constant concentration of CoBF. A series of polymers (**5-8**) were produced (**Table 2.3**).

Reaction	[Monomer] / [CoBF]	[EGDMA] (mol %)	M_w[a] ($gmol^{-1}$)	Đ[a]	Conversion[b] (%)			Time (h)	α[a]	g'
					MAA	EGDMA	Total			
5	29500:1	0	5670	1.58	95	-	95	24	0.39	1
6	25000:1	5	12900	1.75	92	93	92	24	0.23	0.58
7	25000:1	10	58500	3.72	93	> 99	94	24	0.29	0.48
8	25000:1	15	gelled							

Table 2.3; Data for p(MAA-co-EGDMA) with [EGDMA] set at 5 mol. %. [a] Measured by SEC-UC with 2 x PLgel mixed D columns, calibrated with PMMA standards with DMF (5 mmol NH_4BF_4) as eluent. [b] Measured by GC-FID

These reactions produce linear and branched polymers with high conversions as measured by GC-FID (**Figure 2.21**), and a predictable increase in molecular weight and Đ as di-vinyl monomer concentration increases (**Figure 2.3**). At 15 mol % of cross-linker the reactions gelled as chain transfer was not sufficient to mitigate the effects of the Norissh-Trommsdorff gel effect.[24,25] Increasing the [CoBF] would decrease the kinetic chain length of all the materials formed, reducing the M_w and Đ as the amount of chain transfer increases relative to propagation.

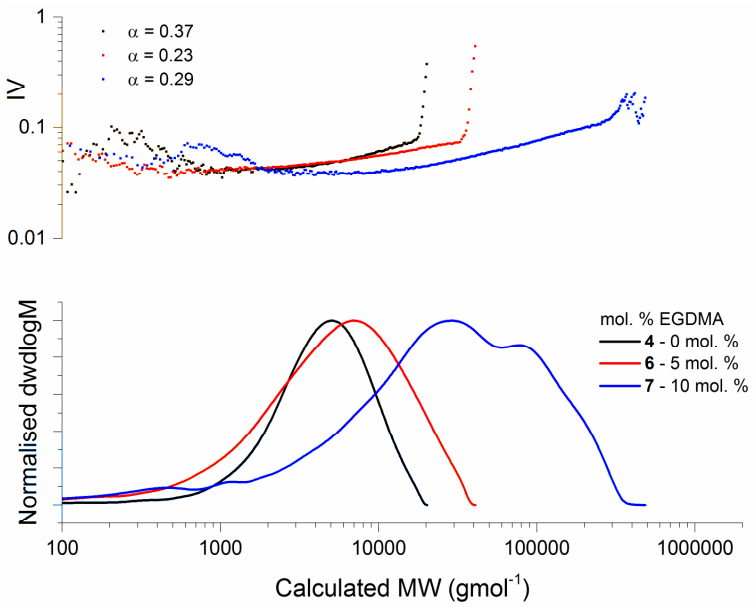

Figure 2.3; SEC-DRI-VISC calculated molecular weight distributions (lower pane), Mark-Houwink plots of IV vs MW (upper pane) for branched polymers of p(MAA-*co*-EGDMA) compared to linear pMAA.

With increasing concentration of di-vinyl monomer relative to the total monomer concentration a decrease in the hydrodynamic volume is observed relative to molecular weight as measured by UC-SEC (**Figure 2.3**). This causes a decrease in the α value from 0.37 in the linear case to 0.23 and 0.29 in the branched cases. The branched polymers also have a lower IV over comparable Mw values – indicative of a smaller hydrodynamic volume. The lower α value associated with **6** relative to **7** and **4** (Figure 2.3) is theorised to be due to the low molecular weight of this material relative to the other polymers synthesised and the similarity between **6** and **7** in α values is hypothesised to be due to similar degrees of branching despite different concentrations of di-vinyl monomer.

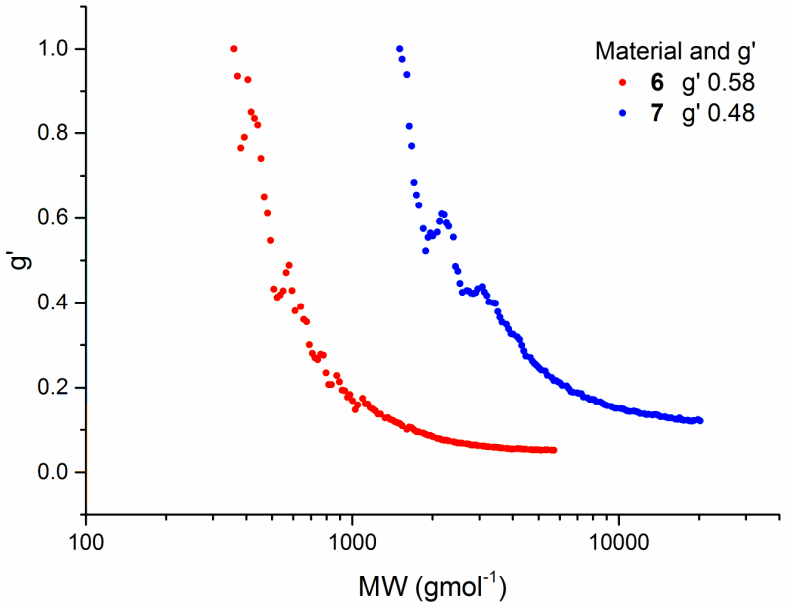

Figure 2.4; SEC-DRI-VISC derived g' plots for branched polymers p(MAA-*co*-EGDMA) 6 and 7, compared to linear pMAA 4 as described in Equation 2.4.

The value of g' can also be derived from comparison of the g' in branched polymers relative to a linear polymer at the same molecular weight when analysed by UC-SEC (**Figure 2.4**). In this case the result of increasing the concentration of divinyl monomer from zero to 10 % causes a significant decrease in the value of g'. This indicates that species with a higher concentration of cross-linker have a significantly lower radius of gyration, caused by an increase in the degree of branching.

2.2.2.2 Variation in the concentration of CoBF

The impact of reducing the concentration of chain transfer agent upon the M_w of polymer with the same concentration of divinyl monomers was assessed by maintaining the ratio of mono-vinyl to di-vinyl monomer constant at 95:5. It was predicted that this would typically cause an increase in the M_w up to a gelation point when cross-linking dominates over chain transfer. Four branched polyacids were synthesised with increasing [MAA]/[CoBF] ratios (**Table 2.4**).

Reaction	[Monomer] / [CoBF]	[EGDMA] (mol %)	M_w[a] ($gmol^{-1}$)	Đ[a]	Conversion[b] (%)			Time (h)	α[a]
					MAA	EGDMA	Total		
9	20500:1	5	12900	1.75	93	95	93	24	0.23
6	25000:1	5	14200	2.83	92	93	92	24	0.27
10	29500:1	5	17600	2.43	99	90	92	24	0.27
11	32000:1	5	42600	3.12	98	99	98	24	0.35

Table 2.4; Data for P(MAA-co-EGDMA) with [EGDMA] set at 5 mol %. [a] Measured by SEC-UC with 2 x PLgel mixed D columns, calibrated with PMMA standards with DMF (5 mmol NH_4BF_4) as eluent. [b] Measured by GC-FID.

As predicted, the four polymers formed show an increase in M_w with decreasing concentration of chain transfer agent (**Figure 2.5)**. Within the range of concentrations employed in this instance for the synthesis of branched polymers, no gelation was observed, implying that chain transfer dominated over cross-linking within the concentration range of 20500:1 to 32000:1.

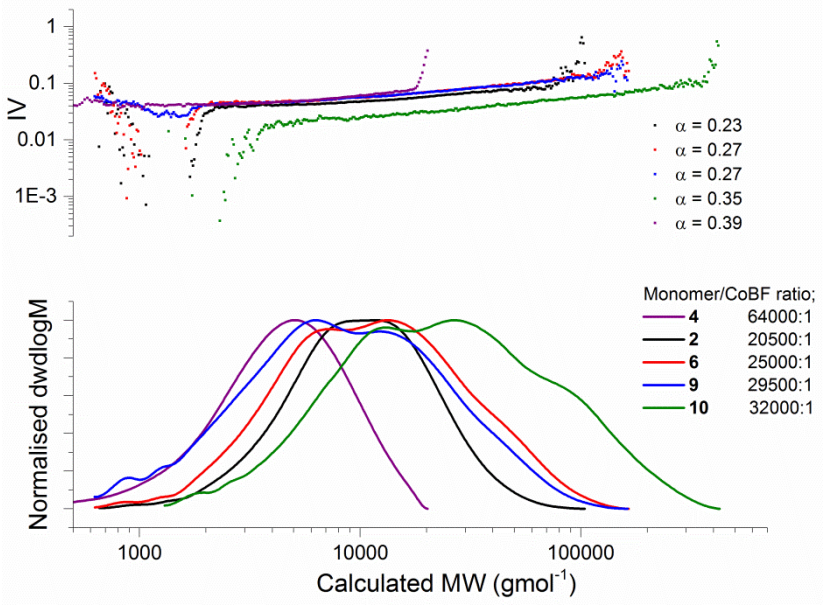

Figure 2.5; SEC-DRI-VISC calculated molecular weight distributions (lower pane), Mark-Houwink plots of IV vs MW (upper pane) for branched polymers of p(MAA-*co*-EGDMA) compared to linear pMAA (4).

Despite an increase in the M_w and Đ of the polymers formed, **Figure 2.5** shows that with decreasing concentration of CoBF there is a decrease in hydrodynamic volume at comparable MW. This indicates a more homogenous distribution of di-vinyl monomer through the polymer forming a less star-like, more tree-like polymer. The increase in α values with decreasing concentration of CoBF is likely to be due to the effects of the increasing molecular weight upon analysis by UC-SEC.[26]

2.2.2.3 Characterisation of the vinyl end group functionality

Due to the difficulties of quantifying the vinyl end groups through ^{1}H NMR, Iodometry through a bromination titration to yield a bromine index (BI) was carried out. This technique has previously been used by Wan *et al.* for the quantification of residual vinyl groups in cross-linked polystyrene spheres.[20,27] The vinyl groups present in the polymers were brominated by molecular bromine generated *in situ* from the reaction of potassium bromate and potassium bromide, in the presence of acetic acid (**Equation 2.6**; and **Scheme 2.3**;).

$$KBrO_3 + 5KBr + 6AcOH \rightleftharpoons 3Br_2 + 6AcOK + 3H_2O$$

Equation 2.6; Potassium bromate and potassium bromide in equilibrium with molecular bromine.

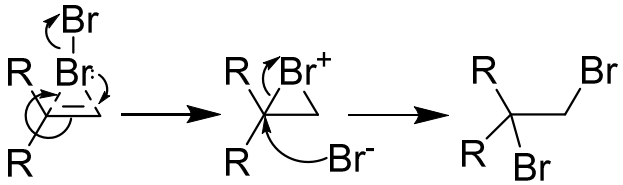

Scheme 2.3; Bromination of vinyl groups with molecular bromine.

Excess bromine was subsequently reacted with potassium iodide and hydrochloric acid to produce iodine (**Equation 2.7**), which is then titrated against sodium thiosulfate

(**Equation 2.8**). The end point is clarified through the use of starch as an indicator towards the end of the titration.

$$6KI + KBrO_3 + 6HCl \rightleftharpoons 2I_2 + KBr + 6KCl + 3H_2O$$

Equation 2.7; Reaction between potassium iodide, hydrochloric acid and excess potassium bromate to form molecular iodine, potassium chloride and water.

$$I_2 + 2Na_2S_2O_3 \rightleftharpoons 2NaI + Na_2S_4O_6$$

Equation 2.8; Reaction between molecular iodine and sodium thiosulphate, used in the titration step.

The moles of bromine used in this reaction are used in the calculation of BI, which is then used to calculate the moles of vinyl group per gram of polymer in solution (**Equation 2.9**).

$$BI = \frac{7990 \cdot (V_1 - V_2) \cdot c}{m}$$

Equation 2.9; Calculation of bromine index (BI), where V_1 and V_2 are the volumes (in mL) of $Na_2S_2O_3$ titrated in the blank and sample solutions, respectively, c is the concentration of the $Na_2S_2O_3$ solution (moldm^{-3}) and m is the mass of the polymer used.

Linear and branched acidic polymers generated by CCTP were tested by iodometry for their respective BI and mmol of vinyl groups per gram of polymer (**Table 2.5**). The number of vinyl groups was expected to decrease with increasing M_w of linear and lightly branched polymer, and to increase with increasing concentration of divinyl monomer due to the formation of branching points with additional vinyl groups. The results show considerable concentrations of vinyl groups in all compounds, comparing favourably to previously reported measurements and essential for the work addressed in later chapters. Unfortunately no clear relationship is seen between M_w of polymers

and concentration of divinyl monomer on the one hand, and, BI and vinyl group concentration on the other. This could be due to a high level of error within the measurement system coupled with the effect of the high levels of variability in the polymers themselves.

Compound	M_w ($gmol^{-1}$)	[EGDMA] (mol %)	BI (mg / 100 g)	Vinyl groups ($mmolg^{-1}$)
1	5000	0	34200	1.71
2	5650	0	54100	2.71
3	6300	0	59300	2.97
4	9800	0	44300	2.21
9	12900	5	46500	2.33
6	14200	5	50500	2.53
10	17600	5	46100	2.31
11	42600	5	56500	2.83
7	58500	10	47700	2.39

Table 2.5; Bromine index (BI) and results of the calculation of the number of vinyl groups per gram of compounds 1-11

Work conducted in this section into the synthesis of branched polymers has shown a library of branched and linear acidic polymers synthesised through the copolymerisation of MAA and EGDMA at different ratios and with different concentrations of the CCTA CoBF. Characterisation of the polymers by universal SEC indicates branching relative to the linear polymers, whereas, iodometry conducted against brominated vinyl terminated polymers indicates substantial vinyl group presence in these polymers. These polymers are subsequently used in Chapters 2 and 3, when investigating the effect they have upon the material properties of monolithic hydrogels.

2.3 Synthesis and optimisation of branched comb polymers

One of the principle issues with the incorporation of MAA based species into materials is the associated high T_g (transition from a glassy solid to a rubbery solid) of pMAA. This can subsequently increase the T_g of the resulting materials rendering them more brittle. As a result, in this work the synthesis of novel branched polymers made with the neutral poly(ethyleneglycol)methyl ether methacrylate (PEGMEMA) monomer are produced using CCTP.[28,29]

In this section the C_s of the CoBF/PEGMEMA system is investigated through synthesis of linear polymers at different [CoBF]/[PEGMEMA] ratios and a pseudo-mayo plot is formed from the results at low conversion. This is followed by the synthesis of a series of linear and branched PEGMEMA polymers with comparable concentrations of EGDMA to the branched acid series above at a range of concentrations of CoBF. The results are analysed using ^{1}H NMR to follow the kinetics of polymerisation in linear pPEGMEMA, UC-SEC as well as iodometry to analyse the branching through determination of the vinyl end group functionality.

2.3.1 Mayo-plot for measurement of C_s of PEGMEMA/CoBF

The Mayo equation (**Equation 2.5**) has two variables which can be changed – the monomer and the chain transfer agent, both of these variables have a profound effect upon the C_s of the system. In this case the monomer has been changed from an acid, to a hydrophilic oligomeric monomer. Whereas methacrylic acid causes acid hydrolysis of the catalyst through the course of the reaction, causing a decrease in the C_s of the

system, this is not expected to occur with PEGMEMA. The mayo equation is again used to show the effects of the change in the concentration of chain transfer agent (**Table 2.6**).

Reaction	[CoBF] (mol)	[CoBF] / [PEGMEMA]	Conversion (%)	M_n [b]	DP
12	7.60×10^{-5}	4.00×10^{-5}	8	4900	10.3
13	5.94×10^{-5}	3.13×10^{-5}	7	6200	13.0
14	2.97×10^{-5}	1.56×10^{-5}	8	10100	21.3
15	1.98×10^{-5}	1.04×10^{-5}	5	13500	28.4

Table 2.6; Data for homopolymerisation of PEGMEMA 12-15 with varying concentrations of chain transfer agent.

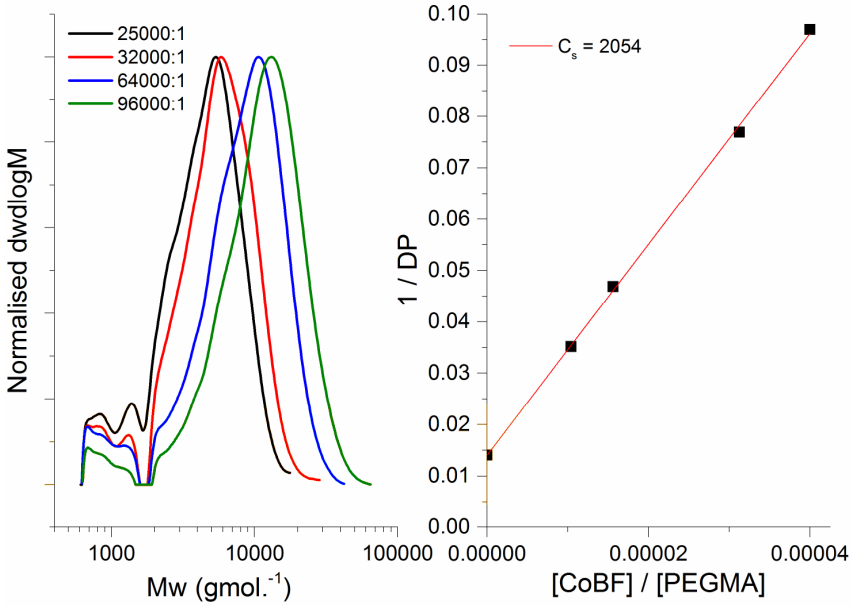

Figure 2.6; SEC traces of p(PEGMEMA) homopolymers at different [PEGMEMA]:[CoBF] stopped at low conversion (left). Mayo plot of 1/DP against [CoBF]/[PEGMEMA] ratios for p(PEGMEMA) homopolymers 12-15 (right).

The pseudo-mayo plot for linear p(PEGMEMA) gives a straight line with a slope C_s of 2,100 (**Figure 2.6**) and a $1/DP_{n,0}$ of 0.01404 (DP of 71) calculated from the intercept. This is significantly higher than the C_s observed from MAA with a value of 440 under the same conditions (**Figure 2.2**). The $DP_{n,0}$ is an accurate representation of the DP in

the absence of CTA as this reflects reasonably the ratio of monomer to initiator. The increase in the C_s between the two systems can be attributed to the absence of the acidic monomer, causing acid hydrolysis of the catalyst.[2] The value of $1/DP_{n,0}$ was found to be 0.01493 which translates to a $DP_{n,0}$ of 67.

2.3.2 Variation in the concentration of CoBF in linear combs

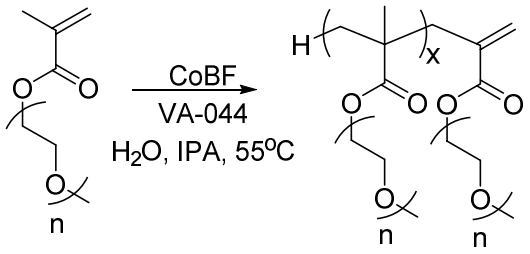

Scheme 2.4; Polymerisation of poly(ethylene glycol) methyl ether methacrylate via CCTP, initiated by VA-044.

Initially, a series of low molecular weight linear pPEGMEMA were synthesised using a binary combination of water and isopropanol (IPA) in order for the system to be identical to that used with the divinyl monomer EGDMA and the MAA system; to ensure that the reaction proceeds in a similar and controllable manner. This was achieved through variation in the ratio of [PEGMEMA]/[CoBF].

Reaction	[PEGMEMA]/[CoBF]	M_w[a] ($gmol^{-1}$)	Đ[a]	Conversion (%)[b]	Time (h)	α[a]
12	25000:1	4800	1.49	69	24	0.13
13	32000:1	5800	1.53	75	24	0.24
14	64000:1	9500	1.4	80	24	0.23
15	96000:1	12500	1.48	86	24	0.46

Table 2.7; Data for linear P(PEGMEMA) with variation of [CoBF]. [a] Measured by SEC with 2 x PLgel mixed C columns, calibrated with PMMA standards with $CHCl_3$ (2 mol % TEA) as eluent. [b] Measured by ^{1}H NMR

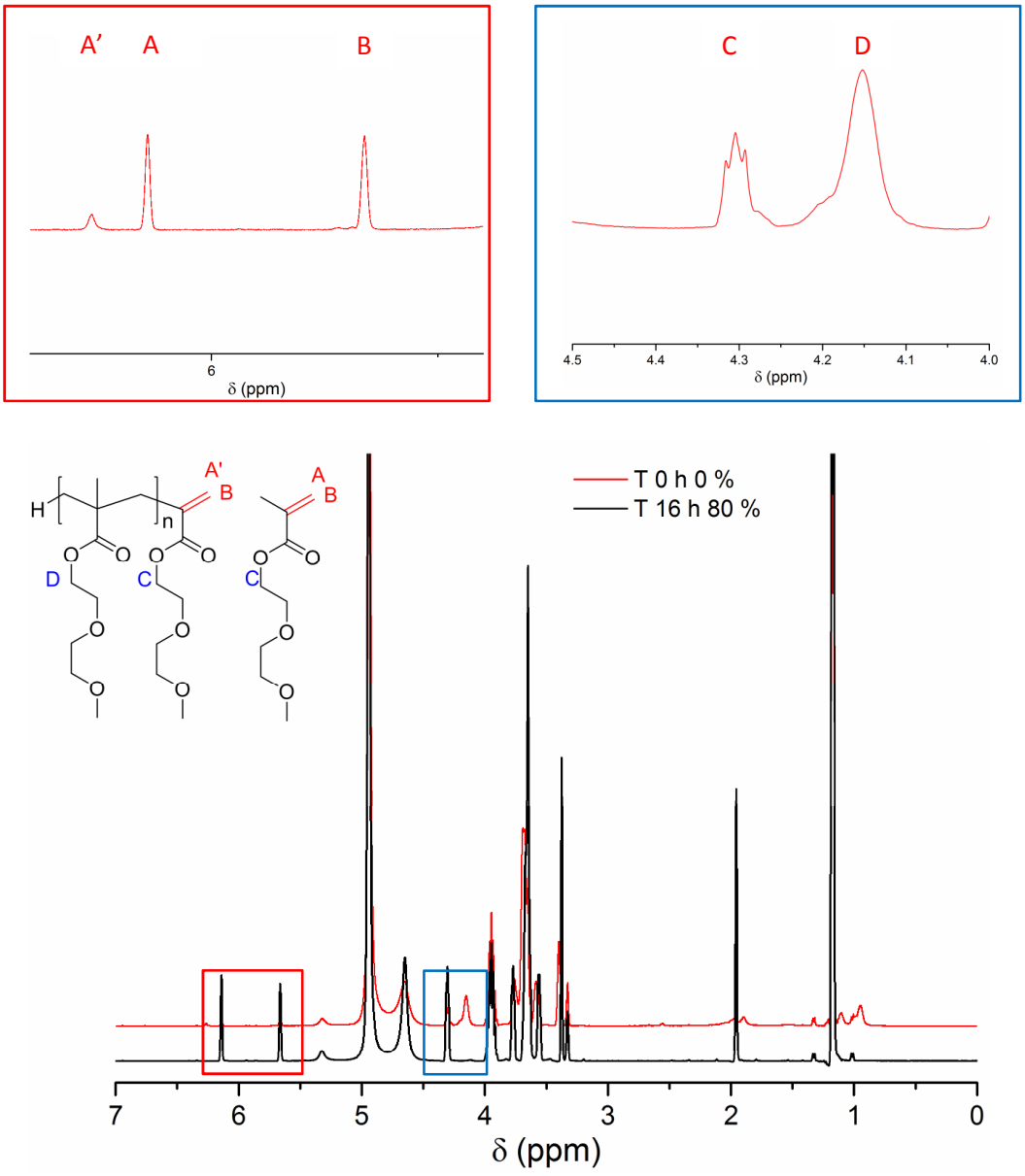

Figure 2.7; Typical ^{1}H NMR of p(PEGMEMA) synthesised by CCTP with characteristic vinyl peaks between 5.6 and 6.4 ppm and the shift in the polymeric ester peak from 4.3 ppm to 4.15 ppm.

The conversion of monomer into polymer for catalytic chain transfer polymerisation is often monitored by GC-FID due to the ease of identification of the monomer peaks and the difficulties in distinguishing end groups of the monomer and polymer by ^{1}H NMR. In this case GC-FID was not possible due to the use of PEGMEMA which, as it exists as an oligomer with a Đ, renders it difficult to monitor the reaction through this method.

One benefit of using PEGMEMA over the MAA monomer used above is the presence of the ester bond (4.30 ppm), which, along with the polymeric ester peak (4.11 ppm) can be used relative to the monomeric vinyl peak (6.14 ppm) to monitor the conversion of the reaction by ^{1}H NMR (**Figure 2.7**).

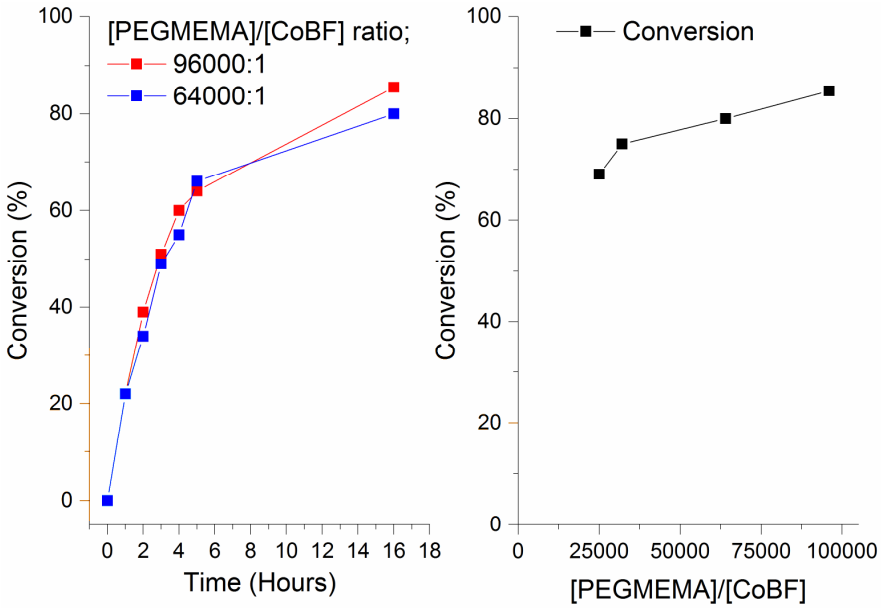

Figure 2.8; Comparison of conversion kinetics for linear pPEGMEMA synthesis by CCTP monitored by ^{1}H NMR (left). Total conversion of pPEGMEMA at different [PEGMEMA]/[CoBF] ratios (right).

The polymerisation of PEGMEMA to form linear pPEGMEMA brushes was followed using ^{1}H NMR, the results show that the majority of the monomer is consumed within 5 hours, however, in order to obtain high conversion (>90 %) the reaction must be left for over 16 hours (**Figure 2.8**). At high conversion the rate of polymerisation slows, this can be attributed to a reduced concentration of initiator and monomer leading to fewer active chain ends and reduction of collision frequency. It is noticeable that the conversion decreases with increasing concentration of CoBF as chain transfer becomes more efficient than propagation leading to the formation of lower molecular weight

and monomeric products.[3] The evolution of Mw of the pPEGMEMA through the reaction was monitored by SEC up to 16 hours, (**Figure 2.9** and **Figure 2.10)**.

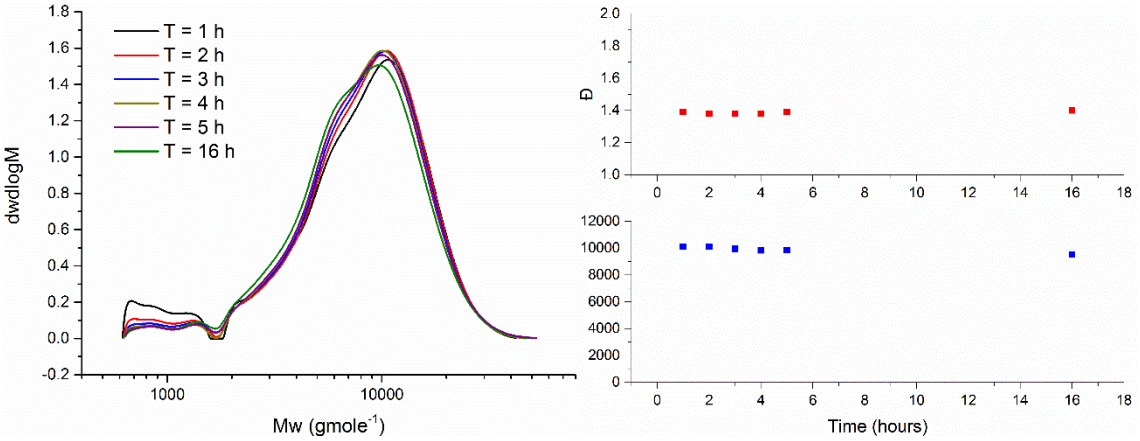

Figure 2.9; Evolution of molecular weight distributions through the homopolymerisation of PEGMEMA 14 with [PEGMEMA]/[CoBF] at 64000 (left). Evolution of the M_w and Đ, measured by conventional SEC, throughout polymerisation (right).

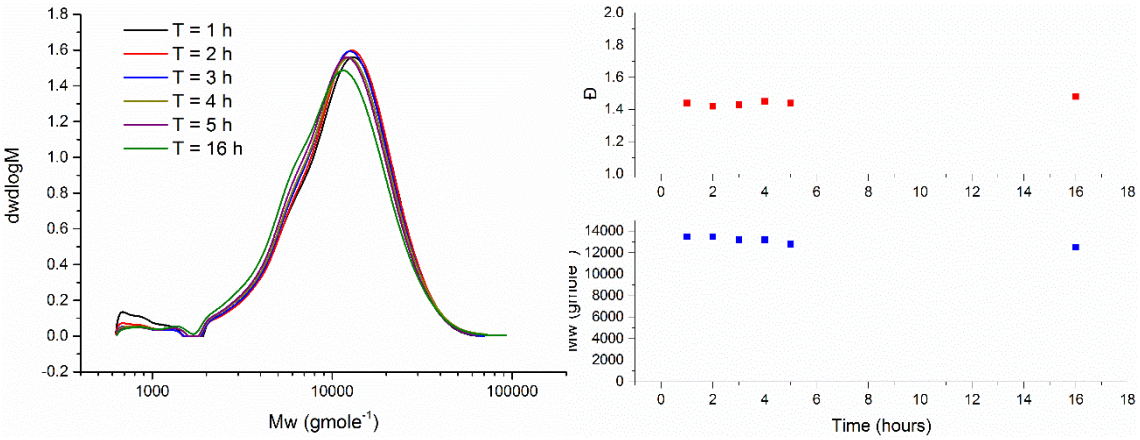

Figure 2.10; Evolution of molecular weight distributions through the homopolymerisation of PEGMEMA 15 with [PEGMEMA]/[CoBF] at 96000 (left). Evolution of the M_w and Đ, measured by conventional SEC, throughout polymerisation (right).

The kinetics of reactions **14** and **15** demonstrate the general trend of the kinetics throughout this series of linear pPEGMEMA polymerisations (**Figure 2.9**, **Figure 2.10**). It can be observed that there is no increase in M_w or Đ with time. This is because

typically in CCTP the rate of chain transfer is so high that the kinetic chain length is obtained effectively immediately and resulting chain transfer prevents any increase in M_w, polymeric products are rarely re-initiated through their terminal vinyl peak due to the low favourability of reacting with the hindered polymeric vinyl group relative to that of the monomer and the competing mechanism of chain transfer from the ω-vinyl group.[16,30] Both **Figure 2.9** and **Figure 2.10** reveal a decrease in M_w with time. This is caused by the [CoBF]/[PEGMEMA] ratio increasing with time as the monomer is consumed, the consequence is an increase in chain transfer (relative to propagation) and a small reduction in the M_w of the polymers being formed. This effect is not substantial because of the rapid conversion of the majority of the monomer to polymer. This effect is not observed in the synthesis of pMAA polymers by CCTP as the CoBF is hydrolysed at a comparable rate to the consumption of monomer allowing the ratio of [MAA]/[CoBF] to remains relatively constant with no molecular weight drift.[20]

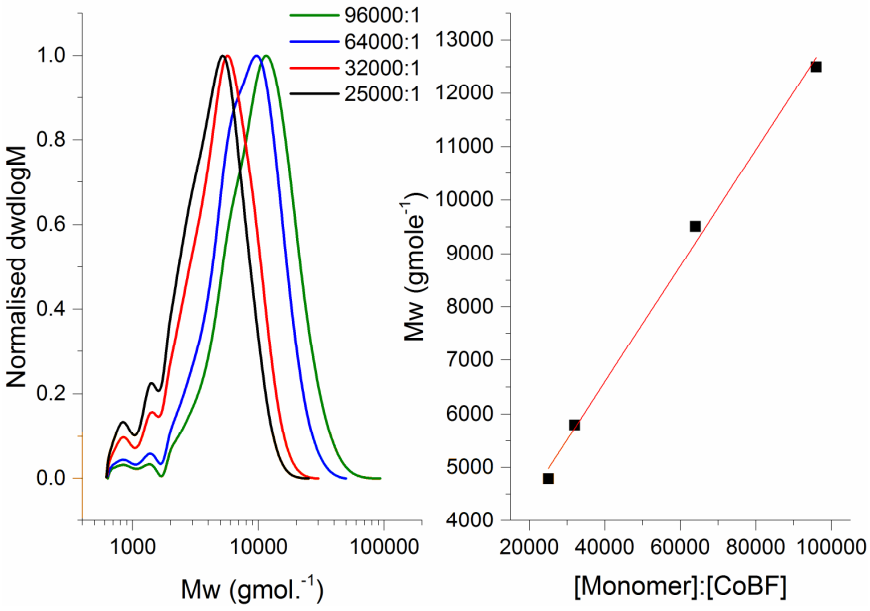

Figure 2.11; Comparison of SEC molecular weight distributions for PEGMEMA homopolymerisations 12-15 through the variation of [PEGMEMA]/[CoBF] ratio.

The four linear polymers prepared in this section show a linear increase in M_w with a decrease in the [PEGMEMA]/[CoBF] ratio demonstrating good control over the M_w of the polymers formed by this process (**Figure 2.11**).

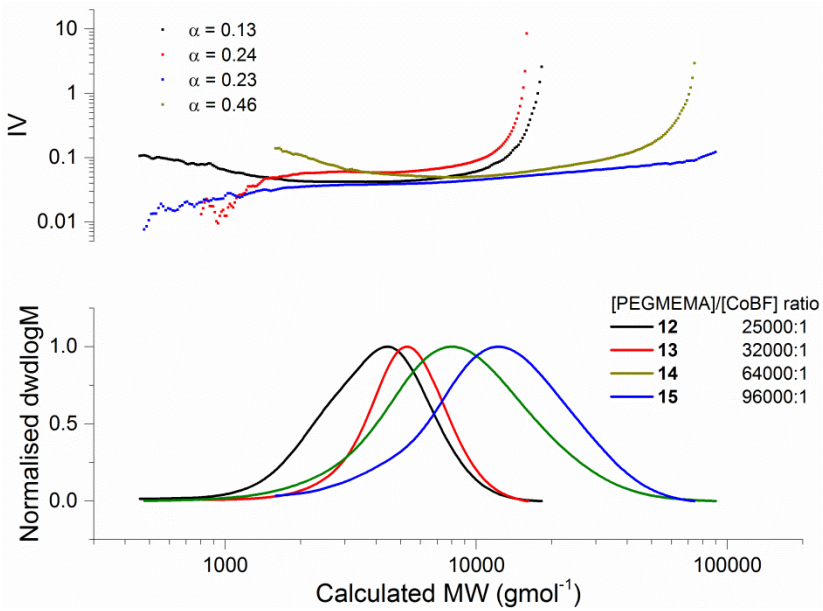

Figure 2.12; SEC-DRI-VISC calculated molecular weight distributions (bottom). Mark-Houwink plots of IV vs MW (top) for p(PEGMEMA).

Compounds **12-15** were analysed using universal calibration from which Mark-Houwink plots according to **Equation 2.2,** were derived (**Figure 2.12**). In this a clear increase in the α value of the polymers with increasing M_w was shown. The α value increases from 0.13 through to 0.46 with the commensurate increase in the M_w of the polymers. This can be explained by the difference in overall architecture between the low molecular weight brush and a high molecular weight brush. A low molecular weight brush more closely resembles a star shaped polymer, which would behave more like a hard sphere than a rigid rod. As the molecular weight of a brush increases it comes to resemble a rigid rod, causing the α value to increase (**Figure 2.13**).

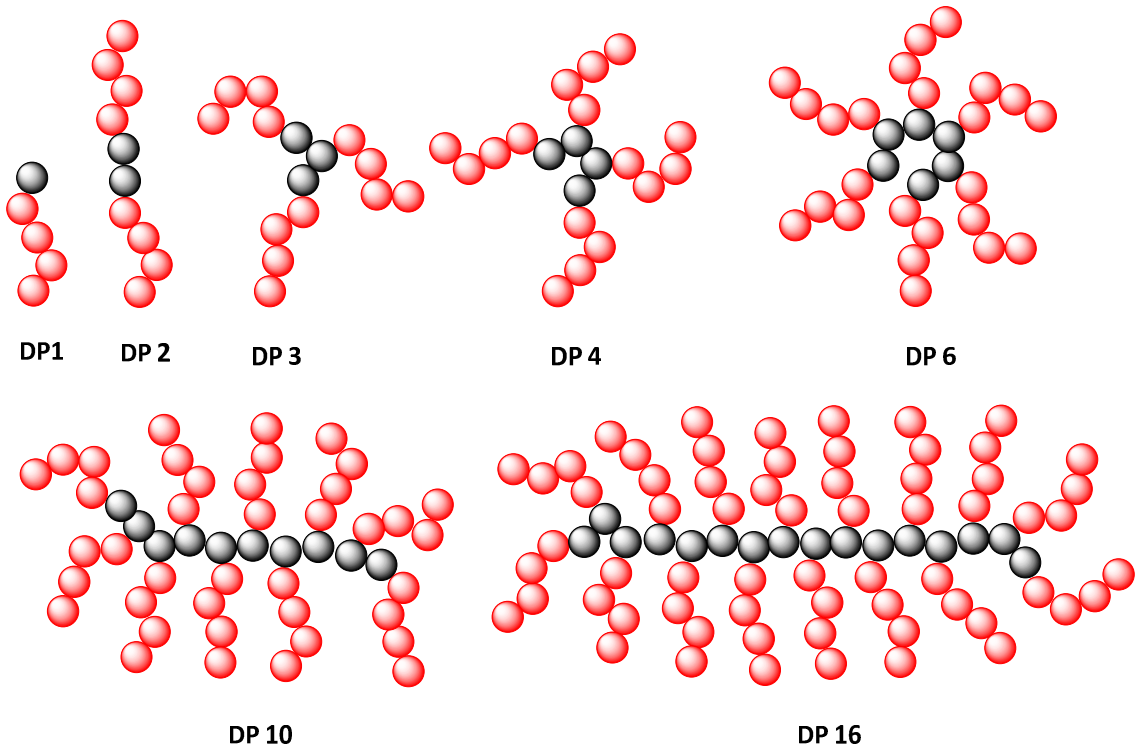

Figure 2.13; Representation of the effect of increase in DP upon morphology of brush polymers. At low DP, star-like morphologies are observed with low α values, with increasing DP the species become more linear with proportionately higher α values.[31]

2.3.3 Variation in the concentration of EGDMA

Following the polymerisation of the linear species and the calculation of C_s for PEGMEMA homopolymerisation, branching was introduced by incorporating EGDMA as the di-vinyl monomer. As with the branched acid species discussed earlier, the limit to the solubility of the branched polymer was found to be around 20 mol %. Three polymers were synthesised at increasing [EGDMA] whilst maintaining a constant concentration of the CCTA.

Reaction	[M]/[CoBF]	[EGDMA] (mol %)	M_w[a] ($gmol^{-1}$)	Đ[a]	Time (h)	α[a]
12	25000:1	0	4800	1.49	24	0.13
15	96000:1	0	12500	1.48	24	0.46
16	25000:1	5	8400	1.47	24	0.30
17	25000:1	10	9000	1.5	24	0.25
18	25000:1	15	10200	1.86	24	0.19

Table 2.8; Data for P(PEGMEMA-co-EGDMA) with variation of [EGDMA]. [a] Measured by SEC with 2 x PLgel mixed C columns, calibrated with PMMA standards with $CHCl_3$ (2 mol % TEA) as eluent.

The ester bond of monomeric EGDMA and PEGMEMA lie at the same ^{1}H NMR shift due to their chemical similarity. As a result of this, monitoring the conversions of these polymers becomes unfeasible by ^{1}H NMR as well as GC-FID, so the conversion of these polymers was not monitored.

With increasing concentration of EGDMA an increase in the molecular weight and the Đ of the polymer was observed. This is indicative of an increase in branching, as more branching points are incorporated into the species at higher [EGDMA]. It is possible in the case of PEGMEMA to use a higher [EGDMA] relative to [CoBF], this is due to the higher rate C_s of the system relative to the MAA system observed earlier. Branched polymers with [EGDMA] up to 15 mol % were synthesised in comparison to the MAA system where a maximum [EGDMA] of 10 mol % was observed before gelation was occurred.

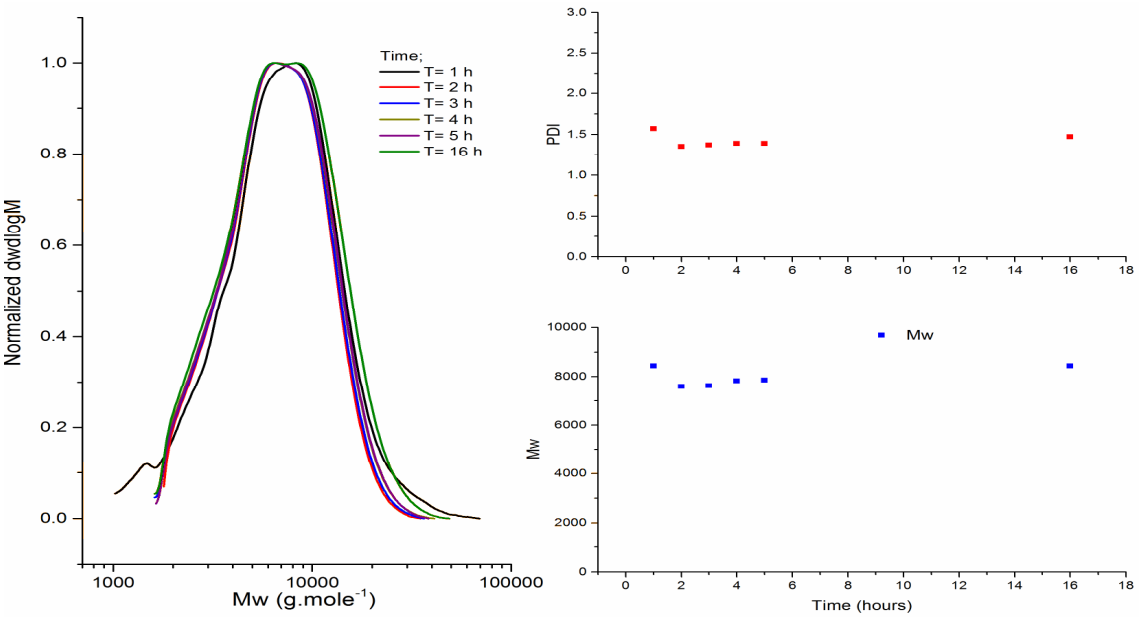

Figure 2.14; Evolution of molecular weight distributions through the copolymerisation of PEGMEMA (95 mol %) and EGDMA (5 mol %) 16 with [M]/[CoBF] at 25000.

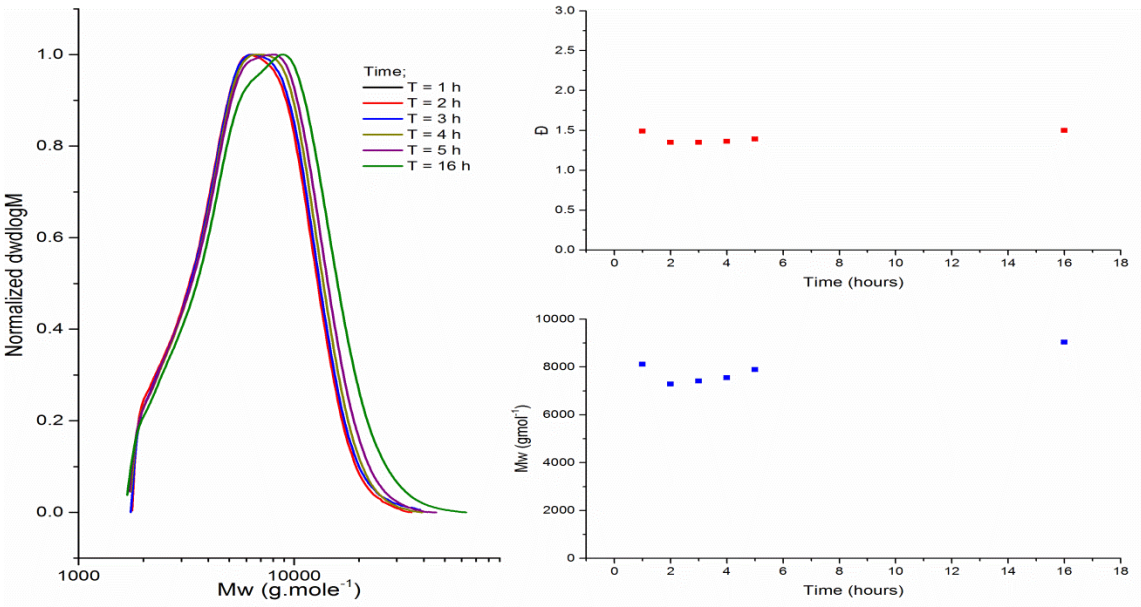

Figure 2.15; Evolution of molecular weight distributions through the copolymerisation of PEGMEMA (90 mol %) and EGDMA (10 mol %) 17 with [M]/[CoBF] at 25000.

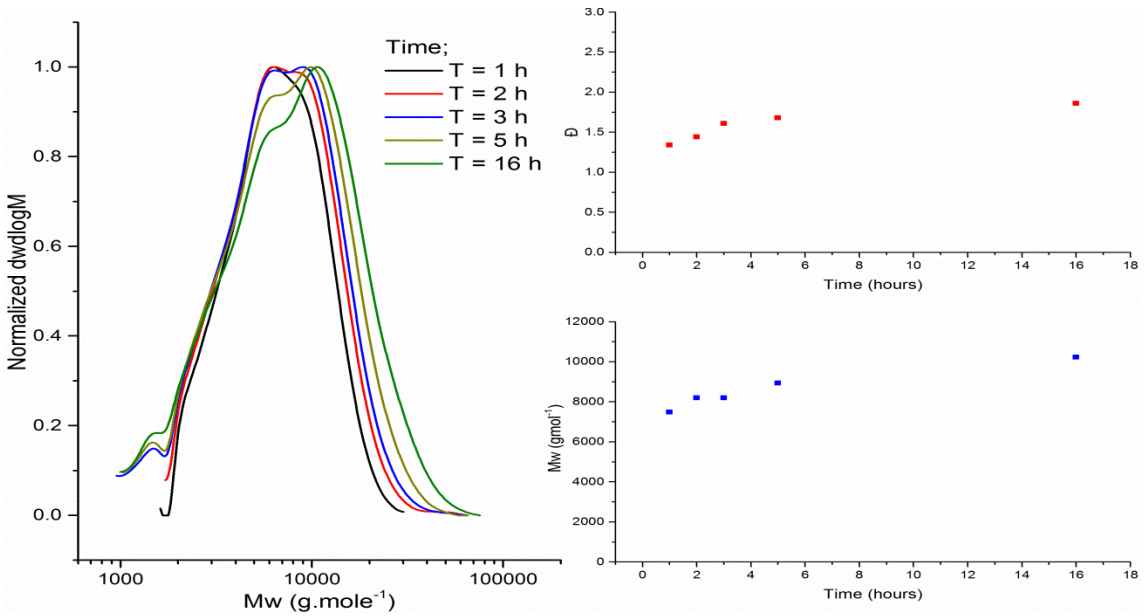

Figure 2.16; Evolution of molecular weight distributions through the copolymerisation of PEGMEMA (85 mol %) and EGDMA (15 mo. %) 18 with [M]/ [CoBF] at 25000.

The effects of increasing concentration of EGDMA upon the evolution of molecular weight as a function of time during the synthesis of branched pPEGMEMA polymers was monitored (**Figure 2.14**, **Figure 2.15** and **Figure 2.16**). In all materials an increase in molecular weight is observed through the reaction as early on in the reaction low molecular weight species are generated which, persist through the reaction. In these materials it is seen that with low concentrations of divinyl monomer there is a small increase in the M_w and Đ with time, but with increasing concentration of the dinvyl monomer, the increase in M_w and Đ with time becomes more pronounced (**Figure 2.14**, **Figure 2.15** and **Figure 2.16**) – as was the case with the MAA-*co*-EGDMA system (although to a lesser extent due to the reduction in the hydrolysis of the catalyst). This effect is due to progressive inclusion of the divinyl monomer, creating irregular branching points, which increases the M_w, but due to its irregularity, also increases the Đ.

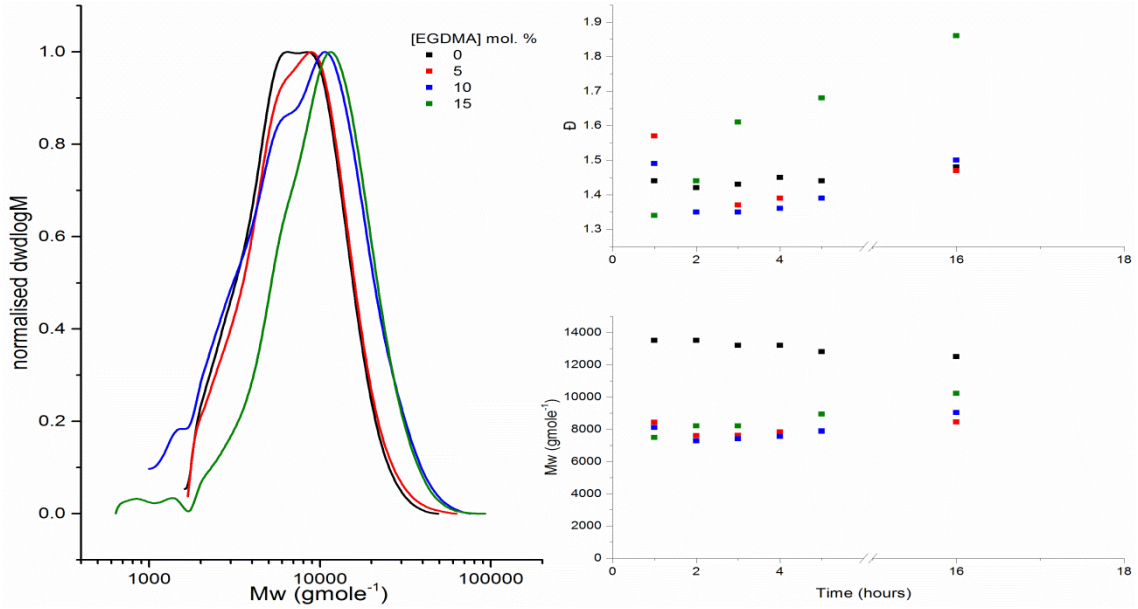

Figure 2.17; Comparison of SEC molecular weight distributions for copolymerisation PEGMEMA and EGDMA with different concentrations of EGDMA at a [M]/[CoBF] of 25000. 15, 16, 17 and 18.

The expected trend where increasing the concentration of divinyl monomer whilst maintaining the concentration of CCTA, causes an increase in M_w and an increase in Đ is observed (**Figure 2.17)**. This effect is caused by the formation of low Mw species early on in the reaction which persist through to the end, whilst at the same time higher Mw species are being formed as the reaction continues with increasing cross-linking (**Figure 2.17**).

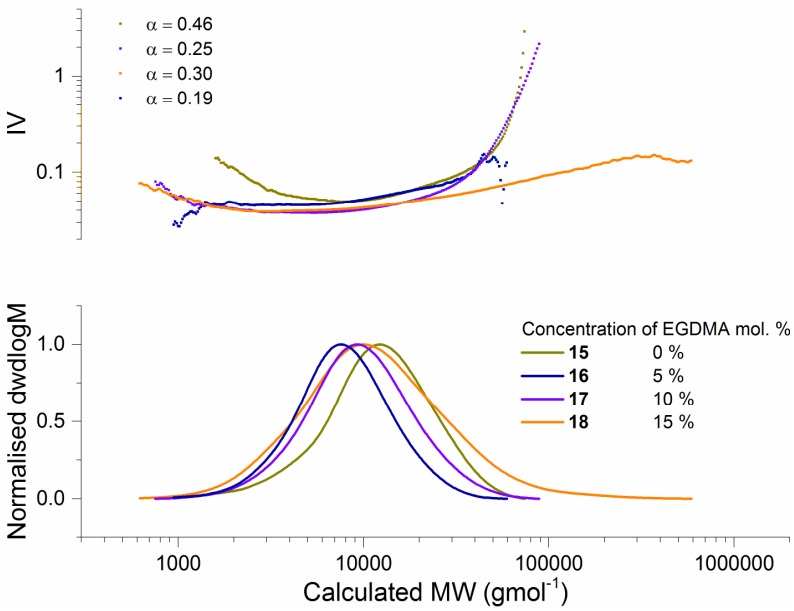

Figure 2.18; SEC-DRI-VISC calculated molecular weight distributions (bottom). Mark-Houwink plots of IV vs MW (top) for p(PEGMEMA-co-EGDMA).

With increasing concentration of cross-linker, a decrease in the α value is observed relative to linear species of a similar MW (**Figure 2.18**). In this case species **16, 17** and **18** are compared to linear species **15** as its MW distribution is more appropriate than that of linear species **11**, which, as a result of having the same [PEGMEMA]/[CoBF] ratio, has a much lower M_w. As seen in **Table 2.8, 15** has an α value of 0.46, indicative of a randomly coiled species. Through species **16** – **18** there is a progressive decrease in the α value caused by increasing degrees of branching. **18** exhibits an α value of 0.19, approaching the region of measurements expected of a hard sphere – indicating a high degree of branching.

2.3.4 Variation in the concentration of CoBF

The final set of tests to be conducted in this study involved the variation of concentration of CTA with a fixed concentration of divinyl monomer at 5 mol %. This divinyl monomer concentration was chosen as it renders the largest range of results

with a divinyl monomer. As with the results represented in **Table 2.7** the [PEGMEMA]/[CoBF] ratio was varied from 25000:1 through to 96000:1 and the resulting polymers were characterised *via* UC-SEC and ^{1}H NMR.

Reaction	[M]/[CoBF]	[EGDMA] (mol %)	M_w[a] ($gmol^{-1}$)	Đ[a]	Conversion[b] (%)	Time (h)	α[a]
16	25000:1	5	8400	1.47	83	24	0.30
19	32000:1	5	13400	1.62	74	24	0.45
20	64000:1	5	18500	1.82	78	24	0.39
21	96000:1	5	23800	1.94	32	24	0.49

Table 2.9; Data for P(PEGMEMA-co-EGDMA) with variation of [CoBF]. [a] Measured by SEC with 2 x PLgel mixed C columns, calibrated with PMMA standards with $CHCl_3$ (2 % TEA) as eluent. [b] Measured by ^{1}H NMR

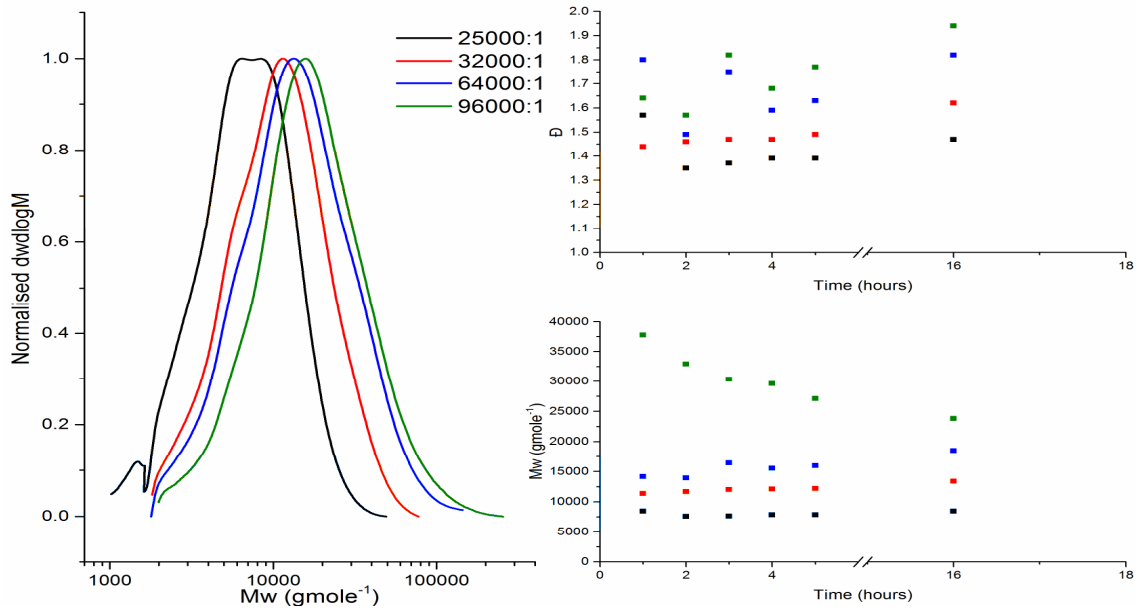

Figure 2.19; Comparison of SEC molecular weight distributions for copolymerisation PEGMEMA and EGDMA with different concentrations of EGDMA at a [M]/[CoBF] of 25000. 11,15,16 and 17.

As is observed with the synthesis of linear polymers, an increase in the [PEGMEMA]/[CoBF] ratio causes an increase in the M_w and Đ due to a reduction in the frequency of chain transfer leading to higher molecular weight species and a broader

range of Mw species being formed (**Figure 2.19**). As with the linear species (**Figure 2.11**) and species with a low degree of branching (**Figure 2.17**), **Figure 2.19** shows that with decreasing concentration of the CCTA the effect of decreasing M_w through the course of the reaction becomes more pronounced. This is caused by an effective decrease in the [PEGMEMA]/[CoBF] ratio, causing lower M_w species to be formed as a result of an increase in the frequency of chain transfer and, therefore, reducing the overall M_w.

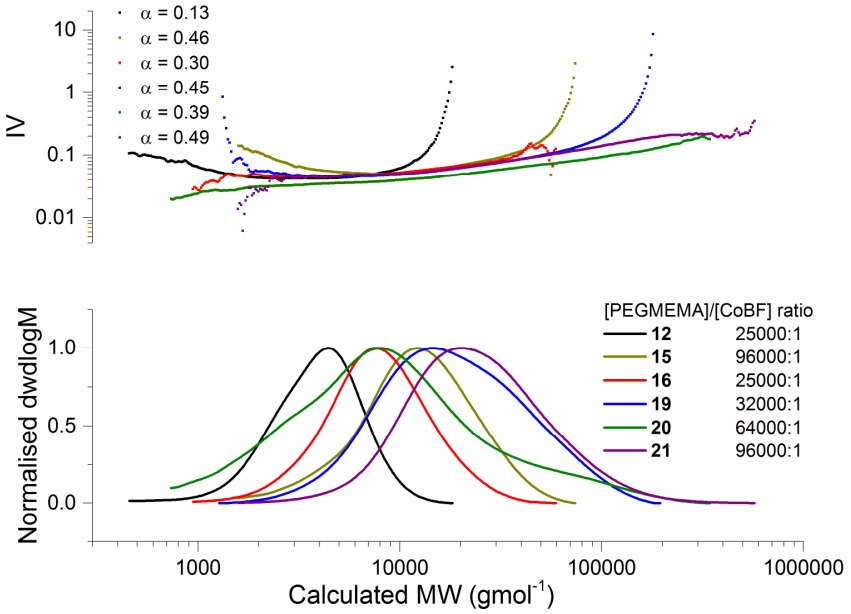

Figure 2.20; SEC-DRI-VISC calculated molecular weight distributions (bottom). Mark-Houwink plots of IV vs MW (Top) for p(PEGMEMA-co-EGDMA).

With increasing [PEGMEMA]/[CoBF] ratio there is no significant change in α, this indicates that all of these materials have a similar degree of branching regardless of Mw (**Figure 2.20**).

2.4 Conclusions

In this chapter a series of branched hydrophilic polymers were synthesised using CCTP and characterised. First, a library of linear and branched polyacids was synthesised. A pseudo-Mayo plot was generated for MAA and CoBF in a water/alcohol mixture to demonstrate the level of effectiveness of the catalyst within the system (a C_s of 434 was found - comparable to previously published literature).[2] Branched polyacids were then synthesised with varying concentrations of divinyl monomer and CoBF. The linear and branched materials were then characterised by GC-FID, NMR and SEC with branching indicated by Mark-Houwink analysis showing a decrease in the hydrodynamic volume as shown by a decrease in the Mark-Houwink parameter from 0.39 to 0.23 with increasing branching and a decrease in the hydrodynamic radius g' from 1 to 0.48 with increasing branching relative to the linear pMAA species.

Following from this a library of linear and branched polyPEGs were synthesised in a similar system. A pseudo-Mayo plot was conducted with the linear pPEGMEMA and found to be more effective than the MAA system due to the lack of acid hydrolysis with a C_s value of 2054. The kinetics of the reactions was monitored by ^{1}H NMR and SEC for linear combs and by SEC for branched polymers. Linear and branched materials were then characterised by ^{1}H NMR, and SEC; including Mark-Houwink plots to demonstrate branching. A clear relationship between concentration of divinyl monomer and decreasing α value was observed from 0.46 in the linear pPEGMEMA to 0.19 in the highest branched species in a comparable molecular weight range.

2.5 Experimental

2.5.1 Materials

All reagents were purchased from Aldrich and used as received unless otherwise stated. 2,2'-azobis[2-[(2-imidazolin-2-yl)propane]dihydrochloride (VA-044) was purchased from Alpha Labs and used as received. CoBF was synthesised *via* a method previously reported.[32,33]

2.5.2 Instruments

^{1}H- and ^{13}C-NMR spectroscopy

All NMR spectra were recorded on either a Bruker Avance III HD 300 MHz, Bruker Avance 300 MHz and a Bruker Avance III 400 MHz spectrometers as in D_2O, CD_3OD or $CDCl_3$ (with TMS) as indicated. Chemical shifts were calculated using the solvent residual peaks for D_2O and CD_3OD as reference or TMS as reference in the case of $CDCl_3$.

Size Exclusion Chromatography (SEC)

Chloroform

$CHCl_3$ SEC experiments were performed on Agilent 390-LC multi-detector suites equipped with a PL-AS RT/MT autosampler, fitted with a PLgel 5µm guard column and two PLgel 5µm Mixed C columns (with an exclusion limit of 2.0×10^6 gmol^{-1}). All data was collected and analysed using Agilent SEC software. Mobile phase was $CHCl_3$ with 2 % triethylamine and a flow rate of 1mL.min^{-1} and an injection volume of 100 µl. Column Sets were maintained at 30 ^{o}C.

Dimethylformamide

DMF SEC experiments were performed on Agilent 390-LC multi-detector suites equipped with a PL-AS RT/MT autosampler, fitted with a PLgel 5µm guard column and two PLgel 5µm Mixed D columns (with an exclusion limit of 4.0 x 10^5 $gmol^{-1}$). All data was collected and analysed using Agilent SEC software. Mobile phase was DMF with 5 mmol NH_4BF_4 and a flow rate of 1mL.min^{-1} and an injection volume of 100 µl. Column Sets were maintained at 50 ^oC.

Conventional SEC

A DRI detector was used for conventional calibration. Calibrations were created using PMMA EasiVial standards (550-2,136,000 $gmol^{-1}$) purchased from Agilent, with a minimum of 9 points fitted with a third order calibration curve. Points with an error greater than 10 % were not included in the final calibration.

SEC-DRI-VISC (universal calibration)

Final polymers were purified by precipitation and dried under vacuum prior to analysis in DMF and $CHCl_3$ in order to ensure accurate sample concentrations. An RI and a 4 capillary viscometer were used as detectors with an inter-detector delay calibrated using a single PMMA narrow standard (M_p 90,250 $gmol^{-1}$) of known concentration. Column calibrations were created using PMMA EasiVial standards (690-1,944,000 $gmol^{-1}$) analysed at known concentrations purchased from Agilent with a minimum of 9 points fitted with a third order calibration curve. g' values were calculated using linear PMAA (for analysis in DMF) and linear p(PEGMEMA) (for analysis in $CHCl_3$) as standards.

Gas Chromatography – Flame Ionisation Detector (GC-FID)

GC-FID was performed using a Varian 450 fitted with a FactorFour™ capillary column VF-1ms, of 15 m x 0.25mm I.D. and film thickness of 0.25 µm. Oven temperature was programmed as follows: 40°C (hold for 1 min) at 25 °C min^{-1} to 200 °C. The injector was operated at 200 °C with the FID at 220 °C. Nitrogen was used as the carrier gas at a flow rate of 1mL min^{-1} and a split ratio of 1:100 was applied. An internal standard of diethylene glycol was used to monitor conversion with the integral of the DEG peak being used relative to the integral of the MAA and EGDMA peaks to determine total and individual monomer conversion. Data was processed using Galaxie software (version 1.9.302.530) before being transferred to Origin Pro (version 9.1) and converted into graphical representations as seen below.

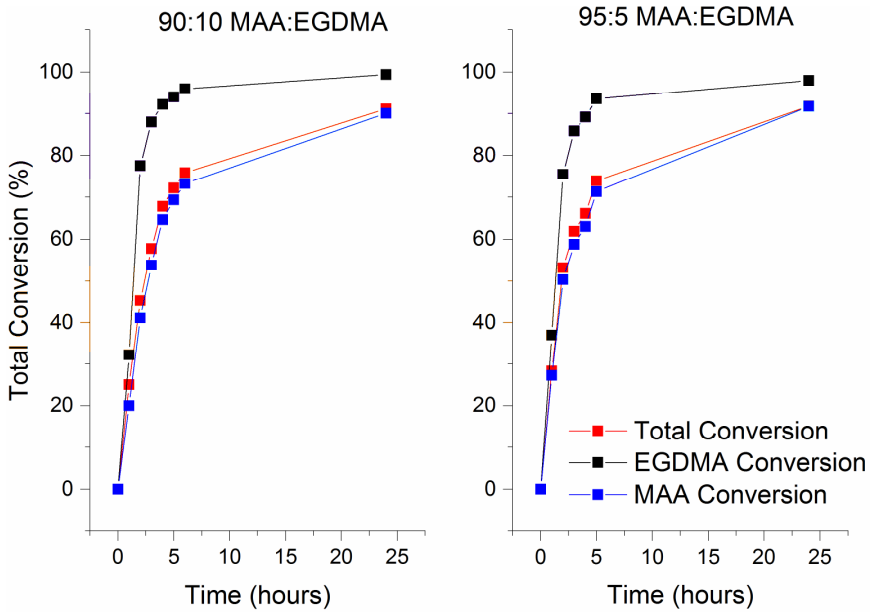

Figure 2.21: GC calculated conversion of MAA-co-EGDMA reaction with 10 mol % EGDMA with a [M]:[CoBF] ratio of 25000:1 (left), GC calculated conversion of MAA-co-EGDMA reaction with 5 mol % EGDMA with a [M]:[CoBF] ratio of 25000:1 (right).

2.5.3 General Procedures

2.5.3.1 Homopolymerisations of MAA

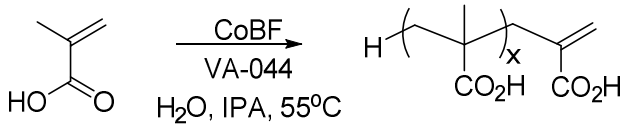

A 500 mL round bottom flask was charged with MAA (164.96 g, 1.92 mol), H_2O (175 mL), IPA (175 mL) and diethyleneglycol (DEG, 5 mL), for use as an internal standard for GC-FID) and equipped with a stirring bar and septum. This mixture was deoxygenated *via* bubbling with a stream of nitrogen for a minimum of 1 hour. A 1 L 3-neck round bottom flask, equipped with nitrogen inlet, septum and stirring bar, containing CoBF and VA-044 (0.6 g , 1.86 mmol), was degassed with four vacuum/nitrogen-backfill cycles before the monomer/solvent mixture was added *via* cannular under positive nitrogen pressure. The resulting reaction mixture was allowed to stir under a positive pressure of nitrogen at ambient temperature until all solids were dissolved, yielding a homogenous solution, at which point the vessel was placed in an oil bath at 55 ^{o}C. After 24 hours, the reaction mixture was precipitated into ice cold acetonitrile (10:1) before being dried under vacuum at ambient temperature.

Reaction	[MAA]/[CoBF]	CoBF (mg)	CoBF (mmol)
1	15000	49.2	1.28×10^{-4}
2	25000	29.5	7.67×10^{-5}
3	32000	23	5.98×10^{-5}
4	64000	11.5	2.99×10^{-5}

Table 2.10; Quantities of CoBF required for linear pMAA polymerisation.

2.5.3.2 Copolymerisations of MAA with EGDMA

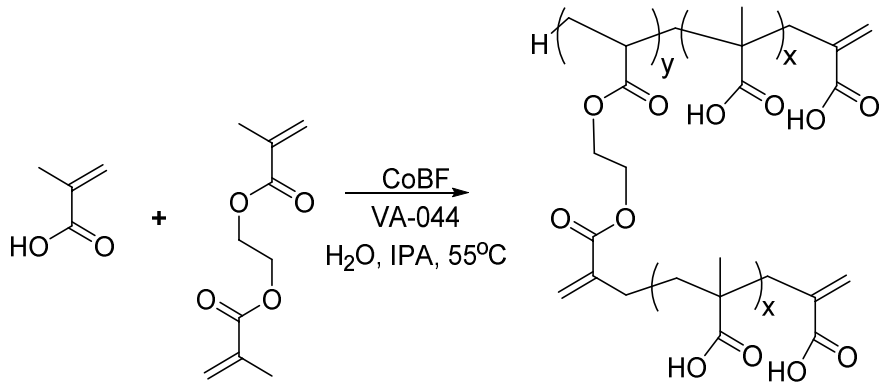

A typical copolymerisation in water-IPA was adapted from the pMAA homopolymerisation conditions described above. With varying wt. % of EGDMA and [monomer]/[CoBF] ratio.

Reaction	EGDMA (wt. %)	EGDMA (mol %)	[monomer]/[CoBF]	CoBF (mg)	CoBF (mmol)
5	10.8	5	20500	35.9	9.33×10^{-5}
6	10.8	5	25000	29.5	7.67×10^{-5}
7	10.8	5	29500	35	6.5×10^{-5}
8	10.8	5	32000	23	5.99×10^{-5}
9	21.6	10	25000	29.5	7.67×10^{-5}
10	32.4	15	25000	29.5	7.67×10^{-5}

Table 2.11; Quantities of CoBF required for branched p(MAA-*co*-EGDMA) polymerisations

2.5.3.3 Homopolymerisations of PEGMEMA

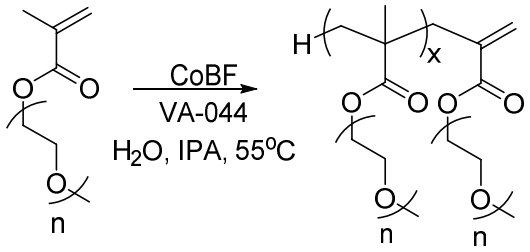

Stock solutions of CoBF in PEGMEMA were prepared using CoBF (2.4 mg, 6.23 x 10^{-3} mol) in PEGMEMA (31.5 g, 0.105mol). PEGMEMA was freeze pump thawed four times in a Schlenk tube then cannulated under nitrogen into the CoBF, degassed *via* vacuum/nitrogen cycles four times. Stock solutions were then stored under nitrogen in a fridge for a maximum of 1 month.

Reaction	[PEGMEMA]/[CoBF]	CoBF (mg)	CoBF (mmol)
11	25000	1.54	4 x 10^{-6}
12	32000	1.2	3.12 x 10^{-6}
13	64000	0.6	1.56 x 10^{-6}
14	96000	0.4	1.04 x 10^{-6}

Table 2.12; Quantities of CoBF required for linear pPEGMEMA polymerisations.

2.5.3.4 Copolymerisations of PEGMEMA with EGDMA

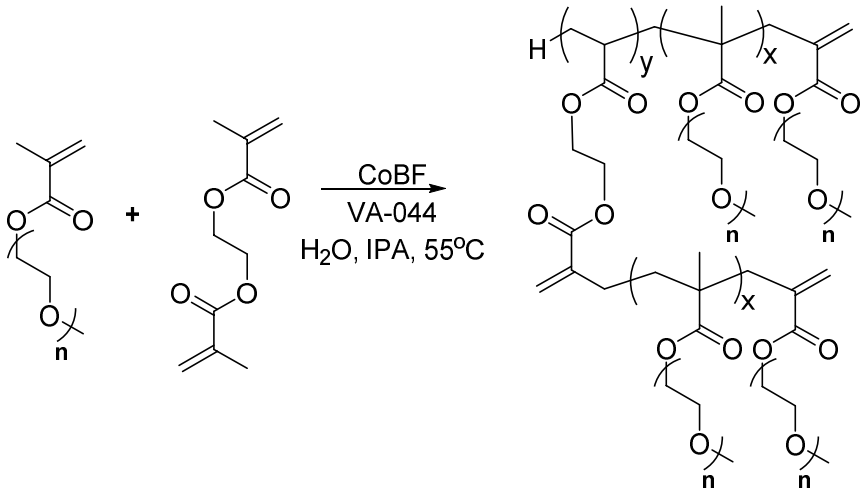

Stock solutions of CoBF in PEGMEMA wCharacteriere prepared using (2.4 mg, 6.23 x 10^{-3} mol) CoBF in of PEGMEMA (35 g, 0.105 mol). PEGMEMA was freeze pump thawed in a Schlenk tube

then cannulated under nitrogen into the CoBF, degassed *via* vacuum/nitrogen cycles four times. Stock solutions were then stored under nitrogen in a fridge for a maximum of 1 month.

Reaction	EGDMA (wt. %)	EGDMA (mol %)	[monomer]/[CoBF]	CoBF (mg)	CoBF (mmol)
15	3.36	5	25000	1.54	4×10^{-6}
16	3.36	5	32000	1.2	3.12×10^{-6}
17	3.36	5	64000	0.6	1.56×10^{-6}
18	3.36	5	96000	0.4	1.04×10^{-4}
19	6.84	10	25000	1.54	4×10^{-6}
20	10.44	15	25000	1.54	4×10^{-6}

Table 2.13; Quantities of CoBF required for branched pPEGMEMA polymerisations.

2.5.3.5 Iodometry bromination

Bromination-titration to yield bromine index (BI) was carried out as follows;

P(MAA-*co*-EGDMA) copolymer (0.2 g) was added to a solution of 9 mL of water, 0.5 mL methanol and 0.5 mL glacial acetic acid in a Erlenmeyer flask. The solution was stirred until dissolution of the copolymer before 50 mL of a solution containing $KBrO_3$ (0.1392 g, 0.834 mmol) and KBr (0.4960 g, 4.165 mmol) in a ratio of 1:5 (total salt concentration 0.1 M) was added. The mixture was stirred in the dark at room temperature for up to 6 hours, at which point the bromination of the vinyl groups was confirmed by ^{1}H NMR.

When bromination was complete the solution was cooled in an ice-water bath, 2 mL concentrated HCl added and the solution stirred for 30 minutes. Potassium iodide (1.5 g) was added and the solution stirred until homogeneous. This solution was titrated with a 0.1 M sodium thiosulfate solution until pale yellow, at which point 0.5 mL of 1 1t. % solution of starch in water was added to give a black solution. Further sodium thiosulfate was added, with the end point a colourless solution.

A "blank" titration, containing no polymer but identical solutions, was also carried out for use in calculation of BI.

Number of vinyl groups per gram was calculated using Bromine Index:

$$BI = \frac{7990 \cdot (V_1 - V_2) \cdot c}{m}$$

Where *BI* is the amount of bromine (mg) consumed by 100 g of polymer, V_1 and V_2 are the volume of $Na_2S_2O_3$ titrated in the blank and sample solutions, respectively; *c* is the concentration of $Na_2S_2O_3$ in moldm^{-3} and *m* is the mass of the polymer in grams.

2.5.4 Characterisation

Characterisation of 1-4. (**1**: linear PMAA with 15000 [MAA]/[CoBF]. **2**: linear PMAA with 25000 [MAA]/[CoBF]. **3**: linear PMAA with 32000 [MAA]/[CoBF]. **4 (5)**: linear PMAA with 64000 [MAA]/[CoBF].)

^{1}H-NMR (300 MHz, CD_3OD at 25 ^{o}C): δ 0.8-1.65 (backbone CH_3), 1.75-2.30 (backbone CH_2), 2.35-2.70 (terminal back bone $C\underline{H}_2$=C), 5.55-5.75 (*cis* to terminal CO_2H C=C$\underline{H}_a$H$_b$), 6.20-6.25 (*trans* to terminal CO_2H C=CH$_a\underline{H}_b$).

Conventional SEC (gmol^{-1}): **1**: M_n 2400, M_w 2380, Đ 1.29. **2**: M_n 2300, M_w 3160, Đ 1.17. **3**: M_n 2740, M_w 3930, Đ 1.17. **4 (5)**: M_n 4500, M_w 6202, Đ 1.38.

SEC-DRI-VISC Universal Calibration (gmol^{-1}): **1**: M_n 3300, M_w 5000, Đ 1.34, α 0.22. **2**: M_n 4230, M_w 5650, Đ 1.51, α 0.2. **3**: M_n 4560, M_w 6250, Đ 1.37, α 0.21. **5**: M_n 6940, M_w 9780, Đ 1.41, α 0.37.

GC-FID (final conversion, %): **1**: MAA 94 %, **2**: MAA 98 %, **3**: MAA 97 %, **4 (5)**: MAA 95 %.

Characterisation of 6-7. (**6**: P(MAA-*co*-EGDMA), 95/5 mol % MAA/EGDMA, [monomer]/[CoBF] 2500. **7**: P(MAA-*co*-EGDMA), 90/10 mol % MAA/EGDMA)

^{1}H-NMR (300 MHz, CD_3OD at 25 ^oC): δ 0.8-1.65 (backbone CH_3), 1.7-2.35 (backbone CH_2), 2.4-2.7 (terminal backbone $C\underline{H}_2$=C), 4.05-4.35 ($OC\underline{H}_2C\underline{H}_2O$), 5.55-5.75 (*cis* to terminal CO_2H C=$C\underline{H}_aCH_b$), 6.20-6.25 (*trans* to terminal CO_2H C=$CH_a\underline{H}_b$).

Conventional SEC ($gmol^{-1}$): **5**: M_n 3500, M_w 5702, Đ 1.65. **6**: M_n 10000, M_w 18000, Đ 1.8.

SEC-DRI-VISC Universal Calibration ($gmol^{-1}$): **5**: M_n 7250, M_w 12900, Đ 1.75, α 0.23. **6**: M_n 15700, M_w 58500, Đ 3.72, α 0.29.

GC-FID (final conversion, %): **5** MAA 91, EGDMA 96, total 92: **6**: MAA 91, EGDMA 97. 91.

Characterisation of 9-11. (**9**: P(MAA-*co*-EGDMA), 95/5 mol % MAA/EGDMA, [monomer]/[CoBF] 20500. **10**: P(MAA-*co*-EGDMA), 95/5 mol % MAA/EGDMA [monomer]/[CoBF]. **11:** P(MAA-*co*-EGDMA), 95/5 mol %)

^{1}H-NMR (300 MHz, CD_3OD at 25 ^oC): δ 0.8-1.65 (backbone CH_3), 1.7-2.35 (backbone CH_2), 2.4-2.7 (terminal backbone $C\underline{H}_2$=C), 4.05-4.35 ($OC\underline{H}_2C\underline{H}_2O$), 5.55-5.75 (*cis* to terminal CO_2H C=$C\underline{H}_aCH_b$), 6.20-6.25 (*trans* to terminal CO_2H C=$CH_a\underline{H}_b$).

Conventional SEC ($gmol^{-1}$): **9**: M_n 6540, M_w 8760, Đ 1.34. **10**: M_n 7960, M_w 13600, Đ 1.7. **11**: M_n 7510, M_w 14500, Đ 1.93.

SEC-DRI-VISC Universal Calibration ($gmol^{-1}$): **9**: M_n 7370, Mw 12900, Đ 1.75, α 0.23. **10**: M_n 7240, M_w 17600, Đ 2.43, α 0.27. **11**: M_n 13700, M_w 42600, Đ 3.12, α 0.35.

GC-FID (final conversion, %): **9** MAA 91, EGDMA 96, total 92: **10**: MAA 91, EGDMA 97. 91. **11** MAA, EGDMA, total.

Characterisation of 12-15. (**12**: linear p(PEGMEMA) with 25000 [PEGMEMA]/[CoBF]. **13**: linear p(PEGMEMA) with 32000 [PEGMEMA]/[CoBF]. **14**: linear p(PEGMEMA) with 64000 [PEGMEMA]/[CoBF]. **15**: linear p(PEGMEMA) with 96000 [PEGMEMA]/[CoBF]).

^{1}H-NMR (300 MHz, CD_3OD at 25 ^oC): δ 0.85-1.35 (backbone CH_3), 2.81-2.15 (backbone CH_2), 3.36 (terminal PEG CH_3), 3.51-3.78 (PEG backbone CH_2), 4.06-4.23 (PEGMEMA and EGDMA ether CH_2), 4.29 (monomeric and terminal ether CH_2), 5.56-5.79 (*cis* to terminal CO_2PEGMA C=C$\underline{H}_a H_b$), 6.07-6.36 (*trans* to terminal CO_2PEGMA C=C$H_a\underline{H}_b$).

Conventional SEC ($gmol^{-1}$): **12**: M_n 3230, M_w 4790, Đ 1.49. **13**: M_n 3800, M_w 5800, Đ 1.53. **14**: M_n 5910, M_w 9510, Đ 1.4. **15**: M_n 7430, M_w 12500, Đ 1.48.

SEC-DRI-VISC Universal Calibration ($gmol^{-1}$): **12**: M_n 3280, M_w 4330, Đ 1.32, α 0.13. **13**: M_n 4670, M_w 5520, Đ 1.18, α 0.24. **14**: M_n 5920, M_w 10900, Đ 1.85, α 0.23. **15**: M_n 9540, M_w 14700, Đ 1.54, α 0.46.

Characterisation of 16-21. (**15**: p(PEGMEMA -*co*-EGDMA), 95/5 mol % PEGMEMA /EGDMA, [monomer]/[CoBF] 25000. **16**: p(PEGMEMA -*co*-EGDMA), 95/5 mol % PEGMEMA/EGDMA, [monomer]/[CoBF] 32000. **16**: p(PEGMEMA-*co*-EGDMA), 95/5 mol % PEGMEMA/EGDMA, [monomer]/[CoBF] 64000. **18**: p(PEGMEMA-*co*-EGDMA), 95/5 mol % PEGMEMA/EGDMA, [monomer]/[CoBF] 96000. **19**: p(PEGMEMA-*co*-EGDMA), 90/10 mol % PEGMEMA/EGDMA, [monomer]/[CoBF] 25000. **20**: p(PEGMEMA-*co*-EGDMA), 85/15 mol % PEGMEMA/EGDMA, [monomer]/[CoBF] 25000).

^{1}H-NMR (300 MHz, $CHCl_3$ at 25 ^oC):δ 0.85-1.35 (backbone CH_3), 2.81-2.15 (backbone CH_2), 3.36 (terminal PEG CH_3), 3.51-3.78 (PEG backbone CH_2), 4.06-4.23 (PEGMEMA and EGDMA ether CH_2), 4.29 (monomeric and terminal ether CH_2), 5.56-5.79 (*cis* to terminal CO_2PEGMA C=C$\underline{H}_a H_b$), 6.07-6.36 (*trans* to terminal CO_2PEGMA C=C$H_a\underline{H}_b$).

Conventional SEC ($gmol^{-1}$): **15**: M_n 5750, M_w 8440, Đ 1.47. **16**: M_n 8260, M_w 13400, Đ 1.62. **17**: M_n 10200, M_w 18500, Đ 1.82. **18**: M_n 12300, M_w 23800, Đ 1.94. **19**: M_n 6020, M_w 9030, Đ 1.5. **20**: M_n 5510, M_w 10200, Đ 1.86.

SEC-DRI-VISC Universal Calibration ($gmol^{-1}$): **15**: M_n 6300, M_w 9300, Đ 1.47, α 0.30. **16**: M_n 5100, M_w 18500, Đ 3.63, α 0.45 **17**: M_n 13300, M_w 25600, Đ 1.93, α 0.39. **18**: M_n 21300, M_w 35600, Đ 1.67, α 0.49. **19**: M_n 7400, M_w 11900, Đ 1.6, α 0.25. **20**: M_n 7600, M_w 19400, Đ 1.56, α 0.19.

2.6 References

(1) Guan, Z. US5767211, **1998**.

(2) Haddleton, D. M.; Depaquis, E.; Kelly, E. J.; Kukulj, D.; Morsley, S. R.; Bon, S. A. F.; Eason, M. D.; Steward, A. G. *J. Polym. Sci., Part A: Polym. Chem.* **2001**, *39*, 2378.

(3) Gridnev, A. A.; Ittel, S. D. *Chem. Rev.* **2001**, *101*, 3611.

(4) Striegel, A., Yau W, Kirkland J, Bly D *Modern Size-Exclusion Chromatography: Practice of Gel Permeation and Gel Filtration Chromatography*; 2nd ed. Wiley & Sons. Inc,, 2009.

(5) Grubisic, Z.; Rempp, P.; Benoit, H. *J. Polym. Sci. B.* **1967**, *5*, 753.

(6) Guan, Z. *J. Am. Chem. Soc.* **2002**, *124*, 5616.

(7) Kostanski, L. K.; Keller, D. M.; Hamielec, A. E. *J. Biochem. Bioph. Meth.* **2004**, *58*, 159.

(8) Gaborieau, M.; Nicolas, J.; Save, M.; Charleux, B.; Vairon, J.-P.; Gilbert, R. G.; Castignolles, P. *J. Chromatogr. A* **2008**, *1190*, 215.

(9) Striegel, A. M. *Anal. Chem.* **2005**, *77*, 104 A.

(10) Dondos, A.; Benoit, H. *Polymer* **1977**, *18*, 1161.

(11) Zimm, B. H.; Stockmayer, W. H. *J. Chem. Phys.* **1949**, *17*, 1301.

(12) Zimm, B. H. *J. Chem. Phys.* **1948**, *16*, 1093.

(13) Zimm, B. H.; Kilb, R. W. *J. Polym. Sci.* **1959**, *37*, 19.

(14) Saunders, G.; Cormack, P. A. G.; Graham, S.; Sherrington, D. C. *Macromolecules.* **2005**, *38*, 6418.

(15) Ahn, S.; Lee, H.; Lee, S.; Chang, T. *Macromolecules.* **2012**, *45*, 3550.

(16) Moad, C. L.; Moad, G.; Rizzardo, E.; Thang, S. H. *Macromolecules.* **1996**, *29*, 7717.

(17) Heuts, J. P. A.; Davis, T. P.; Russell, G. T. *Macromolecules.* **1999**, *32*, 6019.

(18) Mayo, F. R. *J. Am. Chem. Soc.* **1943**, *65*, 2324.

(19) Heuts, J. P. A.; Smeets, N. M. B. *Polym. Chem.* **2011**, *2*, 2407.

(20) Godfrey, J., PhD Thesis, **2014**.

(21) Bakac, A.; Espenson, J. H. *J. Am. Chem. Soc.* **1984**, *106*, 5197.

(22) Gridnev, A. A. *Polym J* **1992**, *24*, 613.

(23) Haddleton, D. M.; Morsley, D. R.; O'Donnell, J. P.; Richards, S. N. *J. Polym. Sci., Part A: Polym. Chem.* **1999**, *37*, 3549.

(24) Trommsdorff, V. E.; Köhle, H.; Lagally, P. *Makromol. Chem.* **1948**, *1*, 169.

(25) Norrish, R.; Brookman, E. *Proc. R. Soc. London, Ser. A* **1939**, 147.

(26) Ferreira, J.; Syrett, J.; Whittaker, M.; Haddleton, D.; Davis, T. P.; Boyer, C. *Polym. Chem.* **2011**, *2*, 1671.

(27) Yang, X.; Zhu, L.-W.; Wan, L.-S.; Zhang, J.; Xu, Z.-K. *J. Mater. Res.* **2013**, *28*, 642.

(28) Smeets, N. M. B. *Eur. Polym. J.* **2013**, *49*, 2528.

(29) Soeriyadi, A. H.; Li, G.-Z.; Slavin, S.; Jones, M. W.; Amos, C. M.; Becer, C. R.; Whittaker, M. R.; Haddleton, D. M.; Boyer, C.; Davis, T. P. *Polym. Chem.* **2011**, *2*, 815.

(30) Engelis, N. G.; Anastasaki, A.; Nurumbetov, G.; Truong, N. P.; Nikolaou, V.; Shegiwal, A.; Whittaker, M. R.; Davis, T. P.; Haddleton, D. M. *Nat Chem* **2016**, *advance online publication*.

(31) Podobnik, B.; Helk, B.; Smilovic, V.; Skrajnar, S.; Fidler, K.; Jevsevar, S.; Godwin, A.; Williams, P. *Bioconjugate Chem.* **2015**, *26*, 452.

(32) Bakac, A.; Brynildson, M. E.; Espenson, J. H. *Inorg. Chem.* **1986**, *25*, 4108.

(33) Haddleton, D. M.; Maloney, D. R.; Suddaby, K. G.; Muir, A. V. G.; Richards, S. N. *Macromol. Symp.* **1996**, *111*, 37.

3. Synthesis and Characterisation of pHEA hydrogels

This chapter details the development of hydrogels synthesised from 2-hydroxyethyl acrylate (HEA). The aim was to synthesise hydrogels from HEA for potential to be used in wound care in combination with the branched polymers discussed in chapter 2. These polymers with their vinyl functionality are synthesised using the technique of catalytic chain transfer polymerisation (CCTP).

2-Hydroxyethyl acrylate is a well understood, hydrophilic monomer which, unlike its methacrylate analogue – 2-hydroxyethyl methacrylate (HEMA) – is water soluble in both monomeric and polymeric forms.[1] This can give rise to a gel that can swell to absorb far larger quantities of fluids than a pHEMA gel which has been used for such applications as contact lenses and other biological applications due to its medically approved status.[2] Thermal polymerisation was initially employed to form hydrogels and optimise the monomer and initiator concentrations before the selected gel system was transferred to photo-curing due to the reduced costs associated with a faster curing process and more consistent gel formation. Both of these systems are then utilised for the addition of branched polymers synthesised by CCTP and the monitoring of the swelling and rheological material properties.

3.1 Background

3.1.1 Hydrogel Swelling

Wound-care materials have to be capable of absorbing large quantities of exudate in order to keep the wound-site well drained and prevent the formation of biofilms.[3-8] As a result of this the extent to which a material can take up fluid and the rate or mechanism by which it does so are important factors in their design. There are two main areas for consideration in swelling; the thermodynamics of the swelling process, which is dependent upon the internal structure of the gel and the kinetics of the swelling process itself.[9,10]

Thermodynamics

The maximum extent to which a network can take up water is defined as the equilibrium degree of swelling, this is the point at which there is zero difference in the chemical potential between fluid inside and outside of the network. There are three other important factors; the first is the polymer volume fraction in the swollen state ($v_{2,s}$), the second is the molecular weight in the polymer chain between two cross-linking points (M_c) and the third is the mesh size (ζ) sometimes referred to as the correlation distance between two cross-link sites (**Figure 3.1**). $v_{2,s}$ is a measure of the amount of fluid imbibed by the network, M_c is a measure of the average degree of crosslinking and within the network and ζ is a measure of the average space between chains and crosslinking sites available for solute diffusion – a measure often used in the study of drug delivery. As this work is not concerned with drug delivery or targeted molecular diffusion, it was decided that the specific knowledge of $v_{2,s}$, ζ and M_c was not required.[9]

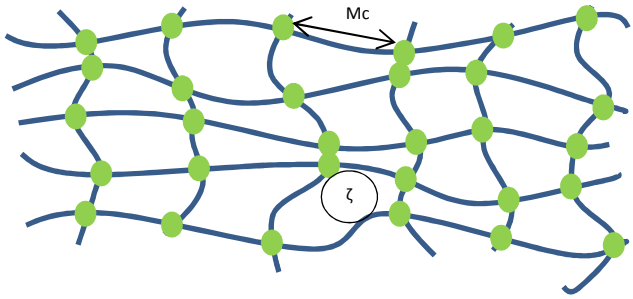

Figure 3.1; Cross-linked network showing cross-linking points, chains, average chain mesh size (ζ) and average distance between cross-linking points (M_c)

Swelling to equilibrium of a non-ionic gel (as is the case with pHEA) can be analysed using the Flory-Rehner theory.[11] This thermodynamic theory states that; a cross-linked network immersed in a fluid and allowed to reach equilibrium with its surroundings is subject to opposing forces; the entropic force of mixing (ΔG_{mixing}) and the enthalpic force associated with the elasticity of the polymer chains ($\Delta G_{elastic}$). At the equilibrium degree of swelling, these two forces are equal and are defined in **Equation 3.1** relative to the compatibility of the mixing of the network and the solvent (ΔG_{mixing}) which is often defined by the polymer-solvent interaction parameter X_1.

$$\Delta G_{Total} = \Delta G_{elastic} + \Delta G_{mixing}$$

Equation 3.1; Relationship between the total Gibbs free energy of relative to the energy of elasticity and mixing.[11]

If **Equation 3.1** is differentiated with respect to the number of solvent molecules whilst keeping temperature and pressure constant, **Equation 3.2** is given where $\Delta\mu$ is the chemical potential of the penetrating solvent.

$$\mu_1 - \mu_{1,0} = \Delta\mu_{elastic} + \Delta\mu_{mixing}$$

Equation 3.2; Chemical potential of the network at equilibrium described by the chemical potential of the solvent in the polymer network (μ_1) and the chemical potential of the pure solvent $\mu_{1,0}$.

When the network is at equilibrium, the chemical potential inside and outside of the gel must be equal and so the forces of mixing and elasticity must balance. When these two forces are equated an expression for the determination of M_c of a neutral network can be written (**Equation 3.3**), this is derived from the heat and entropy of mixing in the case of $\Delta\mu_{mixing}$ and from the theory of rubber elasticity for $\Delta\mu_{elastic}$. [12,13]

$$\frac{1}{M_C} = \frac{2}{M_n} - \frac{\left(v/V_1\right)\left[ln(1 - v_{2,s}) + v_{2,s} + X_1 v_{2,s}^2\right]}{v_{2,s}^{\frac{1}{3}} - \frac{v_{2,s}}{2}}$$

Equation 3.3; Definition of M_c from; the molecular weight of the polymer chains prepared under identical conditions without cross-linker (M_n), the specific volume of the polymer (v), the molar volume of water (V_1), $v_{2,s}$ and the polymer-solvent interaction parameter (X_1).

Equation 3.3 is a useful starting point, but Peppas and Merrill modified this to account for the relaxation of the polymer chains in the presence of water during the process of preparation (**Equation 3.4**). This modification accommodates the volume fraction of the chains during cross-linking and effectively predicts the M_C between crosslinks in neutral networks.

$$\frac{1}{M_C} = \frac{2}{M_n} - \frac{\left(v/V_1\right)\left[ln(1 - v_{2,s}) + v_{2,s} + X_1 v_{2,s}^2\right]}{v_{2,r}\left[\left(\frac{v_{2,s}}{v_{2,r}}\right)^{\frac{1}{3}} - \left(\frac{v_{2,s}}{2v_{2,r}}\right)\right]}$$

Equation 3.4; Definition of M_c taking into account the polymer volume fraction in relaxed state ($v_{2,r}$).

As some of the networks that will be tackled in this work are ionic, these networks have to be dealt with separately. Ionic networks require an additional free energy term ΔG_{ionic}, making the whole endeavour much more complex (**Equation 3.5**).[14,15]

$$\Delta G_{Total} = \Delta G_{elastic} + \Delta G_{mixing} + \Delta G_{ionic}$$

Equation 3.5; Relationship between the total Gibbs free energy of relative to the energy of elasticity, mixing and ionic interactions in an ionic network.

Equation 3.5 can be differentiated as with **Equation 3.1** to give **Equation 3.6**. The additional complexity coming as a result of the addition of the extra term is necessary as it takes into account the degree of ionisation of the polymer chains and the ionisation strength of the medium.

$$\mu_1 - \mu_{1,0} = \Delta\mu_{elastic} + \Delta\mu_{mixing} + \Delta\mu_{ionic}$$

Equation 3.6; Chemical potential of the network at equilibrium described by the chemical potential of the solvent in the polymer network (μ_1) and the chemical potential of the pure solvent $\mu_{1,0}$.

As a result of the strong dependency upon ionic strength not only of the charged network but of an ionic media, the analogous expressions for **Equation 3.4** for anionic and cationic networks prepared in the presence of a solvent are substantially more complex (**Equation 3.7** and **Equation 3.8**).

$$\frac{V_1}{4I}\left(\frac{v_{2,s}^2}{v}\right)\left(\frac{K_a}{10^{-pH} - K_a}\right)^2 = \left[ln\left(1 - v_{2,s}\right) + v_{2,s} + X_1 v_{2,s}^2\right] + \left(\frac{V_1}{vM_c}\right)\left(1 - \frac{2M_c}{M_n}\right)v_{2,r}\left[\left(\frac{v_{2,s}}{v_{2,r}}\right)^{\frac{1}{3}} - \left(\frac{v_{2,s}}{2v_{2,r}}\right)\right]$$

Equation 3.7; Expression for the swelling of anionic networks where I is the ionic strength and K_a is the dissociation constant for acid.[16]

$$\frac{V_1}{4I}\left(\frac{v_{2,s}^2}{v}\right)\left(\frac{K_b}{10^{pH-14}-K_a}\right)^2 = \left[ln\left(1-v_{2,s}\right)+v_{2,s}+X_1 v_{2,s}^2\right] + \left(\frac{V_1}{vM_c}\right)\left(1-\frac{2M_c}{M_n}\right)v_{2,r}\left[\left(\frac{v_{2,s}}{v_{2,r}}\right)^{\frac{1}{3}}-\left(\frac{v_{2,s}}{2v_{2,r}}\right)\right]$$

Equation 3.8; Expression for the swelling of cationic networks where K_b is the dissociation constant for base.

When combined, these equations allow for the quantification of the structure of both neutral and ionic networks.

Kinetics

There are three principle mechanisms for the process of swelling – or transition of a network from an unsolvated glassy or rubbery state to a relaxed rubbery state – this transition is highly dependent upon the thermal properties of the network.

In rubbery networks – those that exhibit a T_g well below the temperature of the medium – a form of transport labelled as Fickian or Case 1 is observed. In this mode the chains have a high degree of mobility and the water can penetrate easily into the network, this means that the limiting step in swelling is the osmotic diffusion of water into the system. The rate of diffusion R_{diff} is significantly lower than the rate of relaxation R_{relax} ($R_{diff} << R_{relax}$). This manifests as a linear increase in the network weight as a function of the square root of time.[10,17]

In glassy networks – those that exhibit a T_g well above the temperature of the medium – a form of transport labelled as non-Fickian or Case 2 is observed. In this mode the chains have a low degree of mobility and water ingresses slowly into the network. In

this case the limiting step to swelling is the chain mobility rather than osmotic diffusion and the relationship relative to time is linear.[10,17,18]

The final form of transport is known as Anomalous transport, this occurs when the rates of diffusion and relaxation are comparable. The modelling of this behaviour generally makes use of Fick's law with modified parameters for non-Fickian behaviour. The relationship relative to time in this case varies from the square root of time to a linear relationship.[19]

Power law equations are the most common way of determining the mechanism of diffusion in a polymeric network.[20,21] The simplest of these can be seen in **Equation 3.9**;

$$\frac{M_t}{M_\infty} = kt^n$$

Equation 3.9; Power law equation describing the diffusion mechanism of polymeric networks. M_t describes the swollen mass at time t, M_∞ describes the equilibrium swollen mass, k and n are characteristic of the solvent polymer system where n is the diffusional exponent.

By determining the diffusional coefficient, n, the mechanism for solute diffusion can be deduced. When n = 0.5 Fickian diffusion is intimated, 0.5 < n < 1.0 indicates anomalous transport and n = 1.0 indicates non-Fickian (relaxation controlled) transport is implied. Although **Equation 3.9** is effective at describing the majority of swelling behaviour of a network, it fails above M_t/M_∞ = 0.60. Above 0.60 the integral of the Berens-hopfenberg differential equation (**Equation 3.10)** is applied.[22]

$$\frac{M_t}{M_\infty} = (1 - Ae^{-k_2 t})$$

Equation 3.10; Integral of the Berens-Hopfenberg differential equation where k_2 (min^{-1}) is the relaxation rate constant (for the network) and A is a constant.

From **Equation 3.10** a plot of $\ln(1-M_t/M_\infty)$ versus t at times later than $M_t/M_\infty = 0.60$ can be used to determine the mechanism of network diffusion.[22]

3.1.2 Hydrogel Rheology

Rheology is used to define viscoelastic properties across a vast range of materials. Rheology is derived from the Greek *rheos* meaning stream and is precisely defined as;

"The study of the deformation and flow of matter, especially the non-Newtonian flow of liquids and the plastic flow of solids".[23]

An applied measure of stress causes a response in both in terms of deformation and elastic recovery of that deformation upon the removal of the stress. The level of deformation (or energy required to deform the material by a set amount) and elastic recovery depend upon the state and properties of the material. A liquid would be expected to deform without recovery displaying viscous properties either in a Newtonian or non-Newtonian manner. A solid would be expected to deform before recovering some of the deformation when force is removed exhibiting an elastic response. Some materials, however, exhibit viscoelastic behaviour – somewhere between a liquids viscous behaviour and a solids elastic behaviour.[23,24]

Stress and Strain

Stress (σ) on a material is defined as the Force (F) applied per unit of initial area (A_0) (Equation 3.11), this in turn elicits a deformation or strain (γ) defined as the ratio of

the change in dimensions relative to the original dimensions (Equation 3.12). As a result of this ratio there are no units for strain and it is normally expressed as a percentage.

$$\sigma = \frac{F}{A_0}$$

Equation 3.11; Definition of stress (σ) as a function of Force (F) in Newtons per area of sample (A_0)

$$\gamma = \frac{dx}{dy}$$

Equation 3.12; Definition of Strain (γ) as a function of the ratio of change of x direction relative to y direction.

A rotational rheometer (**Figure 3.2**) is slightly more complex as the shear force is a displacement gradient acting parallel to the fixed face unlike a tensile deformation which is applied perpendicular to the fixed face. In the shear model, when one plate moves distance, dx, the sample is subjected to strain γ, the velocity of the plate V_x and a shear rate (**Equation 3.13)**.

$$V_x = \frac{dx}{dt}$$

Equation 3.13; Definition of the velocity of the plate (Vx) as a function of the ratio of change in x direction (dx) relative to time (dt).

$$Shear\ rate\ \gamma = \frac{d(\frac{dx}{dy})}{dt}$$

Equation 3.14; Definition of the shear rate (γ) as a function of the ratio of change in dimensions relative to change in time.

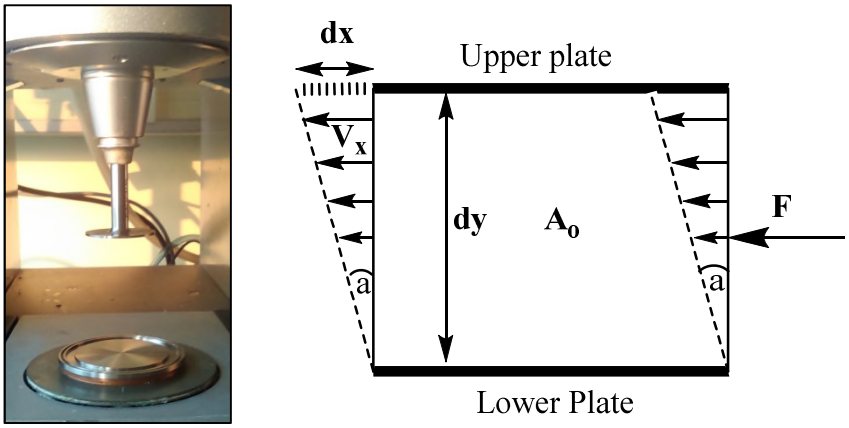

Figure 3.2; A parallel plate set up for a rotational rheometer (left), Shear stress as applied in an idealised cross-sectional parallel plate geometry (right).

The shear modulus of a material G can be defined as the ratio of stress to strain (**Equation 3.15**). This is analogous to the expression of the viscosity of a liquid (η) which can similarly be defined as the ratio of stress to strain rate (**Equation 3.16**).

$$Shear\ modulus\ G = \frac{\sigma}{\gamma} = \frac{(\frac{F}{A_0})}{\tan\alpha}$$

At low amplitude tan α ≈ α and so the shear modulus can be defined as

$$Shear\ modulus\ G = \frac{\sigma}{\gamma} = \frac{F}{A_0 a}$$

Equation 3.15; Definition of the shear modulus (G) as a function of stress and strain

$$\sigma = \eta\boldsymbol{\gamma}$$

Equation 3.16; Relationship between viscosity (η) stress and strain

Measurements can either be stress determined – where the strain resulting from stress is measured, or it can often be more appropriate to measure the force required to commit to a certain degree of strain – a strain controlled instrument. The modulus and viscosity of a material should always be measured in the linear viscoelastic region (LVER explained below) to ensure consistency in results.

Viscous and elastic response.

Materials are able to act as either a solid or a liquid depending upon the time scale of their response. At extremely long time scales a solid material may act as a liquid (10^{65} years for rock), conversely at extremely short time scales a liquid may act as a solid (10^{-8} s for water).[25] As a consequence most materials can be defined as viscoelastic within their own time scales. The LVER of a material is the region in which the modulus is independent of the magnitude of the strain – where there is a directly proportional and linear relationship between the stress applied and the strain resulting from the application of said stress (**Figure 3.3**).[23]

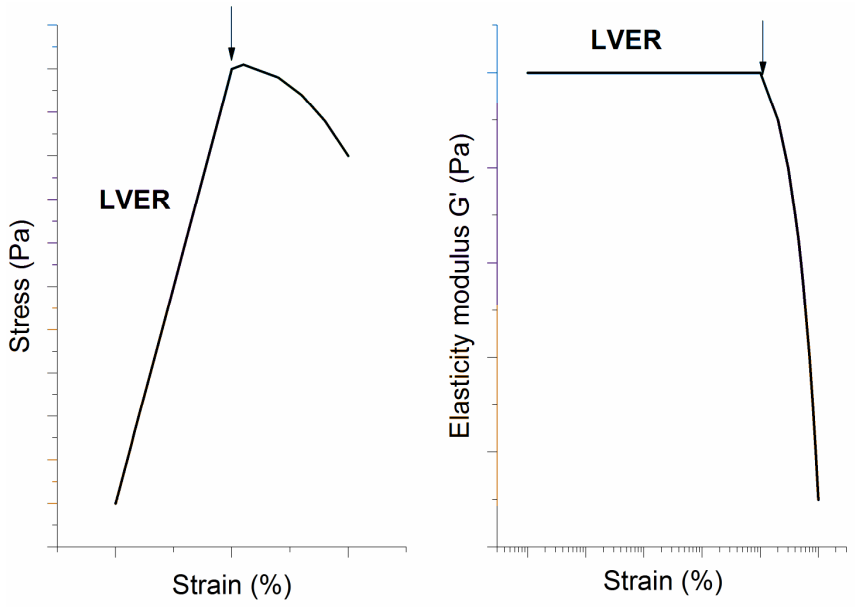

Figure 3.3; Stress vs strain graph showing the LVER, arrow indicates end of the LVER (left). G' vs Strain graph showing LVER, arrow indicates end of the LVER (right).

Viscous flow requires the flow of energy through friction and heat, however elasticity involves the storage of energy thus allowing the material to recover the deformation once force is removed.[26] In oscillatory rheology a sinusoidal wave is applied with a time-varying maximum strain (or amplitude, γ_M), where oscillatory – or angular –

frequency (ω) is applied using a parallel plate. If the material is perfectly elastic then the resulting stress wave will be exactly in phase with the strain wave (for example; steel at low strain). Conversely, if the rate of change of the sinusoidal wave oscillation of stress is a maximum and the strain wave is zero (for example glycerol), this describes a purely viscous system where the stress wave will be exactly 90° out-of-phase from the imposed deformation. The difference in the stress and strain wave can be described using the phase angle (δ) which varies between 0 and 90° as shown in **Figure 3.4**.

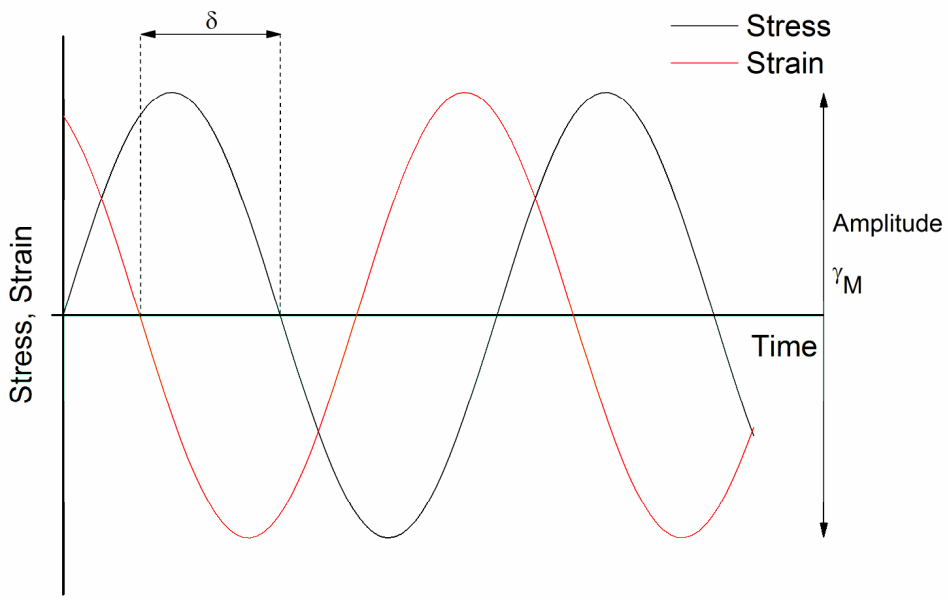

Figure 3.4; Sinusoidal waves of stress and strain created by an oscillatory rheometer upon a viscoelastic fluid with phase angle δ and amplitude γ_M.

The phase angle is a reflection of the ratio of the elastic (in phase) component to the viscous (out of phase component), these components yield an in-phase shear storage modulus G' and an out-of-phase shear loss modulus G'' which can be defined by Equation 3.17;

$$G^* = \frac{\tau^*}{\gamma_M} = (G'^2 + G''^2)^{1/2} \; or \; G' + iG''$$

Equation 3.17; Complex shear modulus G^* resolved to the storage and loss moduli with τ^* representing the complex stress and γ_M representing the maximum amplitude.

Rather than express the phase angle as δ it is more regularly discussed in terms of the loss tangent or tan δ, which is defined as the ratio of the viscous and elastic components as shown in **Equation 3.18**;

$$\tan\delta = \frac{G''}{G'}$$

Equation 3.18; Loss tangent as a function of the phase angle δ or the dynamic loss and storage moduli G'' and G' respectively.

In this case when tan δ >> 1 then the material is behaving as a liquid, when tan δ << 1 then it is behaving as a solid.

The method of rheology can be applied to polymer gels to determine the rigidity of the material in the linear viscoelastic region explained above. This gives an understanding of the workability and toughness of the material under different conditions i.e. levels of cross-liking, levels of hydration and so forth.[24,27]

3.1.3 pHEA hydrogels

Due to its toxicity 2-hydroxyethyl acrylate (HEA) has seen very limited uptake as a hydrogel in any applications, to the best of my knowledge there has been a very limited number of papers published utilising HEA in hydrogels.[1,28-31] 2-Hydroxyethyl methacrylate, unlike its acrylate congener has a long history of use in hydrogels, however, it suffers from a chronic lack of solubility in the polymeric form, HEA

however, has no such problems and as a polymer has seen application due to its hydrophilicity.

3.2 Synthesis and Characterisation of pHEA hydrogels

Hydrogels are highly desirable due to their material properties and also because of the ease at which they can be formed from simple monomeric precursor materials, in facile one step processes. Free radical polymerisation is by far the most common method for the synthesis of hydrogels, in particular chemical hydrogels. Free radical initiation is normally initiated through thermal, redox or photo based reactions. In this work thermal and photo polymerisations are optimised and employed in the synthesis of pHEA hydrogels using the latent EGDA impurity found in standard monomer supply.

Thermal initiation is instigated through a process in which the thermal energy of the environment (in this case an oven) in which the initiating species is located exceeds the bond dissociation energy of the molecule, this leads to homolytic bond cleavage and the generation of two radical species (**Scheme 3.1**).

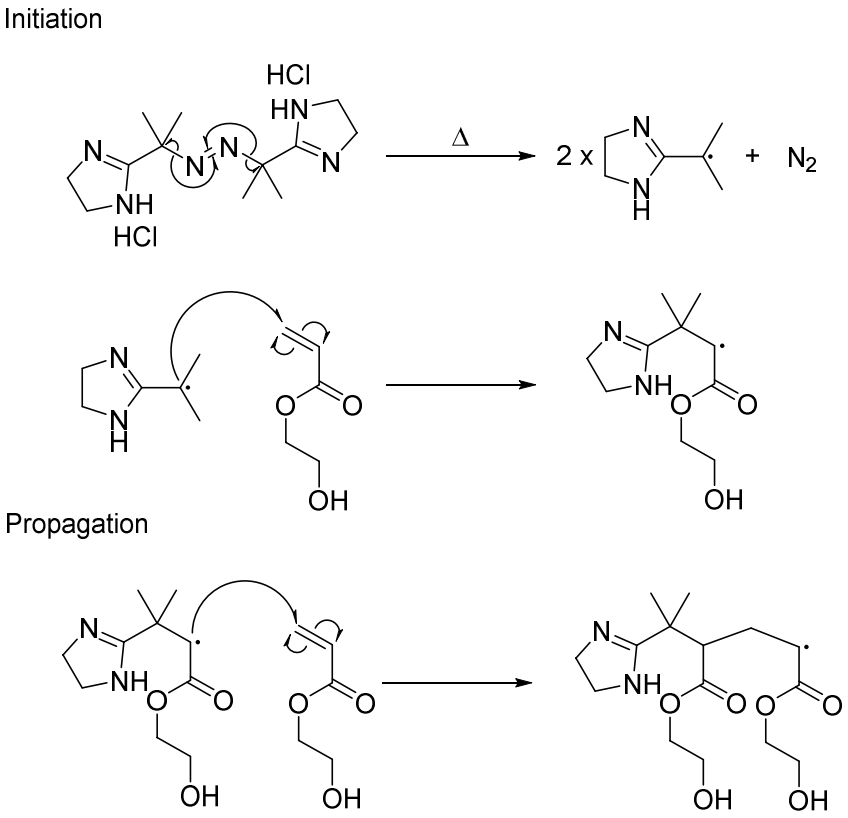

Scheme 3.1; Mechanism of thermal initiation and propagation of HEA monomer

The most significant variables that require tuning in the thermal system are;

- Casting and curing system
- Concentration of cross-linker
- Monomer: solvent ratio
- Type of initiator
- Concentration of initiator
- Temperature of initiation

A sealed casting system into silicon moulds was chosen due to ease of use and the concentration of cross-linker was fixed by the monomer mixture provided at 0.5 mol % of monomer concentration and remained stable for over 2 months over the course of

the study as monitored by GC-FID. A water soluble azo initiator was desirable in this system due to the relatively low costs of azo initiators, their widespread use across industry and their ease of use, handling and storage. From the range of water soluble azide initiators available, VA-044 (**Scheme 3.1**) has a half-life of 10 hours at 44°C,[30] allowing for a relatively slow rate of initiation, in order to prevent the build-up of an exotherm that would potentially lead to the early onset of the gel effect encapsulating unreacted monomer and reducing yield.[32]

3.2.1 Optimisation of thermal polymerisation of pHEA hydrogels

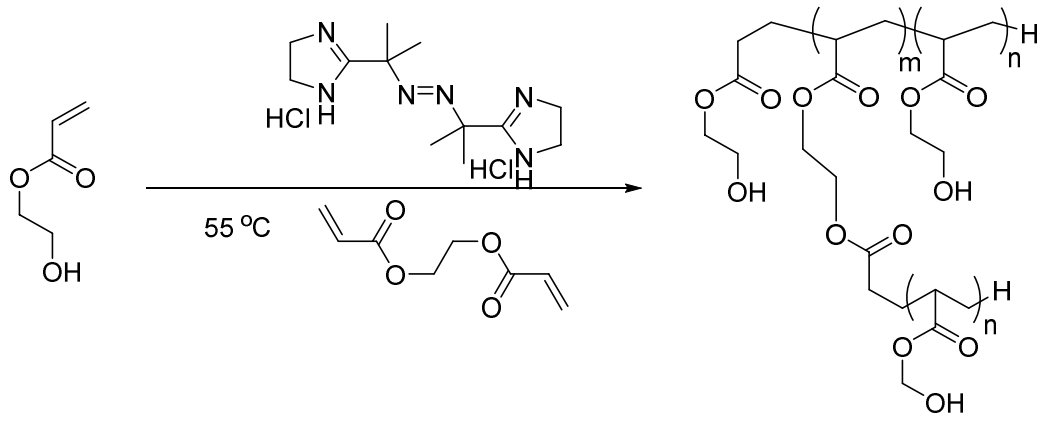

Figure 3.5; Thermal polymerisation of 2-hydroxyethyl acrylate

Since hydrogels synthesised using 2-hydroxyethyl acrylate (HEA) are not widely reported in the literature, the first study required was to optimise the conditions of gelation.[1] Initially thermal polymerisation was explored as a facile route to develop consistent hydrogels that could easily be up-scaled within an industrial scenario to save cost. The two crucial elements identified for initial optimisation with an open cast and cure technique were the concentration of the monomer and initiator respectively. The cross-linker concentration was kept at a constant 0.5 mol % relative to monomer throughout. Initially the concentration of initiator was varied between 0.25 and 1 wt.

% relative to the monomer at a fixed monomer concentration of 30 wt. % of the total content however, in this system no gelation was observed below 0.5 wt. % initiator. The monomer solutions were allowed to polymerise at 60 °C for 16 hours allowing for the initiator (VA-044) to be better utilised in the available conditions.

Reaction	[Monomer] (wt. %)	[Initiator] (wt. %)[a]	Degree of Swelling (%)[b]	G' from amplitude sweep (Pa)[c]	G' from frequency sweep (Pa)[d]
1	30	0.5	1250 (±60)	10040 (±100)	8940 (±1090)
2	30	1.0	1220 (±260)	10200 (±380)	8810 (±1010)
3	40	0.5	1070 (±110)	17430 (±990)	15600 (±6200)
4	50	0.5	1110 (±130)	25600 (±1630)	18420 (±2840)

Table 3.1; Showing material properties of hydrogels; [a] wt. % relative to monomer, b swelling from wet samples, dry weight determined gravimetrically, [c] G' at 1% strain and 10 Hz, [d] G' at 1 Hz.

Hydrogels produced using this method were initially tested by two methods; swelling to equilibrium in deionised water and definition of their linear viscoelastic regions by small oscillation shear rheology. Monitoring the kinetics of the swelling process with variation of initiator concentration revealed a process of swelling to equilibrium taking just over 2 hours. This relatively slow rate of uptake in comparison to the networks described in Chapter 5 is indicative of a swelling process controlled primarily by the rate of relaxation of the polymer network into the solvent rather than solvent uptake into the network. This would be described as non-Fickian where there is a non-linear relationship between a plot of M_t/M_∞ vs $t^{1/2}$ as described in **Equation 3.9** and is confirmed in previous work by Pissis *et al*.[1,28] This is caused primarily by the nano-scale pore size of the networks and the observation that sorption is dominated by the entropic process of mixing the networks to an optimal random coil state rather than the enthalpic elasticity component.[28]

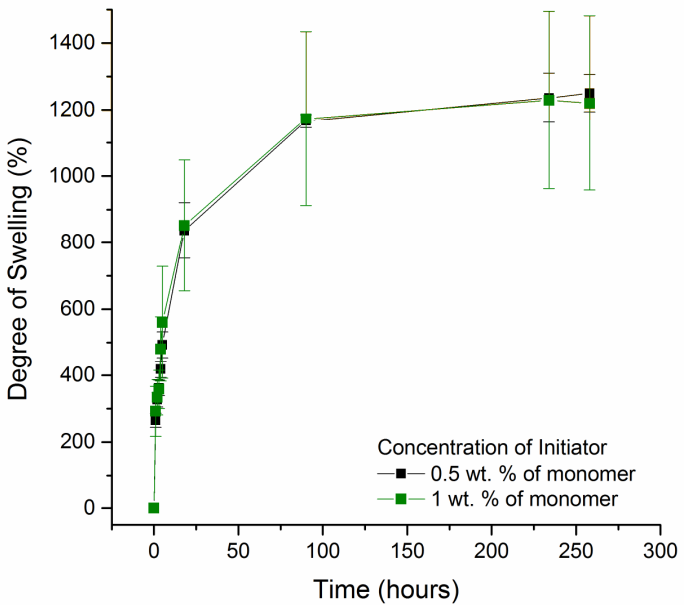

Figure 3.6; Water swelling kinetics for pHEA using two different initial concentrations of initiator.

When testing the effect of variation of the concentration of initiator upon rate and degree of swelling there are two observations; firstly there is no discernible difference in mean equilibrium degree of swelling or rate of swelling, secondly the hydrogels produced at 1 wt. % of initiator exhibited a far higher degree of error associated with the readings (**Figure 3.6**). The first observation shows that these materials must have very similar average mesh sizes, an observation backed up by the rheology data (**Figure 3.7**) where, an increase in the elasticity modulus would have implied a decrease in the mesh size due to increased rigidity. However, the significant degree of error associated with the increase in concentration of initiator suggests that the materials produced with 1 wt. % of initiator may be have significant variation in internal structure and so would be inferior in quality and consistency. One reason for this is that with higher concentrations of initiator, there is a much higher initial concentration of radicals leading to a far higher initial rate of polymerisation and an exotherm associated with

this can caused the formation of macro-defects on the surface of the gel, this can significantly affect the rate of fluid uptake on the surface of the gels.

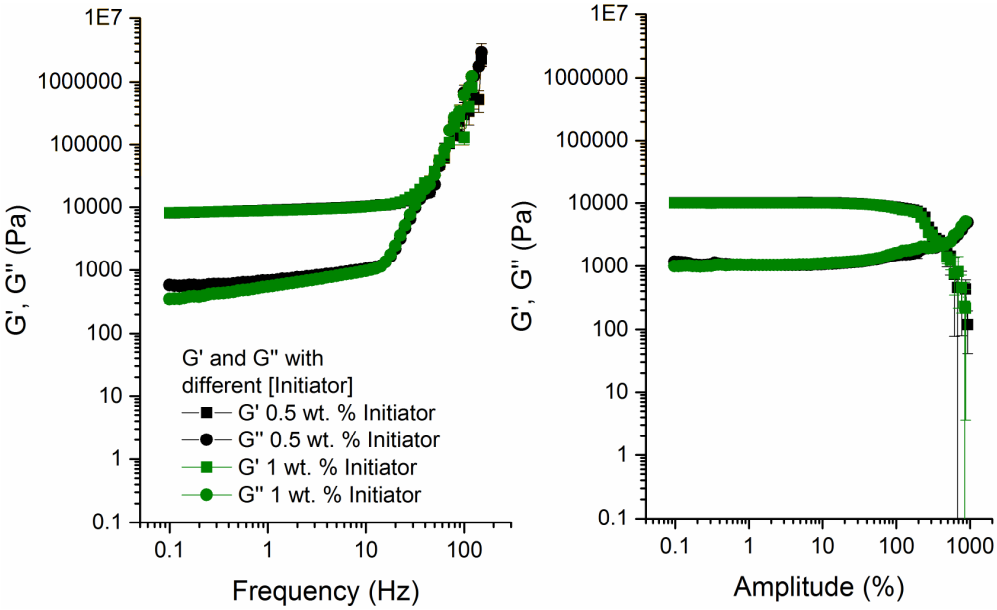

Figure 3.7; The LVER of pHEA hydrogels relative to frequency between 0.1 and 200 Hz with a fixed strain of 1 % at 25 °C (left), the LVER relative to amplitude between 0.1 and 1000 % strain at 1 Hz and 25 °C (right).

Rheological examination of the materials formed from variation in the concentration of initiator show no discernible impact upon the values of the elasticity modulus G' of the pHEA gels, which supports the idea that there has been no overall impact upon the average pore size (**Figure 3.7**). With a larger pore size one would expect to observe a decrease in the value of G' as the rigidity of the material decreases, conversely, an increase in the value of G' would indicate a decrease in the pore size.

Having determined that an initiator concentration of 0.5 wt. % relative to the monomer gave the most consistent results the concentration of the monomer was then varied to determine the optimum concentration. With pHEMA the hydrogels are normally limited to high polymer weight contents of 40 wt. % or above due to the hydrophobicity of pHEMA (which can lead to precipitation of polymer from the

reaction solution prior to gelation and effectively terminating the chain end),[2,33] pHEA hydrogels are not so constrained. Initial testing showed that above 20 wt. % hydrogels could be formed using this thermal polymerisation method (**Figure 3.8**). Materials with concentrations of 30, 40 and 50 wt. % of monomer relative to total reaction mixture were also tested to observe the effects upon properties in this system.

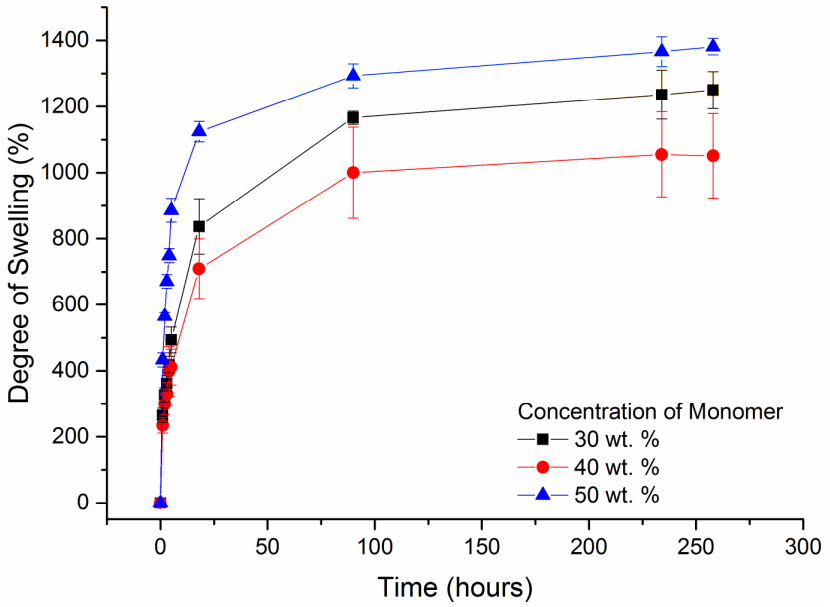

Figure 3.8; The effect upon swelling of variation in the concentration of monomer relative to water.

A decrease in the equilibrium degree of swelling was observed with increasing concentration of the HEA monomer from 30 to 40 wt. % (**Figure 3.8)** indicating that there is a corresponding decrease in the mesh size, limiting the uptake of fluid into the networks. These networks were also studied for their response to shear force by rheology in order to define the relative rigidity and stability of the materials.

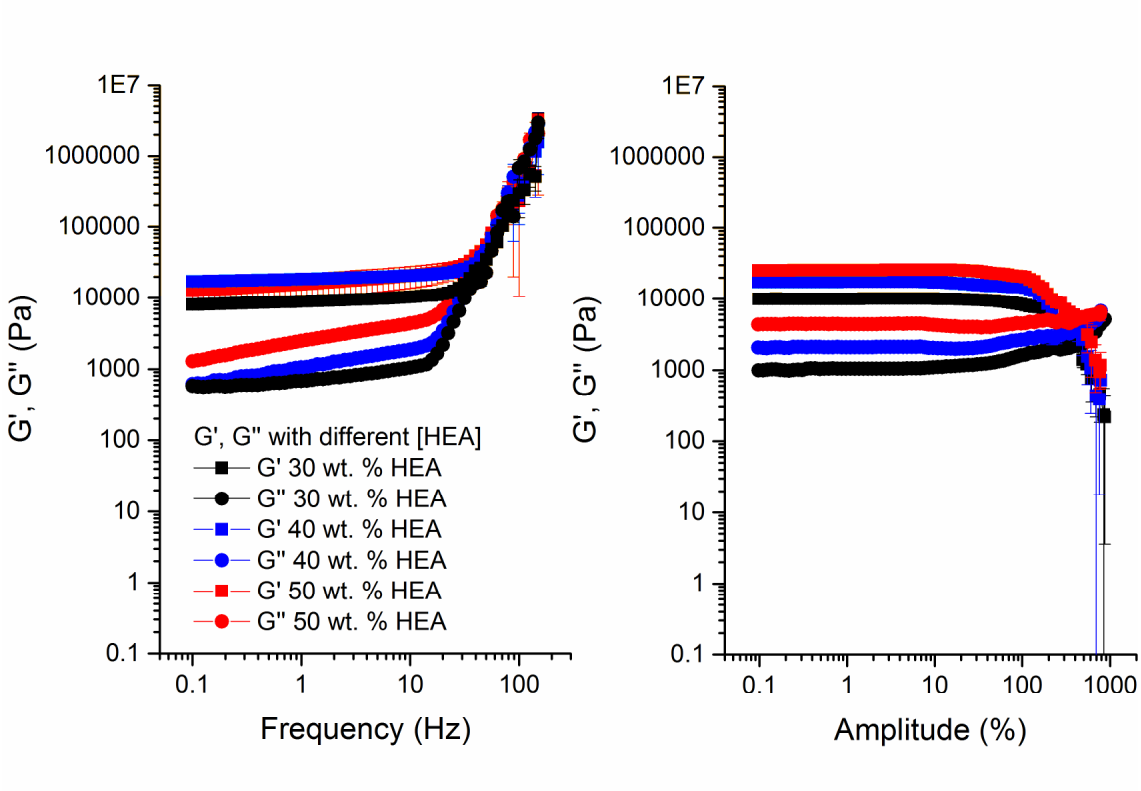

Figure 3.9; Frequency sweep of pHEA hydrogels at different monomer concentrations defining the LVER (left), amplitude sweep of pHEA hydrogels at different monomer concentrations defining the LVER (right).

The impact of the change in the weight % of monomer in the hydrogels upon the LVER of the resulting hydrogels defined with respect to frequency and amplitude under ambient conditions was plotted (**Figure 3.9**), from this two principle observations can be made. Firstly with increasing weight content of monomer in the hydrogels an increase in the value of G' was observed, secondly there is an increase in the error at higher weight content polymer in the hydrogel. The first observation can be explained as an increase in rigidity directly corresponds to a decrease in the pore size of the hydrogel.[26] The second observation derives from the presence of macro defects on the surface of the hydrogel, visible with the naked eye, representing regions of heterogeneity in the samples and therefore inconsistency between samples. For this reason and swelling results the 50 wt. % monomer content in hydrogel was discarded.

30 wt. % was chosen as the optimal monomer content due to the greater reproducibility observed in the material in both swelling and rheology.

Having optimised the composition of the thermal polymerisation of HEA to form a gel, the next step was the addition of CCTP p(MAA-*co*-EGDMA) polymers as an additive and a cross-linker.

3.2.2 Addition of branched polyacids

It has previously been found that the addition of MAA-based polymer has improved the effectiveness of a network for drug delivery due to their ionic character and their pH sensitivity,[34-36] it has also been found that dendritic and branched materials can have a positive influence upon a networks' material properties.[37,38] This research desired to use branched acidic polymers synthesised by catalytic chain transfer polymerisation (CCTP) as an active additive in the hydrogels optimised above. The synthesis and characterisation of these polymers can be found in Chapter 2. The initial branched material chosen for this experiment was the low molecular weight (<20 kDa) species **A** shown in **Table 3.2**.

Compound	[Monomer]/ [CoBF]	[EGDMA] (mol %)	Mwα ($gmol^{-1}$)	Đ[a]	α[a]	Conversion (%)[b]
A	20500:1	5	12900	1.75	0.23	93

Table 3.2; Characterisation of the branched acid used in hydrogel. [a] Measured by SEC-UC with 2 x PLgel mixed D columns, calibrated with PMMA standards with DMF (5 mmol NH_4BF_4) as eluent. [b] Measured by GC-FID.

Compound **A** was added to the previously optimised pHEA hydrogel prior to curing, the initial tests looked at the effect of variation of the concentration of the branched

polymer upon swelling and rheological results, the results of which can be seen in **Table 3.3**.

Reaction	[Branched acid polymer] wt. %[a]	Degree of Swelling (%)b	G' from frequency sweep (Pa)[c]
1	0	1250 (±60)	8940 (±1090)
5	0.5	920 (±10)	14300 (±2300)
6	1	870 (±10)	9990 (±7180)
7	2.5	780 (±10)	7240 (±5210)
8	5	607 (±90)	5390 (±6400)

Table 3.3; Material properties of synthesised hydrogels; [a] wt. % relative to total [monomer], [b] swelling from wet samples, dry weight determined gravimetrically, [c] G' at 1% strain and 1 Hz.

As the swelling profile in deionised water followed the same general kinetic trends as the materials shown in **Figure 3.8** with no significant deviation in its relationship to time (indicating a non-Fickian swelling profile),[9] **Figure 3.10** and **Table 3.3** are only concerned with showing the final equilibrium swelling ratios at 150 hours. These results show that with increasing concentration of branched acid polymer there is a decrease in the degree of swelling (**Figure 3.10**). This is indicative of the branched polymers utilising their ω-vinyl functionality to act as cross-linkers and thus decrease the mesh size of the networks which in turn decreases the equilibrium swelling ratio achievable by these materials. Increasing the concentration of branched polymer clearly has a significant effect upon the degree of swelling (**Figure 3.10**) with a reduced equilibrium degree of swelling corresponding with a decrease in the value of G' implying that a decrease in the mesh size isn't the only cause as this would cause an increase in the value of G'. The reduction in the value of G' can be attributed to the parallel increase in the rate of chain transfer creating more heterogeneous networks.

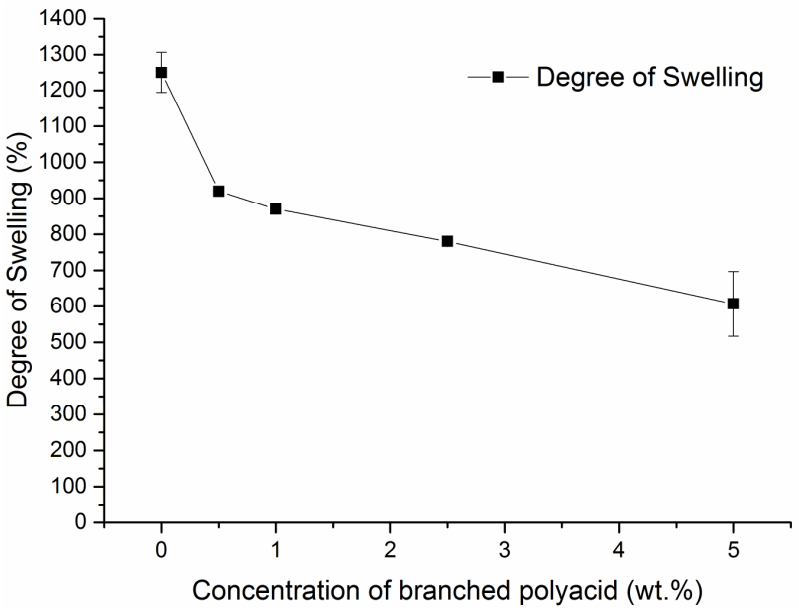

Figure 3.10; Effect of concentration of branched polyacid upon the equilibrium degree of swelling of the hydrogel

Due to the inclusion of methacrylic acid, it was also considered possible that a pH responsive characteristic could be imparted to the materials from the acid's ionisation.[39,40] pMAA has a pKa of 4.66, above the pH of 4.66 significant ionisation can lead to a large increase in ionic repulsion. This manifests in materials through an increase in the degree of swelling above this pH.[39,41] This effect was investigated by subjecting the materials with a fixed concentration of branched acid (0.5 wt. %) to different pH of buffer solution and swelling to equilibrium and comparing to a control without branched acid (**Figure 3.11)**.

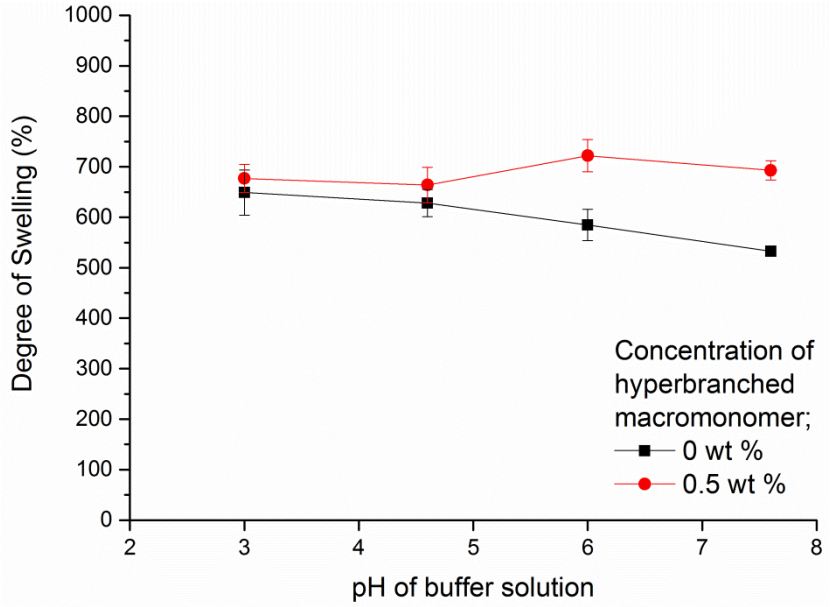

Figure 3.11; Effect of increasing pH upon the degree of swelling of pHEA hydrogels with and without branched polyacid included.

Addition of hydrogels with 0.5 wt. % **A** to solutions with different pH buffer solutions shows that with a pH < 6, the material containing branched acid remains comparable to the material without branched acid, above a pH of 6 there is a significant relative increase in the degree of swelling of the material with the branched acid relative to the material without (**Figure 3.11**). This is most likely due to ionisation of the methacrylic acid leading to greater uptake of free water through coordination to the acid groups according to **Equation 3.7**.

The effect of adding the branched acid polymer upon the rheological characteristics of the gels was also studied. Cured networks with branched acid polymer at 0.5 wt. % were compared to networks without branched acid polymer through a frequency and amplitude sweep used to define the viscoelastic region of the materials. The results of which can be seen in **Table 3.3** and **Figure 3.12**.

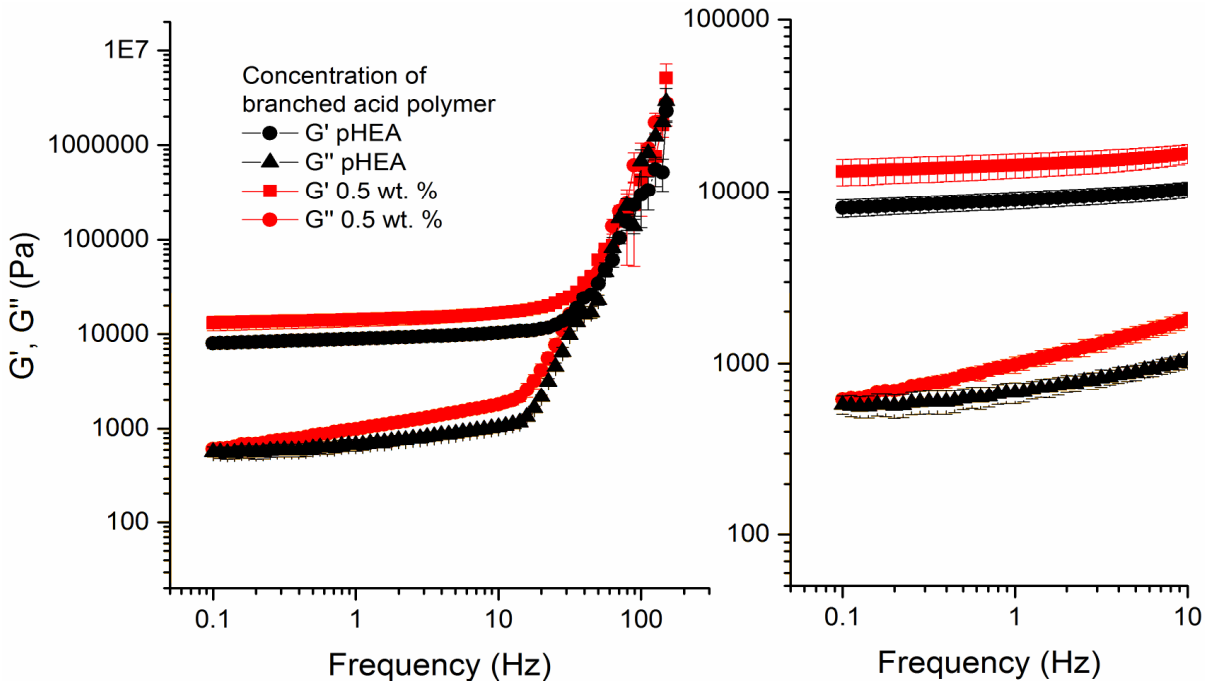

Figure 3.12; Comparison of optimised pHEA hydrogel vs hydrogel with 0.5 wt. % of branched polymer content (left), linear viscoelastic region (right).

The addition of the branched acid polymer significantly increases the value of G' within the LVER as defined by frequency and amplitude at 1 Hz and 1 % strain (**Figure 3.12**). This lends credence to the hypothesis that the branched acid polymers are acting as cross-linking agents in these networks as an increase in the value of G' shows an increase in the rigidity of the material, which in turn is indicative that the materials have a decreased mesh size.

Unfortunately increasing the concentration of branched acid polymers above 5 wt. % of total monomer content creates inhomogeneous materials and also significantly increases the degree of error in the rheological measurements. It was thought to be as a result of chain transfer from to the ω-vinyl groups generated by CCTP – something that has been previously observed.[42] This effect is explored more thoroughly in Chapter 4.

3.2.3 Photo polymerisation of pHEA hydrogels

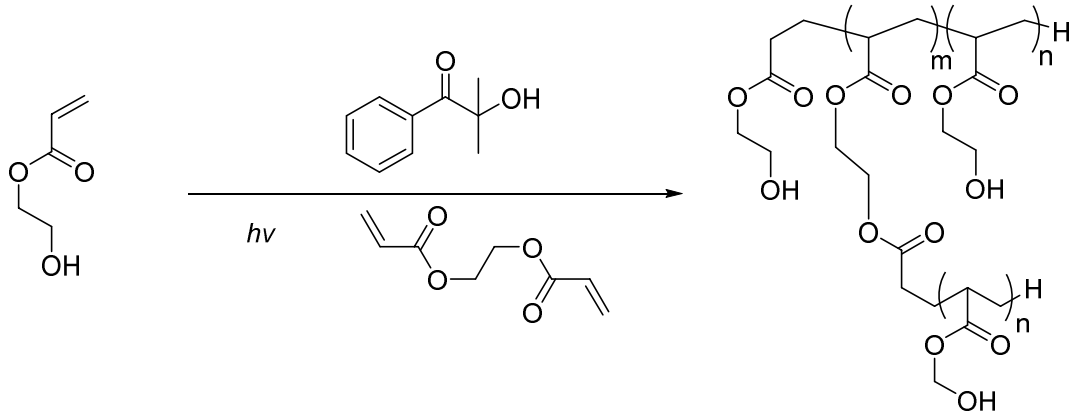

Scheme 3.2; Photopolymerisation of 2-hydroxyethyl acrylate

Thermally initiated polymerisation of hydrogels can be an inherently slow process that typically require temperatures above ambient conditions, leading to evaporation of solvent. In order to counteract this, a photo-polymerisation system was developed and optimised for the synthesis of pHEA monoliths and then compared to the thermal networks previously developed. Previous work by Guan, indicated the potential applications of branched polymers generated by CCTP for photo-curing processes, as a result, it was thought the higher radical concentrations associated with photo-polymerisation may lead to the inclusion of the branched polymers in the curing process as gelators.[43] Branched polymers of the species **A** were then added to observe differences in the effects of their addition in comparison to the thermal system, the results of the testing of these materials can be seen in **Table 3.4**.

Reaction	Polymerisation system	[Branched acid polymer] wt. %[a]	Degree of Swelling (%)[b]	G' from frequency sweep (Pa)[c]
1	Thermal	0	1250 (± 60)	8940 (± 1090)
5	Thermal	0.5	920 (± 10)	14300 (± 2310)
9	Photo	0	1400 (± 40)	950 (± 120)
10	Photo	0.5	1450 (± 40)	210 (± 50)
11	Photo	1	3420 (± 30)	260 (±30)

Table 3.4; Showing material properties of hydrogels; [a] wt. % relative to monomer, [b] swelling from wet samples, dry weight determined gravimetrically, [c] G' at 1% strain and 10 Hz, δ G' at 1 Hz.

Initially the reaction system was adapted for photo-polymerisation; a similar set-up was utilised with open cast moulding and premixing of the reactants in the absence of light, this was followed by photo-polymerisation of the same volume of reactants using a *light hammer™* UV source. The *light hammer™* is designed to emit UV light across a very broad range of wavelengths (between 250 and 400 nm) at relatively high intensity (200 watts/cm); the consequence of this being that it requires a very short period of time for gelation to occur with these materials. Another consequence of this is that far lower concentrations of initiator can be utilised to bring this reaction to gelation. In this case the initiator *Irgacure™* 1173 was utilised at an optimised concentration of 0.14 wt. %.[44-46]

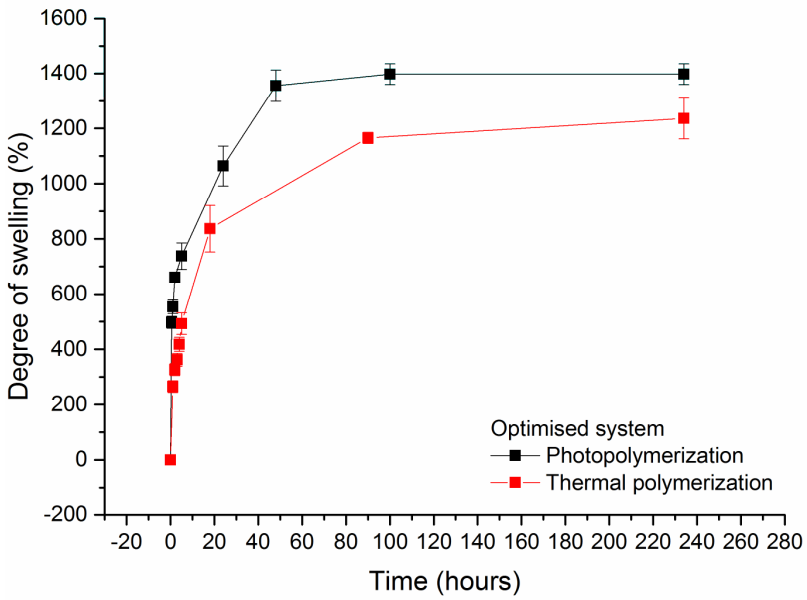

Figure 3.13; Effect of concentration of branched polyacid upon the equilibrium degree of swelling of the hydrogel

Initial comparison of **1** and **9** showed that **9** exhibited significantly lower mass loss through the process of polymerisation due to water evaporation (**Figure 3.13**). There was also no visible evidence of the macro defects that persisted even in the fully optimised thermal networks. Comparison of the swelling profiles of the respective materials shows that the photo-polymerised system reaches a much higher degree of swelling than the thermal system although at a similar rate (**Figure 3.13**). This indicates two things; firstly the mesh size of the photopolymerised system is larger, caused by the lack of evaporation of the solvent from the network during gelation, inhibiting the onset of gelation and preventing the formation of a greater degree of entanglement and smaller mesh sizes; the second is that nothing has inherently changed in the mechanism of uptake and swelling – indicating no significant chemical change to the networks.

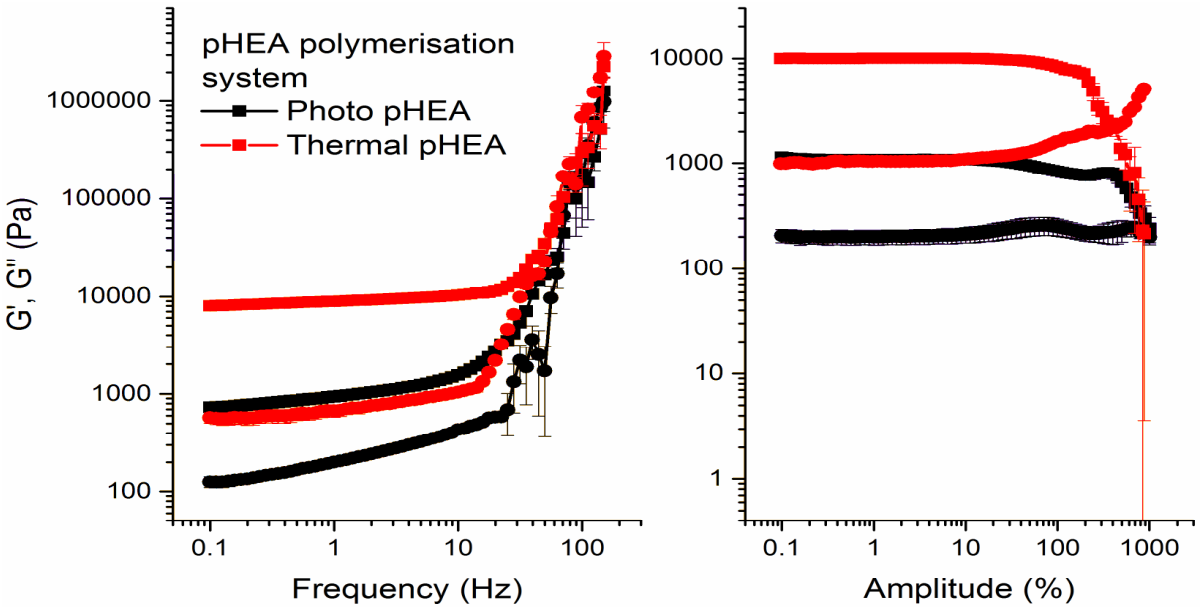

Figure 3.14; Comparison of optimised thermal polymerised pHEA hydrogel vs optimised photo polymerised pHEA hydrogel *via* frequency sweep between 0.1 and 200 Hz (left), comparison of optimised thermal pHEA hydrogel vs optimised photo pHEA hydrogel *via* amplitude sweep between 0.1 and 1000 % (right).

Investigation of the changes in the LVER of the two materials as shown in **Figure 3.14** shows that **9** has a significantly lower value of G' than **1** indicating a softer material. This can be simply explained through the higher concentration of water in the cured gels leading to a softer, less rigid material. A second observation from the rheology profiles of the LVER is that despite differences in the value of G' there appears to be very little change to the limits of the LVER.

After establishing the relative effects of changing the method of gelation, it seemed appropriate to see what effect this would have upon the addition of branched acid polymers to these networks. The same branched acid **(A)** shown in **Table 3.2** was chosen at the same concentrations as reactions **5, 6, 7** and **8** with the same methodology used of premixing of branched acids with the monomer solution in the absence of light. In the event, no gelation was observed at concentrations of branched

polymer above 1 wt. %, materials **10** and **11** were compared to network **9** with respect to their swelling and rheological properties.

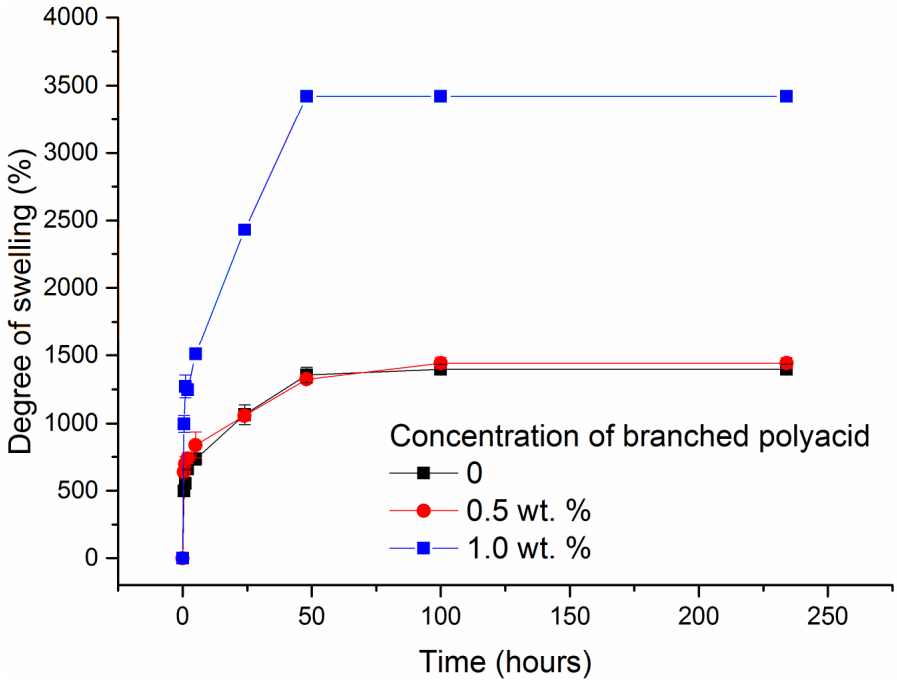

Figure 3.15; Effect of concentration of branched acid polymer upon the swelling in deionised water of photo-polymerised pHEA networks with error.

The swelling profile for **9**, **10** and **11** shown in **Figure 3.15** is surprising in that it represents a departure from the properties seen in the swelling of the thermal networks with branched acid additive. These results show that with an increase in the concentration of branched acid polymer, initially there is no sizeable effect upon the degree of swelling with **10** showing a similar profile and equilibrium degree of swelling to **9** however, with the addition of higher concentrations of the branched acid polymer a much higher equilibrium degree of swelling is observed. This is the opposite of the trend observed with the increase in branched acid content in the thermal networks **5 – 8**. These results indicate that the increased concentration of branched acid polymer has a significant effect in increasing the water uptake of the networks through a combination of increased mesh size and increased hydrophilicity. Once again this has

no effect upon the kinetics of the swelling process, with swelling to equilibrium occurring over the same time period implying that no significant change has occurred to the chemical nature of the gel or its affinity to the solvent system.

The observed effect is confirmed by the rheological properties with the addition of branched polymer showing a decrease in the rigidity of the materials within the LVER as shown in **Figure 3.16**.

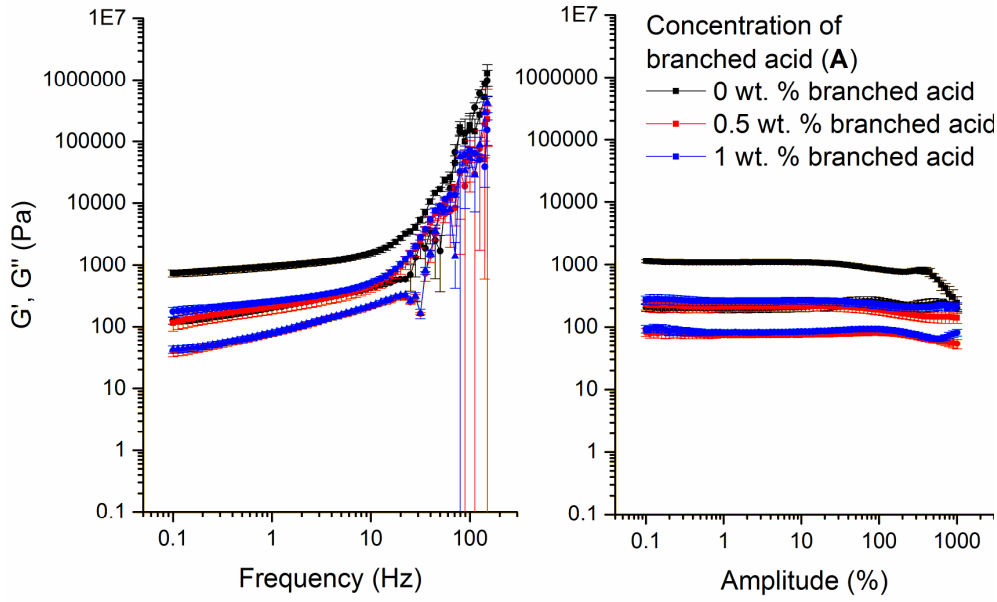

Figure 3.16; Comparison of frequency sweeps across the LVER for optimised photo polymerised pHEA hydrogel vs hydrogel with 0.5 wt. % and 1.0 wt. % of branched polymer (left), linear viscoelastic region within the context of an amplitude sweep (right).

The combination of these results appears to point to the occurrence of chain transfer to the CCTP ω-vinyl end groups of the branched acid polymers causing extensive chain termination competing with cross-linking and so reducing the cross-linking density within the networks. The result of this is that there is an increase in the pore and mesh size of the networks which reduces the rigidity of the networks at any specific degree of swelling but also increases the amount of water the networks can take up.

3.3 Conclusions

A monolithic hydrophilic network was synthesised with HEA through thermal polymerisation. This monolith was first optimised with respect to its monomer and initiator concentration and characterised using swelling and rheology to define the networks. The optimal thermal set up for this network was determined to be a 30 wt. % content of monomer relative to total content and 0.5 wt. % of initiator relative to monomer content. To this optimised network a branched acidic polymer synthesised *via* CCTP with MAA and EGDMA as the cross-linker is applied to functionalise and cross-link the network.

With the thermally polymerised network the branched CCTP polymer has the effect of a cross-linker; decreasing the degree of swelling and increasing the rigidity of the networks according the rheology. Unfortunately the presence of macro-defects in these networks led to a switch to a photo-curing system.

The photo-cured pHEA networks were developed and compared to the thermal networks where the materials properties showed an increase in pore size with an increase in the degree of swelling and decrease in the rigidity of the networks, this is caused by the decrease amount of water that evaporates during the process of polymerisation in the photo-system.

Finally the branched acid polymer was also added to this network to observe and compare the effects relative to the thermally cured network. In this system it was observed that branched acid polymer increased the degree of swelling, decreased the rigidity of the materials and prevented gelation at high concentrations. This indicates that the branched acid polymer's ω-vinyl end groups are causing chain transfer

competing with cross-linking and increasing the mesh size and inevitably inhibiting gelation entirely. These concepts are explored further in Chapter 4.

3.4 Experimental

3.4.1 Materials

Reagents were purchased from Sigma Aldrich and used as received, unless otherwise stated. 2,2'-azobis[2-(2-imidazolin-2-yl)propane]dihydrochloride (VA-044) was purchased from Alpha Labs and used as received.

3.4.2 Instruments

Rheometer

All rheology experiments were conducted upon a Malvern Kinexus Ultra with a Julabo cry-compact circulator CF41 temperature control unit. 20 mm stainless steel parallel plate geometry was used at 37 °C and with a force gap of 1N. Samples were cut to 20 mm using a 20 mm wad punch. The instrument was controlled in a CS-autostrain mode. A minimum of three experiments was conducted for each material. The data was exported as a CSV format and analysed in OriginPro 9.1.

Oven

All thermal gelation experiments were carried out in a Thermo Scientific Heratherm oven OGS180 at 55 °C. Materials were allowed to gel for 16 hours then cooled for 2 hours at room temperature prior to further analysis.

Light Hammer™

All photo gelation experiments were carried out on a Light Hammer 6 equipped with a broad spectrum H bulb and the speed of the conveyer belt unit set at 5 m/min. The H bulb operates between 250 and 400 nm at an optimal intensity of 200 watts/cm.

3.4.3 Thermal method for the synthesis of pHEA networks

A typical thermal gelation would occur according to the following procedure.

A 100 mL round bottom flask equipped with a septum and stirrer bar was charged with 2-hydroxyethyl acrylate (6 g, HEA, 0.052 mol), 14 g of water and degassed for a minimum of 1 hour prior to the addition of VA-044 (0.03 g, 9.28 x 10^{-5} mol) under a blanket of nitrogen. The solution continued to be degassed with stirring until all the initiator has dissolved. The solution was then deposited into the silicone 4 cm diameter cylindrical silicone moulds in 3 mL aliquots by syringe before being covered by an acrylic cover and placed in the oven at 55 °C for 16 hours. After gelation the moulds were removed from the oven and allowed to cool for 2 hours before removing the covering. The materials were stored at 10 °C for up to 1 month.

Reaction	HEA		VA-044		Water	
	(g)	(mol)	(g)	(mol)	(g)	(wt. %)
1	6	0.052	0.03	9.28 x 10^{-5}	14	30
2	6	0.052	0.06	1.85 x 10^{-4}	14	30
3	8	0.069	0.03	9.28 x 10^{-5}	12	40
4	10	0.087	0.03	9.28 x 10^{-5}	10	50

3.4.4 Photo method for the synthesis of pHEA networks

A typical photo gelation would occur according to the following procedure.

A 100 mL round bottom flask equipped with a septum and stirrer bar was charged with 2-hydroxyethyl acrylate (6 g, HEA, 0.052 mol), 14 g of water and degassed for a minimum of 1 hour prior to the addition of *Irgacure 1173* (0.01077 g, 6.56 x 10^{-5} mol) in the absence of light. The solution was then dispensed into the silicone moulds in 3 mL aliquots by syringe in the absence of light before being passed under a *Light Hammer™* 5 times at a rate of 5 $mmin^{-1}$. After gelation the moulds were covered immediately and allowed to cool. The materials were stored at 10 °C for up to 1 month.

Reaction	HEA		VA-044		Water	
	(g)	(mol)	(g)	(mol)	(g)	(wt. %)
1	6	0.052	0.03	9.28 x 10^{-5}	14	30
2	6	0.052	0.06	1.85 x 10^{-4}	14	30
3	8	0.069	0.03	9.28 x 10^{-5}	12	40
4	10	0.087	0.03	9.28 x 10^{-5}	10	50

3.4.5 Synthesis of pHEA networks with branched acid polymers

A typical thermal gelation would occur according to the following procedure.

A 100 mL round bottom flask equipped with a septum and stirrer bar was charged with 2-hydroxyethyl acrylate (6 g, HEA, 0.052 mol), branched polymer (0.05 g, 0.004 mmol), 14 g of water and degassed for a minimum of 1 hour prior to the addition of VA-044 (0.03 g, 9.28 x 10^{-5} mol) under a blanket of nitrogen. The solution continued to be degassed with stirring until all the initiator has dissolved. The solution was then dispensed into the silicon moulds in 4 mL aliquots by syringe before being covered by an acrylic cover and placed in the oven at 55 ^{o}C for 16 hours. After gelation the moulds were removed from the oven and allowed to cool before removing the covering.

Reaction	HEA		VA-044		Branched acid (A)		Water	
	(g)	(mol)	(g)	(mol)	(g)	(mol)	(g)	(wt. %)
5	6	0.052	0.03	9.28×10^{-5}	0.05	0.004	14	30
6	6	0.052	0.03	9.28×10^{-5}	0.1	0.008	14	30
7	6	0.052	0.03	9.28×10^{-5}	0.25	0.020	14	30
8	6	0.052	0.03	9.28×10^{-5}	0.5	0.040	14	30

3.4.6 Swelling

Upon cooling gels were removed from the silicon mould, placed inside a pre-weighed 100 mL screw top jar, weighed then immersed in deionised water for 5 days with changing of water to allow for removal of unreacted material and weighing of mass every 12 hours over the 5 day period. After the 5 day period the gels were removed from solution and dried in a vacuum oven at 40 °C over phosphorous pentoxide (P_2O_5) for 72 hours prior to weighing the dried mass of the gels. A minimum of three repeats was conducted for each material.

3.4.7 Rheology

Cured samples were cut to a 20 mm diameter and 3 mm thick using a 20 mm diameter wad punch. Samples were loaded at 25 °C with and a preload of 1 N was applied and allowed to equilibrate. Frequency sweeps were conducted between 0.1 and 200 Hz with a displacement of 1 %. Amplitude sweeps were conducted between 0.1 and 1000 % at a frequency of 1 Hz. The data was exported as a CSV format and analysed in OriginPro 9.1.

3.5 References

(1) Andreopoulos, A. G. *Biomaterials* **1989**, *10*, 101.

(2) Refojo, M. F.; Yasuda, H. *J. Appl. Polym. Sci.* **1965**, *9*, 2425.

(3) Winter, G. D. *Nature* **1962**, *193*, 293.

(4) Mao, N.; Russell, S. J. *Text. Prog.* **2004**, *36*, 1.

(5) Edwards, J. V. *Future Structure and Properties of Mechanism-Based Wound Dressings*; Springer Netherlands, **2006**.

(6) Boateng, J. S.; Matthews, K. H.; Stevens, H. N. E.; Eccleston, G. M. *J. Pharm. Sci.* **2008**, *97*, 2892.

(7) Velnar, T.; Bailey, T.; Smrkolj, V. *J. Int. Med. Res.* **2009**, *37*, 1528.

(8) Klode, J.; Schöttler, L.; Stoffels, I.; Körber, A.; Schadendorf, D.; Dissemond, J. *J. Eur. Acad. Dermatol.* **2011**, *25*, 933.

(9) Peppas, N. A.; Bures, P.; Leobandung, W.; Ichikawa, H. *Eur. J. Pharm. Biopharm.* **2000**, *50*, 27.

(10) Ganji, F.; Vasheghani-Farahani, S.; Vasheghani-Farahani, E. *Iran Polym J* **2010**, *19*, 375.

(11) Flory, P. J.; Rehner, J. *J. Chem. Phys.* **1943**, *11*, 521.

(12) Flory, P. J. *J. Am. Chem. Soc.* **1956**, *78*, 5222.

(13) Peppas, N. A.; Khare, A. R. *Adv. Drug. Deliver. Rev.* **1993**, *11*, 1.

(14) Vasheghani-Farahani, E.; Vera, J. H.; Cooper, D. G.; Weber, M. E. *Ind. Eng. Chem. Res.* **1990**, *29*, 554.

(15) Grassi, M.; Grassi, G. *Curr. Drug. Deliv.* **2005**, *2*, 97.

(16) Kim, B.; La Flamme, K.; Peppas, N. A. *J. Appl. Polym. Sci.* **2003**, *89*, 1606.

(17) Bajpai, A. K.; Shukla, S. K.; Bhanu, S.; Kankane, S. *Prog. Polym. Sci.* **2008**, *33*, 1088.

(18) Li, H.; Ng, T. Y.; Yew, Y. K.; Lam, K. Y. *Biomacromolecules* **2005**, *6*, 109.

(19) Rossi, G.; Mazich, K. A. *Physical review. A* **1991**, *44*, R4793.

(20) Peppas, N. A.; Colombo, P. *J. Control. Release.* **1997**, *45*, 35.

(21) Siepmann, J.; Peppas, N. A. *Adv Drug Deliv Rev* **2001**, *48*, 139.

(22) Berens, A. R.; Hopfenberg, H. B. *Polymer* **1978**, *19*, 489.

(23) Ross-Murphy, S. B. *Polym. Gels Networks* **1994**, *2*, 229.

(24) Ramazani-Harandi, M. J.; Zohuriaan-Mehr, M. J.; Yousefi, A. A.; Ershad-Langroudi, A.; Kabiri, K. *Polym. Test.* **2006**, *25*, 470.

(25) Dyson, F. J. *Rev. Mod. Phys.* **1979**, *51*, 447.

(26) Kavanagh, G. M.; Ross-Murphy, S. B. *Prog. Polym. Sci.* **1998**, *23*, 533.

(27) Schweller, R. M.; West, J. L. *ACS Biomater. Sci. Eng.* **2015**.

(28) Monleón Pradas, M.; Gómez Ribelles, J. L.; Serrano Aroca, A.; Gallego Ferrer, G.; Suay Antón, J.; Pissis, P. *Polymer* **2001**, *42*, 4667.

(29) Serrano Aroca, A.; Campillo Fernández, A. J.; Gómez Ribelles, J. L.; Monleón Pradas, M.; Gallego Ferrer, G.; Pissis, P. *Polymer* **2004**, *45*, 8949.

(30) Khutoryanskaya, O. V.; Mayeva, Z. A.; Mun, G. A.; Khutoryanskiy, V. V. *Biomacromolecules* **2008**, *9*, 3353.

(31) Song, W.; Liu, Y.; Hou, Y.; Fan, X. *Soft Materials* **2016**, *14*, 228.

(32) Odian, G. In *Principles of Polymerization*; 4th ed.; John Wiley & Sons: **2004**.

(33) Karpushkin, E.; Dušková-Smrčková, M.; Šlouf, M.; Dušek, K. *Polymer* **2013**, *54*, 661.

(34) Milani, A. H.; Saunders, B. R.; Freemont, T.; Bramhill, J. *Soft Matter* **2015**.

(35) Lisovsky, A.; Chamberlain, M. D.; Wells, L. A.; Sefton, M. V. *Adv. Healthc. Mater.* **2015**, *4*, 2375.

(36) Kozlovskaya, V.; Zavgorodnya, O.; Ankner, J. F.; Kharlampieva, E. *Macromolecules.* **2015**, *48*, 8585.

(37) Gao, C.; Yan, D. *Prog. Polym. Sci.* **2004**, *29*, 183.

(38) Voorhaar, L.; Hoogenboom, R. *Chem. Soc. Rev.* **2016**.

(39) Kozlovskaya, V.; Kharlampieva, E.; Mansfield, M. L.; Sukhishvili, S. A. *Chem. Mater.* **2005**, *18*, 328.

(40) Halacheva, S. S.; Freemont, T. J.; Saunders, B. R. *J. Mater. Chem. B.* **2013**, *1*, 4065.

(41) Xiang, Y.; Chen, D. *Eur. Polym. J.* **2007**, *43*, 4178.

(42) Godfrey, J., PhD Thesis, **2014**.

(43) Guan, Z. US5767211, **1998**.

(44) Munro, H. S.; Hoskins, R. US20060068014 A1, **2003**.

(45) Munro, H. S. US20130251665 A1, **2013**.

(46) Tufts, S. A.; Baltezor, M. J.; Ortiz, M.; Flores, J.; Devens, J. R.; Munro, H. S.; Boote, N. US20140235727 A1, **2014**.

4. Synthesis and Characterisation of pAMPS Based Hydrogels for Wound Care

This chapter is concerned with the study of the effects of the addition of branched and linear polymers synthesised by catalytic chain transfer polymerisation (CCTP) to hydrogels of known quality, for application in the field of wound care.[1,2] Initially the theory of the rubber elasticity as it pertains to the compression of hydrogels will be examined.[3-6] This is followed by a brief review of the scanning electron microscopy (SEM) techniques used when imaging hydrogels.[7-9]

Photo-polymerisation for the synthesis of hydrogels is a facile and rapid technique using 2-acrylamido-2-methylpropane sulfonic acid (AMPS) as the principle monomer. The occurrence of chain transfer to the CCTP branched polymer additives is observed to inhibit the formation of strong, cohesive gels except at very low concentrations of the CCTP additive.

4.1 Background

In order to analyse the effects of variation in network precursor constituents upon the properties of the networks formed, the materials need to be tested in multiple dimensions. These include the expansion or swelling of the networks into a solvent and shear testing, as shown in Chapter 3.[6,9-14] There are, however, other techniques that allow for a more comprehensive picture to be assembled, these include; uniaxial mechanical testing (either compression or tensile) and SEM to characterise the effects upon the morphology of the materials formed.

4.1.1 Compression

Compression testing represents a tried and understood technique for determining the network characteristics of swollen and unswollen polymer networks. Not only can it be used to determine the relative stiffness of a material, it can also be used for the determination of cross-linking density (v_e) and effective molecular weight between cross-link points (M_c). In order to determine the relative stiffness and toughness of the materials developed, the compression modulus of cylindrical swollen samples was measured from the linear region of response between stress and strain, typically within the first 15 % of strain.[7,15,16] Unlike rheology, which measures the ability of the polymer network and chains to slide past one another under dynamic stress, compression measures the ability of the network and chains to resist being compacted into a smaller volume under a consistent uniaxial force.[7,9] The experiments were performed through a stress-strain test applied with a constant rate of strain from a preloaded stress of 0.1 N and monitored through a force feed-back loop of the applied stress required to apply the strain.

Rubber Elasticity Theory

For the compression testing of pAMPS networks, the Mooney-Rivlin equation was applied (**Equation 4.1**) as derived from rubber elasticity theory with a stress deformation function for swollen gels.[7,15,17]

$$\sigma = E\left(\lambda - \frac{1}{\lambda^2}\right)$$

Equation 4.1; Compressed Mooney-Rivlin equation of rubber elasticity. σ is the stress or force per cross-sectional area, E is the Young's modulus derived from the linear region of association between stress and strain, λ is the deformation ratio.

Although the overall result shows an exponential increase in force required to displace a hydrogel by a required strain, the initial 20 % of strain regularly gives a linear – non-strain dependent – response. This region allows for the definition of the modulus (E) within a linear region of relationship between stress and strain. This along with the break point provides us with a relative idea of toughness in these materials. Higher E values indicate a stiffer material with a greater elastic response, whereas lower E values represent less rigid softer materials with a 'dampened' response.

The value of E combined with an understanding of the fraction of polymer network in the relaxed (prepared) state ($v_{2,r}$) and the swollen state ($v_{2,s}$) can give an understanding of the v_e.[18,19]

$$E = v_e^4 RT v_{2,r}^{\frac{2}{3}} v_{2,s}^{\frac{1}{3}}$$

Equation 4.2; Relationship between effective cross-linking density v_e, the Young's modulus E, gas constant R, temperature T, fraction of polymer network in relaxed state $v_{2,r}$ and fraction of polymer network in the swollen state $v_{2,s}$.

From v_e can be derived M_c with an understanding of the polymer network density ρ_p (**Equation 4.3**).[20]

$$M_c = \frac{\rho_p}{v_e^4}$$

Equation 4.3; Relationship between effective molecular weight between cross-link points M_c, the polymer density ρ_p and the effective cross-linking density v_e.

4.1.2 Scanning electron microscopy

Scanning electron microscopy (SEM) is the most widely used and established technique for the visualisation of the morphology of polymer networks.[8,21,22] Importantly, the impact of the freezing and drying technique used to form the dehydrated network (xerogel) can have a significant impact upon the morphology visualised.[23,24] The most common forms of freezing are; refrigeration, instantaneous freezing and critical point drying, all followed by lyophilisation to sublime off the solid water. The speed and nature of the freezing process leads to the formation of different morphologies due to the nature of the ice crystals formed. With rapid low temperature freezing – *i.e.* instantaneous immersion in liquid nitrogen, ice is formed as a vitreous mass, this means that ice crystals have minimal impact upon the observed morphology due to an even sublimation process, conversely, with slow freezing processes, large ice crystals can be formed leading to a significant effect upon the observed morphology.[23-25] An alternative method (generally used for biosamples) for xerogel formation is critical point drying, representing another effective method for rapid drying of substrate through water displacement with a transitional solvent (usually acetone), followed by replacement with liquid CO_2, followed by heating for rapid removal, however, as this technique is relatively time consuming and complex, it was not used in this work.[24,26-28]

4.2 Synthesis and characterisation of monolithic pAMPS hydrogels

The AMPS monomer is well suited for use in wound-care, with many already proven applications within the biomedical field in its monolithic form.[1,2,29] Commercially it is used for its properties as a soft, hydrophilic and above all biocompatible material with the capacity for a high degree of swelling.[1,2] The aims of this research were; to investigate the properties of gels formed through the photopolymerisation of the AMPS monomer with variation of cross-linker and then to investigate the impact that the addition of branched and linear polymers synthesised in Chapter 2 would have upon the materials properties of the hydrogels formed.

4.2.1 pAMPS hydrogels formed with a conventional di-vinyl cross-linker

Prior to the addition of the vinyl terminated macromonomers generated by CCTP the pAMPS hydrogel system was tested to see the effect of the addition of different concentrations of the cross-linker poly(ethylene glycol) diacrylate (PEGDA) upon the material properties of the gel.[13,30,31] This brief study was designed to act as a baseline for comparison when branched polymers generated in Chapter 2 – with their potential to act as cross-linking agents – are added into these hydrogels. The addition of the branched polymers with their ω-vinyl end group functionality is anticipated to cause crosslinking which should have an effect upon the value of compression modulus, rheological elasticity modulus and their swelling properties as the branched polymers

impact the mesh size (see Chapter 3).[32-37] To this end this study creates a comparison to a system that is well understood.

Samples with PEGDA concentrations varying between 0.1 and 1 mol % of the total monomer concentration were tested in triplicate through swelling into a simulated body fluid (**Table 4.1**), followed by mechanical analysis by compression and rheology (**Figure 4.4**) with additional observation by SEM (Figure 4.5) in order to observe the impact upon the network morphology.

Reaction	[X-linker] (mol % of monomer)	Equilibrium degree of swelling (%)[a]	Compression modulus E' (MPa)	Rheology Elasticity modulus G' (Pa)
1	0.14	3390 (±60)	5.3×10^{-3} ($\pm 2 \times 10^{-4}$)	950
2	0.25	3250 (±50)	11×10^{-3} ($\pm 1 \times 10^{-3}$)	1910
3	0.5	2230 (±110)	29.5×10^{-3} ($\pm 4 \times 10^{-4}$)	2810
4	1	1470 (±70)	59.2×10^{-3} ($\pm 7 \times 10^{-4}$)	5510

Table 4.1: Mechanical data for the synthesis of pAMPS monoliths with varying concentrations of PEGDA cross-linker. [a] Swollen in SBF for 72 hours at 25 °C.

The trends caused by changing the concentration of cross-linker show that with increasing concentration of PEGDA, the equilibrium degree of swelling in these gels clearly decreases in a directly proportionate manner (**Figure 4.1** and **Table 4.1**). This is caused by a decrease in the chain length between cross-linker points, in turn decreasing the mesh size – the volume between chains occupied by solvent.[4,15] The swelling profile of pAMPS monoliths shows a clear tendency towards non-Fickian (relaxation limited) swelling, with a slow, directly time dependent rate of swelling being indicative of this model.[5,6,11]

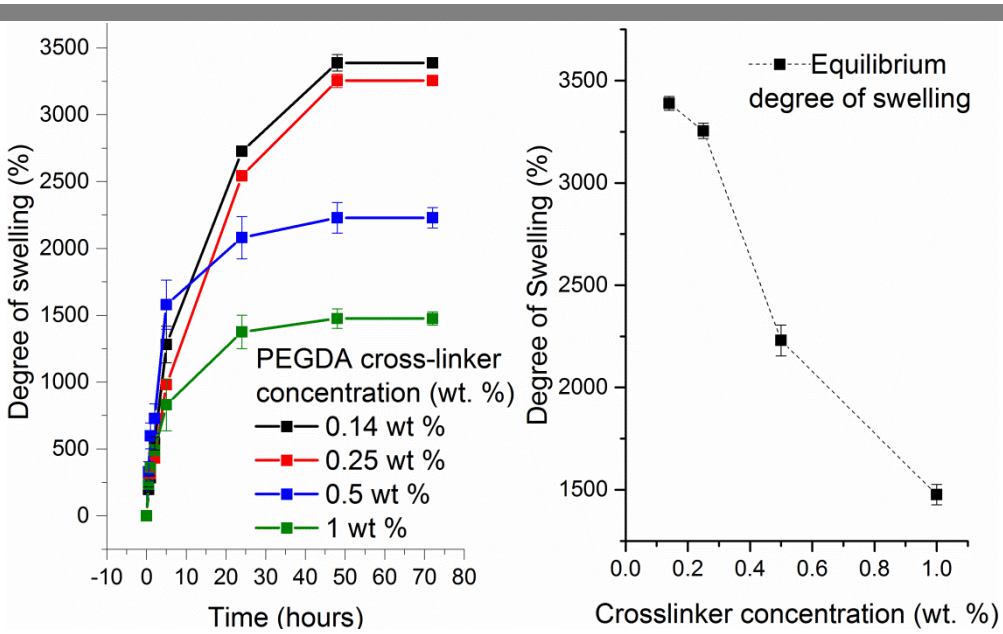

Figure 4.1; Effect of concentration of cross linker PEGDA upon the swelling kinetics of the hydrogel (left). Effect of concentration of cross-linker PEGDA upon the equilibrium degree of swelling (right).

This is confirmed by a study of the compression strength and modulus of these hydrogels at fixed degree of swelling of 10 wt. % (solid component / total mass). The stress strain curves show a decrease in the break point with increasing concentration of cross-linker, this is accompanied by an increase in the elasticity modulus derived from the first 20 % of strain associated with the linear region of fully elastic behaviour (**Figure 4.2**). With increasing concentration of cross-linker a proportionate increase in the elasticity modulus is observed (**Figure 4.3**), according to **Equation 4.2**, this increase in modulus caused by the increase in v_e and the corresponding decrease in the M_c (**Equation 4.3**). As with the swelling this confirms that the increase in the concentration of cross-linker is causing a decrease in the mesh size of the gels, accompanied by an increase in their rigidity and decrease in their elasticity, this is confirmed when manipulating the gels, those with higher concentrations of cross-linker are stiffer and more brittle.[7]

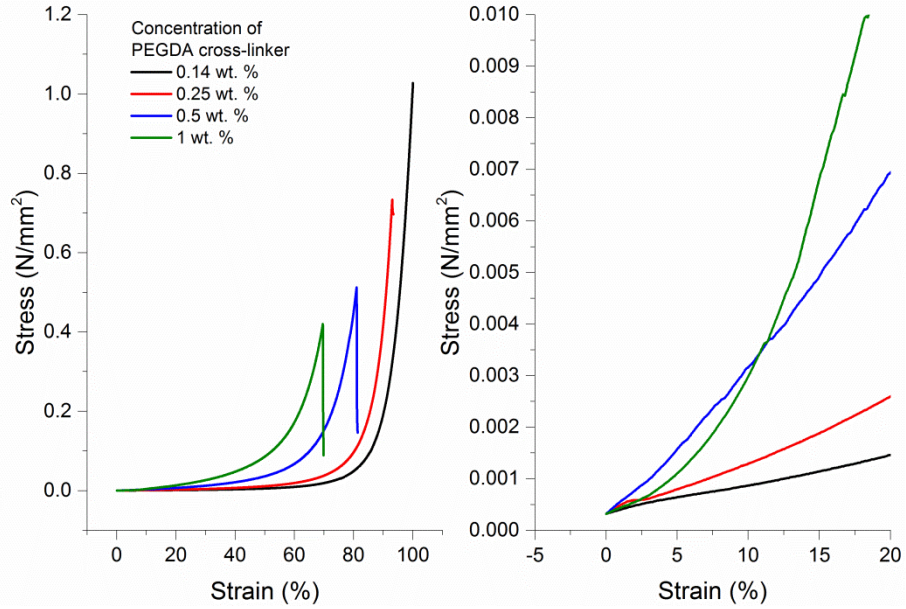

Figure 4.2; Compression to break point of pAMPS gels with PEGDA cross-linker (left), Compression in the linear response region used to calculate modulus E' (right).

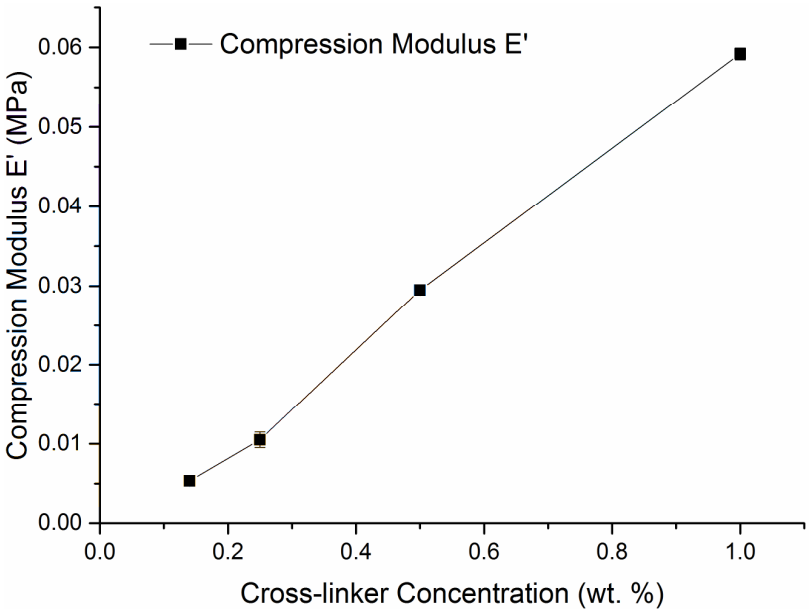

Figure 4.3; Compression modulus E' as a function of cross-linker concentration.

The effect of changing the concentration of cross-linker upon material properties was also analysed by rheology, which monitors the effects of dynamic shear force (as opposed to uniaxial force in compression) upon a network. In these tests, the

frequency of oscillation was varied, whilst maintaining constant amplitude in order to monitor the viscoelastic region (**Figure 4.4**).

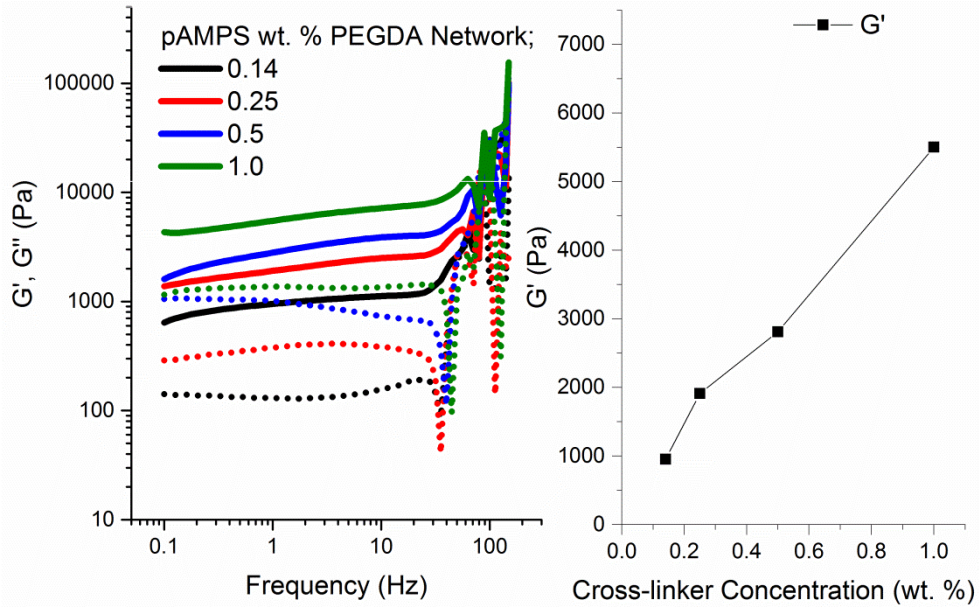

Figure 4.4: Definition of the LVER of monolithic pAMPS hydrogels by a rheological frequency sweep (left). Relationship between cross-linker concentration and elastic modulus (right).

As with compression, with an increase in the concentration of cross-linker there is a proportional increase in the elasticity modulus G' (**Figure 4.4**). At higher frequencies the elasticity modulus increases for all gels due to their inability to recover sufficiently at that time interval.[9,38]

Imaging of these samples by SEM at a constant wt. % and under controlled conditions of 90 wt. % water prior to freezing and lyophilisation were conducted by SEM (**Figure 4.5**).

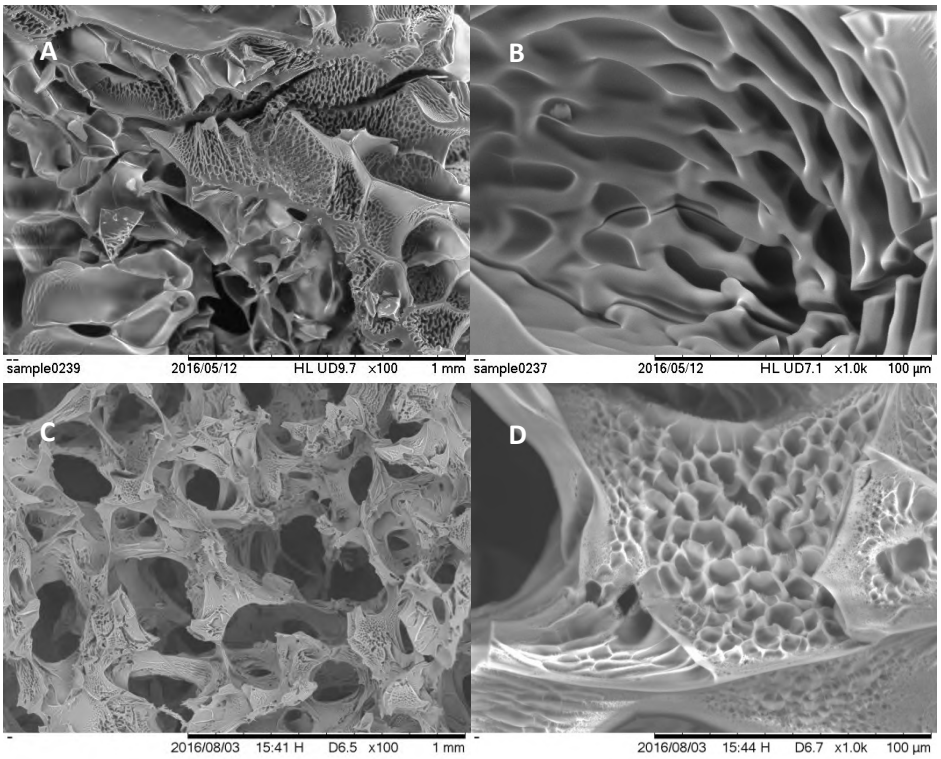

Figure 4.5: SEM images of pAMPS monoliths Clockwise from top left; A – 0.14 wt. % cross-linker x 100 magnification, B – 0.14 wt. % cross-linker x 1000 magnification, C – 1.0 wt. % cross-linker x 100 magnification, D – 1.0 wt. % cross-linker x 1000 magnification.

A random 3D, phase separated structure, on the 100 µm scale, possibly caused by the formation of the ice crystals in the freeze-dry process is seen (**Figure 4.5**). However, on the surface of the gels there is a random pore structure with diameters in the range of 10 µm at the 0.14 wt. % cross-linker used in **1** (**B**). This observable network morphology decreases in size with increasing concentration of cross-linker, with **D** showing a substantially tighter network at the 1.0 wt. % cross-linker concentration used in **4**.

From this initial study a clear understanding of the impact of the change of cross-linker concentration upon the material properties of a hydrogel has been gained. Increasing the concentration of cross-linker increases the elasticity of the materials and decreases

equilibrium swelling ratio. Both of these are indicators of a complementary decrease in pore size (see Chapter 3). This can act as a comparison for the addition of branched acids generated in Chapter 2 to the model monolith **1**.

4.3 Variation in the concentration of branched acid monomer

Catalytic chain transfer polymerisation (CCTP) is a method of free radical polymerisation that makes use of an extremely potent catalytic chain transfer agent (CCTA) to generate low molecular weight polymers without having to resort to either very high concentrations of initiator or thiol CTAs with concentrations approaching equivalency.[39,40] This technique has been used for the synthesis of branched polymers with high concentrations of di-vinyl monomer, something that has previously been very difficult to achieve.[41] One of the consequences of the mechanism of CCTP is the formation of ω-vinyl functionality on the chain ends of the polymers formed, this has allowed for the formation of branched polymers with ω-vinyl functionality with very high fidelity.[42,43] In this work, the utilisation of this ω-vinyl functionality in branched polymers was used in an attempt to create a novel cross-linker for use in free radical gelation.[44]

4.3.1 Branched acid polymer as a gelator

Following from the establishment of a baseline for the behaviour of pAMPS monoliths at different cross-linker concentrations, a series of tests were performed varying the concentration of a branched acid polymer (the same procedure used in Chapter 3), followed by variation of the molecular weight and degree of branching in the branched

polymer. The addition of hydrophilic CCTP branched macromonomers was initially attempted with a branched acid of relatively low molecular weight and degree of branching – that seen in **Table 4.3.**

Compound	[Monomer]/[CoBF]	[EGDMA] (mol %)	M_w[a] ($gmol^{-1}$)	Đ[a]	A[a]	Conversion (%)[b]
A	20500:1	5	12900	1.75	0.23	93

Table 4.2: Characterisation data for MAA/EGDMA branched polymer. [a] derived from triple detection SEC (DMF) 0.2 $mgmL^{-1}$, 1 $mLmin^{-1}$ flow rate, mixed D columns. [b] derived from GC-GID relative to DEG reference.

Initial investigations focused upon attempting to use the branched acid macromonomer as the sole gelator, removing the PEGDA from consideration. A series of tests were performed, in the absence of the di-vinyl PEGDA cross-linker, increasing the concentration of **A** (**Table 4.2**), however, at no point was gelation observed. Addition of other branched polymers yielded similar results. This appears to confirm the results from the photo-polymerised pHEA hydrogels (discussed in Chapter 3) with two contributing factors leading to the inhibition of gelation;

1) The relatively low concentration vinyl groups on the macromonomers in comparison to a conventional cross-linker.

2) The occurrence of chain transfer from propagating radicals to the catalytic chain transfer vinyl end groups competing with the propagation and cross-linking mechanism. This leads to the formation of shorter than kinetic chain lengths terminated by the CCTP polymers.[45,46]

As a result of these discoveries and in order to test this hypothesis, the CCTP branched polymers were subsequently added in the presence of PEGDA cross-linker at the

concentration used for material **1**. This was used in order to investigate in what way these materials would impact the network morphology.

4.3.2 Addition of branched acid polymer as an additive.

The initial study compared the impact of concentrations of compound **A** between 0.1 and 1 wt. % upon the material properties of the hydrogels produced. It was quickly discovered that above 1 wt. % gelation did not occur due to what was interpreted as the dominating impact of chain transfer to the CCTP ω-vinyl end groups.

Reaction	[X-linker] (mol % of monomer)	Equilibrium degree of swelling (%)[a]	Compression modulus E' (MPa)	Rheology Modulus G' (Pa)
1	0	3390 (± 60)	7×10^{-3} ($\pm 2 \times 10^{-4}$)	950
5	0.1	3380 (± 10)	5.6×10^{-3} ($\pm 5 \times 10^{-4}$)	770
6	0.25	3250 (± 40)	8.06×10^{-3} ($\pm 5 \times 10^{-5}$)	1010
7	0.5	3100 (± 200)	5.4×10^{-3} ($\pm 2 \times 10^{-4}$)	720
8	1	2720 (± 70)	6.9×10^{-3} ($\pm 5 \times 10^{-4}$)	320

Table 4.3: swelling and compression data for the synthesis of pAMPS hydrogels with varying concentrations of PEGDA cross-linker. [a] swollen for 72 hours in SBF at 25 °C.

The effect of increasing the concentration of compound **A** results in a decrease in the equilibrium degree of swelling (**Table 4.3** and **Figure 4.6**). Although this is observable, it is significantly less than the effect of varying the degree of the PEGDA cross-linker. If **A** is acting as a chemical cross-linker, the decrease in the degree of swelling can be explained through the increase in the concentration of the cross-linker causing an increase in v_e, the reduced impact could be explained through the lower concentration of vinyl end groups relative to the di-vinyl cross-linker (per gram) causing a reduced impact upon the degree of swelling.

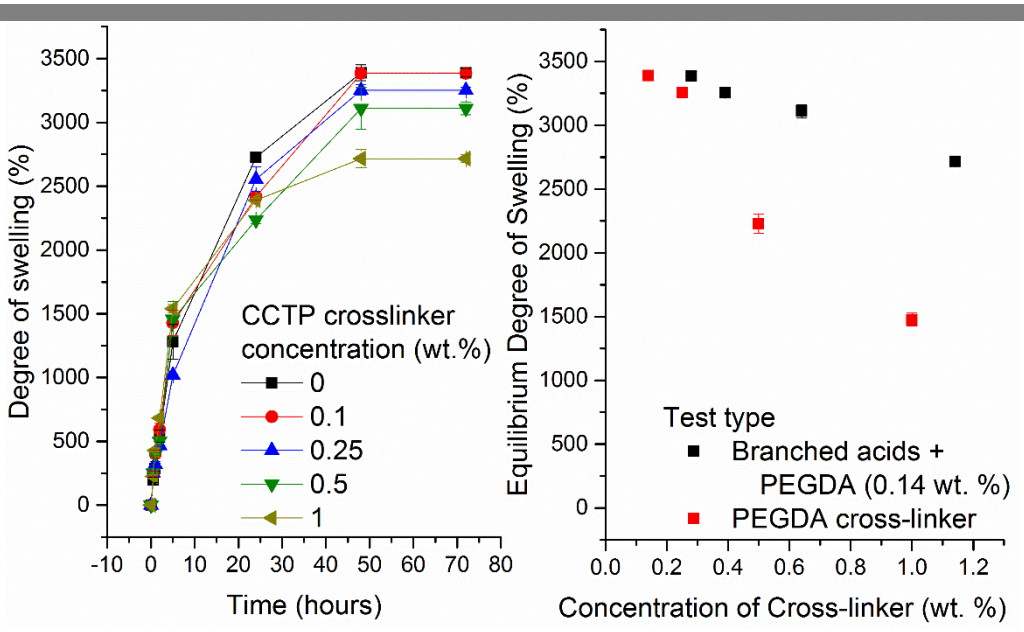

Figure 4.6: Swelling to equilibrium of pAMPS hydrogel with different concentrations of branched acid as additive (left). Equilibrium degree of swelling relative to concentration of branched acid branched acid polymer and cross-linker (right).

Despite this there is no observable increase in compression modulus E' with increasing concentration of compound **A**. As the pore size is directly related to the value of E' (**Equation 4.2**) this implies that, although we see inclusion of compound **A**, it is not acting as a chemical crosslinking agent and so the decrease in the equilibrium degree of swelling should be attributable to other effects such as hydrogen bonding and ionic attractions – caused by the macromonomer filling the space within the mesh without contributing to a reduction in the dimensions of the mesh.[18,19]

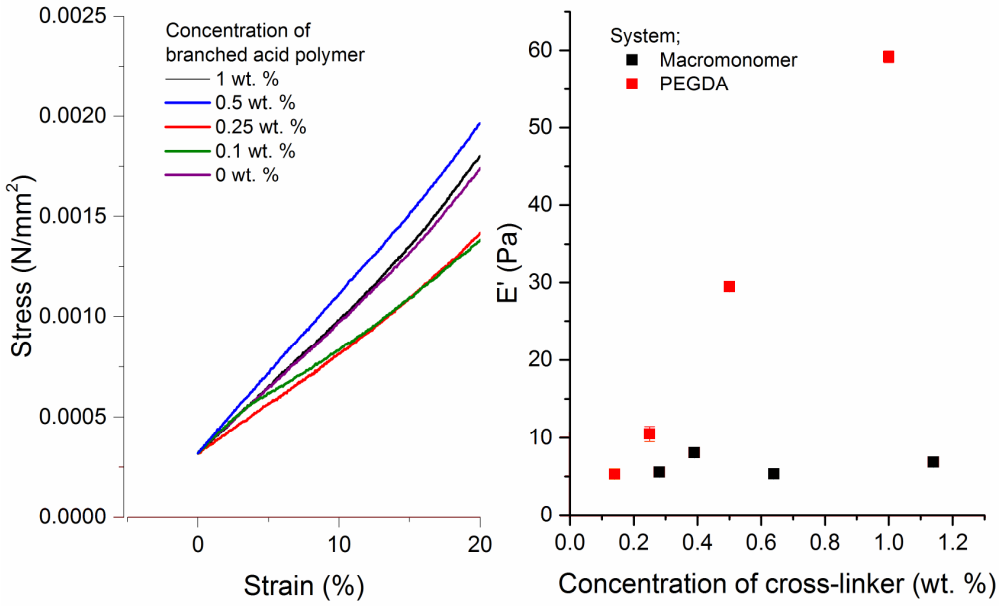

Figure 4.7; Compression of pAMPS hydrogels with different concentrations of branched acid polymer as additive (left). Compression modulus E' as a function of total cross-linker concentration in both pAMPS and pAMPS with branched polymers (right).

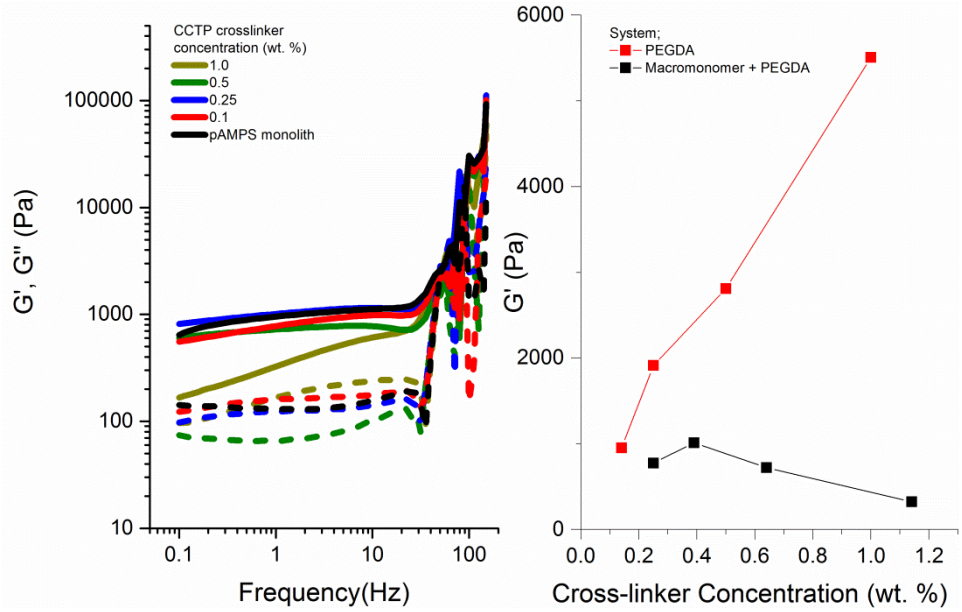

Figure 4.8: Rheology of pAMPS hydrogels with different concentrations of branched acid polymer as additive (left). Elastic modulus G' as a function of total cross-linker concentration in both pAMPS and pAMPS with branched polymers (right).

Analysis of the testing of these materials by rheology also indicates that there is no significant increase in elasticity of the materials with increasing concentration of **A**. In

fact, the value of G' within the LVER appears to decrease with increasing concentration of **A** (**Figure 4.8**).

Three things have been observed in this section indicating that compound **A** is ill suited as a cross-linker, these are;

1) No gelation is observed when attempting to use compound **A** as the sole cross-linker.
2) Above a critical wt % compound **A** prevents the formation of a gel even in the presence of a regular cross-linker.
3) No observable increase in E' (compressive modulus) is observed with increasing concentration of compound **A** and no increase in rheological elasticity modulus is observed.

A reasonable hypothesis for why compound **A** has this affect would be that the size of the molecule makes it unfavourable for propagation from it. This is both due to its increased bulk at the reaction site creating steric hindrance and the large bulk of the molecule meaning that diffusion through the solution is less rapid thereby reducing collision rate. Although this is the case, there is good reason to suggest that compound **A** is being reacted with and included in the hydrogel structure as firstly it has a noticeable impact upon the equilibrium degree of swelling as it inhibits gelation. This implies that initiator or active chain ends react with the compound **A**'s vinyl end groups but then fail to propagate onwards or do so at a seriously reduced rate, most likely due to the large steric bulk of the compound and the action of chain transfer.

4.4 Variation of the degree of branching and molecular weight

In this section a systematic study of the effects of variation of the degree of branching and molecular weight of the branched acids synthesised and characterised in Chapter 2 (shown again in **Table 4.4**) upon the properties of the pAMPS monolith shown above. The degree of branching is varied so that linear, lightly branched and more highly branched polymers can be compared. Following this, the effects of the molecular weight of branched and linear poly acids is investigated with respect to their degree of swelling, compression and rheological results (**Table 4.4**). The concentration of the branched and linear acid is kept to 0.5 wt. % of the total monomer concentration in order to allow for gelation.

Compound	[Monomer]/ [CoBF]	[EGDMA] (mol %)	M_w^{α} ($gmol^{-1}$)	$Đ^{\alpha}$	α^{α}	Conversion (%)$^{\beta}$
B	25000:1	0	5000	1.51	0.22	> 99
C	64000:1	0	9780	1.41	0.28	> 99
A	20500:1	5	12900	1.75	0.23	93
D	25000:1	5	17600	2.43	0.27	95
E	32000:1	5	42600	3.12	0.35	95
F	25000:1	10	50900	5.46	0.31	97

Table 4.4: Characterisation data for MAA/EGDMA branched polymer. $^{\alpha}$ derived from triple detection SEC (DMF) 0.2 $mgmL^{-1}$, 1 $mLmin^{-1}$ flow rate, mixed D columns. $^{\beta}$ derived from GC-FID relative to DEG reference.

4.4.1 Variation in the degree of branching

Initially the effect of varying the degree of branching in the branched acids was investigated making use of three branched acids with three different concentrations of EGDMA but varying molecular weights; **B** – linear pMAA, **D** – branched MAA-co-EGDMA with 5 mol % EGDMA, **F** – branched MAA-co-EGDMA with 10 mol % EGDMA.

Reaction	Branched acid used.	Equilibrium degree of swelling (%)[a]	Compression modulus E' (MPa)	Rheology modulus G' (MPa)
9	B	4240 (± 90)	4.3×10^{-3} ($\pm 5 \times 10^{-4}$)	260
7	D	3100 (± 200)	5.4×10^{-3} ($\pm 2 \times 10^{-4}$)	620
10	F	2570 (± 20)	7.6×10^{-3} ($\pm 3 \times 10^{-4}$)	540

Table 4.5: Swelling, compression and rheology data for the synthesis of pAMPS hydrogels with varying concentrations of PEGDA cross-linker.[a] Swollen in SBF for 72 hours at 25 °C

Swelling results show that with an increase in branching there is a decrease in the equilibrium degree of swelling, however, there were some complications. Firstly, the linear pMAA gives a far higher degree of swelling, even relative to the baseline pAMPS monolith. This is theorised to be due to the relatively high concentration of ω-vinyl end

groups causing chain transfer to dominate without the occurrence of cross-linking to multiple chain ends. As a result, the mesh size of the network increases causing an increase in the equilibrium degree of swelling. The second result of interest is the time scale required to reach equilibrium swelling – in the initial time networks **9**, **7** and **10** take up water at a faster rate than the pAMPS monolith. This is possibly due to the increased hydrophilicity of the network, when the branched acids are incorporated.

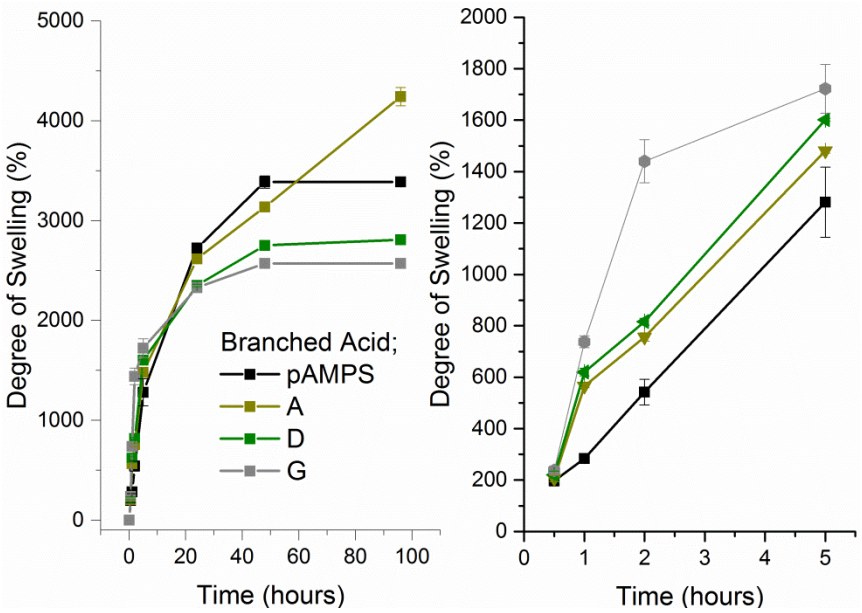

Figure 4.9: Swelling to equilibrium of hydrogels with branched acid polymers incorporated at 0, 5 and 10 mol % cross-linker (left). Initial rate of swelling of the same hydrogels (right).

The compression results agree with the results from the swelling analysis, where the value of E' increases with increasing branching across networks **9**, **7** and **10** – indicating a decrease in the cross-link density with increasing branching (**Figure 4.10**). This also manifests in the point of break, with networks **7** and **10** showing significantly lower points of break due to their increased rigidity. In addition to this, once again the linear species **B** in network **9** decreases the value of E' relative to the network **1** – the pAMPS monolith – again due to chain transfer to the ω-vinyl end group generated by CCTP.

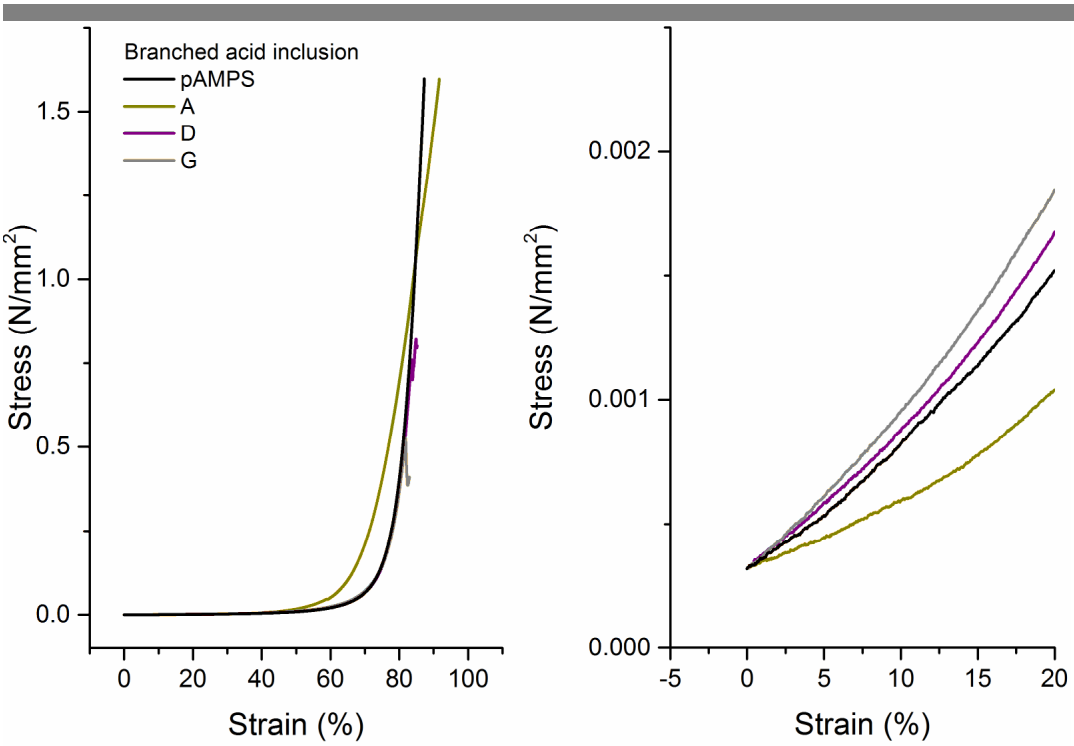

Figure 4.10; Compression of hydrogels with different degrees of branching in the branched acid content (left). Linear region from which the compression modulus E' is calculated (right).

From this work it is seen that with increasing degree of branching in the branched acid polymer, an increase in the rigidity and a decrease in the equilibrium degree of swelling indicate the prevalence of a cross-linking mechanism over the chain transfer mechanism. However, with the linear acid the chain transfer process appears to dominate in the absence of multiple ω-vinyl groups imparted by the branching of the acids.

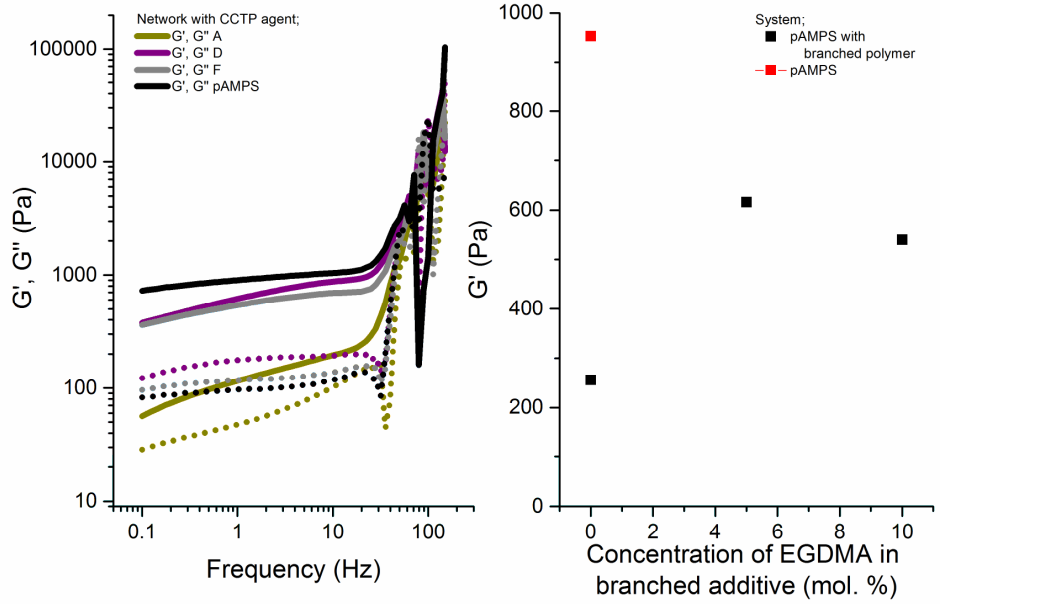

Figure 4.11; Rheology of hydrogels with different degrees of branching in the branched acid content (left). Elastic modulus G' as a function of the degree of branching in the branched polymer additive relative to the pAMPS baseline (right).

In contrast to the results observed by compression and swelling, rheology indicates a different model (**Figure 4.11**). With the addition of the CCTP polymers, a decrease in the value of G' is observed, most significantly with the linear polymer, with the branched polymers imparting a higher degree of stiffness relative to the linear polymer, but still lower than the pAMPS without additive. This could be due to a reduced occurrence of chain transfer due to reduced overall vinyl group concentrations available for chain transfer in these higher molecular weight species.

4.4.2 Variation in the Mw of branched acid

To test this model further, the impact of molecular weight – and therefore ω-vinyl group density – is investigated in both linear and branched acids upon the networks they are incorporated into. If the model above is correct then lower molecular weight linear polymers would show a increased equilibrium degree of swelling and decreased

value of E', in branched polymers, higher lower molecular weight species would have the reverse effect.

Reaction	Branched acid used.	Equilibrium degree of swelling (%)[a]	Compression modulus E' (MPa)	Rheology modulus G' (MPa)
9	B	4240 (± 90)	$4.34 \times 10^{-3}(\pm 5 \times 10^{-4})$	260
11	C	4200 (± 60)	$3.48 \times 10^{-3}(\pm 3 \times 10^{-4})$	770
12	A	4240 (± 90)	5.35×10^{-3} ($\pm 2 \times 10^{-4}$)	120
7	D	3100 (± 200)	6.63×10^{-3} ($\pm 8 \times 10^{-5}$)	620
13	F	2760 (± 6)	5.25×10^{-3} ($\pm 4 \times 10^{-4}$)	540

Table 4.6; Swelling, compression and rheology data for the synthesis of pAMPS hydrogels with varying concentrations of PEGDA cross-linker. [a] Swollen in SBF for 72 hours at 25 °C.

The impact of the addition of branched acid polymers of different degrees of branching upon the observable internal morphology of the hydrogel networks was studied by SEM (**Figure 4.12**). With the addition of linear CCTP generated pMAA (**B**) significant deviation is seen from the morphology generated by a conventionally generated monolith. A greater degree of heterogeneity, with smaller defects or holes observable within the pore structure (**Figure 4.12** - **C**). With the addition of a branched acid (**D**), the same effect is observable, but to a lesser degree (**Figure 4.12** - **E**). This could confirm the observations previously identified in that linear polymers, with a higher vinyl concentration, cause a greater degree of chain transfer termination than the branched polymers, causing a greater degree of disruption to the internal morphology of the networks.

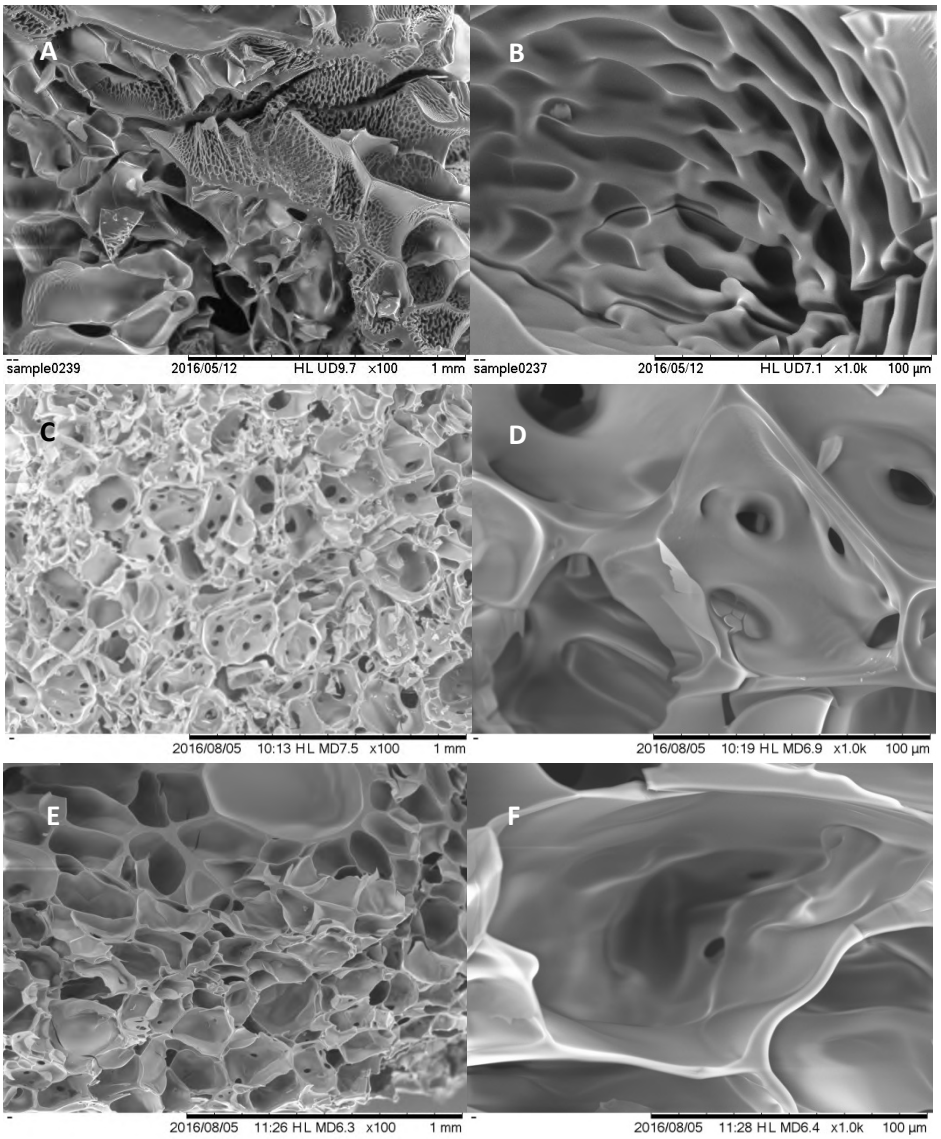

Figure 4.12: SEM images of pAMPS monoliths with branched acids. Clockwise from top left; A conventional monolith x 100 magnification, B conventional monolith x 1000 magnification, C conventional monolith + 0.5 wt. % of B x 100 magnification, D conventional monolith + 0.5 wt. % of B x 1000 magnification, E conventional monolith + 0.5 wt. % of D x 100 magnification, F conventional monolith + 0.5 wt. % of D x 1000 magnification.

Initially linear pMAA was tested in the form of reactions **9** and **11** relative to the network in the absence of branched polymer – **1**. Between **9** and **11** the molecular weight was effectively doubled and, therefore, the concentration of ω-vinyl end groups significantly reduced. Swelling these networks showed once again that the

linear polymers when incorporated into a pAMPS network, significantly increase the degree of swelling over that of the pAMPS monolith. Again this is exhibiting the effects of chain transfer upon the networks (**Figure 4.13**).

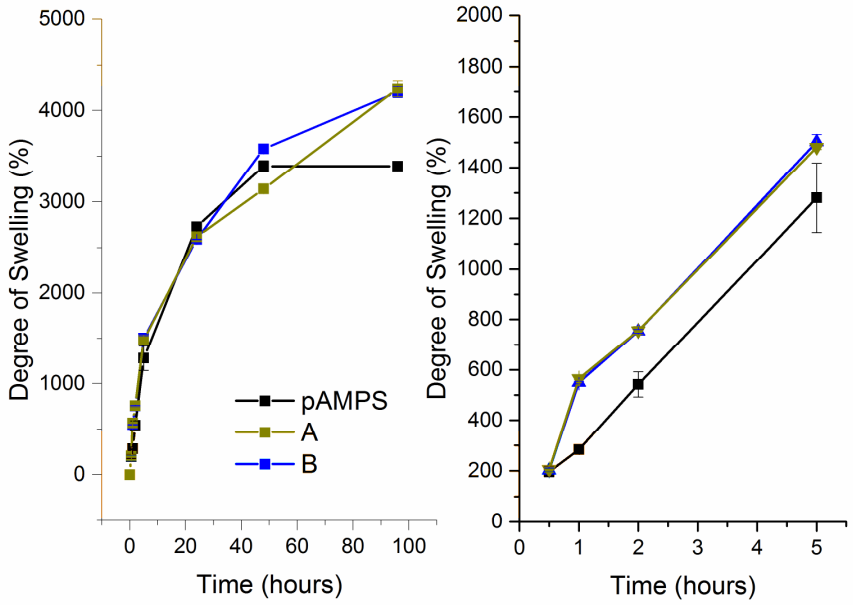

Figure 4.13: Swelling to equilibrium of AMPS hydrogels with different molecular weights of linear pMAA (left). Initial swelling rate of the same hydrogels (right).

Compression of networks **1**, **9** and **11** shows that, the branched polymers exhibit a decrease in the value of E' representing a decrease in their rigidity and an increase in the cross-link density of the networks. Interestingly the impact of increasing the molecular weight, thereby decreasing the concentration of ω-vinyl end groups is also observable with a significant increase in the value of E' from **11** to **9** as the molecular weight of the linear pMAA included increases. This is due to the decrease in the concentration of the ω-vinyl end groups, causing a decrease in the occurrence of chain transfer, allowing the effective cross-link density to increase, increasing the rigidity and E' closer to that exhibited by the model system **1** (**Figure 4.14**).

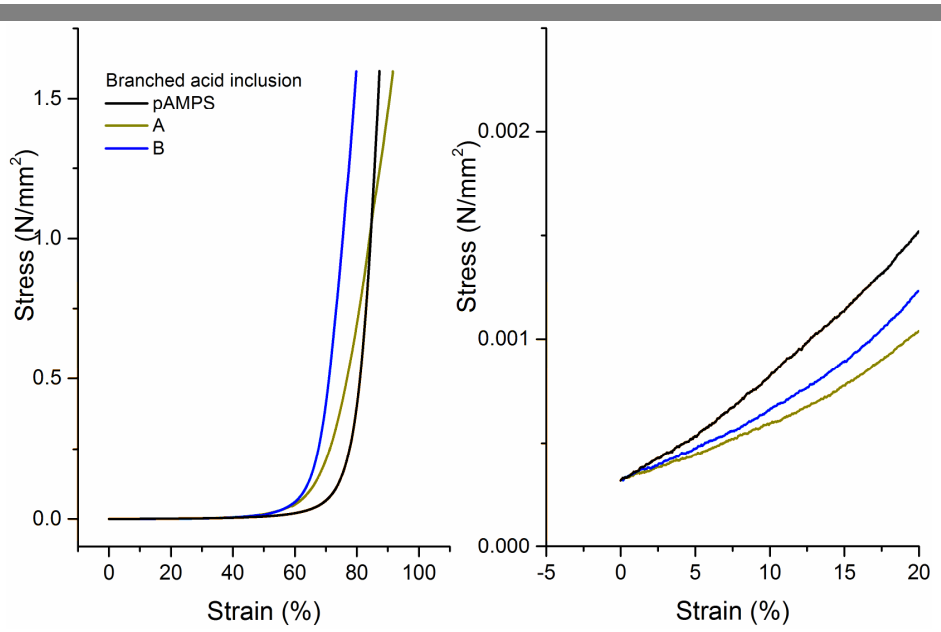

Figure 4.14; Compression of hydrogels with different molecular weights of linear pMAA (left). Linear region from which the compression modulus E' is calculated (right).

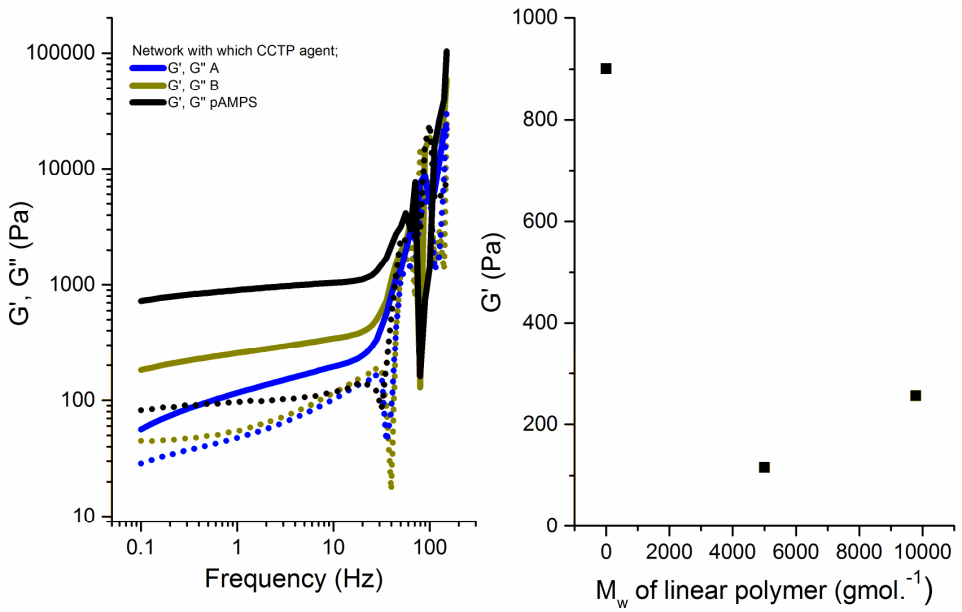

Figure 4.15: Rheology of hydrogels with different molecular weights of linear pMAA (left). Elasticity modulus G' in the LVER in each case (right).

Measurement by rheology with respect to the effect of variation of frequency upon the modulus of the material confirmed the results displayed in **Figure 4.14**, increasing

vinyl concentration, caused by decreasing molecular weight causes a decrease in modulus relative to the pAMPS network without linear pMAA additive (**Figure 4.15**).

After varying the molecular weight of linear pMAA, the next step was to vary the molecular weight of the branched polymers at a fixed concentration of divinyl monomer EGDMA. This was achieved by varying the concentration of the chain transfer agent CoBF relative to the total monomer concentration. Three species were selected at 5 mol % EGDMA relative to the total monomer concentration at three different ratios of CoBF to Monomer. These were 20500:1, 25000:1 and 32000:1 with networks **A**, **D** and **F** respectively. The addition of the branched acid polymers as previously discovered has the effect of decreasing the equilibrium degree of swelling and increasing the value of E', due to causing a decrease in the pore size. This effect is most noticeably observed with addition of **A** in network **12** and then **D** in **7** decreasing the degree of swelling from the baseline network **1 (Figure 4.16**).

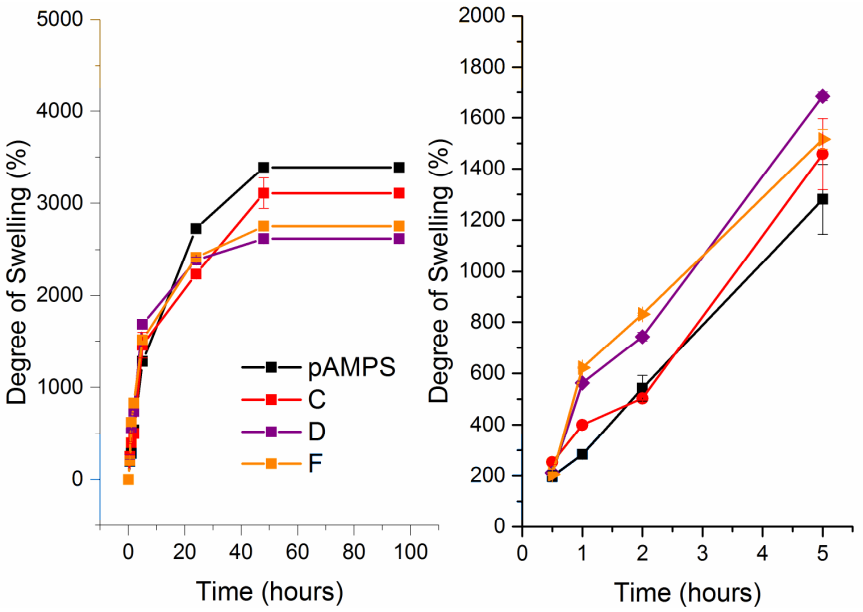

Figure 4.16: Swelling to equilibrium of AMPS hydrogels with different molecular weights of branched acidic polymers (left). Initial swelling rate of the same hydrogels (right).

This is further confirmed with an observed increase in E' relative to **1** (**Figure 4.17**), however, it is observed that with further increases in molecular weight of branched polymer an increase in the value of E' is not seen. This can be explained by the decreasing number of ω-vinyl end groups available and the decreasing concentration of branched polymer as molecular weight increases whilst concentration in wt. % relative to AMPS remains the same. This means that with increasing molecular weight a decrease in the impact upon the value of E' should be observed (**Figure 4.17**).

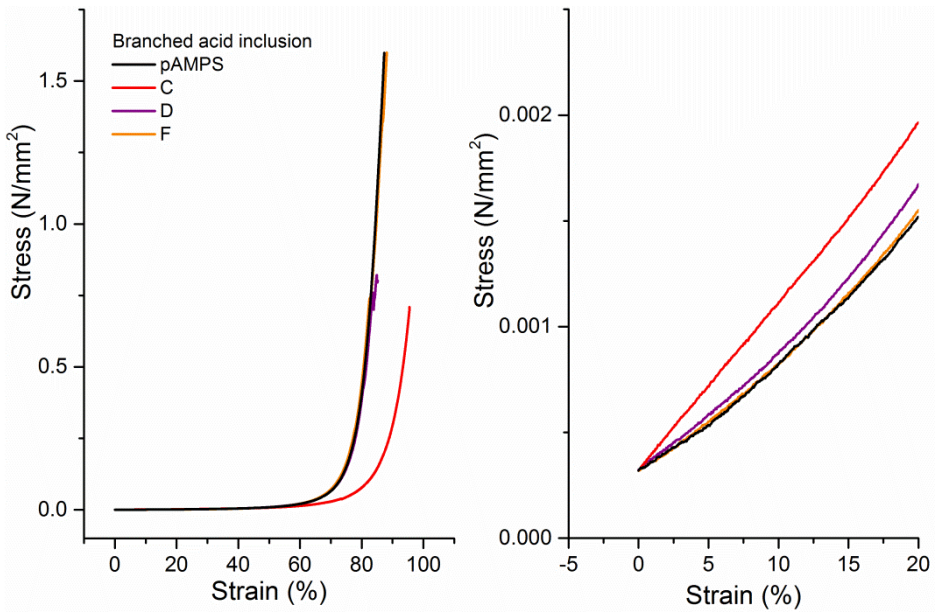

Figure 4.17; Compression of hydrogels with different molecular weights of branched polyacids (left). Linear region from which the compression modulus E' is calculated (right).

This is contrary to what is observed by rheology, with a decrease in the shear modulus being observed upon the addition of the branched material and no significant trend in the impact of molecular weight upon the stiffness of the material (**Figure 4.17**).

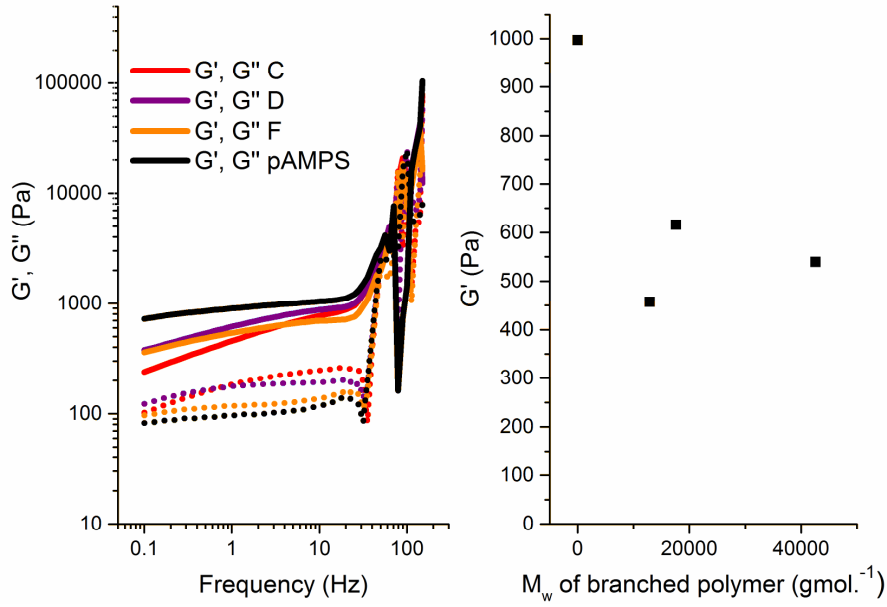

Figure 4.18: Rheology of hydrogels with different molecular weights of linear pMAA (left). Elasticity modulus G' in the LVER in each case (right).

In this work the impact of the molecular weight of the branched acidic polymer additives upon the material properties of the gels they are added to were investigated. Initially the linear polymers were added at different molecular weights and a trend of increasing molecular weight of linear polymers was observed to decrease the impact of chain transfer to the ω-vinyl groups, however, in all cases a decrease in E' with decreasing M_w and increase in equilibrium degree of swelling was observed. After this the molecular weight of branched polymers was changed, maintaining the concentration of PEGDA within the polymers. It was observed that at higher molecular weight the effectiveness of the polymers as a cross-linker was reduced relative to lower molecular weight branched acid polymers, attributed to a decrease in the molar concentration of branched species.[47]

4.5 Conclusions

In this chapter a thorough investigation of the effect of linear and branched acid polymers generated by catalytic chain transfer upon pAMPS monoliths is reported. A fine balancing act between chain transfer and cross-linking has been shown to occur. In the presence of linear pMAA polymers with ω-vinyl groups but no capacity to cause cross-linking, chain transfer is observed to have a significant effect upon the networks, causing an increase in mesh size and, as a result increasing the equilibrium degree of swelling and decreasing the compression modulus.

With the addition of branched polymers a cross-linking effect was observed. This effect is not as significant as with a typical low molecular weight gelator, however, it is observed that with an increased degree of branching a decrease in the degree of swelling and an increase in the compression modulus is observed, contrary to the effects of higher molecular weight. However, these branched polymers are not a viable gelator in their own right, due to both their high molecular weights and the chain transfer caused by their presence. This means that gelation is not viable with these species alone.

4.6 Experimental

4.6.1 Materials

Reagents were purchased from Sigma Aldrich and used as received, unless otherwise stated.

4.6.2 Instruments

Universal Testing Machine

Compression testing was performed on a Shimadzu Autograph AGS-X universal mechanical tester equipped with a 500 N load cell and compressive testing geometry consisting of two parallel stainless steel plates. A preload of 0.1 N was applied at 25 °C. The data was exported as a CSV format and analysed in OriginPro 9.1.

Oven

All thermal gelation experiments were carried out in a Thermo Scientific Heratherm oven OGS180 at 55 °C. Materials were allowed to gel for 16 hours prior to cooling and further analysis.

Light Hammer™

All photo gelation experiments were carried out on a *Light Hammer*™ 6 equipped with a broad spectrum H bulb and the speed of the conveyer belt unit set at 5 m/min. The H bulb operates between 250 and 400 nm at an optimal intensity of 200 watts/cm.

SEM

A Hitachi 3030M desktop SEM was used on all samples at x 100 and x 1000 magnification.

Rheometer

All rheology experiments were conducted upon a Malvern Kinexus Ultra with a Julabo cry-compact circulator CF41 temperature control unit. 40 mm stainless steel parallel plate geometry was used at 25 °C and with a force gap of 1N. Samples were cut to 40 mm using a 40 mm wad punch. The instrument was controlled in a CS-autostrain mode. A minimum of three experiments was conducted for each material. The data was exported as a CSV format and analysed in OriginPro 9.1.

4.6.3 pAMPS hydrogel synthesis

Typical synthesis of pAMPS hydrogels;

2-Acrylamido-2-methyl-1-propansulfonic acid (AMPS, 30.16 wt. %) was mixed with poly(ethylene glycol) diacrylate (M_n 575, 0.14 wt. %) in deionised water (69.84 wt. %) for 10 minutes prior to the addition of 1-hydroxydimethyl phenyl ketone (0.014 wt. %) in the absence of light. The reaction mixture was stirred for 10 minutes and then reacted in silicon moulds under a UV source for 7 passes and until gelation was observed. Gels were then stored in their moulds inside sealable plastic bags for a maximum of a week prior to use.

Reaction	Concentration (wt. %)	Mass added (g)
1	0.14	0.1077
2	0.25	0.2154
3	0.5	0.4308
4	1	0.8616

Concentrations and masses of cross-linker used for variable cross-linker experimentation

4.6.4 Addition of branched acid macromonomer

Hydrogels were synthesised as above but with the branched acid hydrogel added with the monomer and the cross-linker as in the following instances;

Reaction	Branched acid	Concentration (wt. %)	Mass added (g)
5	A	0.5	0.4308
6	B	0.5	0.4308
7	C	0.5	0.4308
8	D	0.14	0.4308
9	D	0.25	0.2154
10	D	0.5	0.4308
11	D	1	0.8616
12	E	0.5	0.4308
13	F	0.5	0.4308
14	G	0.5	0.4308

4.6.5 Swelling

20 mm diameter hydrogel disks are cut out using a 20 mm diameter wad punch and are immersed in 250 mL of simulated body fluid for 96 hours at 25 °C. The wet mass of the gels is measured at regular time points of 0.5, 1, 2, 5, 24, 48 and 96 hours by extracting the hydrogel from the jar, removing excess water with filter paper and weighing. At 96 hours the dry mass of the gels is determined gravimetrically by drying in an oven at 80 ^{o}C for 48 hours. Samples were tested with three replicates.

4.6.6 Compression

20 mm diameter disks of hydrogels are swollen to 90 wt. % water in deionised water for 16 hours. A 20 mm diameter disk of this swollen gel is cut using a 20 mm diameter

wad punch and is preloaded on a compression tester with 0.1 N using a 500N load cell at 25 °C before being subjected to a constant rate of strain at 1 mm min^{-1} until break is detected. Samples were tested with five replicates.

4.6.7 SEM

20 mm diameter disks of hydrogels are swollen to 90 wt. % water in deionised water for 16 hours, the resulting gel is then instantaneously frozen in liquid nitrogen for 10 minutes prior to being lyophilised for 72 hours or until fully dry. The hydrogels are then freeze-fractured with liquid nitrogen, mounted vertically and viewed with a Hitachi 3030M desktop SEM at x 100 and x 1000 magnification.

4.6.8 Rheology

20 mm diameter disks of hydrogels are swollen to 90 wt. % water in deionised water for 16 hours. A 40 mm diameter disk of this swollen gel is cut using a 40 mm wad punch and then preloaded onto the rheometer with a 1 N force gap at 25 ^{o}C with 40 mm parallel plates. A frequency sweep was performed between 0.1 and 200 Hz at 1 % strain, a strain sweep was performed with a fresh sample between 0.1 and 200 % strain at 1 Hz. Each test was conducted with three replicates.

4.7 References

(1) Tufts, S. A.; Baltezor, M. J.; Ortiz, M.; Flores, J.; Devens, J. R.; Munro, H. S.; Boote, N. US20140235727 A1, **2014**.

(2) Munro, H. S. US20130251665 A1, **2013**.

(3) Flory, P. J. *J. Am. Chem. Soc.* **1956**, *78*, 5222.

(4) Flory, P. J.; Rehner, J. *J. Chem. Phys.* **1943**, *11*, 521.

(5) Canal, T.; Peppas, N. A. *J. Biomed. Mater. Res.* **1989**, *23*, 1183.

(6) Peppas, N. A.; Bures, P.; Leobandung, W.; Ichikawa, H. *Eur. J. Pharm. Biopharm.* **2000**, *50*, 27.

(7) Emileh, A.; Vasheghani-Farahani, E.; Imani, M. *Eur. Polym. J.* **2007**, *43*, 1986.

(8) Paterson, S. M.; Casadio, Y. S.; Brown, D. H.; Shaw, J. A.; Chirila, T. V.; Baker, M. V. *J. Appl. Polym. Sci.* **2013**, *127*, 4296.

(9) Kavanagh, G. M.; Ross-Murphy, S. B. *Prog. Polym. Sci.* **1998**, *23*, 533.

(10) Ritger, P. L.; Peppas, N. A. *J. Control. Release.* **1987**, *5*, 37.

(11) Ritger, P. L.; Peppas, N. A. *J. Control. Release.* **1987**, *5*, 23.

(12) Trompette, J. L.; Fabrègue, E.; Cassanas, G. *J. Polym. Sci., Part B: Polym. Phys.* **1997**, *35*, 2535.

(13) Grattoni, C. A.; Al-Sharji, H. H.; Yang, C.; Muggeridge, A. H.; Zimmerman, R. W. *J. Colloid. Interf. Sci.* **2001**, *240*, 601.

(14) Gradinaru, L.; Ciobanu, C.; Vlad, S.; Bercea, M.; Popa, M. *Cent. Eur. J. Chem.* **2012**, *10*, 1859.

(15) Skouri, R.; Schosseler, F.; Munch, J. P.; Candau, S. J. *Macromolecules.* **1995**, *28*, 197.

(16) Wang, L.; Shan, G.; Pan, P. *Soft Matter* **2014**, *10*, 3850.

(17) Anseth, K. S.; Bowman, C. N.; Brannon-Peppas, L. *Biomaterials* **1996**, *17*, 1647.

(18) Şen, M.; Sarı, M. *Eur. Polym. J.* **2005**, *41*, 1304.

(19) Bae, Y. H.; Okano, T.; Kim, S. W. *J. Polym. Sci., Part B: Polym. Phys.* **1990**, *28*, 923.

(20) Huglin, M. B.; Rehab, M. M. A. M.; Zakaria, M. B. *Macromolecules.* **1986**, *19*, 2986.

(21) Chirila, T. V.; Constable, I. J.; Crawford, G. J.; Vijayasekaran, S.; Thompson, D. E.; Chen, Y. C.; Fletcher, W. A.; Griffin, B. J. *Biomaterials* **1993**, *14*, 26.

(22) Miller, D. R.; Peppas, N. A. *Biomaterials* **1986**, *7*, 329.

(23) Trieu, H. H.; Qutubuddin, S. *Colloid. Polym. Sci.* **1994**, *272*, 301.

(24) Baker, M. V.; Brown, D. H.; Casadio, Y. S.; Chirila, T. V. *Polymer* **2009**, *50*, 5918.

(25) Liu, S. Q.; Ee, P. L. R.; Ke, C. Y.; Hedrick, J. L.; Yang, Y. Y. *Biomaterials* **2009**, *30*, 1453.

(26) Chirila, T. V.; Chen, Y. C.; Griffin, B. J.; Constable, I. J. *Polym. Int.* **1993**, *32*, 221.

(27) Andac, M.; Plieva, F. M.; Denizli, A.; Galaev, I. Y.; Mattiasson, B. *Macromol. Chem. Phys.* **2008**, *209*, 577.

(28) Savina, I. N.; Cnudde, V.; D'Hollander, S.; Van Hoorebeke, L.; Mattiasson, B.; Galaev, I. Y.; Du Prez, F. *Soft Matter* **2007**, *3*, 1176.

(29) Munro, H. S.; Hoskins, R. US20060068014 A1, **2003**.

(30) Wachsstock, D. H.; Schwarz, W.; Pollard, T. *Biophys. J.* **1994**, *66*, 801.

(31) Holmes, D. L.; Stellwagen, N. C. *Electrophoresis* **1991**, *12*, 612.

(32) Oudshoorn, M. H. M.; Rissmann, R.; Bouwstra, J. A.; Hennink, W. E. *Biomaterials* **2006**, *27*, 5471.

(33) Pedrón, S.; Bosch, P.; Peinado, C. *J. Photochem. Photobiol., A.* **2008**, *200*, 126.

(34) Pedrón, S.; Anseth, K.; Benton, J. A.; Bosch, P.; Peinado, C. *Macromol. Symp.* **2010**, *291*, 307.

(35) Zhang, H.; Patel, A.; Gaharwar, A. K.; Mihaila, S. M.; Iviglia, G.; Mukundan, S.; Bae, H.; Yang, H.; Khademhosseini, A. *Biomacromolecules* **2013**, *14*, 1299.

(36) Dodiuk-Kenig, H.; Lizenboim, K.; Eppelbaum, I.; Zalsman, B.; Kenig, S. *J. Adhes. Sci. Technol.* **2004**, *18*, 1723.

(37) Liu, H.; Wilén, C.-E. *J. Polym. Sci., Part A: Polym. Chem.* **2001**, *39*, 964.

(38) Ross-Murphy, S. B. *Polym. Gels Networks* **1994**, *2*, 229.

(39) Gridnev, A. A.; Ittel, S. D. *Chem. Rev.* **2001**, *101*, 3611.

(40) Gridnev, A. *J. Polym. Sci., Part A: Polym. Chem.* **2000**, *38*, 1753.

(41) Smeets, N. M. B. *Eur. Polym. J.* **2013**, *49*, 2528.

(42) Smirnov, B. R.; Morozova, I. S.; Pushchaeva, l. M.; Marchenko, A. P.; Enikolopyan, N. S. *Dokl. Akad. Nauk. SSSR.* **1980**, *253*, 609.

(43) Kukulj, D.; Davis, T. P. *Macromol. Chem. Phys.* **1998**, *199*, 1697.

(44) Godfrey, J., PhD Thesis, **2014**.

(45) Moad, C. L.; Moad, G.; Rizzardo, E.; Thang, S. H. *Macromolecules.* **1996**, *29*, 7717.

(46) Engelis, N. G.; Anastasaki, A.; Nurumbetov, G.; Truong, N. P.; Nikolaou, V.; Shegiwal, A.; Whittaker, M. R.; Davis, T. P.; Haddleton, D. M. *Nat Chem* **2016**, *advance online publication*.

(47) Hirst, A. R.; Coates, I. A.; Boucheteau, T. R.; Miravet, J. F.; Escuder, B.; Castelletto, V.; Hamley, I. W.; Smith, D. K. *J. Am. Chem. Soc.* **2008**, *130*, 9113.

5. Synthesis and characterisation of inter-penetrating networks; incorporating polyurethanes

This chapter details the synthesis and development of novel inter-penetrating network (IPN) for potential application in wound-care. IPNs are made up of two orthogonal networks physically intertwined in a single space, these materials have for some time been seen as a way to combine the properties of two networks to prepare a tailor made material for a particular application.[1] In this instance, the targeted application was chronic skin wounds and their treatment with hydrogels (see Chapter 1).[2-6] For this application a fast, high swelling and versatile material is required in order absorb excess exudate and maintain a moist wound environment.[3,4,7] In this chapter the pAMPS networks discussed in Chapter 4 are combined with a hydrophilic commercial polyurethane film (Tecophilic 2000 - TPU) to generate a fully inter-penetrating network.[1,8-10] The level of cross-linker and the relative quantities of the two monomers are varied and compared to the monolithic networks through swelling (both directional and in terms of fluid uptake), rheology, and the ability of the materials to actively absorb calcium ions in order to promote granulation in the networks.[11-15]

5.1 Interpenetrating networks in wound care and material characterisation

As mentioned in Chapter 1, there are a number of different types of interpenetrating networks that have been developed with wound care in mind.[1,16] Some of these species have natural polymers included in one or both of the networks, with the remaineder being made up of networks developed entirely from synthetically derived monomers. Here, the focus lies on synthetic networks where, one of the networks is polyurethane. Networks have been developed from a wide range of monomers however; the principle focus for applications has been in the biomedical field. In the early development of polyurethane-based IPNs, the focus was upon epoxide, styrene and (meth)acrylate polymerisation however, in recent years the focus has coallesed around a selection of hydrophilic monomers. In the late 1990's polyurethane / polyaniline networks were developed unfortunately, despite reasonable mechanical results, the high toxicity of aniline led to these networks being marginalised.[17,18]

Polyurethane (PU)/pHEMA has been the subject of extensive studies by the Karabanova group.[19] Early work focused upon the mechanical properties of these networks, but this soon developed into studies on the homogeneity of the networks.[20,21] Findings through DMTA and DSC analysis showed phase separation of the two networks, in recent years this group has focused upon the attachment of silica nanoparticles for biomedical applications.[22,23]

The Atsushi group has astutely focussed upon the development of the PU/pNIPAM IPNs, this system benefits from NIPAMs LCST of 32 ^{o}C and its biocompatibility. Initial development was followed by research into the tuning of cell adhesion through the

variation of the LCST of pNIPAM followed, by the development of a dual responsive system through the addition of acrylic acid with butyl acrylate to impart pH responsive character.[24-26] This system has been further developed for the inclusion and delivery of silver nanoparticles for antibacterial applications.[27]

Other monomer systems that have attracted some interest include: acrylamides; both in the academic[28,29] and patent literature,[30-32] acrylic acid; in the academic[26,33] and patent literature,[34] and PEG; in the academic[35] and patent literature.[30-32] One monomer that has been developed comprehensively as a monolith as described in Chapter 4 is AMPS however, this monomer has not seen inclusion in any IPNs. The benefits of AMPS are its biocompatibility and its ability to absorb large quantities of water. These properties have seen pAMPS monoliths applied in the biomedical sector for wound care.[8,9,36]

The techniques used to test hydrogels for wound care are designed to simulate and exceed the conditions that the hydrogel would be exposed to at the wound site. To this end the equilibrium degree of swelling and rate of swelling in an excess of a simulated bodily fluid is used, as are stress tests in multiple dimensions in order to ascertain the strength or workability of the material. A good understanding of the hydrogel's adhesion is also necessary in order to determine if the removal of the gel is likely to cause discomfort in the process. This is all without considering the additional factor of delivery and release of specific compounds from the wound site.

5.1.1 Hydrogel adhesion in wound care

The study of the adhesion strength of a hydrogel to the wound environment is an essential component of characterisation as, if the hydrogel adheres too strongly to the

wound site then pain or injury may occur during the process of dressing changes. Despite extensive publication in this field on the subject of hydrogels for application in wound-care there is as yet no standardized procedure with a range of different industrial standard techniques being used as guidance (**Table 5.1**).[37]

Standard	Type of test	Substrate	Adhesive type
ASTM F2258[38]	Tensile	Soft tissue	Surgical adhesives or sealants
ASTM F2256[38]	T-peel in tensile mode	Soft target tissue	Surgical adhesive
ASTM F2458[38]	Tensile	Fresh or frozen porcine skin	Surgical adhesive
ASTM F2255[38,39]	Lap Shear	Soft tissue	Surgical adhesive
ASTM D6195	Loop tack test in tensile mode	Steel and tape	Pressure sensitive tape adhesives
ASTM D1002[40,41]	Lap Shear in tensile mode	Steel	Metal bonding adhesives
ASTM D1876	T-peel in tensile mode	Flexible substrate and adhesive	Wide spread usage
ASTM D3330[42]	180 ^{o} peel test in tensile mode	As appropriate	Pressure sensitive tape adhesive
ASTM D903	180 ^{o} peel test	As appropriate	Tape adhesive
BS EN 1939:2003[37]	180 ^{o} peel test	Stainless steel or own backing	Tape adhesive

Table 5.1; A selection of methods that have been used in the testing of network adhesion for wound care hydrogels.

From the tests shown in **Table 5.1**, the tack test is predicted to be the most appropriate for the application of a wound care hydrogel. In a tack test a probe is lowered onto the surface of the hydrogel with a given preload and then withdrawn. The hydrogel is fixed to a bottom plate so that the force of removal does not cause any slippage. The surface substrate of the probe is crucial as this dictates the level and type of interaction with the material. Historically steel substrates have been used to test the force of adhesion; however, this has been shown to be inadequate due to the disparity in materials properties between steel surfaces and organic tissue.[37] A tack test measures the 'tackiness' or "stickability" of a surface to a substrate through a vertical

lift of the substrate from the surface. In this test the two most important measurements are the peak force – the maximum amount of force required during the process of removal – and the area under the force curve – this denotes the total work done. As porcine skin is difficult to work with, store and maintain in consistency, an alternative substrate was considered. A silex silicone sponge product with a high degree of flexibility offered a potential replacement to living tissue. Previous studies into the relevant silicone sponge have shown comparable tensile and compressive results which often have a significant effect upon the adhesive properties of a material, these materials are also often used when a soft, easily deformable elastic material is required in combination with pressure sensitive adhesives, from this criteria it was decided to use a silicone sponge sheet as a testing substrate.[43]

5.1.2 Hydrogel calcium adsorption

An important aspect incorporated into many modern wound healing materials is the ability to either deliver materials into the wound site or specifically take up harmful substances from the site. Although delivery is attractive in that it can encourage growth through substances such as growth factors or alternatively kill bacterial infections e.g. through the delivery of silver nanoparticles or antibiotics, these methods can be costly to produce materials on the large scale.[2,44-47] The delivery of materials into a wound site usually requires further expensive clinical trials as the material is no longer a non-invasive dressing but a drug delivery agent. The alternative is to target or ensure that the dressing material is able to take up species that are specifically inhibiting the healthy wound healing process – one such species being calcium ions.

Calcium is useful in the initial stages of a normal or acute wound healing process, it is released in hemostasis and inflammation as a cell signalling agent and has been known to regulate a number of processes for some time including; growth factor regulation, cellular mitosis, neutrophil exocytosis, superoxide production and remodelling of the embryonic epithelium.[11,48] Although calcium is important in the process of mitosis, the removal of calcium or the inhibition of its production in the wound site can increase the rate of granulation.[11,49] As inhibition again requires the delivery of material into the wound site, it was decided to investigate as to whether or not the materials developed here were capable of active uptake.

5.2 Synthesis and characterisation of inter-penetrating network hydrogels

An IPN of AMPS and the polyurethane Tecophillic 2000 ™ was generated by photo-initiated free radical polymerisation of the AMPS monomer in the presence of the swollen polyurethane film. This material was subsequently tested for its material properties as well as its ability to interact mechanically in the wound site.

5.2.1 Swelling into simulated body fluid

Wound dressings are expected to absorb a large quantity of exudate in order to remove waste material from the wound site and prevent it from acting as a platform for infection. To this end the IPNs were swollen to equilibrium in a fluid designed to mimic the sodium and calcium concentrations in the blood – a simulated body fluid. The swelling kinetics of the materials was recorded in triplicate until the equilibrium degree of swelling was observed. In the initial tests, the concentration of the PEGDA

cross-linker was varied and the resulting IPN swelling profiles were compared to a monolithic AMPS hydrogel and the swollen TPU film swollen under the same conditions as shown in **Table 5.2**, **Figure 5.1** and **Figure 5.2**.

Material	Network;	[PEGDA] wt. %[a]	Equilibrium Degree of swelling (%)[b]	Volume Ratio of Swelling (X/Y:Z)[c]
A	Monolith	0.14	3390 (±60)	1.049 (± 0.007)
B	Monolith	0.25	3250 (±50)	1.097 (± 0)
C	Monolith	0.5	2230 (± 110)	0.990 (± 0)
D	Monolith	1	1480 (±80)	1.027 (± 0)
E	IPN	0.14	2550 (± 160)	0.822 (± 0)
F	IPN	0.25	2090 (± 70)	0.895 (± 0.006)
G	IPN	0.5	1830 (± 90)	1.002 (± 0.004)
H	IPN	1	1550 (± 70)	0.886 (± 0.001)
I	Monolith	TPU	930 (± 20)	-

Table 5.2; Swelling data for hydrogel networks. [a] Concentration in AMPS monomer solution, with IPNs the TPU is swollen into this. [b] Swollen from cured samples, dry mass obtained by gravimetry. [c] Ratio of degree of swelling at equilibrium in diameter relative to the degree of swelling in height – relative to cured samples.

In Chapter 4 a comprehensive study of the swelling characteristics of the pAMPS monolithic networks at variable concentration of cross-linker was presented. It was shown that one of the most significant determining characteristics of the rate and mechanism of fluid uptake are the thermal properties of the network. In the case of pAMPS the T_g lies well above room temperature (108 °C) leading to a glassy network with a relatively slow rate of water uptake.[50] As the T_g of the TPU is significantly lower than room temperature (-49.6 °C), it should have a marked impact upon the rate of swelling of the IPNs as this helps to create a rubbery network.[51,52]

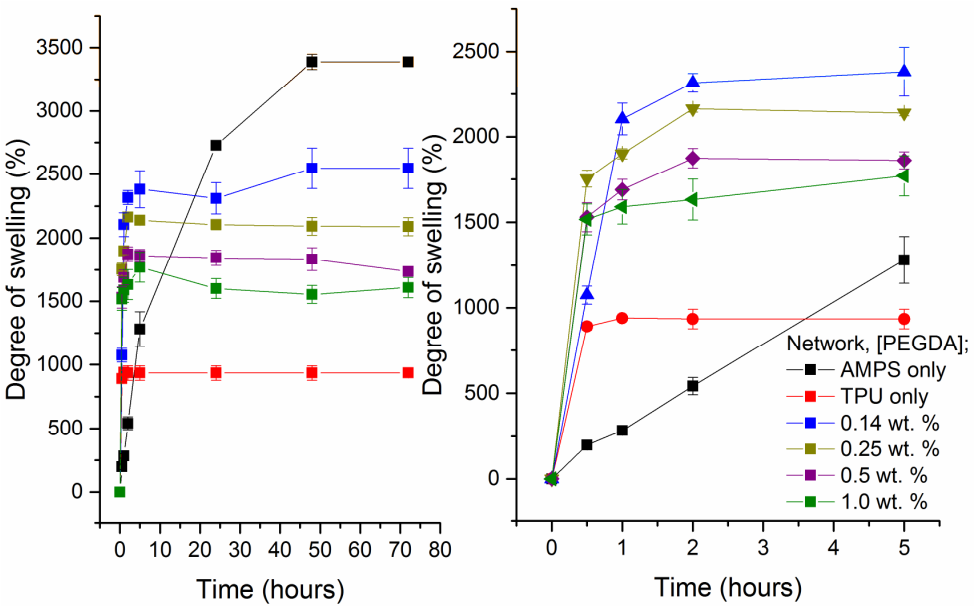

Figure 5.1; Swelling to equilibrium of IPNs at different cross-linker concentrations in comparison to pAMPS and TPU networks (left), initial five hours of swelling (right).

Observation of the swelling behaviour of the IPN hydrogels in comparison to its constituent monoliths of TPU and pAMPS hydrogel showed two notable sets of behaviour (**Figure 5.1**). The IPNs all show a far more rapid rate of fluid uptake in comparison to the monolithic networks, with equilibrium being reached within an hour in comparison to the 2 day time period required for the monolith to reach equilibrium at comparable concentrations of cross-linker. This difference can be attributed to two factors: firstly to the impact of the inclusion of the lower T_g TPU, which, having a significantly lower T_g imparts a rubbery-like (higher chain flexibility) character to the networks and allows for a far more rapid uptake of water.[53] Secondly there is an increased hydrophilicity in the networks reletaive to the TPU monolith due to the inclusion of the pAMPS,, creating a greater osmotic effect..[54,55]

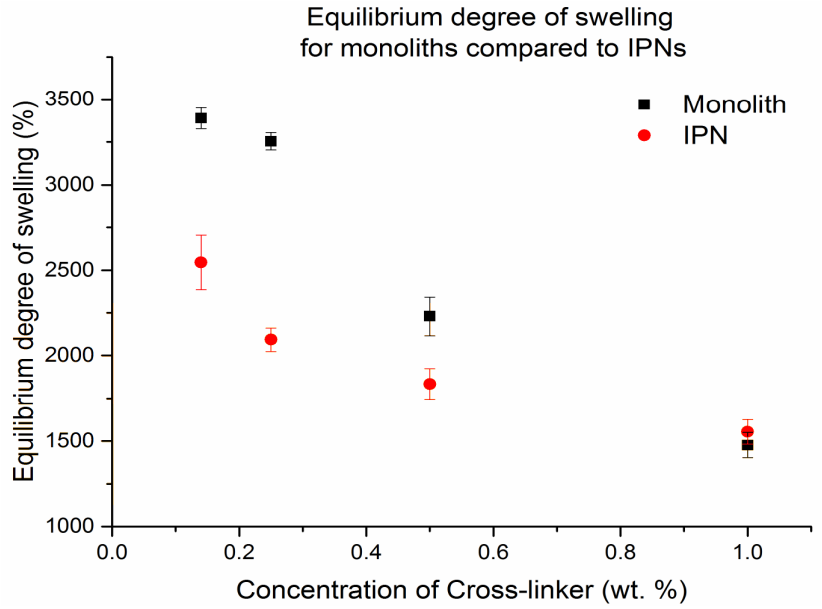

Figure 5.2; Equilibrium degree of swelling of IPNs at different concentrations of cross-linker in comparison to monoliths.

There is a characteristic decrease in the degree of swelling with increasing concentration of PEGDA cross-linker in the second AMPS network caused by a decrease in the mesh size within that network (**Figure 5.2**). Despite the fact that the PEGDA cross-linker is at a significantly reduced concentration relative to the total dry mass of the network, it continues to have a significant impact upon the equilibrium degree of swelling.

The higher degree of swelling seen in the IPNs relative to the TPU monolith can be explained through the inclusion of a high degree of the more hydrophilic, highly swelling pAMPS material (**Figure 5.3**). The lower degree of swelling in the IPN relative to the pAMPS monolith can be explained as the entanglement of the second network in the first network contributes to a relative increase in the cross-linking density in the gel.[1,56,57]

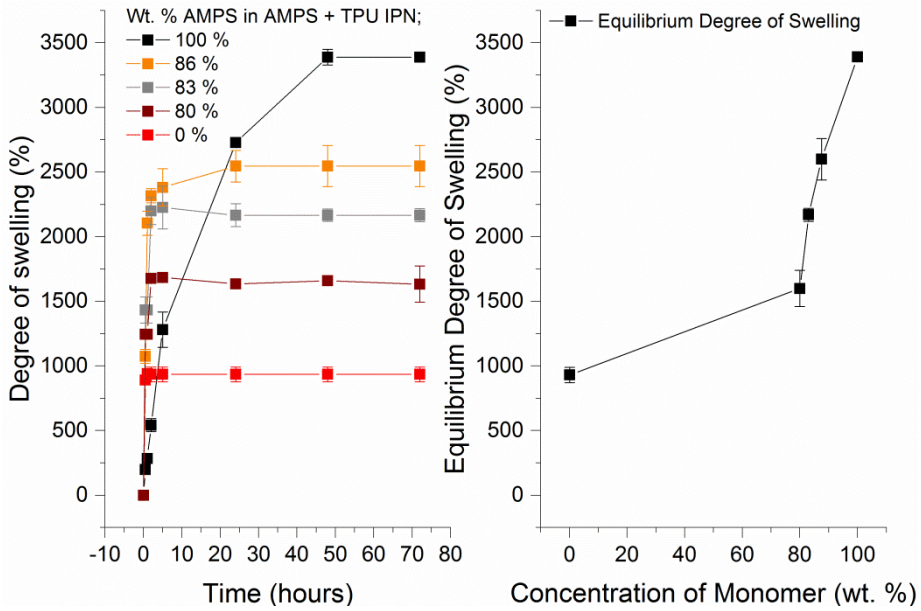

Figure 5.3; Swelling to equilibrium of IPNs with different concentrations of AMPS monomer relative to AMPS and TPU monoliths (left), Equilibrium degree of swelling as a function of AMPS content in IPN (right).

Increasing the concentration of the AMPS monomer relative to the TPU within the network, gives an increase in the equilibrium degree of swelling without there being an impact upon the rate of swelling (**Figure 5.3**). This means that the TPU is still acting as the framework and imparting the 'rubbery like' characteristics necessary for rapid swelling, whereas, the AMPS is imparting increased hydrophilicity – allowing for a higher mass uptake of ordered, coordinated water as opposed to disordered free water, due to the increased osmotic effect. The non-linear increase in the degree of swelling can probably be explained by an exponential increase in the amount of cross-linking caused by increased connectivity through the polyurethane matrix. DSC appears to show that there is no shift in the T_g of the pAMPS network, in a homogeneous network the T_g of the TPU and pAMPS would be expected to merge and create a ssingle T_g, The absence of this phenomenon indicates a heterogeneous

network has been formed where the pAMPS and TPU reside in separate domains (**Figure 5.12**). This allows the TPU to continue to act as the framework imparting the rubbery like characteristics that allow for the rapid uptake of water due to this domain of the IPN residing beneath its T_g.

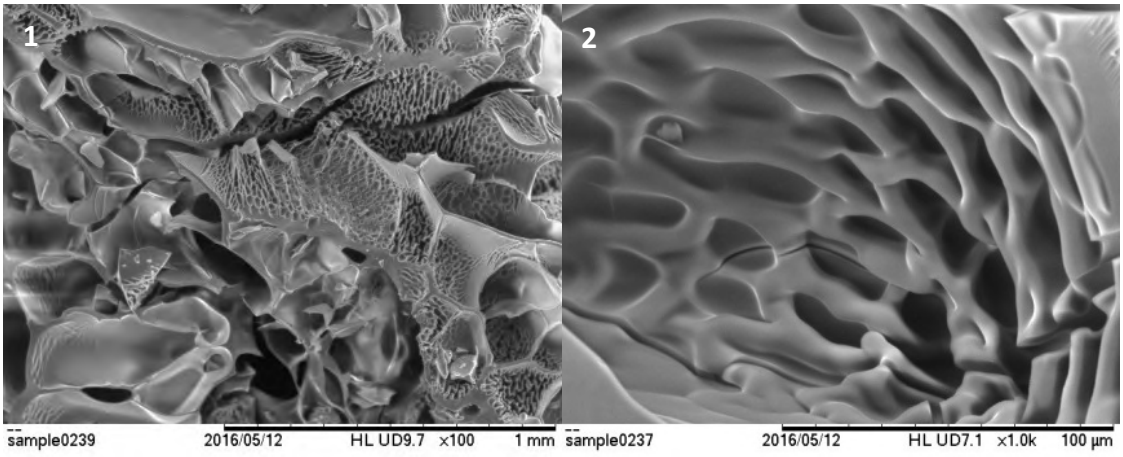

Figure 5.4; SEM micrographs of pAMPS monolith at x 100 magnification (1) and x 1000 magnification (2).

SEM micrographs of the pAMPS network (**A**) show a macroporous network with multiple levels of detail (**Figure 5.4**).[58] At x 100 magnifications the dehydrated network can be seen to have two levels of porosity, those pores on the 100 µm scale and those on the 10 µm scale previously reported, this is complemented at the x 1000 magnification scale, showing a porous structure on the 10 µm scale.[58,59] The macroporosity of these materials lends itself to low mechanical strength but very high water uptake levels as described in Chapter 4. These networks show a random pore structure with no directionality lending itself to a lack of anisotropy in swelling behaviour.

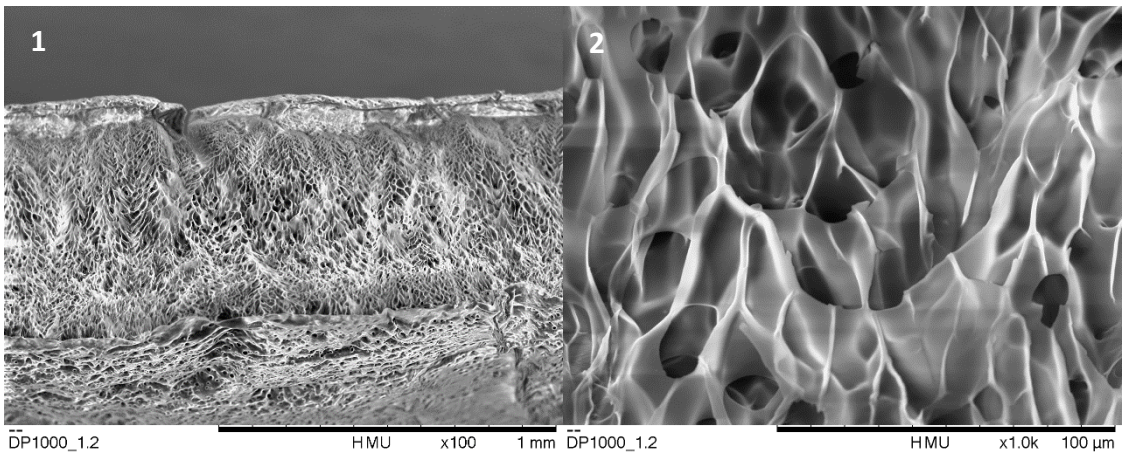

Figure 5.5; SEM micrographs of TPU network at x 100 magnification (A) and x 1000 magnification (B)

SEM micrographs of the TPU network (**I**) show an open cell type network (**Figure 5.5**). Very little directionnality is observed in either the X/Y or Z direction with cells on a 10 µm scale diameter being observable by SEM. These samples were prepared by swelling to 90 wt. % in water, rapidly freezing in liquid nitrogen followed by lyophilising. This type of network with its open cell-like structure is ideal for the formation of an IPN as it allows for the second network precursor to permeate through the first network and form a fully integrated IPN.

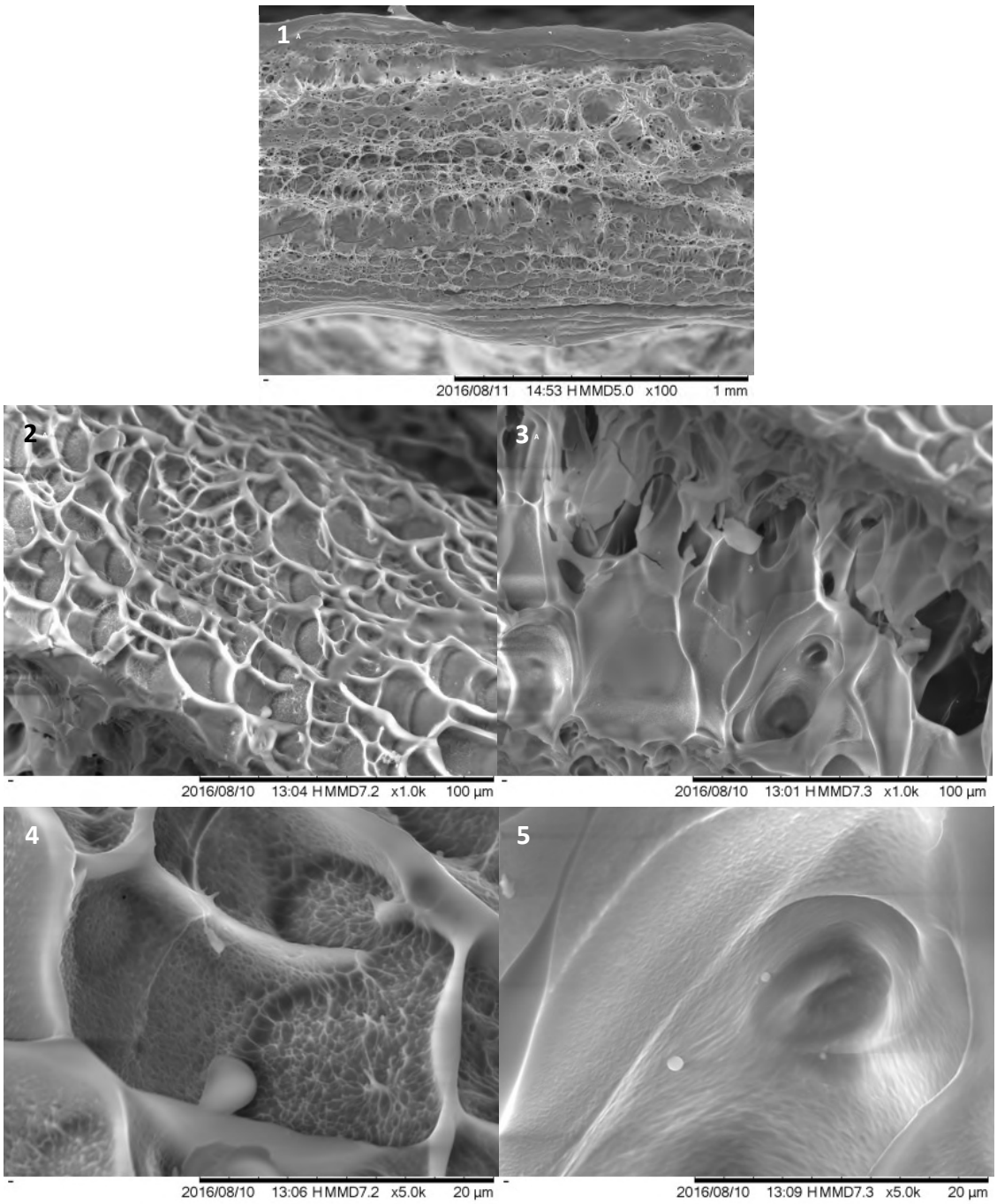

Figure 5.6; SEM micrographs of AMPS/TPU IPN: pAMPS/TPU IPN at x 100 magnification (1), IPN AMPS amorphous domain at x 100 magnification (2), IPN vitreous domain at x 100 magnification (3), IPN amorphous domain at x 5000 magnification (4), IPN vitreous domain at x 5000 magnification (5).

Microscopy of the IPN of the TPU and pAMPS at different magnifications shows the presence of two distinct domains (**Figure 5.6**). A textured porous domain and a vitreous domain are observable, this difference in domains is indicative of a heterogeneous mixture of the two components of the system with phase separation occurring, as seen by DSC (**Figure 5.12**).[19-21] This is readily observable at the lowest level of magnification where the two domains can be seen to contrast directly (**1**, **Figure 5.6**). From observations of the constituent networks, the porous domain is similar in structure to the pAMPS monolith (**Figure 5.4**), the vitreous domain is similar in appearance to the TPU (**Figure 5.5**). These results of heterogeneity are confirmed by the DSC results (**Figure 5.12**).

Anisotropy (or directional dependence) in the swelling of wound care materials is seen as a valuable property as it can mean that the materials can be controlled with respect to the direction they swell into, which makes the design of the bandaging layer securing the dressing to the site much less challenging.[60-62] This property is related to the internal morphology of the materials, where random structures tend to show little or no anisotropy but materials with some degree of internal order demonstrate varying degrees of directionality.[63] As can be seen from the SEM images of the monolithic pAMPS hydrogel, (**Figure 5.4**) there is no readily discernible internal order to the morphology of the pAMPS monolith. This is reflected in its swelling where the ratio of XY to Z axis swelling (explained in **Figure 5.8**) remains close to the value of 1, indicating no anisotropy in its swelling (**Figure 5.7**). This is in contrast to the IPN, which appears to show a degree of internal order as seen in (**1**, **Figure 5.6**). **1** appears to show lateral layers of vitreous TPU (**2** and **3**) regions, interspersed with the randomly structured pAMPS like regions (**4** and **5**), very similar to that seen in **Figure 5.4**. This

appears to have a significant impact upon the anisotropy of the swelling of these materials (**Figure 5.7**).

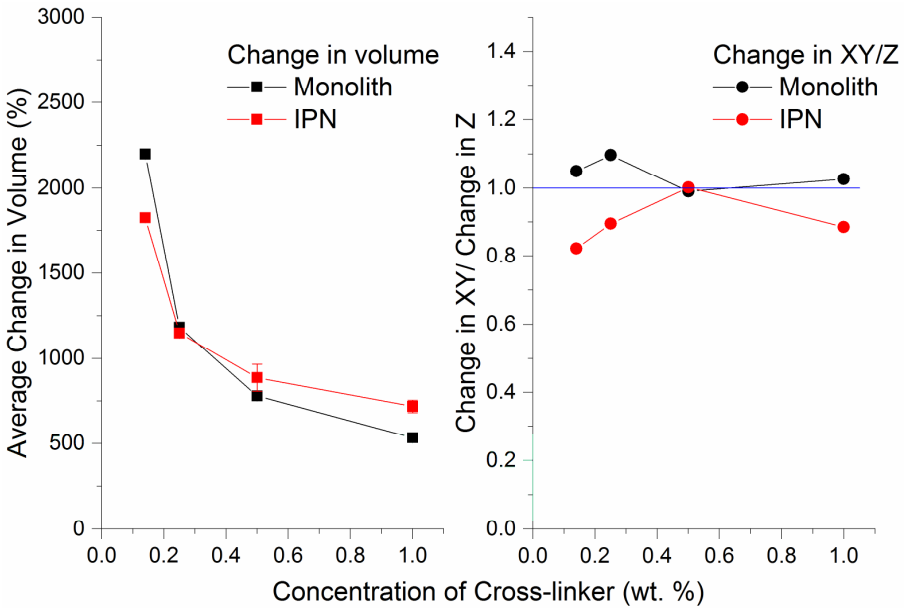

Figure 5.7; Effect of cross-linker concentration upon volume degree of swelling (with error shown) in pAMPS/TPU IPNs and pAMPS monoliths (left), Effect of cross-linker concentration upon anisotropy of swelling (with error shown) in pAMPS/ TPU IPNs and pAMPS monoliths (right).

A small degree of anistropy is observable upon the swelling of the IPN network, with an XY/Z ratio of close to 0.8 in some cases (**Figure 5.7**). This implies a small but significant preference to swelling in the Z direction rather than the XY direction. This is probably caused by the heterogenous structures observed in **Figure 5.6**. This is possibly caused by two things: firstly the layering of pAMPS upon the surface of the network from the swelling process, secondly it is possibly caused by the curing process moving from the surface down into the bulk of the material.

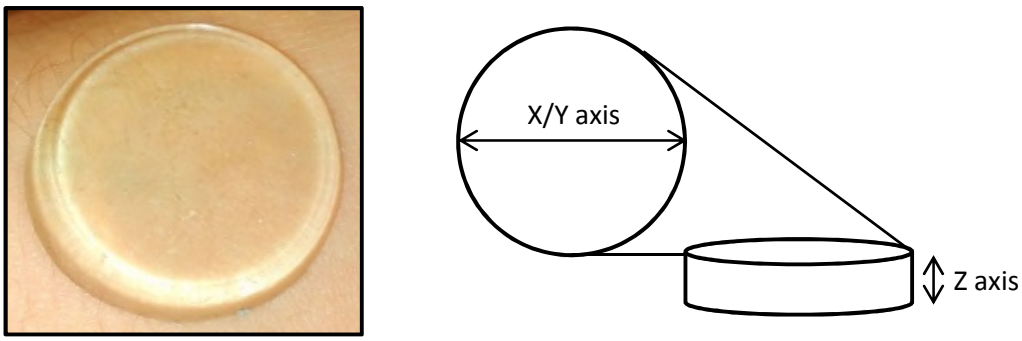

Figure 5.8; Photograph of colourless, transparent pAMPS monolith hydrogel (left), Diagram of discussed axis of hydrogel networks (right).

Having determined the swelling characteristics of the IPN networks as having a significantly more rapid degree of swelling than pAMPS monoliths and exhibiting a combination of behaviours from the TPU and pAMPS monoliths, the next step was to investigate the mechanical characteristics of the networks.

5.2.2 Rheology of cured gels

As the samples are too thin for compression, even in their swollen state, and too soft for use in the tensile grips available to us, rheology was determined to be the best available method for studying the elasticity of the networks. The pAMPS networks developed in Chapter 4 were compared to the IPNs at different concentrations of the cross-linker in the pAMPS network. Frequency sweep experiments were conducted within the linear visco-elastic region (LVER) with respect to amplitude, and compared to frequency sweeps at the same amplitude for the pAMPS monoliths. This will help to gain an understanding of the relative stiffness and rigidity of the two materials at different concentrations of cross-linker.[13,62,64] A full explanation of the theory of gel rheology can be found in Chapter 3. The results from the rheology have been tabulated in **Table 5.3**.

Material designation	Network	[PEGDA] wt. %[a]	G' (Pa) [b]	Tan(δ) [b]
A	pAMPS Monolith	0.14	953	0.14
B	pAMPS monolith	0.25	1913	0.20
C	pAMPS monolith	0.5	2812	0.36
D	pAMPS monolith	1	5506	0.25
E	pAMPS/TPU IPN	0.14	744	0.50
F	pAMPS/TPU IPN	0.25	2001	0.30

Table 5.3; Impact of change in concentration of cross-linker PEGDA upon the elasticity modulus of pAMPS monoliths and pAMPS/TPU IPNs. [a] wt. % as a percentage of total monomer and dry weight content, [b] G' and tan δ recorded at 1 Hz, 1 % strain, 25 °C with 40 mm parallel plates and 90 wt. % water content.

Definition of the pAMPS monoliths by rheology show that an increase in cross-linker concentration causes an increase in the elasticity modulus as the mesh size decreases and the materials become more rigid (**Figure 5.9** and Chapter 4). G' increases at higher frequency due to the inability to recover quickly from deformation.[13] The value of tan δ also increases with increasing cross-linker concentration, showing a smaller different between the viscous and elastic moduli, indicating a more elastic material, this is occurring as the material is becoming more rigid.

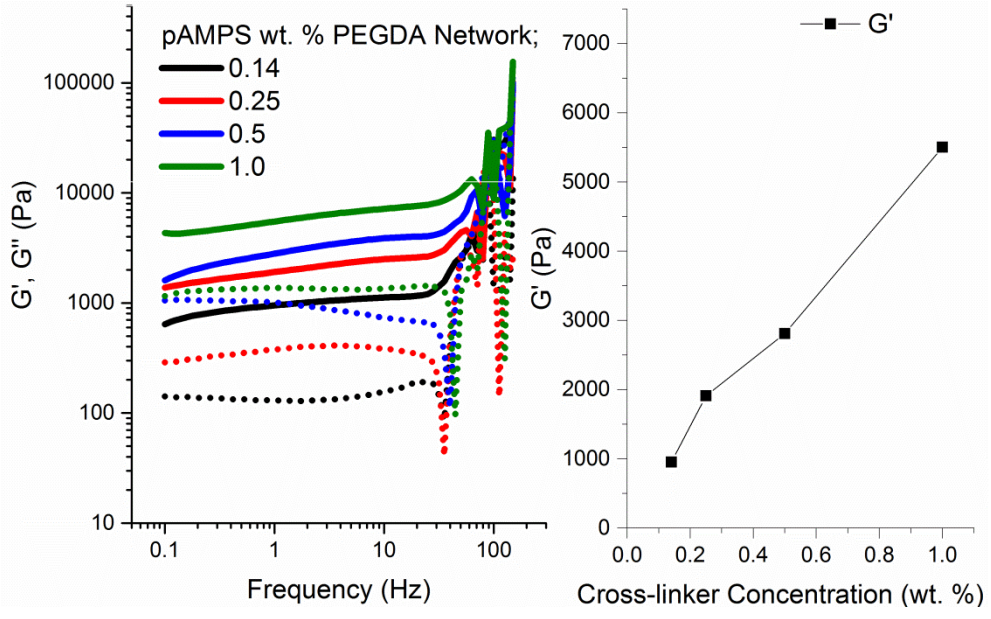

Figure 5.9; Rheological comparison of LVER pAMPS monoliths at different cross-linker concentrations (left), relationship between cross-linker concentration and elasticity modulus in LVER (right).

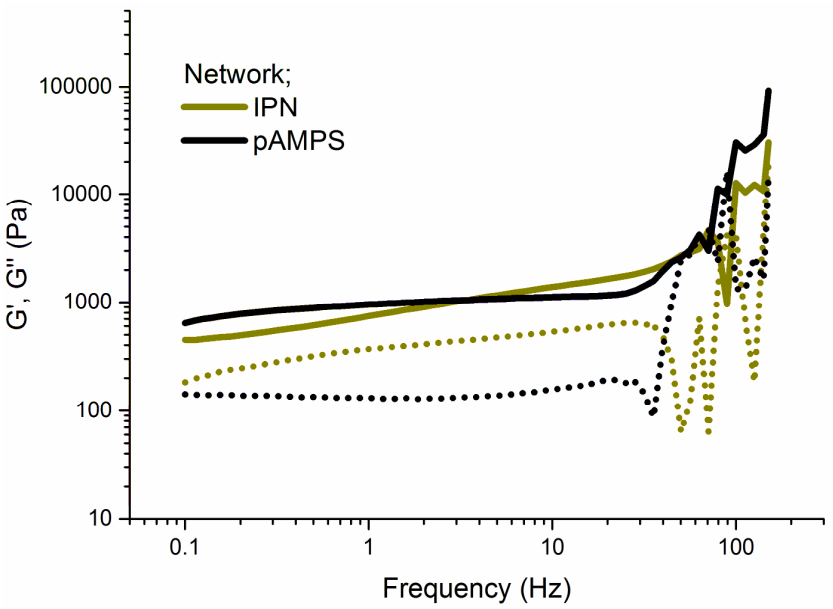

Figure 5.10; Rheological comparison of LVER between a pAMPS monolith and a pAMPS/TPU IPNs at similar cross-linker concentrations within the pAMPS network, 0.1 - 100 Hz at 1 % strain, 40 mm parallel plates, 25 ºC

When comparing the IPN to the pAMPS monolith, the same concentration of cross-linker was used in the AMPS network. The results show very comparable values of G' at the same frequency although the IPN shows a slight frequency dependency even in this region, this indicates that the two materials are very similar with respect to their rigidity (**Figure 5.10**). This is likely to be due to the amplitude being too high for the network to respond to strain in a linear manner. The second value of note from **Figure 5.10** is that the value of tan δ is substantially higher for the IPN. This implies that the 'in phase' and 'out of phase' components are substantially closer leading to a less solid-like material that is better able to flow. The IPN is also able to respond in a linear

fashion to higher frequencies demonstrating that it is able to relax at a faster rate at this amplitude.

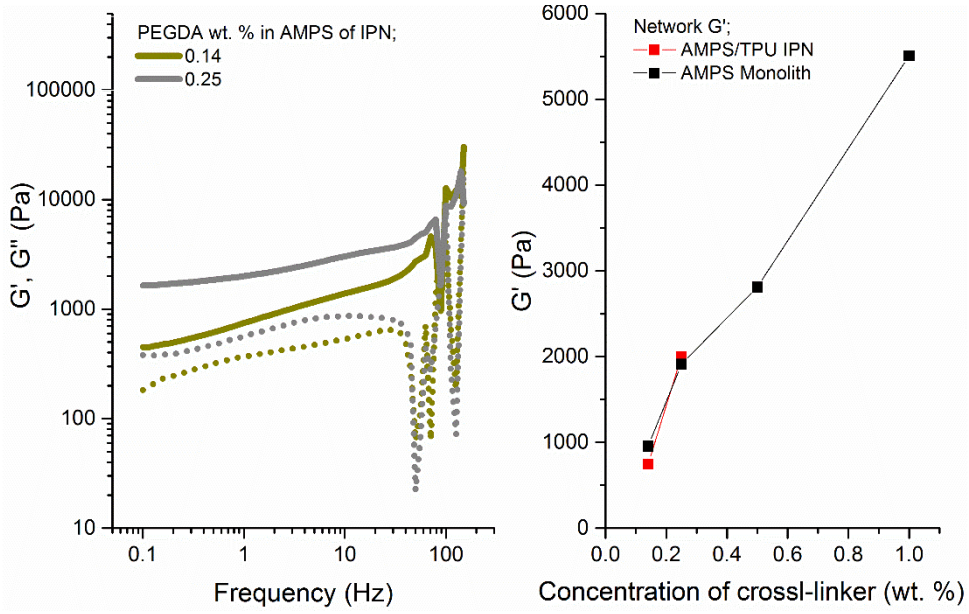

Figure5.11; Rheological comparison of LVER pAMPS/TPU IPNs at different cross-linker concentrations (left), Comparison of the relationship between cross-linker concentration in the IPN network and in the pAMPS monolith (right).

The impact of increasing the concentration of cross-linker in the AMPS network upon the rheological profile of the network is to increase the elasticity modulus, G', as the material becomes more rigid (**Figure5.11**). There is also a decrease in the value of tan δ, indicating a network with a reduced capacity to flow. Both of these can typically be explained through the reduction in the mesh size in the AMPS network. Characterisation of IPN networks at higher concentrations of cross-linker proved to be challenging as the material samples proved too brittle to handle, thereby indicating the impact the divinyl cross linker in the pAMPS network has upon the material properties of the gel.

Investigations into the rheological properties of the IPN has shown that the pAMPS monolithic networks and the IPN formed with the TPU have very similar rheological domains and properties with very comparable moduli under the same conditions. This was expected due to the very high percentage composition of AMPS in the IPN network (86 %).

5.2.3 Thermal properties of IPNs

The thermal properties of a network can yield much information on the nature and homogeneity of the structure as well as their processibility and handling at different temperatures. This is important for wound care materials as a temperature transition within room to body temperature range (10 – 37 °C) could have a serious impact upon the practicality of their use and storage. To this end differential scanning calorimetry (DSC) and dynamic mechanical thermal analysis (DMTA) are utilised to show how the IPN responds to thermal stimuli relative to the monolithic networks.

DSC of the TPU, pAMPS and the IPN show a T_m point associated with the TPU, as would be expected this doesn't shift with inclusion in the IPN (**Figure 5.12**). A T_g is visible for the pAMPS network at 72 °C, this is substantially lower than the reported values for pAMPS of around 150 °C, this is probably due to the reduction in chain mobility caused by cross-linking inteo a network., the T_g is not observed to shift substantially upon inclusion into the IPN. A T_g for the TPU is not visible in the expected range of -50 °C. This could be due to the thermal history associated with the handling of the TPU, I propose that a second heat-cool-heat cycle would probably have observed a T_g for the TPU. From the fact that the T_g for the pAMPS component of the network does not shift, this is indicative that the two networks remain in separate, heterogeneous

domains post-polymerisation and so I propose that no significant increase in the T_g of the TPU component of the network would be observed upon inclusion in the IPN>

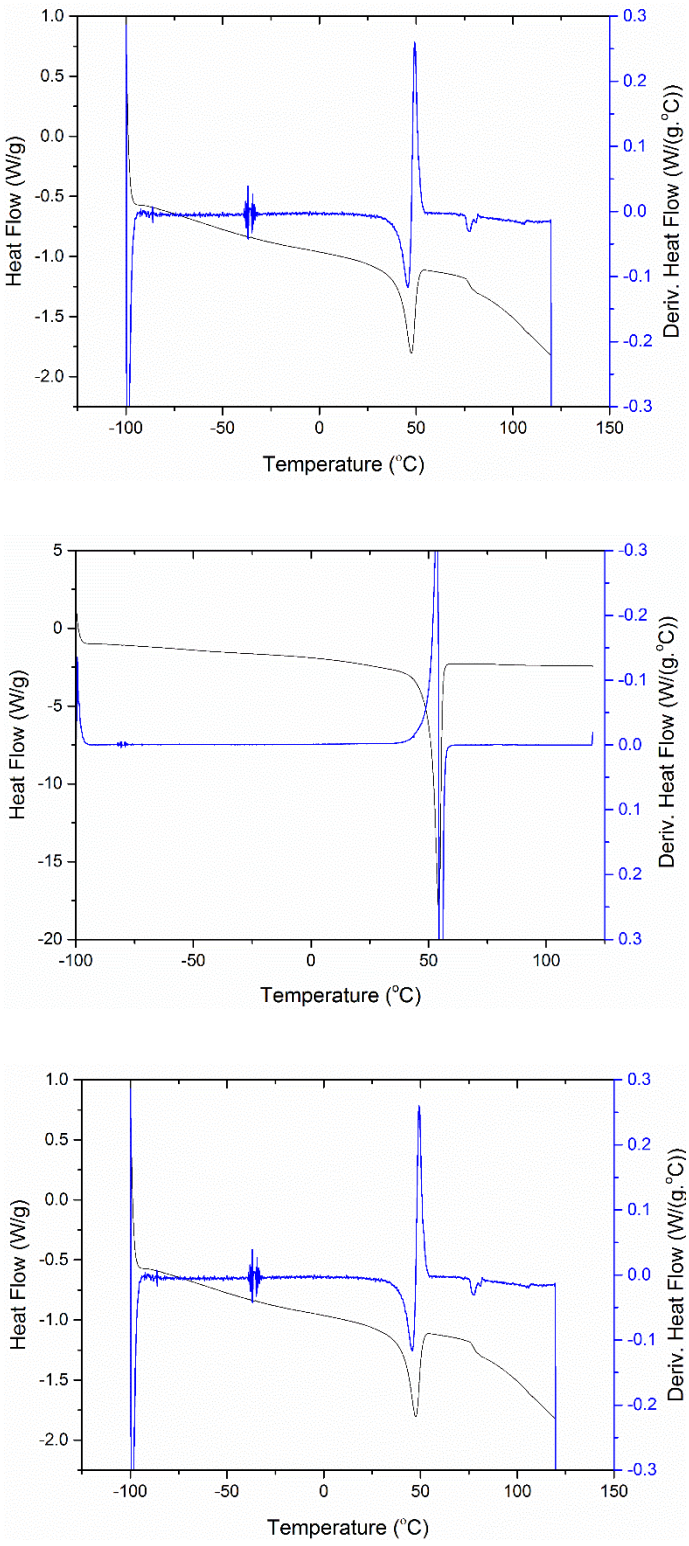

Figure 5.12; First heat cycle of pAMPS monolith with endo down and the first derivative showing the T_g visible at 72 °C (top), first heat cycle of TPU monolith with

no T_g visible (middle), first heat cycle of IPN with first derivative showing clearly the presence of the pAMPS T_g at 77 °C (bottom)

5.2.4 Adhesion of cured gels

The adhesive properties of a dressing for use in chronic wound care have a significant impact upon their practicality. Materials with a relatively high level of adhesion may not only cause significant discomfort upon their removal but also damage any granulated tissue that may be forming upon the wound site.[65]

To this end, this study was designed to investigate the amount of force required to remove a hydrogel from a wound-like surface by a tack-like test. Most tests used to examine adhesion are not designed to be bio-mimetic and use steel plates as described by ASTM E-62 and ASTM F2255-05.[38,39] It has, however, been shown that there is no empirical relationship between the adhesive properties of steel and skin, nor can comparisons be drawn between series of materials tested on steel relative to skin.[37] A silicon foam layer was used to coat the surface of a plastic dolly design (seen in) and the hydrogel was loaded onto a lower plate. The dolly was then lowered onto the lower plate and a preloading force of 1 N was applied and allowed to stabilise to counter slippage. The upper plate was then pulled off the lower plate and the force required to remove the plate with displacement was observed.

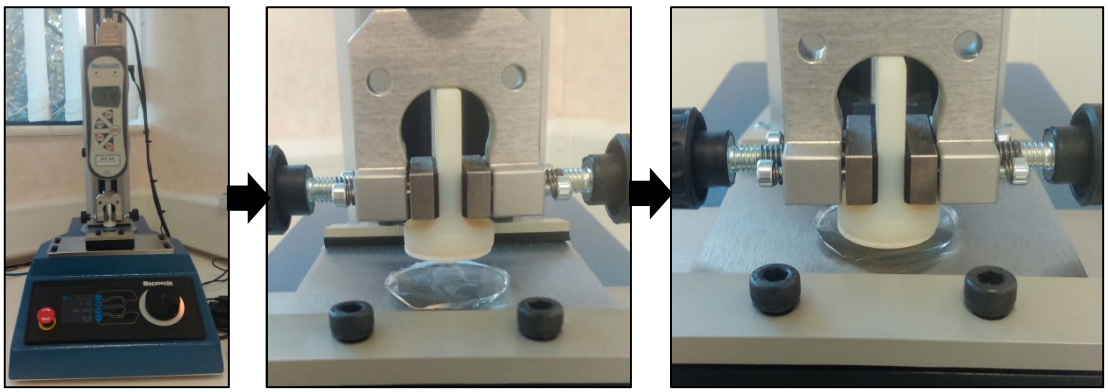

Figure 5.13; Rig used for adhesion testing (left), Dolly applied to surface of gel (Centre), Dolly after removal from surface of gel (right).

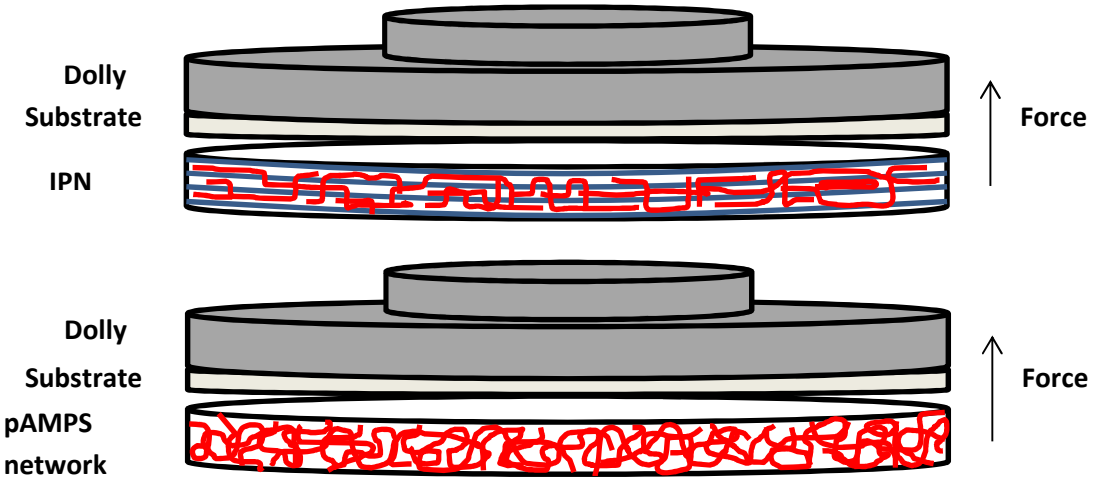

Figure 5.14; Orientation of TPU network (blue) and pAMPS network (red) in an IPN relative to adhesion force and dolly (top), Orientation of pAMPS monolith relative to force and dolly (bottom).

Initially pAMPS monoliths were tested at 90 wt. % water at different degrees of cross-linking, this was followed by testing of the IPNs with variation in cross-linker concentration in the pAMPS network, the results of which can be seen in **Table 5.4**.

Material	Network	[Cross-linker] wt. %	Peak Force (N)	Work Done (Nmm^{-2})
A	Monolith	0.14	0.25 (± 0.009)	14.7 (± 0.5)
B	Monolith	0.25	0.24 (± 0.012)	13.7 (± 0.3)
C	Monolith	0.5	0.05 (± 0.009)	3.11 (± 0.004)
D	Monolith	1	0.06 (± 0.005)	3.9 (± 0.002)
E	IPN	0.14	0.95 (± 0.02)	56 (± 2)
F	IPN	0.25	0.91 (± 0.08)	55 (± 5)
G	IPN	0.5	0.38 (± 0.02)	23 (± 2)
H	IPN	1.0	0.25 (± 0.01)	14.7 (± 0.5)

Table 5.4; Results of adhesion testing of materials including peak force and work done.

An increase of concentration of cross-linker in the materials, results in a decrease in the adhesion peak force and work done in both the AMPS monolith and the IPN (**Table 5.4**). This can be attributed to the increase in rigidity caused by an increase in the concentration of cross-linker which is a symptom of the corresponding decrease in the mesh size of the networks.

Across all concentrations of cross-linker there is a much higher degree of adhesion and peak force associated with the IPNs (**Figure 5.15**). This higher level of adhesion between the substrate and the sample is likely to be due to the inclusion of the polyurethane network and the resulting increase in internal order caused by the curing of the pAMPS network in the presence of the TPU network (**Figure 5.14**).

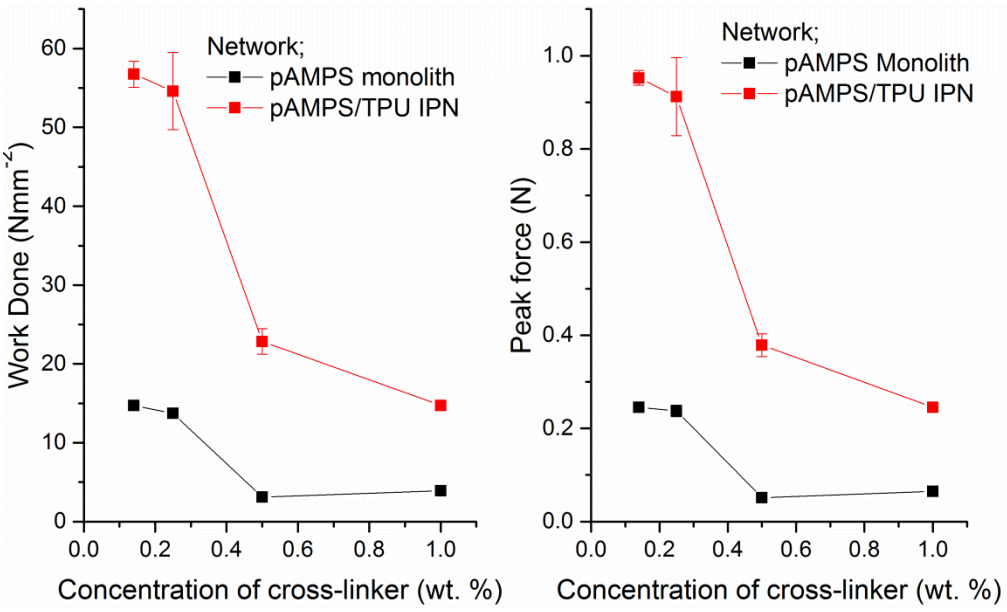

Figure 5.15; Comparison of work done to remove tack dolly from sample between IPNs and pAMPS monoliths at different cross-linker concentrations in the pAMPS networks (left), Comparison of peak force between IPNs and monoliths at different cross-linker concentrations (right).

A comparison between a pAMPS/TPU IPN and a pAMPS monolith at the same concentration of cross-linker within the pAMPS network shows two notable differences between the two networks; firstly the IPN network has a (relatively) ordered presence within the network, the second is that there is a significantly lower concentration of pAMPS per volume than in the pAMPS monolith – due to the volume occupied by the TPU (**Figure 5.14**). The effect of this is to significantly reduce the cross-linking density of the pAMPS network in the IPN relative to the monolith. This effect is exacerbated by the occurrence of chemical cross-linking only in the pAMPS domains lying between the TPU domains meaning there is a reduced amount of crosslinking in the vertical dimension. The result of this is that the network is less rigid in the vertical dimension leading to a degree of anisotropy (**Figure 5.7**) and is able to

deform by a greater amount in the Z direction than the pAMPS monolith, this leads to removal of the dolly from the surface of the network requiring a greater degree of force. In both cases the force required to separate the dolly from the network does not exceed those reported in the literature of skin care devices tested on either steel or skin.[37]

5.3 Calcium uptake of cured gels

As discussed previously in this chapter, the absorption of calcium was identified as a valuable characteristic worth studying due to the impact of calcium upon a chronic wound environment.[11,12,48]

In order to study the concentration of calcium, cured networks were swollen into solutions with a known concentration of calcium (2.5 $mmolL^{-1}$) and the calcium uptake into the hydrogels was detected through the change in the concentration of calcium in the solution. The final concentration of calcium was also adjusted according to the volume degree of swelling of each network. As the calcium ion is divalent (Ca^{2+}) and as such is considered a 'hard' ion, it was desirable to investigate the effects of ionic strength of the monomer in the network upon calcium uptake. AMPS is considered a 'hard' ion due to the highly polar sulfonate group, so a soft oxyanion in the form of sodium acrylate (Na-AA) and acrylic acid (AA) were chosen in both the monolithic and IPN form to act as a comparison.

Network	pH of monomer solution[a]	Calcium uptake (mg/g)	Calcium uptake (mg/mol)
pAMPS monolith	8.14	0.64 (± 0.05)	486 (± 4)
TPU monolith	NA	0	0
pAA monolith	2.55	0.14 (± 0.01)	34 (± 0.8)
pNa-AA monolith	8.52	0.71 (± 0.11)	222 (± 6)
TPU/AMPS IPN	8.14	1 (± 0.11)	1367 (± 223)
TPU/(Na-AA) IPN	8.52	1.52 (± 0.14)	743 (± 140)

Table 5.5; Results of calcium absorption in both mg of calcium absorbed per g of dry content in the network and per mol of AMPS in the network.[a] Solution pH measured of the monomer solution before curing using a broker pH probe.

Six networks were tested; pAMPS monolith, p(Na-AA) monolith, pAMPS IPN and p(Na-AA) IPN and TPU film. A pAA monolith was also tested in order to investigate the effects of pH upon calcium absorption. Initially the monoliths were tested for their calcium uptake, it was thought that an acrylate anion would coordinate calcium more strongly than the acrylamide, however, it was found that pAA hydrogels had a significantly lower uptake than pAMPS hydrogels. This was thought to be a function of pH and indeed the acrylic acid salt – sodium acrylate – at similar pH to the AMPS monomer solution (pH 8.1) showed a far higher degree of uptake – this is thought to be because the charge is less shielded. Per gram of hydrogel the pAMPS gel showed a lower degree of calcium uptake, however, the sodium acrylate molecular weight being far lower showed that per mol of monomer the pAMPS network has a significantly higher degree of uptake. pAMPS has a significantly higher degree of uptake due to the greater degree of electrostatic attraction between the sulfonate group on the AMPS repeating unit and the strong charge of the Ca^{2+}, this contrasts to the weaker dipole on the sodium acrylate group. The pH dependency observed with the pAA vs p(Na-AA) monoliths can be explained by the dipole being more shielded upon the acid, reducing the electrostatic attraction between the acid and the metal ions (**Figure 5.16**).[66]

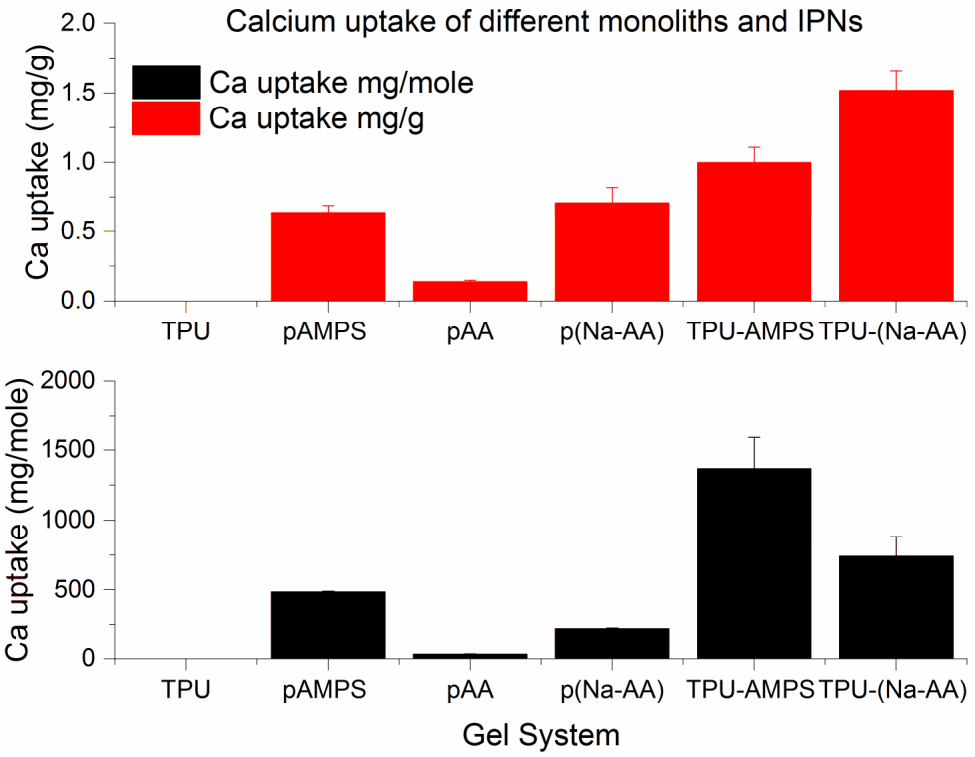

Figure 5.16; Ca^{2+} uptake in mg per g of dry hydrogel for six different networks (top), Ca^{2+} uptake in mg per mol of monomer in the network for 6 different networks (bottom).

A comparison of the networks with respect to their calcium uptake both per gram of solid in the network and per mol of monomer in the network was undertaken (**Figure 5.16**). When the IPNs were tested for their uptake, despite the decreased concentration of polar network and, decreased equilibrium degree of swelling, there was observed a significant increase in the calcium uptake, both in mg per g and mol per g. A similar trend was observed with the pAMPS network showing a significantly higher uptake of calcium per mol of AMPS monomer in the network. As the most significant change between the two systems was addition of the TPU network, this network was tested and was found to have no capacity for the absorption of calcium above the effects of its own equilibrium change in volume.

From these results, it seems that the most likely cause for the increased calcium uptake of the IPNs over their respective monolithic systems is caused by the difference in the morphology of the networks. The layered system of the IPNs could be creating a significantly higher surface area, over which a higher degree of absorption can occur per gram of monomer. This could be tested through the use of pelleted TPU to form IPNs with a more random internal structure with respect to the TPU phase.

5.4 Conclusions

The monolithic pAMPS hydrogel studied in Chapter 4 acted as the platform for the synthesis of a novel fully inter-penetrating network using a biocompatible polyurethane film as the first network swollen into a solution of pAMPS with cross-linker and initiator and then UV cured. Variation in the concentration of cross-linker PEGDA relative to monomer pAMPS in the second network was found to have a significant impact upon the material properties of the gel formed.

The swelling of the material was found to decrease with increasing concentration of cross-linker in the pAMPS network. Swelling was found to be far more rapid than the single network, with equilibrium being effectively reached within an hour in most cases. Anistropic swelling in the Z axis was also found to occur to a greater degree than swelling in the X/Y axis. These differences are thought to be caused by the the comination of the pAMPS network within the TPU network and the curing process leaving a heterogenously distributed morphology.

The rheological characteristic also confirmed these observations with increasing cross-linker concentration, causing an increase in the value of G’ in the LVER denoting a decrease in the pore size of the network. The calcium uptake of the IPN networks were compared to PU and pAMPS monoliths and found to have a significantly higher degree of uptake – creating promise for their potential for targeted absorption. The adhesive properties of the IPN were shown to have a higher degree of adhesion in the experimental system tested here.

The combination of these studies points to a promising material for future use in the biomedical field.

5.5 Experimental

5.5.1 Materials

All reagents were purchased from Aldrich and used as received unless otherwise stated. Tecophilic™ 2000 polyurethane film was obtained from Lubrizol.

5.5.2 Equipment

Rheometer

All rheology experiments were conducted upon a Malvern Kinexus Ultra with a Julabo cry-compact circulator CF41 temperature control unit. 20 mm stainless steel parallel plate geometry was used at 37 ^{o}C and with a force gap of 1N. The instrument was controlled in a CS-autostrain mode. A minimum of three experiments were conducted for each material.

Oven

All thermal gelation experiments were carried out in a Thermo Scientific Heratherm oven OGS180 at 55 °C. Materials were allowed to gel for 16 hours prior to cooling and further analysis.

Light Hammer™

All photo gelation experiments were carried out on a Light Hammer 6 equipped with a broad spectrum H bulb and the speed of the conveyer belt unit set at 5 m/min. The H bulb operates between 250 and 400 nm at an optimal intensity of 200 watts/cm.

Scanning Electron Microscope

A Hitachi TM3030plus portable desktop SEM was used for all SEM imaging.

Differential Scanning Calorimeter

A Mettler Toledo STAR^e instrument under nitrogen and equipped with an autosampler was used in order to carry out single heat-cool-heat cycles between -100 °C and 150 °C with a heating rate of 10 °Cmin^{-1} and a cooling rate of 10 °Cmin^{-1}. The samples were crimped in standard aluminium pans. Experiments were analysed by STAR^e software prior to being exported to OriginPro for graphical represenation.

Plate Reader

A Biotek Synergy HTX multi-mode plate reader was used to measure the absorbance of samples in 96 well plates at 575 nm.

5.5.3 Tecophilic 2000 TPU with pAMPS inter-penetrating network synthesis

A typical synthesis was carried out as follows;

To prepare the AMPS monomer solution; a solution of AMPS (23.2 g, 0.11 mol), water (53.7 mL), PEGDA (0.1077g, 1.23 x 10^{-4} mol) was added to a 125 mL foil lined powder jar equipped with a stirrer bar. To this was added Irgacure 1173 (0.01077 g, 0.01 mL, 6.56 x 10^{-5} mol) in the absence of light and stirred until fully dissolved. To this AMPS monomer solution was added Tecophilic 2000 TPU (10 x 20 mm disks, 0.15 g) in the absence of light and allowed to swell for 16 hours. The swollen material was then weighed and sandwiched between layers of transparent PET sheeting and subjected to a Light Hammer 6 UV source (200 watts/cm, nm) for 7 cycles at 5 m / min. The cured materials were then weighed and sealed in sample bags and stored at ambient temperature.

Reaction	PEGDA (g)	PEGDA (mmol)	AMPS (g)	AMPS (mol)	Water (g)	Irgacure 1173 (g)	Irgacure 1173 (mmol)	Total mass of TPU (g)
1	0.1077	0.123	23.2	0.111	53.7	0.01077	6.56	1.5
2	0.2154	0.246	23.2	0.111	53.7	0.01077	6.56	1.5
3	0.4308	0.502	23.2	0.111	53.7	0.01077	6.56	1.5
4	0.7539	1.00	23.2	0.111	53.7	0.01077	6.56	1.5
5	0.1077	1.23	17.4	0.084	59.5	0.01077	6.56	1.5
6	0.1077	1.23	11.6	0.056	65.3	0.01077	6.56	1.5
7	0.1077	1.23	5.8	0.028	71.1	0.01077	6.56	1.5

5.5.4 Swelling to equilibrium in simulated body fluid

Networks were taken as prepared and immersed in an excess of simulated body fluid (described below) at room temperature. Measurements of mass were taken on a four point weighing scale at times: 0.5, 1, 2, 5, 24, 48 and 72 hours when the sample was taken out of solution, patted with filter paper to remove excess fluid and weighed. At 72 hours, and upon equilibrium swelling. The swollen networks were dried in an oven at 105 °C for 16 hours before the dried weight was taken.[67-69]

Degree of swelling was calculated using the following equation;[53]

$$Degree\ of\ Swelling\ (\%) = \frac{W_S - W_D}{W_D} \times 100$$

In order to determine the volume degree of swelling the networks were measured in their cured state with Vernier calipers in both their diameter and depth. At equilibrium degree of swelling the networks were again measured for their diameter and depth.

The simulated body fluid was made up of sodium chloride (8.2985 g, 142 $mmolL^{-1}$) and calcium chloride (0.2775 g, 2.5 $mmolL^{-1}$) made up to 1 L with deionized water in a 1 L volumetric flask.

All analyses were carried out in triplicate.

5.5.5 Imaging by Scanning Electron Microscopy

Cured samples were swollen in deionised water to 90 wt. % water content before being frozen at -15 ^{o}C for 16 hours. Networks were then lyophilised for 72 hours prior to mounting and analysis. Imaging was performed using a desktop Hitachi TM3030 plus in SE mode at x 100 and x 1000 magnification.

5.5.6 Rheology of gels

Rheology experiments were performed on a Malvern Kinexus Ultra + rheometer equipped with a Peltier plate and hood cartridge. A geometry of 40 mm parallel plates were used with a force gap of 1 N between the plates. All experiments were performed at 25 ^{o}C. The instrument was controlled in strain control mode. Cured samples were swollen to 90 wt. % water content before being cut with a 40 mm diameter wad punch. Frequency sweeps were performed between 0.1 and 1000 Hz at 1 % γ degree of strain. Amplitude sweeps were performed between 0.1 and 1000 % γ at a frequency of 1 Hz.

All results were carried out in triplicate.

5.5.7 Measurement of adhesive properties

Cured samples were swollen to 90 wt. % water content (in deionised water) prior to being cut with a 20 mm diameter wad punch. A preload of 1 N was applied and allowed to stabilise at a constant force of 1 N to counteract creep. The upper plate was then removed at a rate of 20 mm/min off the lower plate and the force required to remove the upper plate was measured. All measurements were conducted a minimum of 5 times with samples showing clear signs of defects – jumps, local maxima – being discarded.

5.5.8 Measurement of Calcium uptake of cured gels

Calcium assays were conducted according to the Calcium colorimetric assay kit provided by Sigma-Aldrich.

Cured networks were immersed into 100 mL of simulated body fluid. A 100 µL sample was taken at time 0 h and upon the reaching of equilibrium swelling at 72 hours a further 100 µL sample was taken. 20 µL of each sample were added separate wells in a 96 well plate and topped up with MilliQue water to 50 µL. 90 µL of a chromogenic reagent was added to each plate followed by 60 µL of Calcium Assay Buffer and then mixed gently. The plate was left to incubate for 20 minutes at room temperature in a dark room before measuring the absorbance at 575 nm using a Biotek Synergy HTX multi-mode plate reader.

All analyses were carried out in triplicate.

5.6 *References*

(1) Dragan, E. S. *Chem. Eng. J.* **2014**, *243*, 572.

(2) Velnar, T.; Bailey, T.; Smrkolj, V. *J. Int. Med. Res.* **2009**, *37*, 1528.

(3) Winter, G. D. *Nature* **1962**, *193*, 293.

(4) Ovington, L. G. *Home Healthcare Now* **2002**, *20*, 652.

(5) Rovee, D. T. *Clin. Mater.* **1991**, *8*, 183.

(6) Jiang, Q.; Wang, J.; Tang, R.; Zhang, D.; Wang, X. *Int. J. Biol. Macromol.* **2016**.

(7) Boateng, J. S.; Matthews, K. H.; Stevens, H. N. E.; Eccleston, G. M. *J. Pharm. Sci.* **2008**, *97*, 2892.

(8) Munro, H. S. US20130251665 A1, **2013**.

(9) Tufts, S. A.; Baltezor, M. J.; Ortiz, M.; Flores, J.; Devens, J. R.; Munro, H. S.; Boote, N. US20140235727 A1, **2014**.

(10) Yin, L.; Fei, L.; Tang, C.; Yin, C. *Polym. Int.* **2007**, *56*, 1563.

(11) Sank, A.; Chi, M.; Shima, T.; Reich, R.; Martin, G. R. *Surgery* **1989**, *106*, 1141.

(12) Lansdown, A. B. G. *Wound. Repair. Regen.* **2002**, *10*, 271.

(13) Kavanagh, G. M.; Ross-Murphy, S. B. *Prog. Polym. Sci.* **1998**, *23*, 533.

(14) Peak, C.; Wilker, J.; Schmidt, G. *Colloid. Polym. Sci.* **2013**, *291*, 2031.

(15) Ganji, F.; Vasheghani-Farahani, S.; Vasheghani-Farahani, E. *Iran Polym J* **2010**, *19*, 375.

(16) Myung, D.; Waters, D.; Wiseman, M.; Duhamel, P. E.; Noolandi, J.; Ta, C. N.; Frank, C. W. *Polym. Advan. Technol.* **2008**, *19*, 647.

(17) Xie, H. Q.; Huang, X. D.; Guo, J. S. *J. Appl. Polym. Sci.* **1996**, *60*, 537.

(18) Chiang, L. Y.; Wang, L. Y.; Kuo, C.; Lin, J.; Huang, C. *Synth. Met.* **1997**, *84*, 721.

(19) Karabanova, L. V.; Boiteux, G.; Gain, O.; Seytre, G.; Sergeeva, L. M.; Lutsyk, E. D. *Polym. Int.* **2004**, *53*, 2051.

(20) Karabanova, L. V.; Boiteux, G.; Seytre, G.; Stevenson, I.; Lloyd, A. W.; Mikhalovsky, S. V.; Helias, M.; Sergeeva, L. M.; Lutsyk, E. D.; Svyatyna, A. *Polym. Eng. Sci.* **2008**, *48*, 588.

(21) Karabanova, L. V.; Boiteux, G.; Seytre, G.; Stevenson, I.; Gain, O.; Hakme, C.; Lutsyk, E. D.; Svyatyna, A. *J. Non-Cryst. Solids* **2009**, *355*, 1453.

(22) Klonos, P.; Chatzidogiannaki, V.; Roumpos, K.; Spyratou, E.; Georgiopoulos, P.; Kontou, E.; Pissis, P.; Gomza, Y.; Nesin, S.; Bondaruk, O.; Karabanova, L. *J. Appl. Polym. Sci.* **2016**, *133*.

(23) Stamatopoulou, C.; Klonos, P.; Koutsoumpis, S.; Gun'ko, V.; Pissis, P.; Karabanova, L. *J. Polym. Sci., Part B: Polym. Phys.* **2014**, *52*, 397.

(24) Reddy, T. T.; Kano, A.; Maruyama, A.; Hadano, M.; Takahara, A. *Biomacromolecules* **2008**, *9*, 1313.

(25) Thimma Reddy, T.; Kano, A.; Maruyama, A.; Hadano, M.; Takahara, A. *J. Biomed. Mater. Res. B.* **2009**, *88*, 32.

(26) Reddy, T. T.; Takahara, A. *Polymer* **2009**, *50*, 3537.

(27) Thatiparti, T. R.; Kano, A.; Maruyama, A.; Takahara, A. *J. Polym. Sci., Part A: Polym. Chem.* **2009**, *47*, 4950.

(28) Merlin, D. L.; Sivasankar, B. *Eur. Polym. J.* **2009**, *45*, 165.

(29) Liu, N.; Shao, H.; Wang, C.-F.; Chen, Q.-L.; Chen, S. *Colloid. Polym. Sci.* **2013**, *291*, 1871.

(30) Turner, J.; Martineau, L.; Shek, P. US20040105880 A1, **2003**.

(31) Peng, H.; Mok, M.; Martineau, L.; Shek, P. US20050218541 A1, **2004**.

(32) Myung, D.; Kourtis, L.; Ward, R.; Jaasma, M. J.; McCrea, K. WO2010017282 A1, **2014**.

(33) Jiménez, M. G.; Armenta, J. R.; Martínez, A. M.; Muñiz, R.; Vazquez, N. R.; Rojas, E. T. *Lat. Am. Appl. Res* **2009**, *39*, 131.

(34) Liliana, M.; Nancy, M.; James, B.; Eric, R.; Andrew, C. WO2015171483 A1, **2015**.

(35) Kim, S. J.; Shin, S. R.; Spinks, G. M.; Kim, I. Y.; Kim, S. I. *J. Appl. Polym. Sci.* **2005**, *96*, 867.

(36) Munro, H. S.; Hoskins, R. US20060068014 A1, **2003**.

(37) Klode, J.; Schöttler, L.; Stoffels, I.; Körber, A.; Schadendorf, D.; Dissemond, J. *J. Eur. Acad. Dermatol.* **2011**, *25*, 933.

(38) Ghobril, C.; Grinstaff, M. W. *Chem. Soc. Rev.* **2015**, *44*, 1820.

(39) Roy, C. K.; Guo, H. L.; Sun, T. L.; Ihsan, A. B.; Kurokawa, T.; Takahata, M.; Nonoyama, T.; Nakajima, T.; Gong, J. P. *Adv. Mater.* **2015**, *27*, 7344.

(40) Sun, L.; Huang, Y.; Bian, Z.; Petrosino, J.; Fan, Z.; Wang, Y.; Park, K. H.; Yue, T.; Schmidt, M.; Galster, S.; Ma, J.; Zhu, H.; Zhang, M. *ACS Appl. Mater. Interfaces.* **2016**.

(41) Balcioglu, S.; Parlakpinar, H.; Vardi, N.; Denkbas, E. B.; Karaaslan, M. G.; Gulgen, S.; Taslidere, E.; Koytepe, S.; Ates, B. *ACS Appl. Mater. Interfaces.* **2016**, *8*, 4456.

(42) Lin, S.-Y.; Chen, K.-S.; Run-Chu, L. *Biomaterials* **2001**, *22*, 2999.

(43) Shergold, O. A.; Fleck, N. A.; Radford, D. *Int. J. Impact. Eng.* **2006**, *32*, 1384.

(44) Choi, J. S.; Yoo, H. S. *J. Biomed. Mater. Res. A.* **2010**, *95A*, 564.

(45) Matthews, K. H. *Advanced Wound Repair Therapies*; Woodhead Publishing, **2011**.

(46) Lin, Y.-J.; Lee, G.-H.; Chou, C.-W.; Chen, Y.-P.; Wu, T.-H.; Lin, H.-R. *J. Mater. Chem. B.* **2015**.

(47) Ham, T. R.; Lee, R. T.; Han, S.; Haque, S.; Vodovotz, Y.; Gu, J.; Burnett, L. R.; Tomblyn, S.; Saul, J. M. *Biomacromolecules* **2015**.

(48) Poenie, M.; Alderton, J.; Steinhardt, R.; Tsien, R. *Science* **1986**, *233*, 886.

(49) Lew, P. D.; Wollheim, C. B.; Waldvogel, F. A.; Pozzan, T. *J. Cell. Biol.* **1984**, *99*, 1212.

(50) Brandrup, J.; Immergut, E. H.; Grulke, E. A.; Abe, A.; Bloch, D. R. *Polymer handbook*; 4th ed.; Wiley New York, **1999**; Vol. 89.

(51) Liaw, D. J. *J. Appl. Polym. Sci.* **1997**, *66*, 1251.

(52) Yilgör, I.; Yilgör, E. *Polymer* **1999**, *40*, 5575.

(53) Peppas, N. A.; Bures, P.; Leobandung, W.; Ichikawa, H. *Eur. J. Pharm. Biopharm.* **2000**, *50*, 27.

(54) Zhang, J.-T.; Bhat, R.; Jandt, K. D. *Acta. Biomater.* **2009**, *5*, 488.

(55) Liu, M.; Su, H.; Tan, T. *Carbohydr. Polym.* **2012**, *87*, 2425.

(56) Wang, H.; Li, W.; Lu, Y.; Wang, Z. *J. Appl. Polym. Sci.* **1997**, *65*, 1445.

(57) Yin, L.; Zhao, Z.; Hu, Y.; Ding, J.; Cui, F.; Tang, C.; Yin, C. *J. Appl. Polym. Sci.* **2008**, *108*, 1238.

(58) Varaprasad, K.; Reddy, N. N.; Ravindra, S.; Vimala, K.; Raju, K. M. *Int. J. Polymer. Mater.* **2011**, *60*, 490.

(59) Ozmen, M. M.; Dinu, M. V.; Dragan, E. S.; Okay, O. *J. Macromol. Sci. A.* **2007**, *44*, 1195.

(60) Mao, N.; Russell, S. J. *Text. Prog.* **2004**, *36*, 1.

(61) Mao, N., PhD Thesis, 2000.

(62) Ross-Murphy, S. B. *Polym. Gels Networks* **1994**, *2*, 229.

(63) Chau, M.; De France, K. J.; Kopera, B.; Machado, V. R.; Rosenfeldt, S.; Reyes, L.; Chan, K. J. W.; Förster, S.; Cranston, E. D.; Hoare, T.; Kumacheva, E. *Chem. Mater.* **2016**, *28*, 3406.

(64) Ramazani-Harandi, M. J.; Zohuriaan-Mehr, M. J.; Yousefi, A. A.; Ershad-Langroudi, A.; Kabiri, K. *Polym. Test.* **2006**, *25*, 470.

(65) Peh, K.; Khan, T.; Ch'ng, H. *J. Pharm. Pharm. Sci.* **2000**, *3*, 303.
(66) Rivas, B. L.; Pooley, S. A.; Luna, M.; Geckeler, K. E. *J. Appl. Polym. Sci.* **2001**, *82*, 22.
(67) Ritger, P. L.; Peppas, N. A. *J. Control. Release.* **1987**, *5*, 37.
(68) Ritger, P. L.; Peppas, N. A. *J. Control. Release.* **1987**, *5*, 23.
(69) Canal, T.; Peppas, N. A. *J. Biomed. Mater. Res.* **1989**, *23*, 1183.